Combinatorial plating characteristics of electroless processes for dense Pd-PSS composite membrane fabrication

Thesis submitted in partial fulfillment of the requirements for the degree of

DOCTOR OF PHILOSOPHY

by

Murali Pujari

Department of Chemical Engineering
Indian Institute of Technology Guwahati
Guwahati - 781039, India

Combinatorial plating characteristics of electroless processes for dense Pd-PSS composite membrane fabrication

Murali Pujari

Combinatorial plating characteristics of electroless processes for dense Pd-PSS composite membrane fabrication

Thesis submitted in partial fulfillment of the requirements for the degree of

DOCTOR OF PHILOSOPHY

by

Murali Pujari
Roll No.: 10610709

Department of Chemical Engineering
Indian Institute of Technology Guwahati
Guwahati - 781039, India

August, 2014

Dedicated To

My Family Members

Department of Chemical Engineering
Indian Institute of Technology Guwahati
Guwahati - 781039, India

CERTIFICATE

This is to certify that the thesis entitled **"Combinatorial plating characteristics of electroless processes for dense Pd-PSS composite membrane fabrication"** being submitted by ***Murali Pujari*** for the award of PhD degree has been carried out under our guidance and supervision. The work documented in this thesis has not been submitted to any other University or Institute for the award of any degree or diploma.

(Dr. Ramgopal V. S. Uppaluri)
Professor
Department of Chemical Engineering
Indian Institute of Technology Guwahati
Guwahati - 781039, India.

(Dr. Anil Verma)
Associate Professor
Department of Chemical Engineering,
Indian Institute of Technology Guwahati
Guwahati - 781039, India.

Acknowledgements

I would like to express my gratitude to all those who helped me in different ways in completing this research work within the time span of four years, directly or indirectly. First and foremost, I would like to express my deep felt gratitude to my supervisors, **Prof. Ramgopal V. S. Uppaluri** and **Dr. Anil Verma** for providing me continuous inspiration and guidance throughout the entire course of work. I am indebted to both of them for their useful suggestions and constant encouragement throughout the entire period.

My first debt of gratitude must go to my main supervisor **Prof. Ramgopal V. S. Uppaluri** for his continuous support, interesting discussions and giving me freedom in handling different issues. His uncompromising approach to complete the experimental part, data analysis, writing manuscripts as well as thesis within the stipulated time period helped me a lot in completing my research work. The numerous brain storming sessions during the project meetings with him were very useful in enriching my analytical power. I also remain indebted for his understanding, support and caring during the times when I was really down and depressed due to personal problems.

I would like to express my sincere gratitude to **Dr. Anil Verma** of the Department of Chemical Engineering for his valuable contribution in my research work. I appreciate very much his flexibility and openness in dealing with the specific and general needs of this research work. I thank him for his patience and helping nature. It has been a great privilege to work with him.

I must also thank my doctoral committee members **Dr. R. K. Upadhyay, Dr. Amit Kumar** of the Department of Chemical Engineering and **Dr. C. V. Sastri** of the Department of Chemistry, for their valuable suggestions and contribution towards my research work.

I also thank all the faculty members of the Department of Chemical Engineering for their kind cooperation during my stay in the department. I am also thankful to all the staff members and scientific officers of the Chemical Engineering Department for their genuine help during my entire research period. I also acknowledge the financial support provided by the **DST, New Delhi.**

I am thankful to the Central Instruments Facility of IIT Guwahati for allowing me to carry out **FESEM** analysis on my own, which has been very important in this research work. In this regard, I should acknowledge the help of **Mr. K. K. Senapati,** Scientific Officer, Central Instruments Facility, IIT Guwahati. He taught me how to use the FESEM instrument and take images at various critical conditions of the sample. I am also thankful to the **Mr. B. Choudhury** of central workshop, IIT Guwahati for helping me in the fabrication of my experimental setup which was very much essential in my research work.

I was fortunate enough to get excellent batch mates like **Rajesh, Amrita, Sriharsha, Chandrasekhar** and **Srinu** for their friendly support and timely assistance whenever needed. I am also thankful to **Shyam, Sanjib Barma, Rajeev**, **Yadav** and **Chola Bhargava** for their friendly behavior and assistance.

Last but not the least, I would like to express my deepest sense of gratitude to my parents and family members. Their love, care, sacrifice and encouragement have made it possible for me to come so far. I appreciate the courage, understanding and dedicated support shown by all of them despite many testing times at their end.

Murali Pujari

Abstract

Dense Pd composite membranes have several functional applications and have been regarded to be important technologies to realize a hydrogen energy based economy. Among various fabrication techniques, electroless plating process (ELP) is one of the promising process in terms of scalability, simplicity of process operation and commissioning. In the recent years, rate enhanced electroless plating processes have been developed as new age technologies for the faster fabrication of dense Pd composite membranes with superior combinations of hydrogen permeability and selectivity.

In the field of electroless fabrication of dense Pd composite membranes, the available state-of-the-art did not address the combinatorial plating characteristics of various rate enhanced electroless plating processes. Precisely, the combinatorial plating characteristics refer to the evaluation of time dependent plating characteristics such as selective conversion (or transport efficiency), plating efficiency, average plating rate, metal film thickness and percent pore densification. The evaluation of time dependent combinatorial plating characteristics of alternate Pd ELP processes will provide significant insights with respect to the screening, scoping and identification of optimal rate enhanced Pd ELP processes and their associated operating parameters.

The thesis research has been broadly carried out in four different areas of research. These are outlined as follows:

a) Identification of optimal rate enhanced Pd ELP processes for the cost effective fabrication of Pd/PSS composite membrane fabrication. The investigated ELP processes include sonication assisted ELP (SOEP), surfactant induced ELP (SIEP), sonication and surfactant induced ELP (SSOEP) and conventional electroless plating

(CEP) processes. Bulk, phase wise (PW) and drop wise (DW) addition of the hydrazine reducing agent were considered as alternate process modifications.

b) Parametric optimization of the optimal rate enhanced Pd ELP process using the relevant combinations of various plating characteristics.

c) Role of nickel diffusion barrier on the combinatorial plating characteristics of optimal Pd ELP process.

d) Effect of chromia and surfactant induced chromia diffusion barriers on the combinatorial plating characteristics of optimal Pd ELP process.

For all experimental investigations, porous stainless steel (PSS) supports were used as substrates to achieve dense Pd composite membranes. The experimental investigations involved (a) support characterization (b) sensitization, activation and Pd electroless plating for 12 – 16 sequential plating steps with 30 min. duration for each step (c) evaluation of room temperature nitrogen flux for membranes fabricated at various cumulative plating time intervals (d) evaluation of Pd solution concentration in spent ELP solutions obtained at various cumulative plating time intervals using atomic absorption spectroscopy and (e) surface characterization of the fabricated dense membrane including FESEM and XRD analyses. Based on the room temperature N_2 flux data, weight gained by the Pd composite membrane after plating process and composition of spent ELP solution, the combinatorial plating characteristics of various Pd ELP processes have been evaluated. Among these parameters, the most important parameters refer to plating efficiency and PPD using which the optimal Pd process can be evaluated.

Identification of optimal Pd ELP process

Among CEP (PW), SIEP (PW), SOEP (PW) and SSOEP (PW) processes, SIEP (PW) and SSOEP (PW) processes provided optimal plating characteristics including PPD and plating efficiency values. For these processes, the process parameters refer to 0.005 M Pd solution concentration, loading ratio of 203 cm^2/L and CTAB surfactant solution concentration of 4 CMC. For the SIEP (PW) process, for a variation in plating time from 2 – 6 h, the selective conversion, plating efficiency, metal film thickness, average plating rate and PPD have been evaluated to vary from 18.51 – 17.35%, 55.32 – 62.8%, 1.61 – 4.47 µm, 2.53 – 2.34 x 10^{-5} $mol/m^2.s$ and 56.83 – 98.46% respectively. However, for SSOEP (PW) processes, superior combinatorial plating characteristics were obtained. For the SSOEP (PW) process, for a variation in plating time from 2 – 6 h, the selective conversion, plating efficiency, metal film thickness, average plating rate and PPD have been evaluated to vary from 29.03-34.45%, 93.33-95.18%, 2.52 – 8.99 µm, 3.96 – 4.70 x 10^{-5} $mol/m^2.s$ and 13.35 – 99.82 respectively. Since 100% dense Pd membranes were not obtained using PW addition of the hydrazine agent, further experimental investigations were carried out for SSOEP (DW) and SIEP (DW) processes.

Using similar process parameters as those deployed for the PW processes, the combinatorial plating characteristics were investigated for SIEP (DW) and SSOEP (DW) processes. Among these, the SSOEP (DW) process provided the optimal combinatorial plating characteristics. For the SSOEP (DW) process, for a variation in plating time from 2 – 7 h, the selective conversion, plating efficiency, metal film thickness, average plating rate and PPD have been evaluated to vary from 30.6 – 26.3%, 72.5 – 80.7%, 3.06 – 8.81 µm, 4.81 – 3.95 x 10^{-5} $mol/m^2.s$ and 37.24 – 99.98%, respectively. Since 100% dense Pd membranes were not obtained further parametric

optimization was carried out for the SSOEP (DW) process which has been inferred to be the optimal rate enhanced Pd ELP process.

Parametric optimality of SSOEP (DW) Pd baths

For a fixed choice of 4 CMC CTAB solution concentration and 203 cm^2/L loading ratio, experimental investigations carried out with variant Pd solution concentrations (0.005 and 0.01 M) indicated that the SSOEP (DW) process provided better combinatorial characteristics for lower Pd solution concentration (0.05 M). Further, for a fixed choice of 0.005 M Pd metal solution concentration and loading ratio of 203 cm^2/L, the SSOEP (DW) process with variant surfactant solution concentrations (1, 2 and 4 CMC) indicated optimal combinatorial characteristics for 2 CMC Pd baths. For these baths, for a variation in plating time from 2 – 8 h, the selective conversion, plating efficiency, metal film thickness, average plating rate and PPD have been evaluated to vary from 35.4 – 31.5%, 90.0 – 95.9%, 3.14 – 11.16 μm, 4.92 – 4.38 x 10^{-5} $mol/m^2.s$ and 96.9 – 100%, respectively. Thus, the basic objective of achieving 100% dense Pd composite membranes were achieved with systematic process engineering approaches and methodologies addressed in this work. Finally, for a fixed choice of other parameters (0.005 M Pd solution concentration and 2 CMC CTAB solution concentration), the loading ratio value for the SSOEP (DW) baths was investigated for two different cases (203 cm^2/L and 407 cm^2/L) in which the loading ratio of 203 cm^2/L provided optimal combinatorial characteristics. Thus, the optimal process parameters correspond to 0.005 M Pd solution concentration, 2 CMC CTAB solution concentration and 203 cm^2/L loading ratio.

Combinatorial plating characteristics of SSOEP (DW) baths for dense Pd/Ni/PSS membrane fabrication

Dense Pd/Ni/PSS membranes were fabricated with 0.5 and 0.1 μm nominal pore size PSS supports. Ni film was deposited on the PSS supports using SSOEP (DW) Ni baths. Among both the cases, optimal combinatorial plating characteristics were obtained for 0.1 μm PSS support. For this case, for a variation in plating time from 2 – 10 h, the combinatorial plating characteristics have been evaluated as 33.73 – 30.92% for selective conversion, 76.54 – 87.01% for plating efficiency, 2.13 – 9.8 μm for Pd film thickness, 3.35 – 3.07 x 10^{-5} mol/m^2.s for average plating rate and 92.98 – 99.989% for PPD. Along with PPD, the combinatorial plating characteristics of dense Pd/Ni/PSS membranes were significantly lower than those obtained for dense Pd/PSS membranes.

Combinatorial plating characteristics of SSOEP (DW) baths for dense Pd/Cr_2O_3/PSS membrane fabrication

The chromia interdiffusion barriers were achieved by first adopting conventional and surfactant induced chromium electroplating followed with oxidation of the chromium deposited on the PSS support. For the dense Pd/Cr_2O_3/PSS membranes fabricated using conventional chromium electroplating and SSOEP (DW) Pd baths, for 7.8 μm thickness of chromia interdiffusion barrier, a variation in total plating time from 2 – 7 h enabled to achieve selective conversion, plating efficiency, plating rate, thickness and PPD in the range of 4.90 – 32.51%, 14.78 – 83.31%, 0.63 – 3.87 x 10^{-5} mol/m^2.s, 0.4 – 8.64 μm and 29.8 – 99.994%, respectively. These characteristics were significantly different from those obtained for Pd composite membrane prepared with 20 μm thick Cr_2O_3 interdiffusion barrier thickness. For this case, the combinatorial plating characteristics correspond to a variation in selective conversion from 29.06 – 21.11%, plating

efficiency from 78.65 – 75.64%, average plating rate from 4.09 – 2.97 x 10^{-5} mol/m^2.s, metal film thickness from 2.6 – 7.58 μm and PPD from 59.47 – 99.91%.

On the other hand, for surfactant induced chromia diffusion barriers, for a variation in total plating time from 2 – 8h, the combinatorial plating characteristics of Pd/Cr_2O_3-surf/PSS membranes (for 7.1 μm thick Cr_2O_3 interdiffusion barrier) were evaluated to vary from 49.29 – 37.6% for selective conversion, 62.11 – 61.18% for plating efficiency, 6.41 – 4.89 x 10^{-5} mol/m^2.s for average Pd plating rate, 4.08 – 12.47 μm for metal film thickness and 49.15 – 99.978% for PPD. On the other hand, for a variation in plating time from 2 – 8h, these characteristics were significantly different for the Pd/Cr_2O_3-surf/PSS membranes prepared with 12.5 μm thick Cr_2O_3 films. For this case, the combinatorial plating characteristics were evaluated to confirm a variation in selective conversion from 41.84 – 28.65%, plating efficiency from 70.60 – 84.78%, average plating rate from 6.26 – 4.28 x 10^{-5} mol/m^2.s, metal film thickness from 3.99 – 10.93 μm and PPD from 98.29 – 99.976%. In summary, the surfactant induced electroplating enabled the realization of higher Pd metal film thickness on the chromia interdiffusion barrier but did not enable the achievement of 100% pore densification. Hence, if it is assumed that the long term performance of 100% Pd/PSS membrane is similar to the 99.99% dense Pd/chromia/PSS membrane, it can be inferred that a reduction in the critical dense Pd film thickness by 2 – 3 μm for the chromia membranes could enhance hydrogen permeabilities. Otherwise, it shall be inferred that the chromia interdiffusion barrier is not at all effective to enhance hydrogen permeabilities in comparison with those obtained with Pd/PSS membranes.

In summary, the Ph.D. thesis addressed the important aspect of fabrication engineering concepts associated to dense Pd/PSS membrane fabrication and various research opportunities available to further the achievement of 100% dense Pd composite membranes with interdiffusion barriers.

Future research in this field needs to be address the tougher challenges posed by interdiffusion barriers to achieve 100% dense Pd composite membranes with lower dense Pd film thickness.

In terms of the thesis novelty, the following have been outlined:

- Evaluation of time dependent combinatorial plating characteristics using which significant insights can be gained for the further optimality of electroless plating processes for dense Pd composite membrane fabrication.
- A framework has been presented to evaluate theoretical selectivity based on the room temperature nitrogen flux. Based on the said approach, high temperature experiments need not be carried out and the deviation of the fabricated membrane from 100% dense Pd composite membrane can be evaluated.
- The optimal process invented for Pd/PSS membrane fabrication refers to the sonication and surfactant coupled Pd ELP bath supplemented with dropwise addition of the reducing agent.
- Parametric optimality for 100 % dense Pd/PSS membrane fabrication has been identified for SSOEP (DW) Pd ELP baths. This refers to utilization of lower Pd solution concentrations.
- Combinatorial plating characteristics for dense Pd/Ni/PSS and Pd/ Cr_2O_3/PSS composite membranes have been evaluated.
- The optimality of SSOEP (DW) baths for dense Pd/PSS membranes does not confirm the optimality for dense Pd membranes with interdiffusion barriers.
- The role of chromia interdiffusion barrier morphology achieved using surfactant induced electroplating process was investigated in the context of combinatorial plating characteristics was investigated.

- The research methodology provided significant insights using which directions for the further refinement in process parameters can be targeted to achieve 100% dense Pd composite membranes.

Contents

Page No.

Page No.

Page No.

Page No.

Page No.

Page No.

Page No.

List of Tables

List of Figures

Abbreviations

PSS	Porous stainless steel
PPD	Percent pore densification
CTAB	Cetyltrimethylammonium bromide
DTAB	Dodecyltrimethylammonium bromide
CEP	Conventional electroless plating
SOEP	Sonication assisted electroless plating
SIEP	Surfactant induced conventional electroless plating
SSOEP	Surfactant induced sonication electroless plating
SEM	Scanning electronic microscopy
FESEM	Field emission scanning electron microscopy
AAS	Absorption atomic spectroscopy
XRD	X-Ray diffraction
LPSA	Laser particle size analyzer
PW	Phase wise
DW	Drop wise
CMC	Critical micelle concentration
HLB	Hydrophilic lipophilic balance
Pcm	Porous composite membrane

Notations

ΔP	Pressure differential, Pascal
JH_{ht}^{df}	Hydrogen flux through dense palladium film at high temperature, $\left(\frac{mol}{m^2.s}\right)$
$Permh_{ht}^{df}$	Hydrogen permeability through dense Pd film at high temperature, $\left(\frac{mol.m}{m^2.s.Pa}\right)$
$Perh_{ht}^{df}$	Hydrogen permeance through dense Pd film at high temperature, $\left(\frac{mol}{m^2.s.Pa}\right)$
$VPerh^{sup}$	Gas Effective permeance, $\left(\frac{m^3}{m^2.s}\right)$
vh	Hydrogen velocity, $\left(\frac{m}{s}\right)$
μh	Hydrogen viscosity, $\left(\frac{kg}{m.s}\right)$
Jn^{sup}	Nitrogen flux through support, $\left(\frac{mol}{m^2.s}\right)$
$Pern^{sup}$	Nitrogen permeability of support, $\left(\frac{mol.m}{m^2.s.Pa}\right)$
μn	Nitrogen velocity, $\left(\frac{m}{s}\right)$
vn	Nitrogen viscosity, $\left(\frac{kg}{m.s}\right)$
JH^{db}	Diffusion barrier film hydrogen permeability, $\left(\frac{mol.m}{m^2.s.Pa}\right)$
$Perh^{df}$	Hydrogen permeability of dense palladium film, $\left(\frac{mol.m}{m^2.s.Pa}\right)$

JH^{df}	Hydrogen flux through dense palladium film, $\left(\frac{mol}{m^2.s}\right)$
$VPern_{rt}^{pcm}$	Nitrogen volumetric permeability of Porous composite membrane at room temperature, $\left(\frac{m^3(STP)}{m^2.s.}\right)$
Q_{rt}^{pcm}	Volumetric flow rate of a gas at room temperature for the Pd composite membrane
$KPern_{rt}^{pcm}$	Knudsen nitrogen permeance at room temperature, $\left(\frac{mol}{m^2.s.Pa}\right)$
$ViPern_{rt}^{pcm}$	Viscous nitrogen permeance at room temperature, $\left(\frac{mol}{m^2.s.Pa}\right)$
$KPern_{ht}^{pcm}$	Knudsen nitrogen permeance at high temperature, $\left(\frac{mol}{m^2.s.Pa}\right)$
Vn_{rt}	Velocity of nitrogen at room temperature, $\left(\frac{m}{s}\right)$
δ^{df}	Dense palladium film thickness, (m)
PR	Partial pressure on retentate side, Pa
PP	Partial pressure on permeate side, Pa
JH^{sup}	Molar hydrogen flux of support, $\left(\frac{mol}{m^2.s}\right)$
$Perh^{sup}$	Hydrogen permeance through support, $\left(\frac{mol}{m^2.s.Pa}\right)$
rp^{sup}	Average pore radius of support, (m)
δ^{sup}	Support thickness, (m)

$\left(\frac{\varepsilon}{q^2}\right)^{sup}$	Support effective porosity
(An)	Slope
(Bn)	Intercept
DEV_i	Deviation of dense Pd membrane flux with respective to porous membrane flux
ΔP_{max}	Maximum pressure, Pascal
rp^{th}	Theoretical pore radius, (m)
$\left(\frac{\varepsilon}{q^2}\right)^{th}$	Support thickness, (m)
$\left(\frac{\varepsilon}{q^2}\right)^{sup}$	Theoretical effective porosity
$\left(\frac{\varepsilon}{q^2}\right)^{opt}$	Optimal effective porosity of the membrane support to always provide H_2 gas flux higher than the dense Pd film hydrogen flux
A_m	Area of membrane, $\left(m^2\right)$
Vn_{ht}	Velocity of nitrogen at high temperature, $\left(\frac{m}{s}\right)$
$VPern_{ht}^{pcm}$	Viscous nitrogen permeance at high temperature, $\left(\frac{mol}{m^2.s.Pa}\right)$
μn_{rt}	Viscosity of nitrogen at room temperature, $\left(\frac{kg}{m.s}\right)$
μn_{ht}	Viscosity of nitrogen at high temperature, $\left(\frac{kg}{m.s}\right)$
JN_{ht}^{pcm}	Nitrogen flux of porous composite membrane at high temperature, $\left(\frac{mol}{m^2.s}\right)$

$JH_{ht}{}^{pcm}$	Hydrogen flux of porous composite membrane at high temperature, $\left(\frac{mol}{m^2.s}\right)$
δ^{pcm}	Thickness of porous composite membrane, (m)
$Permh^{pcm}$	Hydrogen permeability of porous composite membrane, $\left(\frac{mol.m}{m^2.s.Pa}\right)$
$Perh^{pcm}$	Hydrogen permeance through porous composite membrane, $\left(\frac{mol.}{m^2.s.Pa}\right)$
$AJH_{ht}{}^{pcm}$	Average hydrogen flux of porous composite membrane at high temperature, $\left(\frac{mol}{m^2.s}\right)$
$PR_{\max}$	Maximum allowed upstream pressure (5 bar)
$PR_{\min}$	Minimal upstream pressure (0.01 bar)
$AJN_{ht}{}^{pcm}$	Average nitrogen flux of porous composite membrane at high temperature, $\left(\frac{mol}{m^2.s}\right)$
$\alpha_{av}{}^{pcm}$	Average selectivity of porous composite membrane
y_{H2}	Mole fraction of hydrogen in the permeate stream
y_{N2}	Mole fraction of nitrogen in the permeate stream
x_{H2}	Mole fraction of hydrogen in the feed stream
x_{N2}	Mole fraction of nitrogen in the feed stream
d_p	Pore diameter, μm
PH	Hydrogen pressure, (pascal)
T	Temperature, K

Chapter 1:

Introduction and Literature Review

Chapter 1

INTRODUCTION AND LITERATURE REVIEW

After presenting a brief introduction on Pd composite membranes in section 1.1, section 1.2 presents an overview of various membrane fabrication methods with specific emphasis upon electroless plating (ELP). Thereby, section 1.3 elaborates upon the state-of-the-art in conventional (section 1.3.1) and rate enhanced ELP processes (section 1.3.2) for dense Pd composite membrane fabrication. Eventually, section 1.3.3 presents a brief overview of various fabrication methodologies to achieve Pd composite membranes with interdiffusion barriers such as chromia, ceramic, yttria stabilized zirconia, ZrO_2, oxidized porous stainless steel (PSS), and nickel. Section 1.4 elaborates upon various prominent issues in literature with emphasis upon engineering aspects of rate enhanced electroless plating process. Based on these insights, the scope for further research is outlined in section 1.5 followed with objectives and thesis organization in sections 1.6 and 1.7 respectively.

1.1 Introduction

In the past decade, the demand for the production and utilization of ultrapure hydrogen has enormously increased due to emphasis on novel technologies. Ultrapure hydrogen is an important constituent as an energy and processing resource for fuel cells, semiconductor manufacturers, petrochemical processing and metallurgical processing [1-3]. Commercially available hydrogen contains impurities such as CO, CO_2, O_2, N_2, H_2O and CH_4, which must be separated to obtain high purity hydrogen. A major challenge for the widespread use of hydrogen and a hydrogen-based economy is to target and develop inexpensive technologies for H_2 separation, purification and production. Various ongoing technological developments in the field

of hydrogen separation and purification are highly dynamic with rapid growth in their success rate. Pure hydrogen can be achieved with various separation technologies such as pressure swing adsorption (PSA) [4], catalytic purification, cryogenic separation [5], polymer membranes [6], metal hydride separation, solid polymer electrolyte cell and palladium membranes [7]. Amongst these, ultra pure hydrogen can be obtained with pressure swing adsorption, catalytic purification and palladium membrane diffusion. In these few technologies, PSA is expensive for compact and medium scale processing and catalytic purification is used for H_2 feed streams containing O_2 impurity. To produce high purity hydrogen, membrane processes are considered to be one of the most promising technologies. Among several kinds of membranes, palladium-composite membranes are considered to be the best choice. This is due to their catalytic activity for hydrogen dissociation, high hydrogen permeability and resistance to oxidation [8].

1.1.1 Palladium membranes

For the past 10 years, significant amount of research has been focused on Pd composite membranes. This is due to their high hydrogen adsorption capacity, high catalytic activity and resistance to oxidation. Due to high cost and low mechanical strength, commercially available palladium foils are not suitable for industrial/commercial applications. It is well known that the permeation rate or H_2 flux of membrane systems is inversely proportional to membrane thickness and therefore thicker foils give poor H_2 fluxes. To overcome this problem, palladium composite membrane consisting of thin dense Pd layer on a porous substrate is the optimal choice due to higher combination of mechanical strength and hydrogen permeance and lower membrane cost [9]. Typically, pure palladium membranes for hydrogen separation cannot be used below 573 K due to the lattice expansion caused by dissolved hydrogen which leads to membrane embrittlement. Since Pd is an expensive rare earth metal, palladium membrane technology

research involves the engineering of thin palladium films on porous supports. There by, fabrication engineering aspects are very important to analyze various factors and issues that enable the reduction in the expensive Pd composite membrane cost [10].

Details with respect to companies that manufacture dense Palladium membranes one represented in Table 1.1. Typical applications for Pd composite membranes include

a) Technology component for lab scale H_2 generators
b) Purification of H_2 produced in steam reforming reactions
c) Enhancement in conversion by selective removal of H_2 in membrane reactors
d) Reduction of CO concentration in the H_2 feed stock supplied to PEM fuel cells (i.e. Pd membranes to serve as guard units)
e) High purity H_2 generation for semi-conductor processing and various other novel applications.

Table 1.1: A summary of commercial dense Pd membranes.

S.No	Corporate institution	Membrane fabricated	Support used	Applications
1	ECN Netherlands [11]	Palladium composite membrane	Commercially available ceramic support	• Hydrogen generators • Steam reforming • Membrane reactors • Fuel cell applications • H_2 for Semiconductor processing
2	Johnson Matthey [12]	Palladium composite membranes	Porous stainless steel	

1.2 Membrane fabrication methods

Various fabrication methods deployed to achieve thin and dense Pd membrane films on porous substrates include magnetron sputtering [13-14], physical vapor deposition, chemical vapor deposition (CVD) [15-17], electroplating [18-19] and electroless plating [19-22]. A brief outline of these methods is presented in the following sub-sections.

1.2.1 Magnetron sputtering

During sputtering, a low pressure gas with large number of ions and free electrons (referred as plasma) is created using a high energy electric field. The bombardment of solid (target) with high energy chemically inert ions extracted from the plasma causes ejection of atoms from the target which are eventually deposited on the surface of the substrate using magnetic field generated by permanent magnets. The main advantage of this technique is that ultra-thin nano-structured films with minimal impurity can be prepared with greater flexibility for synthesizing alloys. Despite providing good quality films sputtering is not a scalable process. This is due to its high cost of procuring sophisticated setup and high energy requirements.

1.2.2 Physical vapor deposition

Physical vapor deposition (PVD) is a vaporization coating process in which the basic mechanism refers to an atom by atom transfer of material from the solid target phase to the vapor phase and eventually to the porous support. Prolonged deposition gradually enables the growth of Pd film on the substrate surface. For the case of reactive deposition, the noble metal reacts with a gaseous environment of co-deposited material to form a film of the metal compound, such as a nitride, oxide, carbide or carbonitride. Physical vapor deposition is a less laborious technique

and provides faster deposition rates. It allows to achieve better control of the film thickness. In contrast to CVD, the metal film can be obtained at relatively low temperatures. This avoids damage to the support due to lack of thermal stresses. Compared to the sputtering technique, PVD setup is inexpensive to commission and therefore is one of the cheapest process to achieve metal composite membranes. However, the transport efficiency of the PVD process is very poor due to deposition of the metal on surfaces other than the support.

1.2.3 Chemical vapor deposition

Chemical vapor deposition involves facilitating a precursor gas to flow into a chamber containing one or more heated objects to be coated. Thereby, chemical reaction occurs on and near the hot surfaces. This enables the deposition of a thin film on the surface. The chemical vapor deposition process has the advantage of depositing metallic or dielectric coatings of low and high temperature melting materials with high deposition rates. Also it is very easy to control the thickness of the film in the range of sub-micron scale. Further, since only the element that needs to be coated is heated, the transport efficiency of the CVD process is very high. CVD requires fairly sophisticated setup but is inexpensive compared to magnetron sputtering. However, since high temperature reactions are involved, safety related aspects of the process need to be taken seriously during frequent operation.

1.2.4 Electroplating

During electroplating process, the metal ions prevalent in a solution are moved towards an electrode using an electric field. Thereby the metal ions deposit on the electrode to achieve the desired metal film. Hence, the process uses electrical current to reduce cations of a desired

material from a solution and coat a conductive object with a thin layer of the material, such as a metal. Electroplating is therefore only relevant to deposit films on conducting surfaces such as metals etc.

1.2.5 Electroless plating

Electroless plating involves metal deposition without any electrical current being applied. The electroless Pd deposition process involves the autocatalytic reduction of the Pd metal precursors present in the plating solution on an activated membrane support surface. The reduction is facilitated using a reducing agent such as hydrazine or hypophosphite. Electroless plating is a promising technique due to several advantages. These include the metal plating ability on both conducting and non-conducting surfaces, uniformity of deposits on complex geometry, hardness of the deposits, low preparation cost and simplicity of the equipment [19 – 22]. Further, an interesting feature of the electroless plating is that it enables the metal deposition at significantly lower temperatures (40 – 80 ^{o}C), thus indicating low energy requirements. Hence, electroless plating is possibly the simplest means to achieve Pd composite membranes. Further, electroless plating offers the widest choices of parametric optimization in terms of support quality, surface activation methods, electroless plating procedures and bath chemistry which are very easy to implement and achieve. The important parameters during electroless fabrication of Pd composite membranes are to achieve promising combinations of membrane permeability, selectivity, film thickness and stability. An additional promising feature of electroless plating is its susceptibility for scale up which is very cumbersome for other techniques such as sputtering and CVD.

Conventional Pd electroless plating constitutes two steps namely:

a) Seeding a porous support surface with Pd metal particles (seeds) using a sequence of sensitization and activation processes.

b) Plating of the Pd layer on top of the activated porous support.

1.2.5.1 Sensitization and Activation

The seeding process involves sequential steps of sensitization, activation and rinsing using baths of various compositions. The process of sensitization is accomplished by placing the substrate surface into acidic tin ($SnCl_2$) solution to first adsorb Sn^{+2} ions on the porous support. Following this step, activation process facilitates the deposition of Pd metal nuclei on the membrane support as presented in the following reaction.

$$Sn^{+2} + Pd^{+2} \rightarrow Sn^{+4} + Pd^{o}$$

Intermittent rinsing with dilute HCl baths is anticipated to promote better Pd metal nucleation on the porous support. Thus, the process of seeding the porous support involves the sequence of sensitization-rinsing-activation-rinsing to complete a cycle. About 8 – 10 cycles are usually carried out to achieve a support with uniform Pd seeds. The uniformity of the seeding is one of the most important mandatory requirements to enable uniform Pd plating, as the electroless plating reaction is an autocatalytic reaction with Pd seeds available on the support surface acting as the catalyst to drive the surface conversion of noble metal ions to Pd metal particles.

1.2.5.2 Metal deposition

The electroless plating solution consists of noble metal ions and stabilizing agent in an ammonia rich solution. To initiate plating, the reducing agent (such as hydrazine) is added to the plating solution after achieved the plating temperature. The reaction is initiated by the oxidation of reducing agent to release electrons, which reduce the metal ions on the support surface. The reduction of the metal ions on the support surface is facilitated by the Pd nuclei that was

uniformly distributed in the sensitization and activation step prior to the ELP. Further, since electroless plating process is an auto-catalytic reaction, the reactions occurs only at specific sites where Pd metal is present. Also, care needs to be taken during the ELP process to facilitate the plating reaction on the porous support but not solution. Thus, plating reaction needs significant care and attention, given the fact that faster plating on porous supports may generate metal nuclei in solution due to attrition. This is not desired feature and shall be eliminated to the best possible extent during the ELP.

In summary, among various fabrication techniques, electroless plating is the most promising technique to achieve dense Pd composite membranes. This is due to its simplicity and process scalability perspectives in achieving the desired fabrication. Considering these desired features, the next section elaborates upon the state-of-the-art for electroless fabrication of dense Pd composite membranes. Since the thesis orients towards research emphasis on the engineering aspects of the ELP, literature survey would be confined to these issues.

1.3 State-of-the-art in electroless fabrication of dense Pd composite membranes

The state-of-the-art in electroless fabrication of dense Pd composite membranes is presented for two cases namely (a) conventional and (b) rate enhanced ELP. In the following sub-sections, the relevant state-of-the art is briefly outlined.

1.3.1 Conventional electroless plating

Cheng et al. [23] studied the effects of plating chemistry on palladium deposition, plating efficiency and membrane microstructure for hydrazine and hypophosphite Pd ELP baths. The

bath solution Pd precursor composition was varied in the 5 – 20 x 10^{-3} M and 2.5 – 15 x 10^{-3} respectively for hydrazine and hypophosphite baths. For a Pd solution concentration of 10 mM, the reducing agent solution concentration was varied in the range of 1.5 - 9.9 x 10^{-3} M and 1.5 – 136 x 10^{-3} M for hydrazine and hypophosphite precursors. All experimental investigations were conducted for Pd seeded vycor glass (5 nm) and porous stainless steel (PSS) (nominal pore size of 0.2 μm). For the chosen variation in Pd solution concentration, the plating efficiencies varied from 80-38% and 58 – 43% for hypophosphite and hydrazine plating baths respectively. On the other hand, for a variation in reducing agent concentration, the plating efficiency varied from 1 – 45% and 1 – 55% respectively. In other words, both processes can be evaluated to provide lower efficiencies (< 50%). The authors have also confirmed that the phase wise addition of hydrazine (twice, once at 0 and second time at 50% of the total plating time in one plating step) enhanced the efficiency from 65 – 78%. Further, the authors also provided a model to predict accurately the plating rate and film thickness as a function of plating parameters. In summary, it has been concluded that the plating chemistry played a vital role on both plating performance and film microstructure.

Yeung et al. [24] prepared palladium membranes on porous Vycor glass tube (5 nm nominal pore size) using electroless plating technique. The authors used 5 – 40 mM $PdCl_2$ and 2 – 15 mM hydrazine solution concentrations. Eventually, the authors developed mathematical models for hydrazine based plating baths to predict film thickness and plating rate as a function of plating parameters such as reactant concentrations, temperature and time. From film surface micro structure analysis, the authors found that the grain structure was dependent on both plating chemistry and plating rate. Also, from hydrogen permeation study it was evaluated that film

structure has significant influence on the high temperature performance of palladium composite membrane.

Kitiwan and Atong [20] studied the influence of α-alumina support porosity and plating time on electroless plating of Pd composite membranes fabrication. The α-alumina supports with variant porosities (56, 51, 45 and 38%) were achieved by varying sintering temperatures (1200, 1300, 1400 and 1500 ^{o}C). Simultaneously, the average pore size of the membrane got varied in the range of 0.25 – 0.30 μm. Using 0.01 M Pd solution concentration, the authors conducted Pd ELP and found that the deposition of palladium film was very rapid during first 30 min of plating and after which the dense layer was gradually formed. The morphology of palladium film was analyzed as a function of plating time and a dense layer of the membrane was available after plating for 3 h of sequential Pd ELP. In summary, the authors concluded that the porosity of ceramic support had a profound effect on the microstructure of deposited Pd film and supports with low porosity provided a defect free palladium membrane.

Shi et al. [25] fabricated Pd composite membrane using PSS support (200 nm nominal pore size) and Pd solution concentration of 0.011 M. The authors focused upon the morphological variations in due course of plating (030 – 300 s and 60 min) to achieve the dense Pd composite membrane. It was analysed that during the initial stage of plating, the palladium metal was deposited around the pore area on the stainless steel substrate. However, as time progresses, the palladium deposits on the wall of the pores and makes a strong palladium peer to attract and deposit nano-sized Pd particles. With the extension of the deposition time, a network structure around pore was built. With the establishment of a network structure, the Pd was easily deposited on the network structure and forms a thin membrane that fully covers the pore area. To summarize the plating process, a bridge model was presented to describe upon the membrane

formation around the pore area of the substrate. The model, together with the micrographs confirmed upon the deposition progress on the pore areas. The proposed bridge model was anticipated to provide greater insights into the deposition process to engineer the effective fabrication of the Pd composite membrane with alterations to the support morphology and plating parameters. Experimental investigations with the dense Pd composite membrane provided a hydrogen selectivity of infinity for a trans-membrane pressure differential of $3.5x10^5$ Pa (H_2 gas) in the temperature range of 300 – 550 ^oC.

Using electroless plating method, Umeiya et al. [26] prepared a palladium-silver alloy membrane on the outer surface of porous alumina cylinder with a nominal pore size of 0.2 μm. The authors reported that the hydrogen permeability and selectivity of a composite membrane consisting of miscible palladium-silver alloy film has significantly higher hydrogen flux than commercially obtainable palladium based membranes due to both reduction in film thickness as well as enhancement in hydrogen solubility. The palladium-silver alloy membrane containing 23-26 wt% of silver exhibited 100% selectivity for hydrogen separation even at comparatively low temperatures of 473 K. The hydrogen permeability increased with silver content and reached maximum at 23 wt%.

Keuler et al. [27] prepared palladium and silver coated membranes on γ-Al_2O_3, ZrO_2, Y_2O_3 supports using electroless plating. Palladium-silver alloy membranes were synthesized by successive palladium and silver depositions using Pd and Ag solution concentrations of 0.09 M and 0.004 M respectively. The deposition of Pd and Ag were conducted at 72 and 65 ^oC for 3 and 2 h respectively using 20 ml plating solution. The authors investigated the effect of palladium and silver deposition sequence on coating adhesion and metal distribution in the alloy matrix after heating the membrane for 5 h in hydrogen atmosphere at 650 ^oC. By depositing first silver

and then palladium, the palladium to silver ratio across the thickness of the metal film remained constant after heat treatment and it resulted in only a small amount of the alloy penetrating into the support membrane pores. However, when palladium was deposited first, then alloy penetrated at least 3 μm into the support and the palladium and silver concentration profiles across the thickness of the film were asymmetric. Also, the authors noticed that the palladium deposit was about 99.75% pure with the main impurities being tin (deposited during the pre-treatment step), 700 ppm silver, 100 ppm mercury and 100 ppm lead. The silver film was about 99.5% pure with tin (0.49%) and iron (250 ppm) as the main impurities. It was found that the palladium deposit was column like and indicated the formation of a continuous dense layer covering the entire substrate surface. The silver deposit was non-homogeneous and clusters were deposited randomly over the palladium film or on the activated surface.

Umeiya et al. [28] conducted experiments on characterization of hydrogen separation by a composite membrane consisting of a thin palladium film supported on the outer surface of a porous glass cylinder of an average pore size of 300 nm. The Pd composite membrane was prepared using electroless plating method whose process parameter choice were not mentioned. The composite membrane was highly permeable to hydrogen, having an extremely high selectivity for hydrogen. The addition of copper or silver to the palladium film improved the selectivity for hydrogen separation, making it suitable to be utilized below 573 K, at the same time. The rate of hydrogen permeation however was reduced by the addition of these elements causing the film to become inhomogeneous.

Roa et al. [29] prepared Pd-Cu composite membranes on tubular porous ceramic supports by successive electroless deposition of Pd and Cu. The authors used symmetric α-alumina (200 nm nominal pore size), asymmetric zirconia on α-alumina (50 nm nominal pore size), and

asymmetric γ-alumina on α-alumina (5 nm nominal pore size) as supports. To induce intermetallic diffusion and obtain homogeneous metal films, the obtained metal/ceramic composite membranes were heat treated between 350 – 700 ^{o}C for 6 to 25 days. The layers of Pd and Cu films were sequentially deposited on these substrates by using 0.03 and 0.04 M Pd and Cu solution concentrations at a temperature of 65 – 70 ^{o}C followed by annealing at high temperature in the presence of flowing hydrogen. The hydrogen permeation experiments were conducted on the composite membrane with 11 μm thick, 10 wt% Cu film on a nominal 50 nm pore size asymmetric ultra filter with zirconia top layer at 450 ^{o}C and at H_2 feed pressure of 345 kPa. The obtained hydrogen flux and selectivity (H_2/N_2) were 0.8 mol/m^2.s and 1150 respectively. It was also reported that the support with 200 nm pores required more Pd to plug the pores than the asymmetric membranes with smaller pore size. On the other hand, the authors could not deposit leak-free films on supports with smaller pore size (5 nm γ-alumina) due to surface defects and lack of adhesion between the metal film and the membrane surface. Thus, it was confirmed that lower average pore size of the membrane support provides smoother surfaces which could not provide good adhesion of the dense Pd film with the membrane surface.

Collins and Way [30] fabricated palladium-ceramic composite membranes by depositing 11.4 - 20 μm thick Pd films on the inner surface of asymmetric tubular ceramic substrates using electroless plating method. The ELP experiments were conducted using Pd solution concentration of 0.03 M with occasional shaking of the plating bath to drive out the bubbles produced during plating. During ELP, the authors changed the plating solution after every 1 h and continued ELP for prolonged time periods to achieve the desired Pd film thickness. For the fabricated Pd membranes, permeation experiments were conducted using hydrogen, nitrogen and helium gases at 723 – 913 K and 160 – 2445 kPa. Based on these experimental investigations,

the authors reported that membrane with 11.4 μm Pd film thickness provided the hydrogen permeability and selectivity of $3.23x10^{-9}$ $mol.m/m^2.s.Pa^{0.602}$ and 380 respectively at a temperature and transmembrane pressure difference of 823 K and 1500 kPa respectively.

1.3.2 Rate enhanced electroless plating

The conventional electroless plating process is an extremely slower deposition process. Typical plating rates using the CEP are about 1 – 1.5 μm. Therefore, to achieve a typical 15 – 20 μm thick dense Pd films, about 15 – 20 h of total plating time is required. To circumvent this problem, rate enhanced Pd ELP processes have been investigated. Among these, some processes are also used to repair the pinholes that exist in near dense Pd composite membranes.

1.3.2.1 Osmosis

Li et al. [31] fabricated dense palladium composite membrane on the outer surface of a porous α-alumina support (average pore size of 0.16 μm) by CEP using Pd solution concentration of 0.016M. After 8 h of plating, the authors reported that the dense Pd film thickness is 7.6 μm. The membrane exhibited poor selectivity during H_2 and N_2 permeation experiments. Thereby, the authors conducted Pd film repairing using electroless plating process coupled with osmosis. Using osmosis assisted ELP, the dense Pd/PSS composite membrane at 467 ^oC and pressure differential of 1.03 bar with an initial H_2/N_2 permeation ratio of 10 could be repaired to achieve a separation factor of 1000 without causing a large reduction of its hydrogen permeation flux and without significant increase in the dense Pd film thickness.

Souleimanova et al. [32] studied the fabrication of Pd composite membranes on porous vycor glass support (average pore size and porosity of 4 nm and 0.28 respectively) using

electroless plating coupled with osmosis technique. The authors investigated the influence of osmosis on metal grain size and penetration into the porous vycor glass substrate. They analyzed the microstructure of the Pd membrane by both scanning electron (SEM) and atomic force (AFM) microscopy and reported that microstructure of the deposited Pd film was more finer and regular when the membrane was seeded with osmosis. From energy dispersive X-ray analysis (EDX), it was confirmed that the osmosis improved the adhesion between the substrate and deposited film which subsequently enhanced the mechanical properties of the composite membranes.

Li et al. [33] prepared a dense Pd/PSS composite membrane on the outer surface of porous stainless steel tube of average pore size 0.1-0.2 μm using osmosis coupled ELP process. The conventional ELP experiments were conducted using Pd solution concentration of 0.016 M for 30 h. Eventually, the membranes were repaired for 10 h using 3 M NaCl solution to repair and densify the Pd deposited film. Using weight gain method, the membrane film thickness was evaluated to be 10 μm. The hydrogen permeation flux of the composite membrane was as high as 12 cm^3/cm^2 min at 480 ^oC and differential pressure of 1 bar. The highest H_2/N_2 separation factor was achieved about 1000 at higher permeation temperatures.

Li et al. [34] fabricated a defect-free Pd composite membrane on an α-Al_2O_3 support (average pore size of 0.16 μm) using 0.016 M Pd solution concentration. To repair the defects present on the composite membrane with a palladium film thickness (10.3 μm), the authors coupled electroless plating technique with osmosis. To do so, 3 M NaCl solution was circulated through the tube side of the membrane at 60 ^oC while doing ELP for an additional plating time of 6 h. It was analyzed that the osmotic pressure of salt solution created necessary condition to force the material towards the inside of the support tube and this contributed enormously towards the

densification of the Pd film. In the temperature range of 320 – 577 ^{o}C, the apparent activation energy for H_2 transport was 12.3 kJ/mol. It was also analyzed that both sweep gas and a higher total feed flow rate improved the hydrogen permeation through the membrane.

1.3.2.2 Vacuum electroless plating

Zhang et al. [35] prepared thin dense Pd composite membrane on α-Al_2O_3 support (average pore size of 0.3 μm) using vacuum assisted ELP process with a Pd solution concentration of 0.025 M. It was evaluated that the application of vacuum on the both ends of the tubular substrate enabled the achievement of thin dense Pd composite membranes with finer and more uniform microstructure. Thereby, significant enhancement in high temperature hydrogen permeance and thermal stability of the membranes was obtained in comparison to those fabricated with the CEP process. For the fabricated membrane, H_2 permeance of 22.4 m^3/m^2.h.bar and H_2/N_2 selectivity of 3000 was obtained at 500 ^{o}C. Further, the membranes were analyzed to be stable over a period of 470 h and for 10 temperature cycles under H_2 or Ar atmosphere. Also, the membranes were analyzed to exhibit good thermal stability over a period of 2000 h and could resist temperature fluctuations.

1.3.2.3 Surfactant coupled ELP

Ke et al. [36] fabricated thin dense palladium membrane on α-alumina supports (average pore diameter of 320 nm) by dispersing an anionic surfactant (SDS) in conventional electroless plating baths. The surfactant assisted ELP experiments were conducted for 8-12 h total plating time with a Pd solution concentration of 0.19 M at a loading ratio of 262 cm^2/L. During the process, the plating solution was changed after every 4 h with intermittent shaking of the beaker

to drive out the bubbles adsorbed on the surface. The hydrogen permeance of the Pd composite membrane was as high as 2.45×10^{-6} mol/m^2.s.Pa. Further, H_2/N_2 selectivity of about 700 at 623 K was evaluated at a transmembrane pressure difference of 0.1 MPa. Also, the membrane exhibited good thermal stability at 623 K for over 200 h. It was also analyzed that in comparison with the thin Pd film, the ceramic support provided major H_2 permeation resistance for the composite membrane.

Islam et al. [37] fabricated Pd-Cu composite membranes on microporous stainless steel support (200 nm average pore size) using surfactant induced electroless plating baths (SIEP). The authors conducted plating experiments using Pd solution concentration of 0.015M. The DTAB cationic surfactant at a solution concentration of 4CMC was dispersed in Pd and Cu electroless plating baths. The performance of SIEP baths were compared with the CEP for dense Pd composite membrane fabrication. It was evaluated that the SIEP process enabled a significant improvement in the membrane morphology in terms of metal grain structure and grain agglomeration in comparison with the CEP baths. Finally, the authors reported that the membrane fabricated in SIEP baths provided higher perm-selectivity as compared to CEP membranes.

Ilias et al. [US 2010/0068391 A1] [38] fabricated Pd/PSS composite membranes using surfactant dispersed conventional electroless plating baths. Various type of surfactants were studied by the authors which include cationic (dodecyl trimethylammonium bromide), anionic (sodium Dodecyl benzene sulfonate) and non-ionic (Triton X-100) surfactants in the concentration range of 0.5 – 4 CMC. It was analyzed that the metal plating rates were significantly enhanced using SIEP process. The surface morphology of the membranes fabricated at 4 CMC surfactant concentration was analysed by SEM analysis and it was evaluated that the

membrane fabricated with DTAB surfactant provided narrow size grain distribution in the range of 1-3 μm.

To study the effect of surfactant on the electroless nickel-phosphorus deposits over the brass substrate, Chen et al. [39] dispersed surfactants in acidic hypophosphite plating baths. The authors reported that the addition of surfactant enabled a reduction in the interfacial tension between gas bubbles and plating solution, due to which the gas bubbles size reduced along with their faster removal. Due to this effect, the pore densification characteristics of the membrane were significantly altered. It was analyzed that there was minimal pitting effect for the Ni-P deposits. Further, the authors analyzed that the addition of excessive amount of surfactant could cause grain agglomeration over the substrate surface. This promotes uneven charge distribution over the substrate surface and thereby non-uniform metal deposition on the substrate. In other words, higher surfactant solution concentration and prolonged periods of plating are detrimental towards achieving dense Pd composite membranes.

1.3.2.4 Sonication coupled ELP

Chiba et al. [40] studied the effect of sonication and vibration on the electroless Ni-B deposited film from acid baths containing 4.8g/dm^3 of $NiCl_2.6H_2O$, 4.4 g/dm^3 of sodium acetate and 0.01 g/dm^3 of sodium lauryl sulphate at a pH of 4 and temperature of 341 K. The authors found that plating rate was in the order of sonication (45 kHz)> mechanical agitation (250rpm) > vibration (1.6MHz) > vibration (1.6MHz)> stationary state. The deposited film formed with sonication assisted ELP reduced the corrosion resistance in 3% NaCl solution. However, cracks on surface were significant for these membranes.

1.3.2.5 Agitated ELP baths

Using agitated Pd ELP baths, Ayturk and Ma [41] studied the electroless Pd and Ag deposition kinetics for composite Pd and Pd/Ag membrane fabrication. The authors deposited Pd and Ag films on porous inconel tubes (average pore size of 0.1 μm) using 0.0078 – 0.015 and 0.003 – 0.012 M Pd and Ag solution concentrations respectively. It was analyzed that the both Pd and Ag electroless plating were strongly affected by the external mass transfer limitation and hence agitation substantially improved the plating characteristics. The external mass transfer limitations for both Pd and Ag deposition were minimized at or above an agitation rate of 400 rpm, where a maximum conversion of the plating reaction along with uniform film deposition was achieved. Bath agitation indicated about 60% improvement of the plating bath efficiency in comparison to that of the Pd and Ag runs conducted under the static conditions. Eventually, the authors fabricated 16 – 20 μm thick composite Pd/Ag membranes (10 – 12 wt% Ag) and only Pd membrane with hydrogen selective dense Pd layer of 4.7 μm thickness. The H_2 permeance for the 4.7 μm thick Pd membrane at 400 ^{o}C was as high as 63 m^3/m^2-h-$atm^{0.5}$. The long-term permeance testing for all membranes fabricated using agitated plating baths indicated a relatively slow leak growth. This is due to the improvement in the membrane morphology with improved plating conditions.

1.3.2.6 Other approaches

Zeng et al. [42] reduced defects in Pd and Pd-Ag membranes by directed electroless plating. The process involved feeding the metal source and the reducing agent from opposite directions to the defect zone. It was analyzed that the surface texture of the metal layers was well preserved in the vicinity of cracks and pinholes, thereby confirming that the Pd deposition was

effectively restricted to defect sites. The ideal H_2/N_2 selectivity was improved by more than an order of magnitude by adopting the directed ELP process. Also, very high H_2 permeability of the membrane was achieved. This confirmed that the overall metal layer thickness had not increased with the directed ELP process.

Table 1.2 summarizes some of the relevant combinatorial plating characteristics reported in the literature for dense Pd composite membrane fabrication using rate enhancement techniques.

1.3.3 Fabrication of Pd membranes with interdiffusion barriers

1.3.3.1 Chromia interdiffusion barrier

Samingprai et al. [43] fabricated dense Pd/oxidized PSS and Pd/Cr_2O_3/oxidized PSS membranes on oxidized porous stainless steel tubes (average pore size 0.1 μm and porosity 17%) using electroless plating with a Pd solution concentration of 0.015M. The fabricated Pd/oxPSS membrane was subjected to hydrogen permeance studies and was found to provide a reduction in H_2 flux at temperatures higher than 400 ^oC. From SEM-EDX analysis, it was confirmed that intermetallic diffusion occurred at 500 ^oC and this was responsible for the reduction in hydrogen flux. To inhibit the intermetallic diffusion at high temperatures, the authors deposited chromium oxide layers of different thicknesses on oxidized PSS disks by conventional chromium electroplating process followed with oxidation in air at 700 ^oC. The dense palladium membrane was obtained after depositing 32 μm thick Pd film on 2 μm thick chromia film. For the Pd/chromia/PSS membranes, the membrane hydrogen permeance was evaluated to vary from 0.84 to 1.51 $m^3/m^2.h.atm^{0.5}$ for a variation in temperature from 350 to 500 ^oC. It was also analyzed by the authors that the chromia diffusion barrier did not reduce the minimal Pd thickness required to achieve a dense Pd composite membrane.

Table 1.2: Combinatorial plating characteristics reported in the literature for dense Pd composite membranes fabricated with rate enhanced Pd ELP baths.

S. No	Type of support	Initial Pd solution concentration (g/l)	Total time of plating	Selective conversion	Plating Temperature	Rate enhancement technique	Support avg. pore size (nm)	Thickness of dense Pd film (µm)	Selectivity	H_2 permeation flux	References
1	PSS	4 Pd $(NH_3)_4$ Cl_2	30 h	-	60 °C and pH 11.2	Osmosis	100 - 200	10	1000 for H_2/N_2 above 400 °c	12 cm^3/cm^2.sec at above 480 °c and Δp of 1 bar	Li et al.[33]
2	PSS	2 Pd Cl_2	-	-	60 °C	-	200	1.5 - 2	Infinity	-	Shi et al. [25]
3	Porous α-Alumina	4.4 Pd $(NH_3)_4$ Cl_2	8 h 11 h 14 h	-	60 °C and pH 11.2	osmosis	160	7.6 (initial) 9.2 (after 1st repair) 10.3 (final)	10.27 (initial) 970 (2nd repair) for H_2/N_2	1.4956 cm^3/cm^2.sec ((initial)) 0.6686 cm^3/cm^2.sec 2nd repair)	Li et al. [34]
4	α- Al_2O_3	4.43 Pd Cl_2		-	40 °C	Vacuum	300	5 to 6	3000 (H_2/Ar)	22.4 m^3/m^2.h at 500 °c and of ΔP of 1 bar	Zhang et al. [35]
5	PSS	4 Pd $(NH_3)_4$ Cl_2 H_2O	10	-	60 °C	Surfactant	200	7.68	250 (H_2/N_2)	0.28 mol/m^2.s at 723 K and Δp of 20 psi	Islam et al. [37]
6	α-Al_2O_3	33.6 mg/ml	8-12 h	-	35 °C	-	320	2 for 8 h 3 for 12 h	35 (H_2/N_2) 700 (H_2/N_2)	For 3 µm 19.75 m^3/m^2.h	Ke et al.[36]
7	Pd/Al(OH)$_3$/Inconel	2.0-4.0	15 min	94%	60 °C	Agitation	100	4.7	310 (H_2/He)	63 m^3/m^2-h-atm $^{0.5}$ at 400 °C	Ayturk et al.[41]
8	Pd/PSS	4.343 g/L $PdCl_2$	-	-	40 °C and pH 11	Vacuum	300	5 - 6	3000 (H_2/N_2)	22.4 m^3/m^2 h at 500 °C	Zhang et al.[35]

1.3.3.2 Ceria interdiffusion barrier

Tong et al**.** [44] prepared Pd/CeO_2/PSS composite membranes using improved electroless plating techniques. The tubular supports with nominal pore size of 0.2 μm were first modified with cerium hydroxide particles by applying suction from the interior side of the tube for 1 h and suction coupled with sonication (using an ultrasonic bath) for 2 h. The Pd film deposition was carried out using CEP for first 1 h plating at a pH of 7 and temperature of 303 – 318 K to preserve the cerium oxide particles in the porous structure. Following this step, further ELP was carried out at a regular pH of 5 and temperature of 323 – 343 K. Thereby, the dense Pd composite membranes with a film thickness of 6 and 10 μm were obtained. For the membrane with 6 μm thickness of the Pd film, the hydrogen permeation flux and H_2/Ar separation factor were 0.235 mol/m^2.s and 14 at 773 K and 100 kPa. The membrane with thickness of 10 μm Pd film had a reduced hydrogen flux of 0.178 mol/m^2.s with an increased selectivity of 108. Further, additional CVD based Pd film deposition was carried out by the authors to remove defects present in the 6 μm Pd film membrane. After the CVD treatment for three times, the membrane hydrogen flux did not reduce but the separation factor increased significantly to565.

1.3.3.3 Titania interdiffusion barrier

Zhang et al. [45] prepared dense Pd/TiO_2/Ti-Al alloy composite membranes on porous Ti-Al supports (thickness 2.5 nm and an average pore size of 6 μm) by electroplating of Ti followed with electroless plating of Pd (0.022 M Pd solution concentration). The authors observed that the intermediate TiO_2 layer was effective as diffusion barrier for Pd membranes on Ti-Al alloy supports after 40 h of treatment with hydrogen at 973 K. The obtained thickness of

Pd film was about 14 μm and hydrogen permeance through Pd composite membrane was $1.07x10^{-3}$ mol/m^2 s $Pa^{0.5}$ at 773 k and a differential pressure of 0.3 MPa. The membrane was analysed to provide very good combinations of thermal stability and hydrogen selectivity in the temperature range of 623 – 773 K.

1.3.3.4 Ceramic interdiffusion barrier

Li et al. [46] prepared thin and pinhole-free Pd based membrane on a porous stainless steel substrate of 0.2 μm average pore size using 0.02 M Pd solution concentration. They observed that the Pd film did not become pinhole-free until its thickness reached 35 μm. The prepared membrane was analysed to provide a reduced hydrogen flux after 22 h at 923 K which was about 10% of the initial flux. Subsequently, the authors pre-treated the substrate surface by polishing and etching followed by successive coating with aluminium oxide sols of different particle sizes. The resultant membrane with ceramic interdiffusion barrier was evaluated to be pinhole-free with a Pd film thickness of 5μm. The obtained hydrogen permeation flux of Pd/ceramic/PSS membrane was about 95 m^3/m^2 h at 823 K and 3.4 bar and was stable during long term hydrogen permeability studies.

1.3.3.5 Yttria stabilized zirconia diffusion barrier

Huang and Dittmeyer [47] prepared thin defect-free palladium membranes on porous stainless steel tubes (average pore size of 500 nm) with three different interdiffusion barriers. The authors used Zirconium dioxide (ZrO_2), Yttria-stabilized zirconia (YSZ) and Titanium dioxide (TiO_2) as porous barriers between palladium membrane and sinter metal support. The interdiffusion barrier was fabricated by coating the porous SS supports with YSZ using

atmospheric plasma spraying technique to yield an interdiffusion barrier thickness of 10 – 70 μm). Other than this membrane, two other membranes were prepared with zirconia and titania interdiffusion barriers. For the second membrane support, 2 μm zirconia oxide layer was deposited using magnetron sputtering technique. The third membrane support was achieved by depositing 40 – 60 μm titania layer using wet spraying method. The three membrane supports were analyzed to possess variant combinations of interdiffusion barrier thickness, pore size, surface roughness and porosity. Eventually the Pd composite membranes were fabricated on these supports using 0.03 M Pd solution concentration at room temperature. The plating was allowed to achieve desired thickness of palladium with a plating time of 1.5 h for each plating step. The Pd composite membranes on APS – YSZ, WPS – TiO_2 and MS – ZrO_2 with 15 – 20, 18 – 20 and 7 μm thick Pd films respectively were annealed at 600 ^oC in hydrogen environment for 23 days. Among all interdiffusion barriers, the authors identified that YSZ is the most promising barrier with minimal intermetallic diffusion of the Pd metal to the support layer.

1.3.3.6 Tungsten diffusion barrier

Grayaznov et al. [48] utilized the high melting point of tungsten (3410 ^oC) in an attempt to eliminate the thermal expansion mismatch between Pd and the stainless steel support. The authors deposited 0.8 μm thick tungsten film by sputtering technique at argon pressure from 0.1-1 Pa followed with Pd deposition using sputtering technique. Eventually, the authors found that a tungsten intermediate layer was successful to prevent the intermetallic diffusion at elevated temperatures (800 ^oC). However, the thin tungsten layer did not significantly reduce the pore size distributions of the substrate. Thereby, relatively thick Pd film thickness (>10 μm) was required to produce a pinhole-free layer. It is anticipated that a further enhancement in the tungsten layer

would reduce the surface pore size distributions of the support and would thereby enable the requirement of thin Pd film to achieve dense Pd composite membranes. Such an approach might be effective to reduce the larger pore size of the support but could adversely fill the smaller pores of the support structure. This inturn reduced the hydrogen permeability.

1.3.3.7 α-Fe_2O_3 and γ-Al_2O_3 diffusion barriers

Yepes et al. [49] fabricated Pd-Ag composite membranes on a modified porous stainless steel substrate of 0.2 μm by sequential electroless plating of Pd and Ag with the solution concentrations of 0.02 and 0.03 M respectively. To improve the stability of Pd-Ag alloy, the authors introduced α-Fe_2O_3 and γ-Al_2O_3 as diffusion barriers. The γ-Al_2O_3 and α-Fe_2O_3 were deposited by wash coating of the support with γ-Al_2O_3 suspension and oxidation of PSS support respectively. The Pd and silver film deposition was targeted using sequential deposition approach to achieve 16-20 μm thick Pd-Ag alloy films. Among both membranes, it was analysed that the membrane with α-Fe_2O_3 barrier exhibited higher selectivities than γ-Al_2O_3 barrier but the H_2 permeability was 2 times lower than those obtained with γ-Al_2O_3 interdiffusion barrier. From Auger depth profiles the authors also confirmed that the γ-Al_2O_3 layer effectively blocked the intermetallic diffusion.

1.3.3.8 Zirconia oxide diffusion barrier

Wang et al. [50] fabricated palladium membrane on zirconia modified porous stainless steel tube using Pd ELP process. The tubular porous stainless steel substrate (average pore size of 200 nm) was modified by depositing zirconia oxide particles on the surface using coupled sonication and vacuum application. Eventually, the authors deposited 10 μm thick Pd dense film

using electroless plating. The authors analyzed that the introduced zirconia oxide particles offered additional permeation resistance to reduce hydrogen flux in comparison to the Pd-PSS membranes.

1.3.3.9 Pencil coating diffusion barrier

Hu et al. [51] fabricated highly permeable and hydrogen selective Pd/pencil/Al_2O_3 composite membrane on low cost macro porous Al_2O_3 substrate (average pore size 3.3 μm) using electroless plating technique. The authors modified alumina support surface by 2B pencil and the average pore size of alumina substrate was reduced to 1.2 μm. The Pd film with a thickness of 5 μm was achieved on the modified support using 0.03 M Pd solution concentration. The N_2 flux through the Pd/pencil/Al_2O_3 membrane was evaluated to be about 0.01 $m^3/(m^2$ h bar) which indicated that the membrane is almost pinhole free. The obtained hydrogen permeability and selectivity of Pd/pencil/Al_2O_3 membrane at 723 K and 1 bar pressure were 25 m^3/m^2 h and 3700 respectively. Also, the membrane was found to be stable during 330 h of continuous operation at 723 K.

1.3.3.10 Oxidized porous stainless steel diffusion barrier

Rothenberger et al. [9] fabricated thin palladium films (22 μm) on the outer surface of oxidized porous stainless steel tubular substrate (200 nm average pore size) using electroless plating technique. The authors evaluated the membrane performance in the temperature range of 623 – 723 K and pressure differentials of 100 – 2800 kPa. The H_2/He selectivity value was as low as 12 for a total transmembrane pressure differential of 2800 kPa. It was also found that the hydrogen flux through the membrane was proportional to the H_2 partial pressure in the retentate

raised to an exponent of ~0.55 for one membrane and ~0.64 for the other. This indicates that bulk diffusion was the rate limiting step for the hydrogen transport through the composite membrane. The high temperature H_2 permeance of the membrane remained invariant at values of ~$1.5x10^{-4}$ and ~$2.9x10^{-4}$ mol/m^2.s.$Pa^{0.5}$ from 623 – 726 K and 2800 kPa which reduced by ~35% upon cooling the membrane to 623 K. This indicated degradation of the membrane under high pressure testing conditions.

1.3.3.11 Nickel diffusion barrier

Researching upon nickel as interdiffusion barrier, Lin et al. [52] addressed nickel electroplating on porous stainless steel substrate (4 μm average pore size) followed with sequential electroless deposition of palladium and silver. On 16.9 and 27.2 μm thick nickel films, 18.4 and 17.8 μm thick Pd films were deposited respectively. The membranes were eventually subjected to hydrogen permeance studies. The permeation experiments at 723 K and 8 atm confirmed that the hydrogen flux was more critically dependent on the Pd film thickness but not nickel film thickness. This indicates that the interdiffusion barrier did not reduce the minimum Pd film thickness required to achieve dense Pd composite membranes and the nickel interdiffusion barriers were not providing additional resistance for H_2 permeation.

Ryi et al. [53] fabricated nickel porous membranes for the separation of hydrogen or as a metal support for Pd or Pd-alloy dense membranes. The authors fabricated Ni porous membranes using Ni powder with two different particle size distributions (average particle size of 0.15 and 5 μm and pore diameter of 33, 115 μm, respectively). Thereby, the authors confirmed that the particle size distribution had a significant influence on the membrane packing degree and H_2 selectivity. The authors conducted single gas permeation experiments using N_2 and H_2 gas above

200 ^{o}C and reported that the hydrogen permeation was contributed by Knudsen and surface diffusion. It was also analysed that the membrane permeance was similar to and the selectivity was lower than that obtained for the dense Pd membrane prepared without interdiffusion barrier. In summary, the authors confirmed that porous nickel membrane can be developed as a new material for porous membrane fabrication and will be very good substrate for Pd and Pd based alloy membranes due to its high mechanical strength.

Table 1.3 summarizes the combinatorial plating characteristics for dense Pd composite membranes fabricated with various interdiffusion barriers.

1.3.4 Summary

Due to their high hydrogen flux and selectivity, Pd-composite membranes have great commercial potential compared with other hydrogen-selective composite membranes. In addition to the reduction in cost, thin Pd films contribute towards enhancement in the hydrogen flux. For micro-porous membranes such as silica composite membranes, the separation factor and flux are governed by Knudsen diffusion mechanism, whereas for palladium membranes, the flux and separation factor are governed by surface activation followed with diffusion of hydrogen atoms through the dense metal matrix. Such mechanism is far superior to the Knudsen diffusional mechanism in terms of hydrogen flux and selectivity. Porous substrates successfully reduce the material costs and provide greater mechanical strength to the film for functionality at desired higher pressure differentials. The materials that are commonly used as porous substrates include ceramics [54, 55], glass [28] and metals such as stainless steel (PSS) [25], inconel [56] and nickel [53]. Each of these has their own advantages and disadvantages. Ceramic membrane supports are inexpensive and can offer pore sizes ranging from 5-500 nm. Typically α-Al_2O_3 is

Table 1.3: Literature data for the combinatorial plating characteristics of dense Pd composite membranes fabricated with interdiffusion barriers and ELP processes.

S.No	Type of support	Pd solution concentration (g/l)	Total time of plating	Plating Temperature	Support avg. pore size (nm)	Thickness of dense Pd film (µm)	Selectivity	H_2 permeation flux	References
1	Ce_2O_3/MPSS	-	7 h	50-70 °C pH 5-6	200	13 (Pd)	Infinity	2750 cm^3/cm^2s at 550 °c	Tong et al. [44]
2	Cr_2O_3 on PSS	4 $Pd(NH_3)_4$ $Cl_2.H_2O$	4 h 30 min	60 °C	100	2 (cr_2o_3) 32 (Pd)	-	8.95 m^2/m^2.h at 500 °c	Samingprai et al. [43]
3	Pd/Ti/Ti-Al alloy	4.0 $PdCl_2$	-	40 °C	6000	14	Infinity	27.41 m^3/m^2.h at 773 K and ΔP 0.3 MPa	Zhang et al.[45]
4	Pd/Pencil coating / α- Al_2O_3	4.0 $PdCl_2$	-	30 °C	3300	5	3700	25 m^3/m^2 h	Hu et al. [51]

regarded as the commonly and widely used ceramic porous substrate. γ-Al_2O_3 offers a pore size of about 1-5 nm. However, a major disadvantage of ceramic membranes is their brittle nature, which thereby requires careful operations during the assembling and disassembly of membranes in permeation units. Further, ceramic membranes cannot be welded as well and hence, the usage of high temperature graphite seals that do not offer 100% leakage proof towards gases will remain an important problem. Further, while fabricating α-Al_2O_3 membranes is relatively easier, deposition of γ-Al_2O_3 on α-Al_2O_3 is a difficult to achieve task.

Stainless steel supports are very expensive and offer pore sizes within the range of 100 - 1000 nm. These supports have advantages such as non-brittleness, ability to get welded to the permeation setups and hence they are widely studied and investigated for metal (Pd/Ag/Ni) composite membrane research. However a major disadvantage of the SS porous support is the intermetallic diffusion between the palladium layer and the support that contributes to slow and gradual decline of the hydrogen permeability upon temperature cycling. However, inter-metallic diffusion can be prevented if a non-metallic barrier is applied to avoid direct contact of the palladium membrane with the metallic support. Common practices to form an inter diffusion barrier layer refer to coating a thin interdiffusion barrier such as α-Fe_2O_3 [49], γ-Al_2O_3 [49], CeO_2 [44], Cr_2O_3 [43], ZrO_2 [50], YSZ [47], Ni [52], Tungsten [48] and TiO_2 [45, 47] on SS supports. Till date, porous supports such as Ni and Inconel were not widely investigated. This is possibly due to higher cost for inconel when compared to the SS supports and difficulty to obtain porous Ni supports using easier fabrication process.

1.4 Prominent Issues in Literatures

1.4.1 Rate Enhancement Techniques and Process modifications

Till date, rate enhancement techniques addressed for Pd electroless plating processes include osmosis [31-34], stirring [41, 58], vacuum [35], agitation [41, 58] and surfactant [36 – 39]. Amongst all these techniques, surfactant induced electroless plating appears to highly promising when compared to other rate enhancement techniques such as stirring, hydrothermal and vacuum. While the osmosis is scalable, it needs careful design of experimental process so that the salt solution does not leach and disturb the electroless plating bath stability. Stirred baths could enhance plating rate. However, metal delamination is significantly high during electroless plating which further deteriorates the quality of plating in terms of the plating efficiency. Hydrothermal coupling to the electroless plating process could not be automated for sufficiently high number of plating steps for prolonged plating time (about 8 to 10 h) in a scalable process. Vacuum coupled electroless plating is not cost effective for membranes with huge surface area. In addition, the application of vacuum assisted electroless plating for ceramic supports require sophisticated setup with high quality shock resistant seals that restrict the cracking of the brittle ceramic structures during loading, unloading and vacuum application for prolonged plating time periods. In summary, only surfactant and sonication can be regarded to be scalable rate enhancement techniques that can be coupled to ELP baths for dense Pd composite membrane fabrication.

A critical observation of the literatures indicates that several studies targeted the dense Pd composite membrane fabrication without addressing upon the combinatorial plating characteristics such as selective conversion, efficiency, average plating rate, metal film growth rate and pore densification. Also, while few studies have been carried out independently, a

comparative assessment of scalable and promising rate enhancement techniques was not addressed till date. In summary, combinatorial plating characteristics were not targeted and only membrane characteristics were targeted.

To further improve the efficacy of Pd electroless plating techniques, process modifications can be suggested which could refer to semi-batch mode of contacting between the reducing agent and the metal ion precursors in the plating solution. Till date, no such studies were targeted, even though phase wise addition was addressed by Yeung et al. [24], whose results were encouraging towards furthering the optimality of the contacting pattern.

1.4.2 Parametric Optimality

Few literatures that address dense Pd composite membrane fabrication using SIEP Pd plating baths did not elaborate upon the role of surfactant and Pd solution concentration on combinatorial plating characteristics. For instance, Islam et al. [37] fabricated dense Pd/PSS composite membrane using SIEP process with palladium and surfactant (DTAB) solution concentrations of 0.015 M and 4 CMC respectively. However, to achieve dense membrane the authors used a high Pd concentration. Also, the authors did not elaborate upon the role of surfactant concentration and the combinatorial performance characteristics of electroless plating baths during the fabrication of Pd/PSS membranes. In the field of dense Pd composite membranes using electroless plating process, it is well known that high concentrations of reactants (Pd precursors and reducing agent) could provide higher plating rates but achieve poor quality of films deposited on the substrate surface with poor densification and low adhesion strength. This results in the delamination of metal particles from the substrate surface while carrying out the plating process. The undesirable delamination of metal particles during plating enables metal reduction in the solution and hence lower plating efficiencies.

There is a possibility to get dense membranes with lower Pd solution concentration along with various concentrations of surfactant and loading ratios. Therefore, in those circumstances, the formulation that provides the optimal combinations of selective conversion, high temperature performance and stability, dense Pd film thickness may be the recommended choice, despite the fact that it may or may not demand higher number of plating steps.

In summary, investigations in the literature report discrete sets of successful fabrication parameters that yielded membranes with good separation characteristics. A systematic exploration of fabrication parameters such as loading ratio, rate enhancement technique parameters, Pd solution concentration, hydrazine solution concentration etc. was not addressed for Pd membranes, given the fact that Pd is very expensive and repeatability issues cannot be ignored in materials research that targets 100% dense Pd composite membranes.

1.4.3 Fabrication of Pd composite membranes with interdiffusion barriers using Electroless Plating technique

In the literature, significant amount of research addressed the fabrication of multi-layered and multi-metallic composite membranes to reduce the critical thickness of Pd layer and thereby enhance their hydrogen permeance. Another advantage of the interdiffusion barrier is that they reduce intermetallic diffusion during temperature cycling effect and contribute towards the enhancement of shelf life of the membranes [43-52]. For dense Pd composite membranes, various types of interdiffusion barriers investigated include yttria stabilized zirconia [47], TiO_2 [45, 47], CeO_2 [44], α-Fe_2O_3 [49], γ-Al_2O_3 [49], W [48], ZrO_2 [50], Cr_2O_3 [43] and Ni [52]. Some of these investigations indicated that despite achieving 100% dense Pd composite membranes, the interdiffusion barrier could not reduce the achieved critical dense Pd film thickness [43, 47]. On the other hand, while interdiffusion barriers reduced the critical dense Pd

film thickness, they did not enhance hydrogen flux due to additional transport resistance contributed by the barrier itself [44, 48, 50]. Amongst several diffusion barriers, Cr_2O_3 can be regarded as the most competent due to higher chemical stability under high pressure hydrogen environment. Also, few researchers suggested nickel composite membranes for hydrogen separation due the high hydrogen adsorption capacities [52 – 53]. Few others have proposed that porous nickel membranes could serve as new generation supports for dense Pd composite membranes [53]. All other interdiffusion barriers summarized above are either expensive or difficult to fabricate in terms of process scale up. While chromium can be easily electroplated to a conducting surface, nickel electroless plating is versatile and there have been numerous articles in this field of research (Bulasara et al. [58 – 59]). Thus, it is apparent that from scale up and cost perspective, nickel and chromia interdiffusion barriers appear to be the most promising and research emphasis shall be towards the engineering of these films using the rate enhanced modified Pd electroless plating technique.

Researching upon nickel as interdiffusion barrier Lin et al. [52] addressed nickel electroplating on porous stainless steel substrate (4 μm average pore size) followed with sequential electroless deposition of palladium and silver. On 16.9 and 27.2 μm thick nickel films, 18.4 and 17.8 μm Pd thick films were deposited which were then subjected to hydrogen permeance studies. The authors observed that the enhancement of hydrogen flux was more critically dependent on the Pd film thickness but not nickel film thickness. Also, the obtained higher Pd film thickness values for dense composite membranes are indicative to confirm that nickel interdiffusion barrier did not reduce the critical dense Pd film thickness significantly. Further, the nickel film was deposited by the authors using electroplating technique, which is not suitable for deposition of metal films on non-conductive surfaces such as α-Al_2O_3, γ-Al_2O_3 and

porous vycor glass etc. Also when compared with stainless steel substrates, nickel films offer lower surface conductivities and lower surface activation. This does influence the combinatorial plating characteristics of Pd ELP baths. Therefore, it will be interesting to evaluate how nickel interdiffusion barriers pose a challenge towards Pd electroless plating during dense Pd composite membrane fabrication.

An even tougher challenge is to deposit Pd films on chromia diffusion barriers, as chromia is anticipated to be having lower conductivity than the nickel film. Also, it is apparent from literatures that investigations with respect to diffusion barriers (DB) also did not elaborate to a large extent the intrinsic technical features involved (such as number of fabrication steps to achieve the desired thickness of the diffusion barrier) and their role in significantly altering the plating characteristics of the dense Pd film. Such studies would be relevance to evaluate the possibility of reducing critical dense Pd metal film thickness. For instance, dense Cr_2O_3/PSS membrane has been reported in the literature that refers to 32 μm thick Pd films on 2 μm thick Cr_2O_3 film [43]. However, the only publication available, did not elaborate upon the role of diffusion barrier to reduce the critical thickness of Pd film for achieving the dense palladium membrane. Further, the effect of support morphology (pore size and its distribution characteristics) on the Cr_2O_3 interdiffusion layer thickness and eventually on the Pd film thickness has also not been investigated [43]. All investigations reported till date with respect to interdiffusion barriers [43-52] ignored the combinatorial plating characteristics for dense Pd composite membranes. Also, a comparative assessment of Pd/DB/PSS membranes with Pd-PSS membranes had not been carried out. Such studies could provide significant insights with respect to the quality of deposition and the associated challenges in fabrication engineering of dense Pd composite membranes. In summary, studies pertaining to the achievement of dense Pd composite

membranes with PSS supports modified with interdiffusion barriers such as chromia and nickel are encouraging to address the following challenges for dense Pd composite membrane fabrication:

a) The availability of interdiffusion barriers with low and non-conducting nature on PSS invoke poor surface activation and henceforth poor plating rates, process efficiencies and pore densification rates. Thus, the efficacy of rate enhanced modified Pd electroless plating process is an interesting issue to investigate and identify its ability for the enhancement of combinatorial plating characteristics within a short span of the plating time.

b) The role of nickel interdiffusion barrier morphology in influencing the combinatorial plating characteristics of dense Pd composite membranes. These specifically refer to the nickel film average pore size, thickness and adhesion strength which are complex functions of nickel solution concentration, rate enhancement technique parameters and other relevant process modifications.

c) A further challenge for the dense Pd composite membrane is to enable Pd deposition on non-conducting interdiffusion barriers (such as chromia) on a non-conducting support (such as alpha alumina). However, since this is the most challenging case for dense Pd composite membrane achievement, case (a) needs to be investigated prior to case (c) to generate reference data and to gain substantial insights with respect to the associated time dependent variation of combinatorial plating characteristics.

d) A further challenge towards the fabrication of dense Pd composite membranes using chromia interdiffusion barrier is to develop chromium electroless plating to achieve chromia interdiffusion barrier. Till date, there has not been any major literature to

elaborate upon chromium electroless plating on PSS and ceramic supports. Thus there is a substantial need to promote the development of optimal rate enhanced metal electroless plating processes for the sequential plating of chromium and palladium on both conducting and non-conducting supports. Pertinent challenges will be towards engineering the morphological characteristics of the chromia interdiffusion barrier by varying the electroless plating parameters of the chromium electroless plating baths.

1.5 Possible scope for research

From literature survey, it can be inferred that significant amount of research was focused towards the fabrication of dense Pd composite membranes. These membranes provided good performance characteristics such as higher combinations of hydrogen permeability, selectivity and durability. Given the fact that palladium is highly expensive metal, the literatures did not emphasize upon comparative assessment of process efficiencies to achieve dense Pd composite membranes. Thus, combinatorial plating characteristics comprising of both process and membrane performance characteristics have not been studied in a systematic format for the desired objective. With this as a central theme, few areas for the possible scope of research are summarized as follows:

1.5.1 Targeting an Efficient and Scalable Rate Enhanced Pd ELP process

The possible objective for the assessment of combinatorial plating characteristics for dense Pd composite membrane fabrication using electroless plating is to achieve higher combinations of conversion, plating efficiency, plating rate and pore densification. For electroless plating processes, while rate enhancement techniques may address enhancement of plating rates, they need not effectively target pore densification. Therefore, process modifications in addition could play an important role to further refine the combinatorial plating characteristics.

1.5.2 Parametric studies for identified rate enhanced Pd electroless plating processes

Once an optimal rate enhanced modified Pd ELP process has been identified, the optimality of the chosen process parameters needs to be assessed. These specifically refer to precursor solution concentrations (metal and surfactant if any) and loading ratio for the identified optimal concentration variation of hydrazine in the solution with time. These studies envisage to identify the potential and sensitivity of the fabrication parameters to influence the combinatorial plating characteristics. For instance, it is important to conceive how variations in the loading ratio influence pore densification. Similarly, while lower Pd solution concentrations might be favourable, it is also important to figure out whether higher Pd solution concentrations significantly reduce the total plating time or not to achieve a dense or near dense Pd composite membrane. Also, the adhesion strength of the Pd film as a function of fabrication parameters also needs to be assessed, as the developed scalable Pd ELP process must ensure the achievement of durable Pd composite membranes.

1.5.3 Fabrication of dense Pd/Ni/PSS and Pd/Cr_2O_3/PSS composite membranes

The objective of the preliminary investigations would be is to assess upon the role of nickel film and chromia film on the combinatorial plating characteristics of rate enhanced modified Pd ELP baths during fabrication of Pd/Ni/PSS, Pd/Cr_2O_3/PSS composite membranes. These specifically refer to the time dependent variation of adhesion strength, pore densification rate, plating efficiencies and selective conversions, film growth rate etc. A critical issue for investigation will be is to identify optimal support morphology that can provide optimal combinatorial plating characteristics for dense Pd composite membranes.

1.5.4 Role of surfactant during interdiffusion barrier engineering for dense Pd composite membrane fabrication

It has been well documented in the literature that surfactant induced electroless plating baths provide better combinations of uniformity in metal deposition and pore densification on porous stainless steel supports. Therefore, it is anticipated that surfactant induced chromium electroplating might provide interdiffusion barrier with better morphological properties such as narrow pore size distribution. Thereby, it will be interesting to investigate whether the consideration of surfactant in the engineering of chromia interdiffusion barrier has any role in altering the combinatorial plating characteristics of dense Pd chromia PSS composite membranes.

1.5.5 Repeability and Confidence Parameters

Finally, Pd membrane fabrication research needs to identify fabrication parameters and also needs to ascertain confidence levels associated with these. In almost all the investigations reported so far, repeability is not at all considered, which is an important issue. It is a fact that any membrane procured even commercially has a distinct pore size distribution which could not be determined without damaging the membrane and by only doing gas permeation experiments. Even by doing gas permeation experiments, the pore size distributions of the membrane are not known, even though it is possible to evaluate its average pore size and porosity. Further, if the membranes are fabricated in the laboratory, the ambiguity in average pore size and pore size distribution would be even higher. Considering these aspects in research is very important to consolidate the benchmarks with respect to the performance characteristics of various electroless plating processes to achieve dense Pd composite membrane fabrication.

1.6 Objectives of this work

The objective of this work is to prepare low cost thin dense Palladium composite membrane on porous stainless steel substrate. The reduction in palladium film thickness will be targeted by fabricating an interdiffusion barrier with appropriate thickness to reduce the membrane flux by 25 – 50%. Based on the available state-of-the-art and associated limitations, two different types of interdiffusion barriers will be extensively researched namely nickel and chromia. Amongst these, chromia interdiffusion barrier is anticipated to be deposited by electroplating method and nickel layer through electroless plating technique. Further details with respect to the desired objectives of this work are presented in the following paragraphs.

1.6.1 The role of rate enhancements during electroless plating towards the fabrication of better performing palladium membranes

To study the efficacy of different rate enhancement techniques on the performance characteristics of palladium electroless plating baths, sonication coupled electroless plating (SOEP) baths, surfactant induced electroless plating baths (SIEP) and both surfactant and sonication coupled electroless plating baths (SSOEP) will be investigated. The Pd deposition on the PSS supports was facilitated using hydrazine electroless plating bath. Based on the combinatorial plating characteristics (bath selective conversion, plating efficiency, average plating rate, average Pd film thickness and percent pore densification (PPD)), the optimal rate enhancement technique would be identified for the fabrication of Pd/PSS composite membranes.

1.6.2 Optimality of Process Parameters for Optimal Rate Enhanced Pd ELP process

In this work, the role of fabrication parameters such as palladium solution concentration (0.01 M and 0.005 M), surfactant concentration (CTAB at 1, 2 and 4 CMC) and loading ratio (203 cm^2/L

and 406 cm^2/L) on the time dependent combinatorial plating characteristics (selective conversion, plating efficiency, plating rate, Pd film thickness and percent pore densification) are to be studied during fabrication of Pd/PSS composite membranes with the identified optimal rate enhancement technique.

1.6.3 Effect of Nickel-stainless steel membrane morphology on the deposition characteristics of Pd films using hydrazine based electroless plating baths

In this work, the focus is upon the fabrication of palladium films on Ni-porous stainless steel substrates using electroless plating. The Ni/PSS membranes are to be prepared by depositing nickel on 500 and 100 nm PSS support by electroless plating technique. The Pd plating characteristics will be investigated by depositing palladium on the Ni-PSS supports using the identified optimal Pd ELP process. The combinatorial plating characteristics during dense Pd/Ni/PSS composite membrane fabrication would be investigated which refer to selective conversion, plating efficiency, plating rates, palladium film thickness and percent pore densification (PPD). Thereby, the role of nickel as an interdiffusion layer to reduce Pd film thickness will be investigated.

1.6.4 Effect of Chromia-stainless steel membrane morphology on the deposition characteristics of Palladium films using Hydrazine based electroless plating baths.

In this study, chromium oxide layers with different thickness values one to achieved on PSS supports using chromium electroplating technique followed with oxidation. The Pd plating characteristics will be investigated by depositing palladium on the Cr_2O_3-PSS supports using ELP process. Once again combinatorial plating characteristics will be investigated for their

optimality in conjunction with Pd/PSS membrane plating characteristics. Thereby, the role of chromia as interdiffusion layer to reduce Pd film thickness will be evaluated.

In all above experimental investigations, the repeability issue has to be given priority. The membrane permeance before and after surface modification using Cr_2O_3/Ni/Pd is regarded as a key parameter to deduce systematic conceptual insights into the fabrication processes and thereby pave the way towards furthering the development of multi-layered multi-metal low cost palladium composite membranes.

1.6.5 Engineering chromia interdiffusion barrier with surfactant induced electroplating and evaluation of combinatorial plating characteristics of dense Pd Chromia PSS composite membranes

Few sets of experiments will be designed to engineer chromia interdiffusion barrier using surfactant induced chromium electroplating baths and subsequent oxidation of the chromium metal to achieve chromia interdiffusion barrier. Thereby, the eventual experimental investigation will target the role of surfactant engineered chromia interdiffusion barrier on the combinatorial plating characteristics of dense Pd-Chromia-PSS membranes.

1.7 Organization of the thesis

Chapter 2 presents the experimental procedures for the fabrication of Pd composite membranes. The experimental procedures first refer to the evaluation of optimal Pd ELP process for dense composite membranes amongst CEP, SOEP, SIEP and SSOEP. Further, the effect of the contacting pattern of reducing agent in terms of bulk, phasewise and dropwise addition was also investigated. Further, the procedures adopted for the evaluation of plating characteristics were presented. Following this, a novel approach to evaluate the theoretical selectivity based on room

temperature permeation data has been elaborated. Finally, the chapter refers to the experimental procedures followed towards the parametric optimality of SSOEP Pd plating baths, and combinatorial plating characteristics of Pd/Ni/PSS and Pd/chromia/PSS membranes.

Chapter 3 presents the role of rate enhancements and process modifications on the combinatorial plating characteristics of Pd/PSS membranes. Based on the combinatorial plating characteristics and associated tradeoffs, the optimal rate enhancement technique coupled to Pd ELP and further modifications in the contacting pattern of the reducing agent were identified. The identified novel process refers to the coupled sonication and surfactant induced Pd ELP baths supplemented with drop addition of the reducing agent (SSOEP (DW)).

Chapter 4 addresses the parametric optimality of SSOEP (DW) plating baths in terms of Pd solution concentration (0.005 and 0.01 M), surfactant concentration (1, 2 and 4 CMC) and loading ratio (203 and 407 cm^2/L). Based on the combinatorial plating characteristics to achieve dense Pd composite membranes, the optimal set of surfactant and Pd solution concentration at the optimal loading ratio were identified. These parameters were utilized to fabricate dense Pd/Ni/PSS and dense Pd/chromia/PSS membranes.

Using optimal process parameters identified in Chapter 4, **Chapter 5** addresses the combinatorial plating characteristics of Pd ELP (SSOEP (DW)) baths for dense Pd/Ni/PSS composite membrane fabrication. Specifically, the target of the investigations was to evaluate the role of Ni interdiffusion barrier in altering the plating characteristics. Specific interest was to understand the role of Ni barrier film thickness on the critical Pd film thickness required for dense Pd/Ni/PSS composite membranes.

The results obtained during the fabrication of Pd/Cr_2O_3/PSS composite membranes using SSOEP (DW) Pd ELP baths are presented in Chapter 6. Two approaches were investigated to evaluate

upon the interdiffusion barrier morphological properties. These refer to (a) conventional chromium electroplating to achieve chromia interdiffusion barrier with variant chromia film thickness after oxidation and (b) surfactant induced chromium electroplating to achieve variant chromia interdiffusion barrier thicknesses. Eventually, based on the combinatorial plating characteristics, the role of interdiffusion barrier was evaluated in comparison with the obtained plating characteristics of baths deployed for Pd/PSS composite membrane fabrication.

Based on the most important findings obtained in several experimental investigations, various important conclusions obtained in the undertaken research work are presented in Chapter 7. Further, the scope for further research work is also presented in the same chapter in the context of (a) further alterations to process parameters for achieving 100% dense Pd composite membranes (b) further engineering aspects of coupling ELP with other fabrication techniques and (c) furthering the challenges associated to the fabrication of dense Pd/Ni/PSS and Pd/chromia/PSS membranes.

Chapter 2:

Experimental

Chapter 2

EXPERIMENTAL

This chapter summarizes the relevant experimental procedures adopted for the assessment of combinatorial plating characteristics of ELP baths for dense Pd composite membranes. Section 2.2 details upon the procedures adopted for the characterization of the porous stainless steel support. With hierarchial emphasis towards the identification of optimal ELP process, section 2.3 addresses the fabrication of dense Pd/PSS, Pd/Ni/PSS and Pd/chromia/PSS composite membrane fabrication. Section 2.4 summarizes various mathematical expressions developed for the assessment of combinatorial electroless plating characteristics. Finally, section 2.5 outlines a methodology for the evaluation of theoretical selectivity of dense Pd composite membranes.

2.1 Introduction

The Ph.D. thesis addresses the optimality of Pd ELP processes for dense Pd composite membrane fabrication. Since the process optimality is desired to achieve a product, the correlation between process parameters and its variables has to delineate in terms of various combinatorial plating characteristics. Therefore, the approach adopted in the thesis refers to the evaluation of both process and membrane characteristics. The overall assessment methodology for the optimality of various competent ELP processes and their associated parameters needs the evaluation of variables such as selective conversion, plating efficiency, average metal plating rate, metal film growth rate and percent pore densification. Therefore, experimental procedures shall involve the assessment of both variables associated to plating solution and membrane properties. In the next section, details with respect to the procedures adopted for the characterization of the porous support are presented along with a few results.

2.2 PSS support characterization

Porous stainless steel circular discs (dia of 36 mm and thickness of 1 mm) with a nominal particle retention size of 0.1 µm and 0.5 µm were purchased from Mott Corporation, USA. These stainless steel discs were sonicated (Model: S30H, ELMA) with acetone to remove the grease, oil, dirt, corrosion products and other contaminants present on the surface and were subsequently dried at 393 K in an oven (Model: ROV/DG, REICO) for 2 h. Subsequently, the porous stainless steel discs were characterized by scanning electron micrographs and room temperature nitrogen permeation experiments which are explained briefly in the following sub-sections.

2.2.1 Surface characterization

Figure 2.1 shows the surface morphology of porous stainless steel disc of 0.1 µm nominal pore size which was examined by scanning electron micrograph **(**Make: Zeiss, Model: Sigma). The pore size of the support was analyzed by Image J software and it was evaluated that the pores are distributed in the range of 2.06 – 9.8 microns. The average pore size of the support is about 6.04 µm.

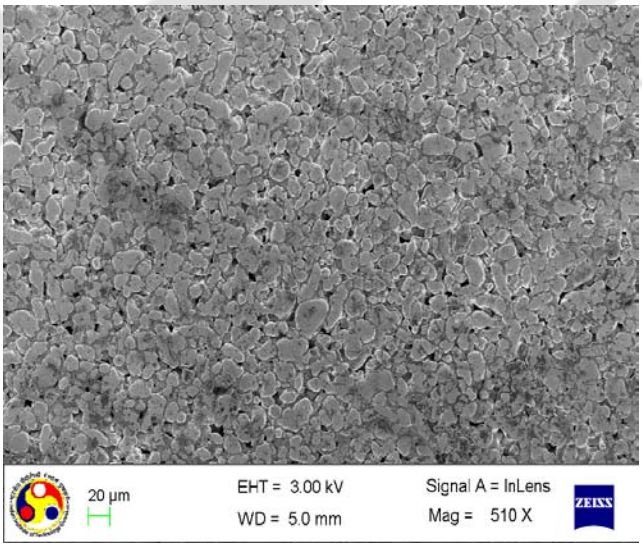

Figure 2.1: FESEM micrograph of 0.1 µm PSS support.

2.2.2 N_2 Permeation experiments

To evaluate the performance of PSS supports, nitrogen gas permeation experiments were conducted in a membrane module shown in Figure 2.2. The setup consists of a stainless steel tubular cell with a flat circular steel base plate. The support was placed in the membrane housing provided on the base plate and was sealed with rubber gaskets. The cell was pressurized with nitrogen gas and the outlet was connected to a flowmeter (rotameter/digital gas flow meter) for measuring gas flow rate at various transmembrane pressures. All permeation experiments were conducted at room temperature.

From the nitrogen permeation experiments, the measured data corresponds to flow rate (Q) vs pressure differential (ΔP) that was generated for the PSS support. The nitrogen permeation flux (J) of support was calculated using the expression 2.1.

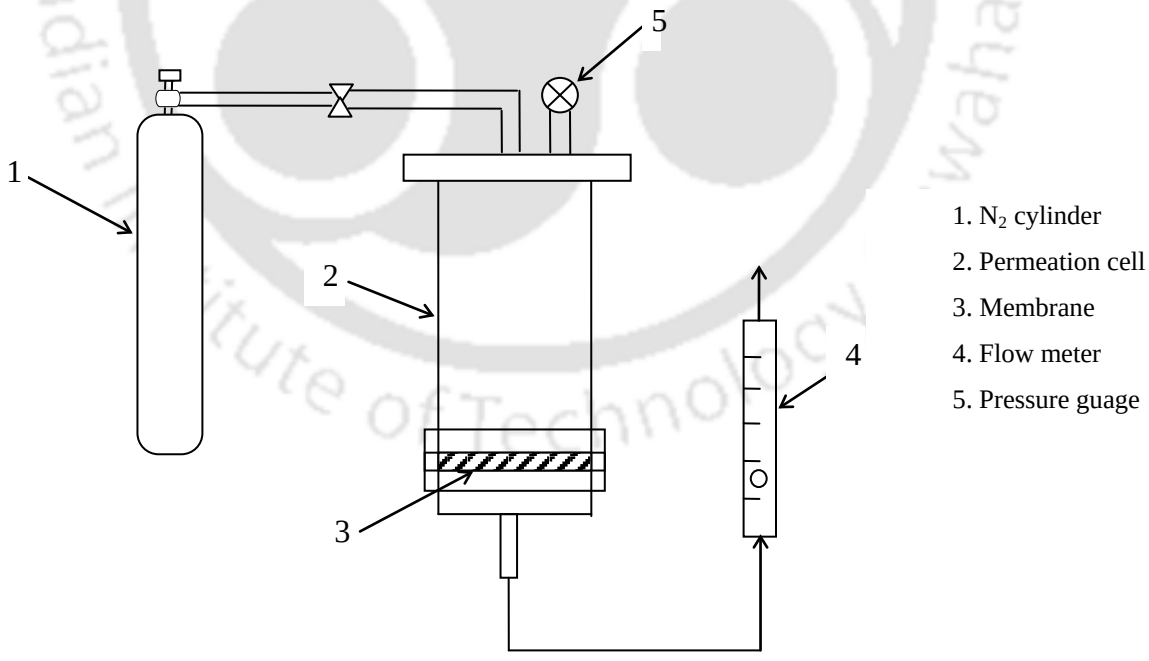

Figure 2.2: Experimental setup for room temperature N_2 permeation tests.

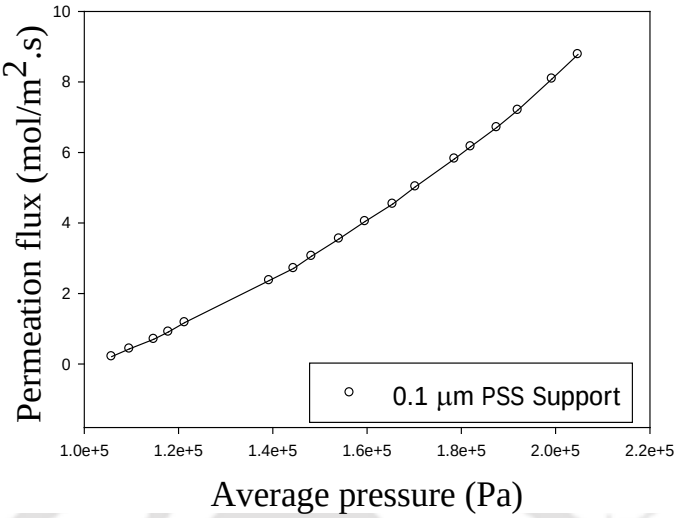

Figure 2.3: Variation of N_2 flux with average pressure for 0.1 μm PSS support.

$$J = \frac{Q}{S} \qquad (2.1)$$

where S is the surface area of PSS support. For the PSS support with nominal pore size of 0.1 μm, the obtained Nitrogen permeation flux (J) vs. Average pressure (P_{avg}) data is shown in Figure 2.3.

For the evaluation of PPD, the average membrane flux of the porous support is to be determined. From Figure 2.3, the average nitrogen permeation flux ($\overline{J}$) of the support can be evaluated using the following expression:

$$\overline{J} = \frac{\int_{P_1}^{P_2} JdP}{P_2 - P_1} \qquad (2.2)$$

where P_1 and P_2 corresponds to the minimal and maximum retentate pressures during an experimental test to measure the nitrogen gas permeance at room temperature. The expression presented in Eq. (2.2) is also applicable for Pd composite membranes.

2.3 Dense Pd composite membrane fabrication using Electroless Plating Processes

2.3.1 Process Description

Electroless plating involves the autocatalytic deposition of metallic films on substrate by the reduction of metallic complex ions in the solution using a reducing agent. Typically, palladium electroless plating requires seeding of the support with Pd nuclei to initiate a uniform deposition. The seeding process involves sequential steps of sensitization, activation and rinsing using baths of various compositions (Table 2.1). The process involves placing the stainless steel substrates in the sensitization bath ($SnCl_2$ solution) for 5 min, rinsing with water and then contacting the membrane supports in activation bath ($PdCl_2$ solution) for 5 min followed by rinsing in acid bath (0.1 N HCl) for 2 min. These steps were repeated 9 to 10 times to obtain a completely activated surface, which was confirmed by observing uniform dark-brown colour on the membrane surface. After seeding, the membrane was dried overnight in an oven at 393 K to measure its dry weight (w_1) before plating.

Table 2.1: Sensitization and activation bath compositions.

Constituent	**Amount used in each bath**	
	Sensitization	**Activation**
$SnCl_2.2H_2O$ (g/L)	1.0	-
$PdCl_2$ (g/L)	-	0.1
35% HCl (ml/L)	0.1	0.4
Operating Temperature	293 K	293 K
pH	4 - 5	4 - 5

The electroless deposition of palladium can be summarized using the following chemical reactions:

$$2Pd(NH_3)_4^{2+} + 4e^- \xrightarrow{Pd^o} 2Pd^o + 8NH_3 \quad (2.3)$$

$$N_2H_4 + 4OH^- \rightarrow N_2 + 4H_2O + 4e^- \quad (2.4)$$

Overall reaction

$$2Pd(NH_3)_4^{2+} + N_2H_4 + 4OH^- \rightarrow 2Pd^o + N_2 + 8NH_3 + H_2O \quad (2.5)$$

In the literature, researchers fabricated dense palladium composite membranes using palladium solution concentration of 0.02 - 0.03 M (2128.42 - 3192.63 ppm). Due to these higher Pd solution concentrations, Pd membrane fabrication cost is high. In this work, preliminary experiments were conducted on a stainless steel disc of 0.1 µm average pore size using 0.02 M $PdCl_2$ solution concentration at a loading ratio of 203 cm^2/L. These preliminary experiments indicated that a solution concentration as low as 0.005M could be used for plating, which is not the case in the literature. Table 2.2 summarize the composition of the electroless plating baths for palladium solution concentrations of 0.02 M (case a) and 0.005 M (case b).

Table 2.2: Pd ELP bath compositions.

S.No	Component	Amount used in each bath (a)	**(b)**
1	$PdCl_2$	3.6 g/l	0.8866 g/L
2	Na_2EDTA	76 g/l	14.89 g/L
3	$NH_3.H_2O$ (25%)	650 ml/l	110 ml/L
4	N_2H_4	10 ml/l	1.81 ml/L
5	CTAB	0-4 CMC	0-4 CMC
6	pH	11	11
7	Temperature	60^{o}C	60 ^{o}C

2.3.2 Fabrication of Pd/PSS membranes using CEP, SOEP, SIEP and SSOEP processes

The present study addresses the fabrication of palladium composite membranes on an activated MPSS supports using conventional electroless plating (CEP), sonication assisted electroless plating (SOEP), surfactant induced electroless plating (SIEP) and both surfactant and sonication coupled electroless plating (SSOEP) baths. Specific details with respect to the steps involved in the Pd deposition using CEP, SIEP, SOEP and SSOEP baths are presented as follows:

Conventional electroless plating (Figure 2.4a) involves heating the plating solution containing $PdCl_2$, NH_4OH and Na_2EDTA in a constant temperature water bath to achieve a plating temperature of 333K. Once the temperature was achieved, hydrazine was added with stirring, along with the activated substrate. The plating was allowed to proceed without further stirring for 30 min to complete one plating step.

The sonication assisted electroless plating process (Figure 2.4b) refers to placing the plating bath in an ultrasonic cleaning bath (Elmasonic, S30H) that also consists of a heating element and various modes of sonication operation (constant, degas and sweep modes of sonication). During the SOEP, the Pd bath was maintained at a constant plating temperature of 333 K, a constant frequency of 50/60 Hz and degas mode of sonication. Once the plating temperature was achieved, hydrazine was added with stirring, along with the activated substrate to initiate Pd deposition.

For both SIEP and SSOEP Pd electroless plating processes, a cationic surfactant Cetyltrimethylammonium bromide (CTAB) was dispersed in the plating solution containing $PdCl_2$, NH_4OH and Na_2EDTA, whose composition has been presented in the Table 2.2 (case b). Subsequent steps during SIEP and SSOEP plating process refer to those presented earlier for the CEP and SOEP, respectively.

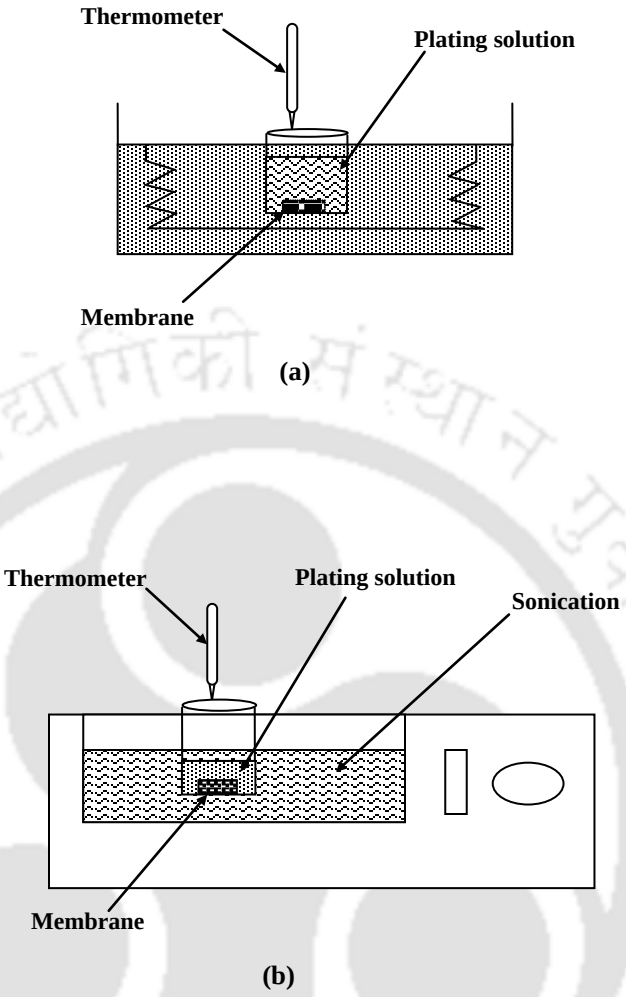

Figure 2.4: Schematic of (a) CEP and SIEP and (b) SOEP and SSOEP Pd ELP baths.

In addition to these cases, further experimentation involved minor modifications to the experimental procedure related to the addition of the reducing agent (hydrazine) to the plating solution. The variation in the addition of the reducing agent is based upon on the physical examination of plating solution after plating, as metal particles in the solution after plating are indicative towards nucleation in the solution and plating inefficiency which needs to be eliminated for noble metal deposition.

The experimentation involved with the variation in the reducing agent contacting pattern has been broadly categorized into two different categories namely:

(a) Phase wise (PW) addition of reducing agent for CEP, SOEP, SIEP and SSOEP baths

(b) Drop wise (DW) of reducing agent to SIEP & SSOEP baths. For these investigations, only SIEP and SSOEP Pd baths were considered due to their superior performance in comparison with CEP and SOEP processes.

The phase wise addition of reducing agent involves the addition of hydrazine reducing agent in three subsequent equal time intervals during one plating step of 30 min. duration. On the other hand, the drop wise addition of reducing agent refers to the continuous addition of the total amount of hydrazine during plating using a burette. In this as well as other plating bath operations, the plating baths were covered with a lid to avoid the loss of vapors and restrict solution volume loss.

The experimental setups for SIEP (DW) and SSOEP (DW) processes are shown in Figure 2.5a and 2.5b respectively. The experimental procedure for the plating process is as follows. The surfactant induced sonication assisted electroless plating (SSOEP (DW)) process involves dispersing a cationic surfactant (CTAB) in the plating solution containing palladium chloride, liquor ammonia and sodium salt of ethylene dinitrilo tetra acetic acid. Then the plating solution was kept in an ultrasonic cleaning bath (Elmasonic, S30H) that also consists of a heater element and various modes of sonication operation (constant, degas and sweep modes of sonication). During the SSOEP, the Pd bath was maintained at a constant plating temperature of 333 K, constant frequency of (50/60 Hz) and degas mode of sonication. Once the plating temperature was achieved, hydrazine was added to the plating solution continuously throughout the plating time using a burette.

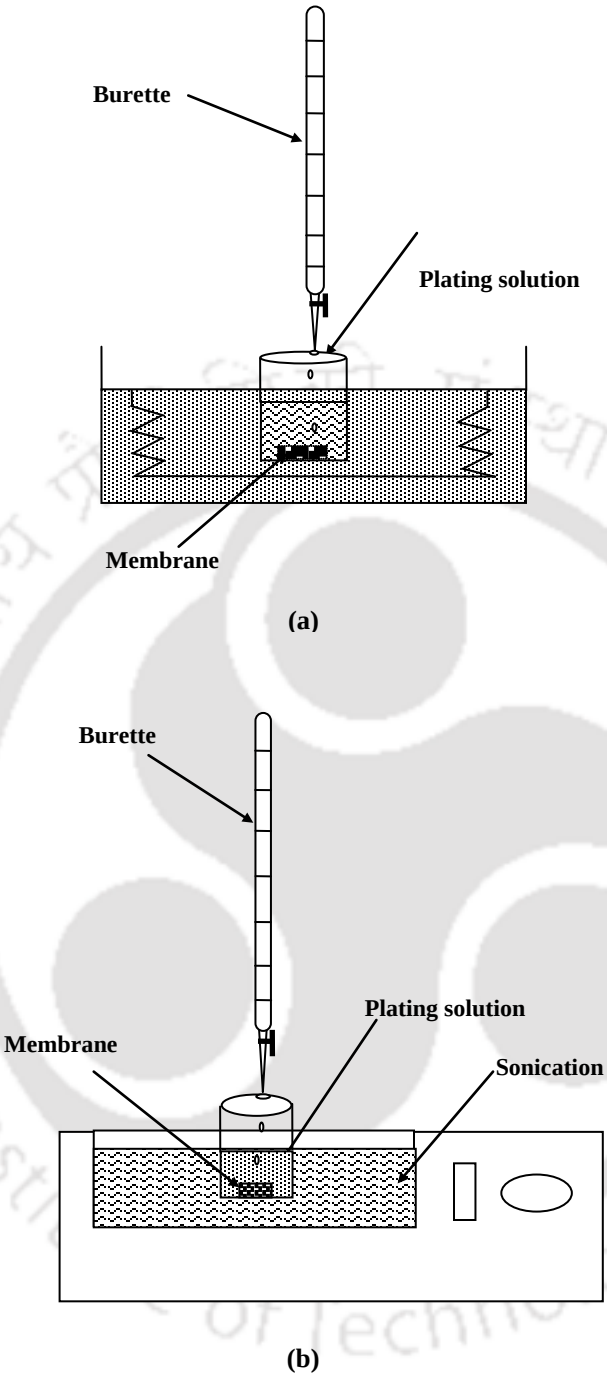

Figure 2.5: Schematic of (a) SIEP (DW) and (b) SSOWP (DW) plating baths.

Similarly in surfactant induced conventional electroless plating (SIEP (DW)) process, the plating solution consists of cationic surfactant (CTAB), palladium chloride, liquor ammonia and

sodium salt of ethylene dinitrilo tetra acetic acid. Prior to SIEP (DW) based Pd ELP, the solution was kept in a beaker to maintain the plating temperature of 333 K. Once the plating temperature was achieved, hydrazine was added to the plating solution continuously throughout the plating time using a burette.

2.3.3 Optimality of SSOEP (DW) Pd baths for dense Pd/PSS membrane fabrication

Among various Pd ELP processes, SSOEP (DW) process provided highest PPD values for Pd/PSS composite membrane fabrication. Therefore, further optimality of the process parameters associated to SSOEP (DW) has been addressed. The procedures for the fabrication of Pd/PSS composite membrane are similar to those presented in the previous section (section 2.3.2). The effect of Pd solution concentration was investigated for two different Pd bath compositions (0.005 and 0.01 M) for fixed choice of CTAB surfactant (4 CMC) concentration and loading ratio (203 cm^2/L). Based on optimal combinatorial plating characteristics for the Pd metal solution concentration, the optimality of surfactant solution concentration was investigated for 1, 2 and 4 CMC ELP baths with fixed choice of 0.005 M Pd metal solution concentration and loading ratio of 203 cm^2/L. Finally, based on the optimal combinatorial plating characteristics for Pd metal and surfactant solution concentrations, the optimality of loading ratio was investigated for two different cases (203 and 407 cm^2/L).

2.3.4 Fabrication of Pd/Ni/PSS membranes using SSOEP (DW) baths

2.3.4.1 Nickel interdiffusion barrier fabrication

To deliberate upon the role of Nickel diffusion barriers in influencing combinatorial plating characteristics, prior to palladium plating the Pd seeded supports were subjected to Ni ELP using SSOEP (DW) plating baths to achieve Ni/PSS composite membranes. Corresponding nickel electroless plating bath composition is presented in Table 2.3. Experimental setup for the Ni ELP

Table 2.3: Ni ELP bath composition

S.No	Constituent	Amount used in each bath
1	Nickel sulfate ($NiSO_4$. $7H_2O$)	0.08 mol/L
2	Hydrazine hydrate (20%) ($N_2H_4.H_2O$)	40 ml/L
3	Trisodium citrate ($Na_3C_6H_5O_7.2H_2O$)	0.16 mol/L
4	Sodium hydroxide (NaoH)	pH: 10-11
5	CTAB	4 CMC
6	Temperature	80 ^oC

is similar to that presented in Figure 2.5b. The Ni interdiffusion barrier was achieved for 0.1 μm and 0.5 μm support pore size. Ni interdiffusion barriers of low and high thickness were achieved for a total plating time of 2 and 5 h respectively. These variations in the Ni interdiffusion barrier were achieved to target upon their role in influencing the combinatorial Pd plating characteristics.

2.3.4.2 Pd Electroless plating

Pd electroless plating was carried out on the Ni/PSS supports using the Pd plating bath composition shown in Table 2.2 (case b). For the Ni/PSS supports, additional seeding and activation steps were conducted to ensure the activation of the Ni/PSS supports with Pd seed particles. Eventually, all plating experiments were conducted with the surfactant and sonication induced electroless plating baths supplemented with drop wise addition of reducing agent (SSOEP-DW) at a loading ratio of 203 cm^2/L. For all investigations, the performance characteristics of Pd electroless plating baths were determined initially after every four sequential plating steps (2 h of plating time). Later, after PPD reached 90%, all relevant plating characteristics were determined after every two sequential plating steps whose time period for each step was about 30 min.

For all membranes, 12 to 16 sequential plating steps with an average plating time of 30 minutes for each step were carried out. After completing the electroless plating, the Pd membranes were intermediately rinsed using de-ionized water to remove salts adsorbed in pores of the porous support or entrapped in the Pd coating layer. Finally the membrane was dried in an oven at 393 K for 6 h.

To evaluate the membrane performance and identify the presence of defects, the room temperature nitrogen gas permeation experiments were conducted in a membrane module shown in Figure 2.2.

2.3.5 Fabrication of Pd/Chromia/PSS membranes using SSOEP (DW) baths

2.3.5.1 Chromia interdiffusion barrier

To deliberate upon the role of chromia diffusion barriers in influencing combinatorial plating characteristics, prior to palladium plating the porous PSS supports were coated with chromia interdiffusion barrier using conventional chromium electroplating process. The typical experimental setup used for chromium electroplating is shown in Figure 2.6. The process consists of lead as an anode and porous stainless steel support as a cathode with H_2CrO_4 plating solution (250 g/L concentration). The electroplating process was operated at a current density of 133 mA/cm^2. The total time of plating was varied as 10 and 30 min for two different cases to obtain chromia films of variant thickness values. Eventually, the deposited chromium metal film was subjected to oxidation at 700 ^oC for 6 h in a muffle furnace to achieve chromia interdiffusion barrier. Further, few membranes were fabricated using surfactant induced chromium electroplating process to evaluate upon the role of surfactant induced chromia interdiffusion barrier on the combinatorial plating characteristics of Pd composite membranes. To do so, the conventional chromium electroplating process is supplemented with 2 CMC CTAB cationic

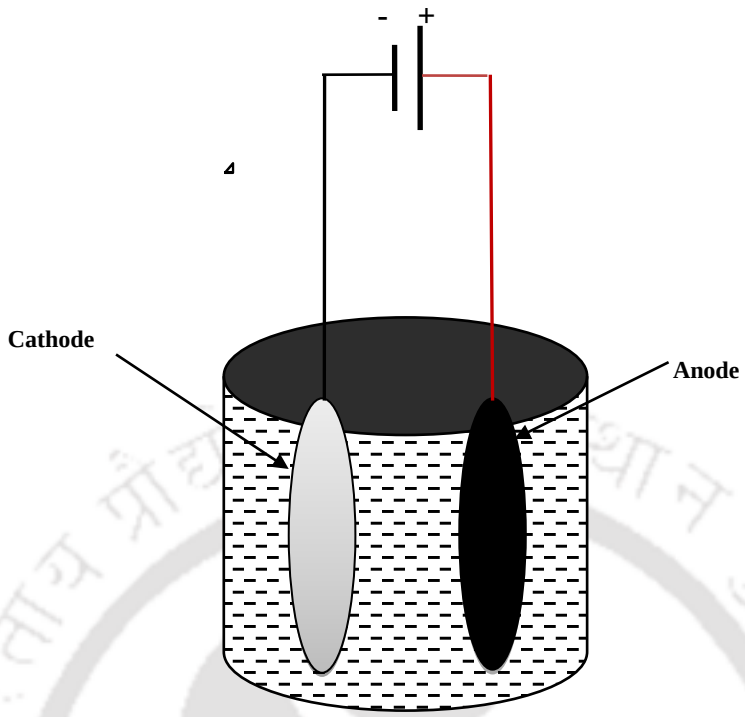

Figure 2.6: Schematic of experimental setup for conventional/surfactant induced chromium electroplating.

surfactant (CMC) in the solution composition presented in the previous paragraph. To achieve chromia interdiffusion barrier of variant thickness values, the surfactant induced chromium electroplating was conducted for 10 and 20 min respectively to yield chromia barriers with two different thickness and morphologies.

2.3.5.2 Pd ELP

The procedure followed for the fabrication of Pd/chromia/PSS and Pd/surf-chromia/PSS membranes is similar to that presented in section 2.3.4.2.

2.4 Evaluation of combinatorial plating characteristics

The performance characteristics evaluated for the Pd electroless plating baths are namely plating bath conversion (χ), selective conversion, plating efficiency (η), Pd film thickness (δ), average plating rate $\left(\bar{r}_{Pd}\right)$, average permeation flux $\left(\bar{J}\right)$ and percent pore densification (PPD).

The plating bath conversion is evaluated as the ratio of the amount of Pd metal ion reacted to the amount of palladium present initially in the plating solution, and is expressed as:

$$\chi\,(\%) = \frac{C_i - C_f}{C_i} \times 100 \qquad (2.6)$$

where C_i and C_f are initial and final concentration (mol/L) of Pd in the plating solution. These were determined using atomic absorption spectroscopy (AAS) (Model: FS 240, Varian Spectra) at a wavelength of 247.6 nm. Appendix A and B summarizes the relevant calibration curves required for the evaluation of unknown Pd plating solution concentrations after Pd ELP.

Plating efficiency (η) is evaluated as the ratio of amount of the palladium deposited on the activated substrate surface to the amount of palladium converted during the plating step and is expressed as follows.

$$\eta\,(\%) = \frac{w_2 - w_1}{w_o} \times 100 \qquad (2.7)$$

where w_1 is the dry weight of membrane (g) before plating, w_2 is the dry weight of membrane after plating and w_o is the amount of palladium metal converted during plating. In the above expression, w_o is calculated using the equation:

$$w_o = (C_o - C_i)\, n V_o M_{Pd} \qquad (2.8)$$

where, n is the number of sequential plating steps, V_o is the volume of plating solution (L) in each plating step and M_{Pd} is the molecular weight of palladium metal.

The selective conversion is defined as the product of plating efficiency and conversion of plating bath and is expressed as:

$$\text{Selective conversion (\%)} = \frac{\eta \times \chi}{100} \qquad (2.9)$$

The thickness of deposited palladium film is evaluated by using weight gain method and is expressed as follows.

$$\delta = \frac{w_2 - w_1}{\rho_{Pd} A_m} \tag{2.10}$$

where ρ_{Pd} is the density of palladium metal (g/cm^3), A_m is the membrane surface area (cm^2). Since it was assumed that the palladium film is dense even in intermediate steps, the evaluated thickness corresponds to the theoretical value and the actual value will be apparently lower than the evaluated value. However, since it is not possible to measure membrane porosity, thickness calculations omitted the same.

The average plating rate $\bar{r}_{Pd}$ (mole/m^2.s) is evaluated by using the following expression.

$$\bar{r}_{Pd} = \frac{w_2 - w_1}{M_{Pd} \times A_m \times t} \tag{2.11}$$

where, t is the corresponding total plating time.

Pore densification during the plating process is defined as the fractional volume of the pores covered by the deposited metal and is expressed as PPD. It is calculated using the following expression.

$$PPD\ (\%) = \frac{\bar{J}_o - \bar{J}_i}{\bar{J}_o} \times 100 \tag{2.12}$$

where $\bar{J}_o$ is the average room temperature nitrogen permeation flux of the porous stainless steel substrate (mol/m^2.s) and $\bar{J}_i$ is the average room temperature permeation flux of the palladium composite membrane fabricated after i^{th} depositional plating step. The average room temperature nitrogen permeation flux is calculated by using the expression.

$$\overline{J} = \frac{\int_{P_1}^{P_2} JdP}{P_2 - P_1} \qquad (2.13)$$

where P_1 and P_2 corresponds to the minimal and maximum retentate pressures during an experimental test to measure the nitrogen gas permeance at room temperature.

2.5 Model for the assessment of theoretical selectivity

Typically for palladium composite membranes, high temperature H_2/N_2 single and binary gas selectivities are determined after achieving a dense palladium membrane. However, depending upon the PPD values of the palladium composite membranes, one can also estimate the theoretical selectivity. In this work, for the first time, we have reported a procedure to estimate the theoretical selectivity, which will serve as an important guideline towards the time dependent pore densification effectiveness of the palladium composite membranes during fabrication. Thus, using the following procedure, one can eliminate carrying out rigorous experimentation until one refines and obtains the best quality palladium composite membranes. Thereby, one can also identify optimal combinations of plating process parameters with minimal experimentation. The procedure to evaluate the theoretical selectivity of the palladium composite membrane is presented as follows:

a) For the porous palladium composite membrane, room temperature permeation experiments can be conducted with nitrogen gas.

b) From room temperature N_2 flow rate vs. pressure differential data, the average volumetric nitrogen permeance of the porous palladium composite membrane (pcm) can be calculated using the expression:

$$Pern_{rt}{}^{pcm} = \frac{Q_{rt}{}^{pcm}}{A_m} \times \frac{1}{(PR - PP)} \quad (2.14)$$

c) Plot a graph between $Pern_{rt}{}^{pcm}$ and $\frac{(PR + PP)}{2}$ to obtain slope and intercept. These correspond to Viscous and Knudsen nitrogen permeance values at room temperature, respectively. Thus,

$$Pern_{rt}{}^{pcm} = KPern_{rt}{}^{pcm} + ViPern_{rt}{}^{pcm} \frac{(PR + PP)}{2} \quad (2.15)$$

where $KPern_{rt}^{pcm}$ and $ViPern_{rt}^{pcm}$ corresponds to the graphically determined Knudsen (slope) and Viscous nitrogen permeance values at room temperature.

Since volumetric Knudsen permeance is proportional to average velocity, corresponding Knudsen permeance for nitrogen gas for the same metal composite membrane at higher temperature (573 K) can be estimated using the expression:

$$KPern_{ht}{}^{pcm} = KPern_{rt}{}^{pcm} \frac{vn_{ht}}{vn_{rt}} \quad (2.16)$$

On the other hand, viscous permeance is inversely proportional to viscosity and the high temperature (573 K) nitrogen gas viscous permeance for the same metal composite membrane is determined using the expression:

$$ViPern_{ht}{}^{pcm} = ViPern_{rt}{}^{pcm} \frac{\mu n_{rt}}{\mu n_{ht}} \quad (2.17)$$

Using the computed values of $KPern_{rt}^{pcm}$ and $ViPern_{rt}^{pcm}$, the high temperature nitrogen flux is determined using the expression:

$$JN_{ht}{}^{pcm} = \left[KPern_{ht}{}^{pcm} + ViPern_{ht}{}^{pcm} \frac{(PR + PP)}{2} \right] \times \frac{[PR - PP]}{PP} \times \frac{1000}{22.4} \qquad (2.18)$$

Corresponding hydrogen flux through the porous palladium membrane is computed by assuming that the film is highly dense and consists of pinholes through which nitrogen gas passes through and hydrogen passes through the dense palladium film. Thereby, the theoretical hydrogen flux of the palladium composite membrane at higher temperature is estimated using the expression:

$$JH_{ht}{}^{pcm} = \frac{Permh^{dm}}{\delta^{pcm}} \times \left(PR^n - PP^n \right) = Perh^{pcm} \times \left(PR^n - PP^n \right) \qquad (2.19)$$

where $Permh^{dm}$ is assumed to be the dense palladium membrane permeability from literature data [60] (66.8×10^{-13} mol.m/m^2.s.Pa at 573 K) and δ^{pcm} corresponds to the thickness of the palladium film determined by weight gain method.

The theoretical hydrogen flow rate is evaluated as a function of membrane area and is expressed as:

$$Q_{H_2}^{th} = JH_{ht}{}^{pcm} A^{pcm} \qquad (2.20)$$

Having known the values of $JH_{ht}{}^{pcm}$ and $JN_{ht}{}^{pcm}$ at higher temperatures, the average hydrogen and nitrogen flux values were determined using trapezoidal rule applied for the flux vs. pressure differential data. The average hydrogen and nitrogen flux values are evaluated using the expressions:

$$AJH_{ht}{}^{pcm} = \frac{\int_{PR_{\min}}^{PR_{\max}} JH_{ht}{}^{pcm}.dP}{(PR_{\max} - PR_{\min})} \qquad (2.21)$$

$$AJN_{ht}{}^{pcm} = \frac{\int_{PR_{\min}}^{PR_{\max}} JN_{ht}{}^{pcm}.dP}{(PR_{\max} - PR_{\min})} \tag{2.22}$$

Having known the average flux values of the palladium composite membrane at higher temperature, the theoretical selectivity $(\bar{\alpha}_{av})$ for an equimolar feed mixture of H_2/N_2 is estimated using the expression:

$$\bar{\alpha}_{av} = \frac{\frac{y_{H_2}}{y_{N_2}}}{\frac{0.5}{0.5}} = \frac{AJH_{ht}{}^{pcm}}{AJN_{ht}{}^{pcm}} \tag{2.23}$$

For tradeoff related studies, the average theoretical hydrogen flow rate is estimated using expressions similar to (2.21) and (2.22) and is presented as:

$$\bar{Q}_{H_2}^{th} = \frac{\int_{PR_{\min}}^{PR_{\max}} Q_{H_2}^{th}\, dP}{(PR_{\max} - PR_{\min})} \tag{2.24}$$

The theoretical membrane selectivity has been evaluated using literature hydrogen permeance value (33.4×10^{-7} mol/m^2.s.Pa for 2 μm dense Pd film thickness) at 573 K [60]. However, in due course of sequential electroless deposition involving several plating steps, dense palladium films were only obtained in the last step and all other intermediate palladium composite membranes are porous membranes. The theoretical membrane selectivity also ignored the hydrogen flux through the pores (i.e., pinholes in the later stages of sequential electroless deposition) which is also significant. Therefore, the net hydrogen flux in principle should have been taken as the sum of the hydrogen flux through the dense palladium matrix and hydrogen flux through the pinholes. However, since dense palladium film hydrogen flux could be overestimated using literature

values, the contribution of hydrogen flux through the pinholes is ignored in the evaluation of theoretical membrane selectivity so as to obtain a lower prediction for theoretical selectivity values.

This work also cites upon the relevance of theoretical membrane selectivity as an important index in the tradeoffs associated to fabrication and plating parameters. Theoretical membrane selectivity is an alternate index compared to the PPD. While PPD represents a depositional characteristic, the theoretical selectivity refers to the separation characteristic of the membrane. Therefore, both PPD and theoretical selectivity indices are extremely relevant indices to identify and screen amongst various parametric and rate enhancement alternatives of the Pd electroless baths to achieve low cost dense Pd membrane fabrication.

Fundamentally, for a fully dense palladium composite membrane, the theoretical selectivity value shall be infinity and for a porous palladium composite membrane with minimal selectivity, the theoretical selectivity value will be close to the separation factor achievable with purely Knudsen diffusion phenomena. Therefore, the evaluation of theoretical selectivity value will be useful to screen various processes and time dependent electroless plating characteristics could thereby identify potential routes for integrated process and product development i.e., developing an electroless plating that can simultaneously maximize theoretical selectivity, PPD and plating efficiency and minimize PPD. In other words, in due course of sequential plating, the palladium composite membrane theoretical selectivity values need to increase to about infinity and identification of process conditions that provide high selectivity values is an interesting subject in the fabrication research of palladium composite membranes.

Chapter 3:

Identification of Optimal Rate Enhanced Pd ELP Process for Dense Pd/PSS Membrane Fabrication

Identification of Optimal Rate Enhanced Pd ELP Process for Dense Pd/PSS Membrane Fabrication

Targeting dense Pd/PSS membrane fabrication, this chapter addresses the results obtained for CEP, SIEP, SOEP and SSOEP Pd ELP baths. Section 3.2 summarizes few results obtained for SOEP process with bulk addition of hydrazine reducing agent. Section 3.3 addresses combinatorial plating characteristics, tradeoffs and surface characterization results obtained for the chosen processes supplemented with phasewise addition of the reducing agent. Section 3.4 discusses the efficacy of SIEP and SSOEP processes for drop wise addition of the reducing agent in terms of the combinatorial plating characteristics, surface characterization and tradeoffs. Section 3.5 addresses the cost assessment of SSOEP (DW) Pd ELP baths with those documented in the literature. Finally section 3.6 presents a summary of the obtained results.

3.1 Introduction

In the literature, SIEP process with bulk addition of the hydrazine has been patented. Therefore, further research in the SIEP process with bulk addition of reducing agent has not been considered in this work. On the other hand, SOEP process has not been investigated till date for the combinatorial plating characteristics associated to the bulk addition of the reducing agent. Therefore, the next section presents few important findings for SOEP processes to gain important insights upon the pertinent plating characteristics.

It has also been documented in the literature that the contacting pattern of the reducing agent is an important parameter that needs to be given its due attention in the research associated to the fabrication of dense Pd composite membranes [24]. The phase wise addition of the reducing

agent has been proven to be effective in enhancing the plating efficiency. However, the effect of phase wise addition of the reducing agent on the PPD and other plating characteristics were not investigated and will be addressed in this chapter. Also, further improvement in the PPD values (to 100%) needs to be targeted by additional modifications to the contacting pattern of the reducing agent. This is due to the reason that phasewise addition of the reducing agent may not provide 100% PPD.

The next section addresses few characteristics of SOEP Pd ELP processes that were operated with the bulk addition of the hydrazine reducing agent. SIEP Pd ELP with bulk addition of the hydrazine reducing agent is not considered due to the available prior art [24].

3.2 Characteristics of SOEP Pd ELP baths with bulk addition of the hydrazine reducing agent

3.2.1 Physical Examination

Using the ELP bath composition presented in Table 2.2 (a), Pd/PSS composite membranes were fabricated using CEP and SOEP process. The Pd solution concentration for the investigated case is about 0.02 M and 0.005 M for SOEP and 0.02 M for CEP process. Higher solution concentration was used for CEP process as the process provides lower Pd plating rates and enhancement of solution concentration could facilitate faster deposition. Figure 3.1a and 3.1b illustrate the images of the plating solution and membrane obtained after 4 h of total plating time (1 h time duration for each step) for a Pd solution concentration of 0.02 M. Similar images were obtained for membranes fabricated with SOEP process at 0.005 M Pd solution concentration While conducting the plating experiments, it was observed that for both CEP and SOEP processes, that the bulk addition of reducing agent enabled the formation of Pd metal particles in

(a)

(b)

Figure 3.1: Photographs of (a) spent ELP solution and (b) Pd/PSS composite membrane obtained with 0.02 M SOEP Pd bath and 30 min. plating time.

the plating solution after 7 min. of plating for all sequential Pd plating steps. After plating, it was also evaluated that the Pd deposited on the membrane surface did not adhere to it properly. This indicates poor plating characteristics. Hence, other plating characteristics such as selective conversion, metal film thickness etc., were not investigated for these cases.

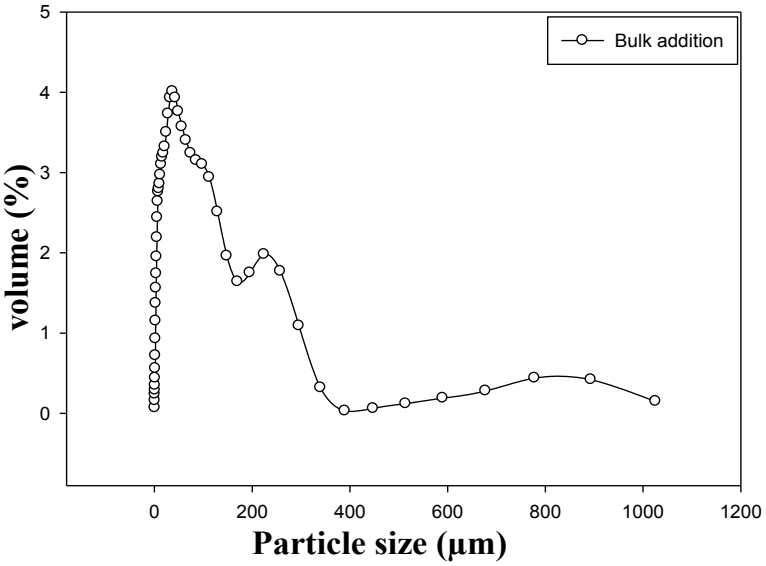

Figure 3.2: Particle size distribution in spent solution obtained using 0.02 M SOEP Pd bath and 30 min. plating time.

3.2.2 Particle size distribution analysis

The particle size distribution in the plating bath solution was measured by using laser particle size analyzer. Figure 3.2 summarizes the same and it can be observed that the plating solution after plating with SOEP process had palladium metal particles in the range of 1 - 1000 microns. From the particle size distribution graph, the average particle size has been estimated as 66.5 μm. Therefore, it is apparent that bulk addition is not at all favourable for large scale Pd membrane fabrication using electroless plating technique.

3.2.3 Summary

Bulk addition of reducing agent (such as hydrazine) is not recommended for rate enhanced ELP process such as SOEP even at low Pd metal solution concentration of 0.005 M. Therefore, the next section addresses phase wise addition of the hydrazine reducing agent for all cases namely CEP, SOEP, SIEP and SSOEP processes.

3.3 Pd ELP Baths supplemented with phase wise addition of hydrazine

In this section, the combinatorial plating characteristics of various Pd ELP baths facilitated with phase wise addition of reducing agent are presented. Table 2.2 (b) summarizes the plating bath compositions. The evaluated combinatorial plating characteristics include selective conversion, plating efficiency, average plating rate, metal film thickness, percent pore densification (PPD) and palladium film thickness for CEP, SIEP, SOEP and SSOEP Pd ELP processes. Thereby, the evaluated combinatorial plating characteristics are anticipated to provide insights with respect to the efficacy of the best process and further enhancement in the process performance by suitable variation to the contacting pattern of the reducing agent.

3.3.1 Selective conversion and Plating efficiency

Figure 3.3a and 3.3b summarize the effect of plating time on selective conversion and plating efficiencies for CEP, SIEP, SOEP and SSOEP baths. For a variation in total plating time from 2 – 6 h, it can be observed that for CEP and SIEP baths, the selective conversions varied from 13.46 – 11.77% and 18.51 – 17.35% respectively. Corresponding plating efficiencies varied from 29.60 – 28.44% and 55.32 – 62.80%, respectively. In this regard, it can be noted that the plating efficiencies of the CEP process are significantly low and hence phase wise addition of the reducing agent with hydrazine is not a good choice. However, for SOEP and SSOEP Pd ELP baths, the selective conversions varied from 42.66 – 34.95% and 29.03 – 34.45% respectively. Corresponding plating efficiencies varied from 84.03 – 80.07% and, 93.33 – 95.18%, respectively. Thus higher plating efficiencies are achieved for SOEP and SIEP processes in comparison with SIEP baths.

Also, compared to the CEP, it is apparent that CTAB surfactant played a significant role to enhance both selective conversions and plating efficiencies for SIEP baths. However, compared to the SIEP, higher plating efficiencies are obtained for the SSOEP plating baths. In agreement with the trends presented in the literature, the selective conversion and plating efficiencies for SOEP process are higher than those obtained for the CEP process. In this regard, the literature (Bulasara et al. [61]) refers to the superior performance of SOEP Ni ELP baths for the fabrication of porous Ni ceramic composite membranes. It is further interesting to note that SSOEP provide better plating efficiency profiles in comparison with the SOEP process. This is due to the combined effect of surfactant and sonication for the SSOEP process.

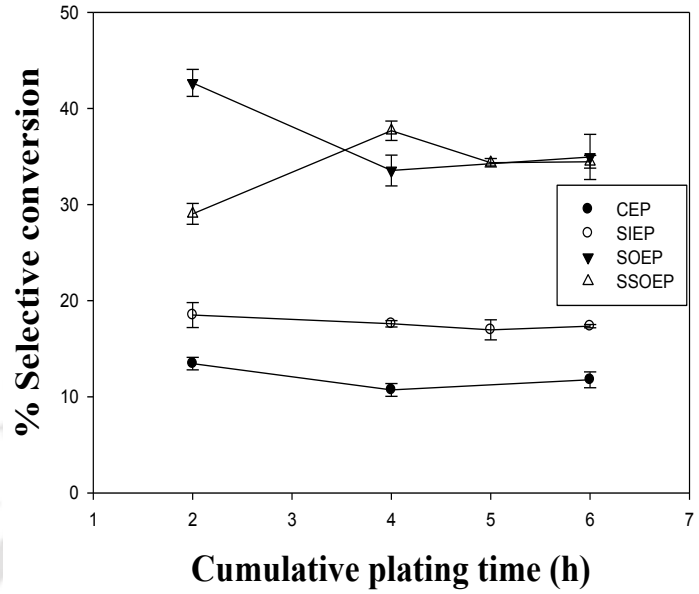

(a)

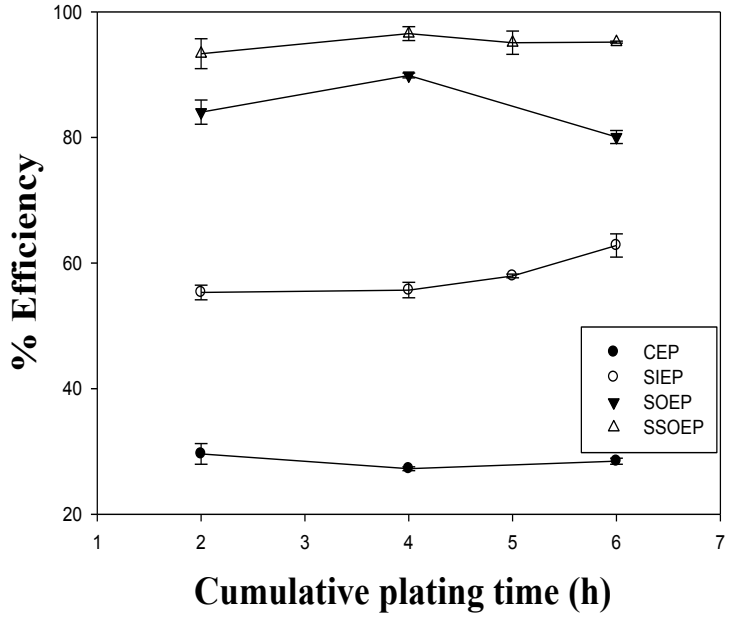

(b)

Figure 3.3: Effect of plating time on (a) Selective conversion and (b) Plating efficiency for CEP (PW), SOEP (PW), SIEP (PW) and SSOEP (PW) Pd baths.

Table 3.1 Time dependency of average plating rate for CEP (PW), SIEP (PW), SOEP (PW) and SSOEP (PW) processes.

Process	Average plating rate (mol/m^2.s)x10^5 for various total plating time (h)			
	2	4	5	6
CEP (PW)	2.01	1.60	-	1.76
SIEP (PW)	2.53	2.37	2.29	2.34
SOEP (PW)	5.28	4.58	-	4.77
SSOEP (PW)	3.96	5.14	4.69	4.70

3.3.2 Plating rate

Table 3.1 presents the average Pd plating rate values for CEP, SIEP, SOEP and SSOEP baths. It can be observed that, for a variation of total plating time from 2 – 6 h, the average Pd plating rates varied from 2.01x10^{-5} to 1.76x10^{-5} mol/m^2.s for CEP, 2.53 x10^{-5} to 2.34x10^{-5} mol/m^2.s for SIEP, 5.28x10^{-5} to 4.77x10^{-5} mol/m^2.s for SOEP and 3.96 x10^{-5} to 4.70x10^{-5} mol/m^2.s for SSOEP process. The plating rates for sonication baths (SOEP and SSOEP) are higher than those obtained for CEP and SIEP baths. The probable reason for the same is that the applied ultrasound accelerated the transfer of metal particles from the plating solution to the membrane surface due to cavitation effect [61].

3.3.3 Nitrogen flux profiles

Figure 3.4 depicts the nitrogen permeation flux trends for various total plating time cases for the Pd-PSS membranes fabricated with CEP, SIEP, SOEP and SSOEP baths. It can be observed that the CEP process enabled the flux reduction from 0.26-8.95 mol/m^2.s (for an average pressure of 1.05 – 2.04 bars) to 0.20 – 8.68 mol/m^2.s (for an average pressure of 1.05 – 2.04 bars) after 6 h of Pd ELP. For the same time period, the SIEP process enabled the flux reduction from 0.24 – 8.58

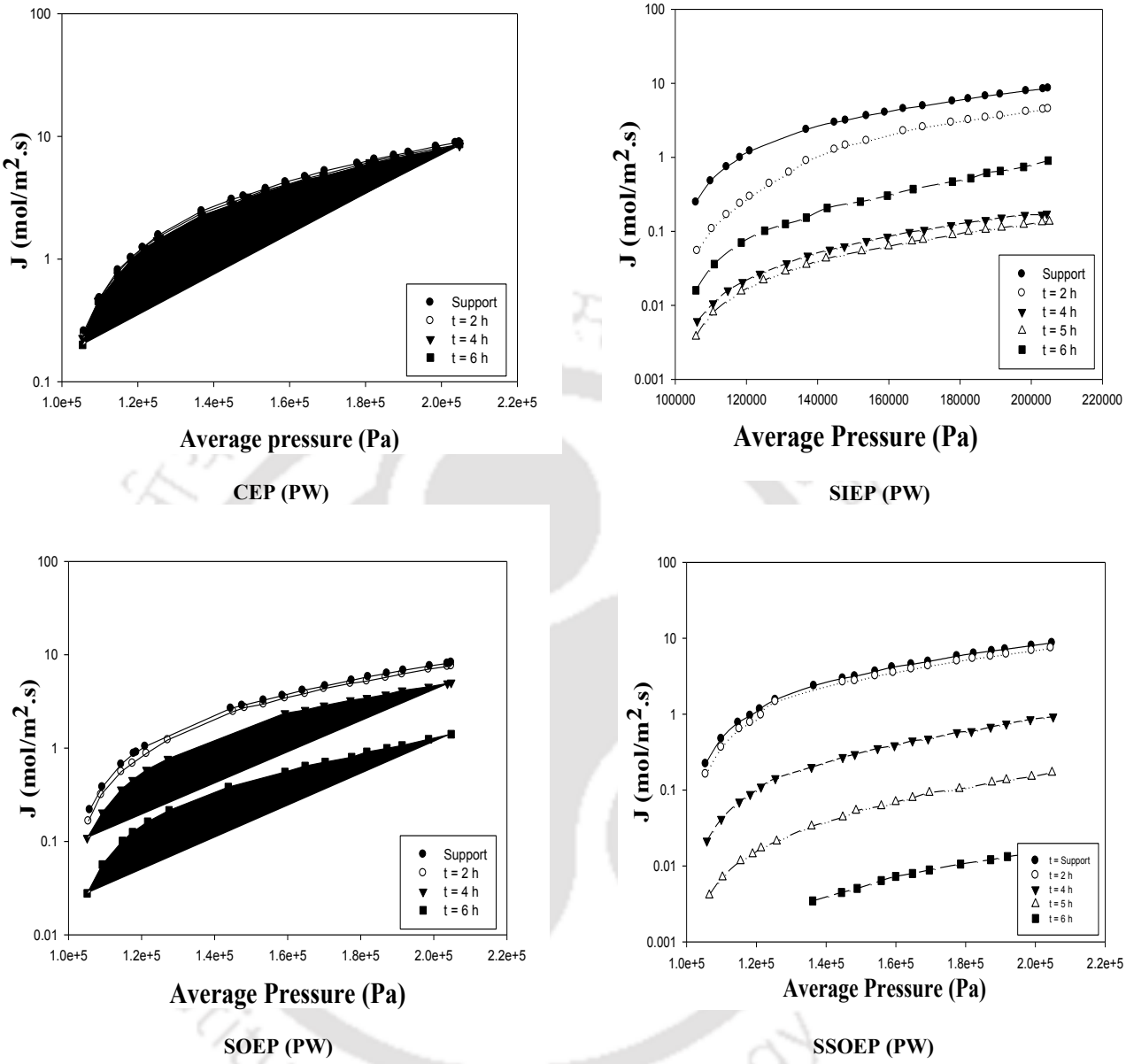

Figure 3.4: N_2 flux vs. average pressure plots for various membranes achieved with CEP (PW), SIEP (PW), SOEP (PW) and SSOEP (PW) processes.

mol/m^2.s (for an average pressure of 1.05 – 2.04) to 0.016 – 0.90 mol/m^2.s (for an average pressure of 1.05 – 2.04 bar). In other words there is no reduction in nitrogen flux after 6 h of plating using CEP. Further, the obtained flux after 6 h with CEP process is significantly lower than the nitrogen permeation flux obtained after 2 h plating with SIEP baths. For SOEP and

SSOEP baths, the flux reduced from 0.22 – 8.28 mol/m^2.s (for an average pressure of 1.05 – 2.04 bar) to 0.028 – 1.41 mol/m^2.s (for an average pressure of 1.05 – 2.04 bar) and 0.221 – 8.68 mol/m^2.s (for an average pressure of 1.05 – 2.04 bar) to 3.46×10^{-3} – 0.014 mol/m^2.s (for an average pressure of 1.36 – 1.99 bar) after 6 h of sequential palladium deposition. Also, it can be observed from the figure that for both SOEP and SSOEP baths, the reduction of nitrogen flux during the initial 2 h plating time is low. This indicates that initial Pd metal deposition occurred to normalize the pore size distributions on the substrate surface. Also, for both SOEP and SSOEP processes, after 4 h of plating time, the nitrogen flux reduced significantly. For SSOEP baths, the surfactant contributed significantly to the reduction of nitrogen flux. Compared to CEP and SOEP, significant reduction in N_2 permeation flux has been obtained for SIEP and SSOEP baths. Therefore, it is apparent that surfactant was effective to reduce the nitrogen permeation flux and contributed to PPD enhancement. However, for SIEP, the nitrogen flux increased after 6 h of total plating time. The enhancement in nitrogen flux is not desired, given the fact that dense Pd composite membranes should not undergo metal delamination at prolonged plating times. However, this is not the case for SSOEP Pd ELP baths where the nitrogen flux profiles continuously decreased with increasing total plating times. Hence, based on the nitrogen flux profiles, the SSOEP Pd ELP baths provided better performance. Further assessment of the SSOEP bath performance in terms of pore densification is addressed in the next section.

3.3.4 Percent Pore Densification

Based on the reductions in average nitrogen flux, the time dependent PPD profiles for various Pd ELP processes are presented in Figure 3.5a. It can be observed that, for CEP Pd ELP bath after 6 h of total plating time, the maximum PPD obtained is 7.16% only. This indicates that a significantly higher plating time will be required for the CEP process to achieve dense Pd/PSS

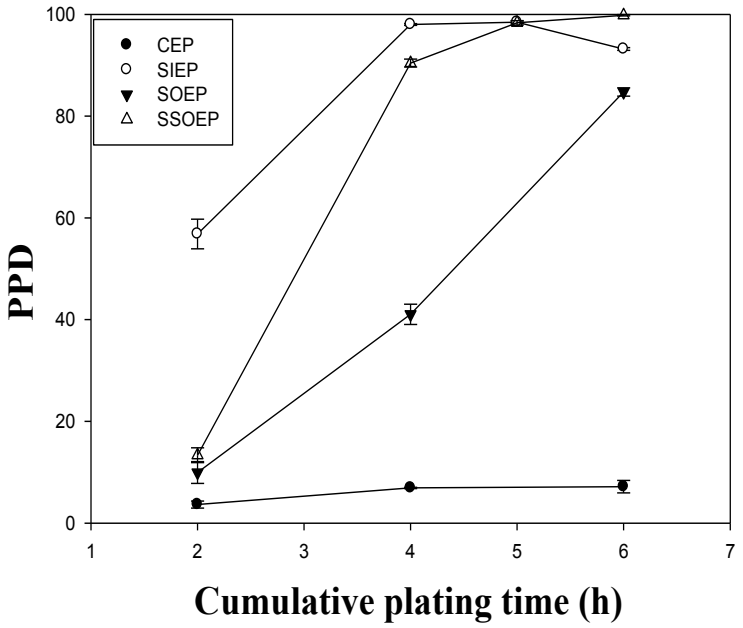

(a)

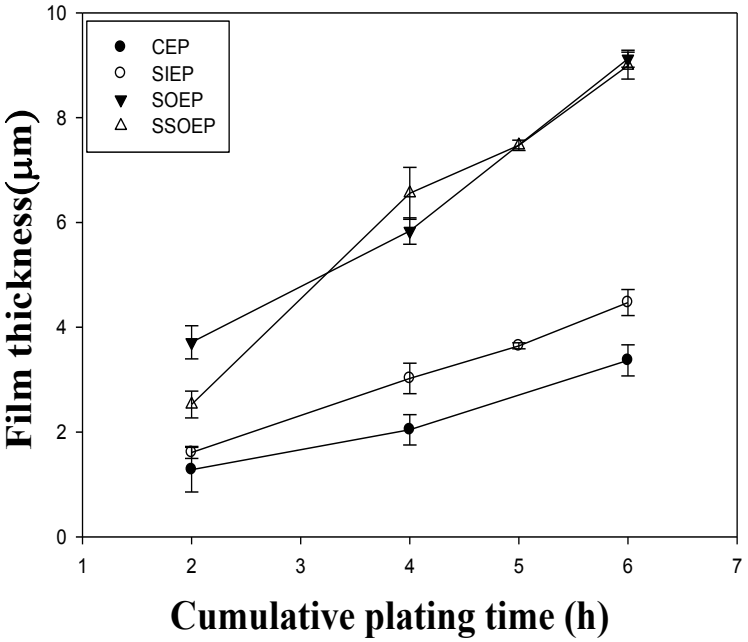

(b)

Figure 3.5: Variation of (a) PPD and (b) film thickness with plating time for CEP (PW), SOEP (PW), SIEP (PW) and SSOEP (PW) processes.

composite membranes. However, for SIEP ELP baths, the first 5 h of total plating time demonstrated an enhancement in PPD to 98.46% followed with reduction to 93.29% for an additional 1 h of Pd ELP. The possible reason for the reduction in PPD is the delamination of palladium particles from the membrane surface which could be eliminated by altering the bath chemistry and plating parameters. For both SIEP and SSOEP baths, higher PPD values have been obtained in shorter deposition time. For SOEP and SSOEP baths, the maximum PPDs obtained are 84.74 and 99.82%, respectively. While dense Pd/PSS membranes were not achieved by the SSOEP Pd ELP baths, the obtained maximum value of the PPD after 6 h of total plating time are promising. Also, SOEP did not enable a significant enhancement in the PPD even after 6 h of plating in comparison with the SSOEP. This is possibly due to the layering effect. In other words, the cavitation effect during sonication did not effectively contribute towards pore densification, which is the most important desired feature of the dense Pd composite membrane fabrication. The best reported literature data corresponds to the PPD trends reported by Islam et al. [37]. The authors have inferred that compared to the CEP process, the SIEP process with bulk addition of hydrazine provides dense and thinner Pd films (7.68 µm) on PSS substrates for lower total plating time (10 h) values.

3.3.5 Thickness

The effect of plating time on the Pd film thickness for Pd/PSS membranes fabricated with CEP, SOEP, SIEP and SSOEP baths is shown in Figure 3.5b. It can be observed that, for CEP and SIEP baths, the time dependent Pd film thickness varied from 1.28 – 3.36 µm and 1.61 – 4.47 µm for a variation of total plating time from 2 to 6 h. For similar time periods, the thickness of Pd film varied from 3.71 – 9.12 µm and 2.52 – 8.99 µm for SOEP and SSOEP Pd plating baths, respectively. Thereby, it has been analyzed that for SIEP baths, the Pd film thickness is 1.25 –

1.32 times higher than that obtained with CEP baths. These observations are in agreement with the results presented by Chen et al. [39] who reported that the addition of a suitable surfactant to the electroless plating bath increases the deposition rate by 25%. However, when compared to the SOEP baths, the SSOEP baths did not indicate upon a significant role of surfactant to enhance the Pd film thickness. Overall, the metal film thickness for SOEP, SSOEP baths are higher than that obtained with CEP and SIEP baths.

3.3.6 Morphological and surface characterization

Since SSOEP provided best performance, the surface characterization studies were carried out only for membranes obtained with the process. Figure 3.6a shows the FESEM micrograph of Pd/PSS membrane fabricated with SSOEP bath. The microstructure of the Pd film is studied using ImageJ software. It has been evaluated that on the membrane surface, palladium grains distributed uniformly and the average grain size is around 16 μm. The observations are in agreement with the uniformity and grain size distributions reported by Islam et al. [37] who indicated that the grain size of Pd deposited using SIEP bath varied from 2 – 17 μm using DTAB surfactant.

Figure 3.6b shows the XRD pattern of Pd/PSS composite membrane fabricated in SSOEP bath with 4 CMC surfactant concentration. The XRD spectra indicate the existence of Pd reflection peaks at a diffraction angle (2θ) of 40.2°, 46.76° and 68.28° due to diffraction of (1 1 1), (2 0 0) and (2 0 2) plane and it confirmed the deposited Pd metal to be highly pure. No peaks associated to stainless steel composite membrane (that are not shown in a separate figure) have been observed and this indicates that the deposition has been dense from the perspective of the XRD analysis. The extent of pore densification could not be confirmed by the XRD analysis and this can be only confirmed from room temperature nitrogen flux data that was reported earlier.

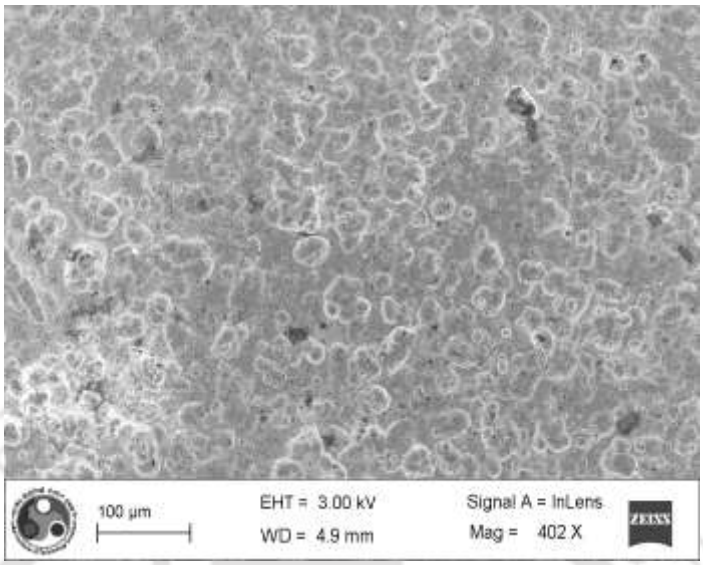

(a)

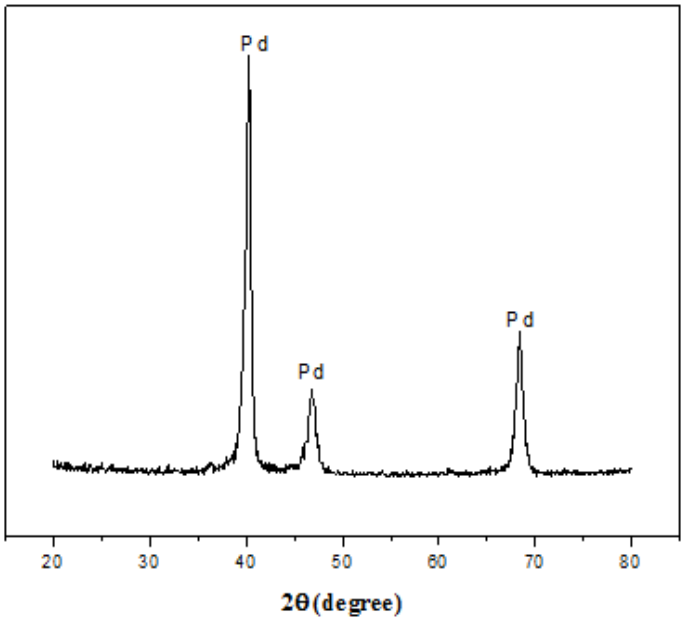

(b)

Figure 3.6: (a) FESEM micrograph and (b) XRD pattern of the Pd/PSS membrane fabricated with SSOEP (PW) bath at 0.005 M Pd and 4 CMC CTAB initial concentration and plating time of 6 h.

3.3.7 Tradeoffs

Conceptually, thin palladium film supported on a porous substrate is the most desired to obtain high hydrogen permeation flux and lower membrane cost. In general, using any deposition process, the PPD of membrane increases with increasing Pd film thickness. However, an efficient fabrication process targets high PPD values for low Pd film thickness and therefore ensures both process and membrane optimality. Therefore higher values of $\frac{PPD}{\delta}$ and PPD are desirable during the fabrication of dense palladium composite membranes and the process or processes that provide these combinations can be referred to be the optimal choices. Figure 3.7a illustrates the $\frac{PPD}{\delta}$ vs PPD profiles for all investigated Pd ELP baths. It can be observed that after completion of 6 h of total plating time, for CEP and SIEP baths, the $\frac{PPD}{\delta}$ values varied from 2.84 – 2.12 and 35.28 – 20.86 respectively. On the other hand, for SOEP and SSOEP baths, the $\frac{PPD}{\delta}$ varied from 2.68 – 9.79 and 5.28 – 11.09 respectively. For SIEP bath, $\frac{PPD}{\delta}$ profile indicated reducing trend after 5 h of total plating time. However, for SSOEP bath, the $\frac{PPD}{\delta}$ profile did not indicate saturation even after 6 h of Pd sequential plating. Therefore, it is evident that SSOEP baths are the optimal choices for the cost effective fabrication of dense Pd composite membranes. Since dense Pd composite membranes are not obtained with the phase wise addition of the reducing agent, further investigations are required for suitable process modifications.

Figure 3.7b illustrates (100 – PPD) vs. selective conversion profiles for CEP, SIEP, SOEP and SSOEP baths. The best scenario of plot refers to lowest value of (100 – PPD) (y-axis value) and highest value of selective conversion (x-axis value). For CEP baths, the selective conversion is in

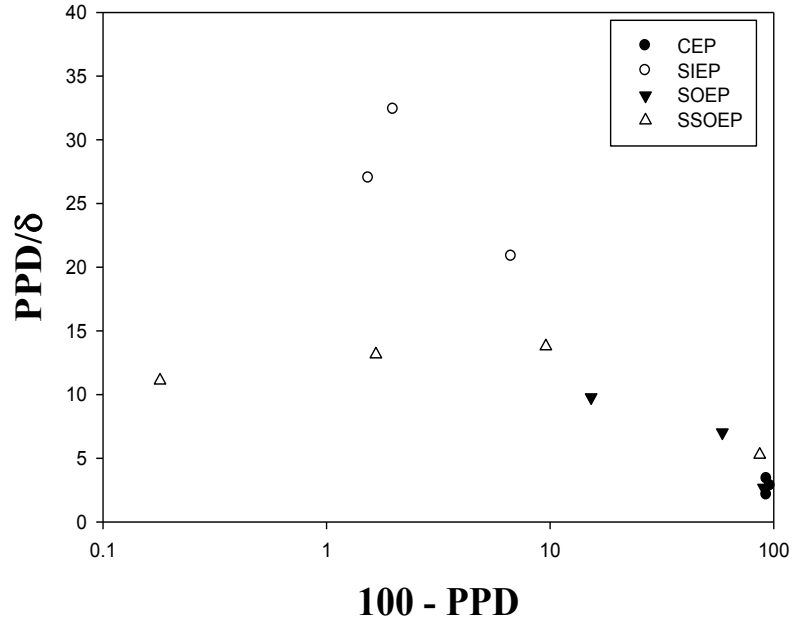

(a)

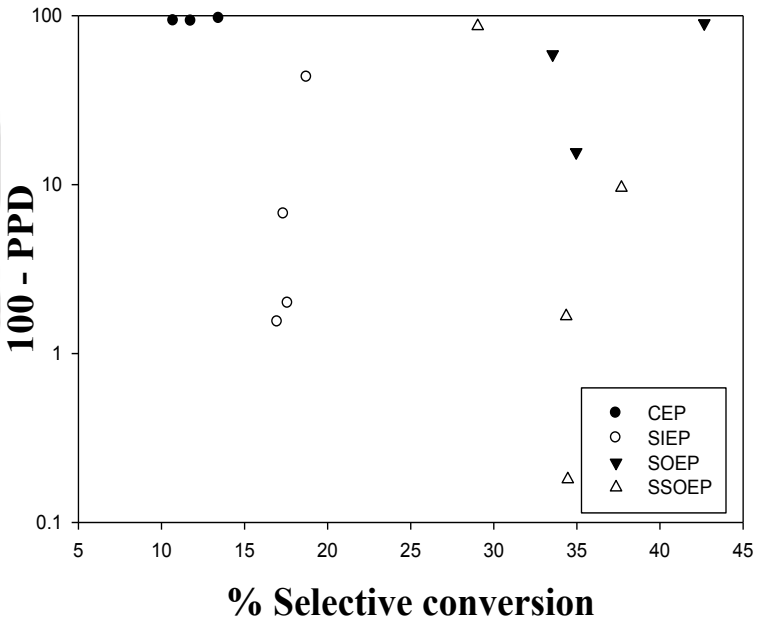

(b)

Figure 3.7: Tradeoffs of (a) PPD/δ vs (100 - PPD) and (b) (100 - PPD) vs selective conversion for CEP (PW), SIEP (PW), SOEP (PW) and SSOEP (PW) processes.

the range of 13.45 – 11.77% and the maximum PPD obtained is too low. For SIEP baths, the selective conversion and PPD varied from 18.74 – 17.34 % and 56.83 – 93.19 % respectively. For SOEP baths, the selective conversion and the PPD varied from 42.66 – 34.95 % and 9.94 – 84.73 % and for SSOEP baths, the selective conversions and PPD varied from 29.03 – 34.45 % and 13.35 – 99.82%. In other words, best combination of selective conversion and PPD are obtained for SSOEP.

3.3.8 Particle size distributions in the spent ELP solution obtained with SSOEP Pd baths

The particle size distribution in the plating bath solution during phase wise addition of reducing agents was measured using laser particle size analyzer. Figure 3.8 summarizes the same and it can be observed that the plating solution after plating had palladium metal particles in the range of 0.2 – 500 microns. From the particle size distribution graph, the average particle size has been estimated as 24.5 μm. The obtained average particle size distribution is lower than that obtained for the CEP with bulk addition of hydrazine. Therefore, it is apparent that phase wise addition is

(a) **(b)**

Figure 3.8: Photographs of (a) spent plating solution and (b) Pd/PSS membrane obtained for SSOEP (PW) process.

not at all favourable for large scale Pd membrane fabrication using electroless plating technique. Figure 3.8a and 3.8b pictorially presents the plating solution and membrane after 6 h of total plating time for SSOEP Pd ELP baths supplemented with phase wise addition of the reducing agent. The formation of Pd metal particles in plating solution was observed occasionally for the phase wise addition of the reducing agent. Therefore a better process needs to be investigated to eliminate the further minimize or significant reduction of metal ions in the plating solution.

3.3.9 Summary

The phase wise addition of reducing agent has improved the depositional characteristics of Pd using CEP, SIEP, SOEP and SSOEP. Based on the maximum values of the PPD obtained in minimal total plating time (6 h), it has been confirmed that the best processes for dense Pd membrane fabrication are SIEP and SSOEP. However, the phase wise addition of N_2H_4 to the plating baths needs further investigations, as it has not eliminated reduction of metal ions in the solution i.e., metal nucleation in the solution. Also, the phase wise N_2H_4 addition to the plating baths did not materialize dense Pd membranes even after 10 – 12 plating steps with a time duration of 30 min. for each plating step. This further indicates that dense Pd membrane fabrication is a very difficult area of research and researchers often have not addressed these issues in the light of consistent process development and research in process engineering. To further enhance process efficiencies and PPD values, the next section addresses the combinatorial plating characteristics of Pd ELP baths for SIEP and SSOEP baths supplemented with the drop wise (DW) contacting pattern of the reducing agent. Both CEP and SOEP are not addressed in the next section due to the fact that both have not been effective to reduce the PPD values significantly.

Conventional electroless plating involves the formation and evolution of gas bubbles on the porous substrate surface in due course of the autocatalytic redox reaction. The N_2 gas bubbles would leave the surface after buoyancy forces are satisfied and thus, it is possible that smaller hydrogen bubbles that do not meet the surface force requirements occupy the surface. This would give raise to pits or unwanted voids in the metal film. During SIEP, the surfactant adsorption on the substrate surface facilitates variation of wettability characteristics of the deposited substrates and thereby contributes to a reduction in the interfacial tension between the gas bubbles generated on the membrane surface. Therefore, in an SIEP process, the gas bubble size will reduce and smaller bubbles have better tendencies to leave the substrate surface quickly (Karuppusamy and Anantharam [62]). Due to this reason, quicker removal of smaller hydrogen/nitrogen gas bubbles from the membrane surface minimize pitting. Also, cationic surfactants have a tendency to participate in the ELP reaction and thereby promote the shifting of the slow Pd ELP reaction in the forward direction to thereby enhance the plating rate. Thus, surfactant addition favors enhancement in the deposition rate and reduction of pitting observed during the conventional electroless plating process. It has been reported in the literature as well that during electroless plating, cationic surfactants with lower hydrophilic lipophilic balance (HLB) values are very effective towards enhancing the plating rate and metal film quality [39]. SSOEP process indicates an even better alternative to the SIEP process. The SSOEP process furthered the Pd plating characteristics with additional sonication effect that carefully promoted the PPD values significantly, without indicating upon any lapse mode of PPD trends.

3.4 Depositional Characteristics of SIEP and SSOEP baths with drop wise (DW) contacting pattern of the reducing agent

Table 2.2b summarizes the plating bath compositions adopted to carry out SIEP and SSOEP Pd ELP with dropwise contacting pattern of the reducing agent (DW). Figures 2.5a and 2.5b illustrate the relevant experimental setups for SIEP (DW) and SSOEP (DW) Pd ELP processes for dense Pd/PSS membrane fabrication. In the following sub-sections, the combinatorial plating characteristics of both ELP baths are presented.

3.4.1 Selective conversion and Plating efficiency

Figure 3.9a and 3.9b illustrates the variation of selective conversion and plating efficiencies with plating time for SIEP and SSOEP baths. For SIEP baths, for a variation in total plating time from 2 – 4 h, the selective conversion and plating efficiencies varied from 14.5 – 13.75% and 47.80 – 45.23%, respectively. For the same time period, for SSOEP baths, the selective conversion and plating efficiencies varied from 30.61 – 29.10% and 72.53 – 72.44%, respectively. Further ELP was not carried out for SIEP (DW) process due to poor combinatorial plating characteristics in comparison to those obtained with SSOEP (DW) process. For SSOEP bath after completion of 7 h of total plating time, the selective conversion and plating efficiencies are 26.31% and 80.69%, respectively. For comparison, it can be observed in the previous section that the best selective conversion and plating efficiencies for SSOEP (PW) bath are 29.03 – 34.45 and 93.33 – 95.17%, which are higher than the SSOEP (DW) baths. However, an important issue that needs to be investigated is the PPD, as higher conversions and plating efficiencies need not translate into higher PPD. For the DW plating baths, it can be concluded that the selective conversion and plating efficiencies for SSOEP (DW) baths are much higher than the SIEP (DW) baths.

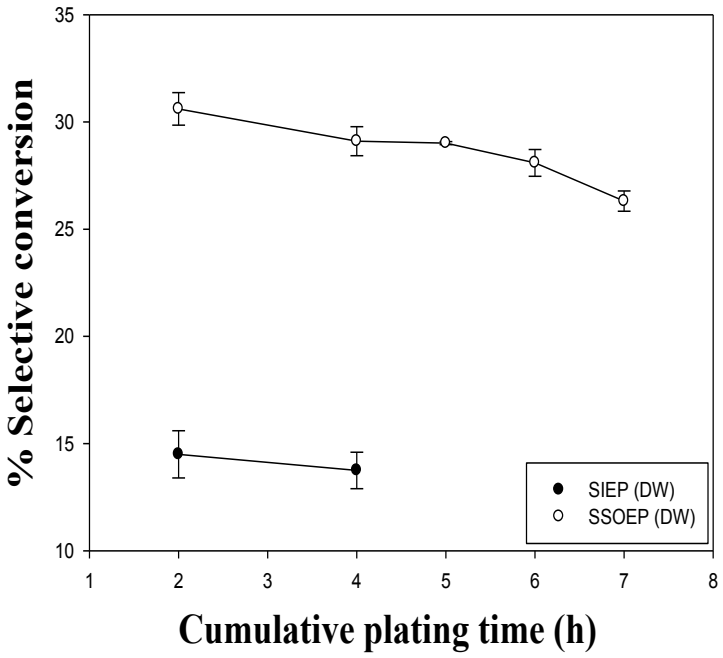

(a)

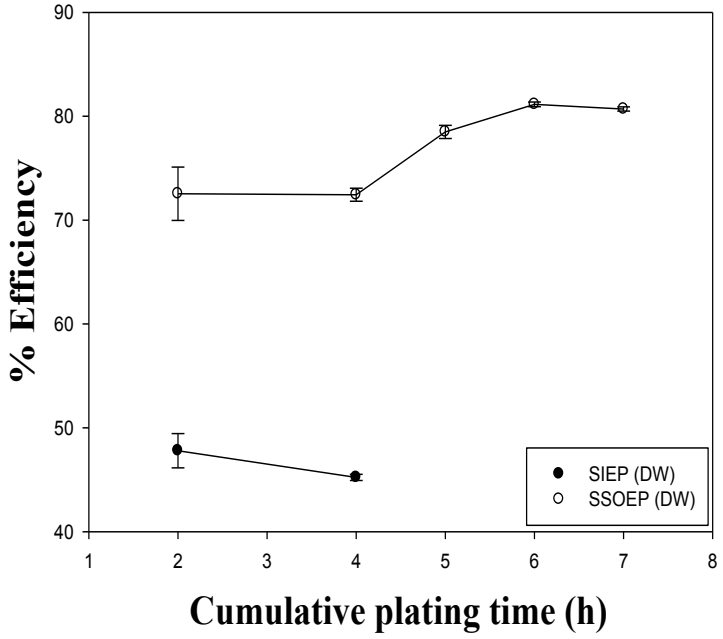

(b)

Figure 3.9: Effect of plating time on (a) Selective conversion and (b) Plating efficiency for SIEP (DW), SSOEP (DW) Pd baths.

Thus, it is apparent that, in terms of plating efficiency and selective conversions, there could exist better performance of the PW Pd ELP processes in comparison with the DW processes. This is possibly due to the variations in the adhesion strength of the Pd film during the initial stages of plating. It is hypothesized that DW processes would reduce metal nucleation in the solution by reducing effectively the available hydrazine solution concentration. However, it may not be able to enhance metal adhesion to the porous support. It might be the case that during DW processes in the initial stages of plating, the film adhesion strength could be comparatively poor, due to which metal attrition from the porous surface is higher and this favors greater metal nucleation in the plating solution. Therefore, the alteration of process parameters such as surfactant solution concentration could improve the plating efficiency and is worth investigating from the perspective of improving plating efficiency.

3.4.2 Plating rate

The rate of Pd metal deposition for both SIEP (DW) and SSOEP (DW) baths are summarized in Table 3.2. For SSOEP baths, the rate of metal deposition varied from 4.81 – 3.95 x 10^{-5} mol/m^2.s, whereas for SIEP baths the plating rate varied from 2.17 – 1.77 x 10^{-5} mol/m^2.s. It can be observed that the rate of palladium deposition for SSOEP (DW) baths are 2.2 – 2.6 times higher than those obtained for SIEP (DW) baths but slightly lower than those obtained for SSOEP (PW) bath which varied from 3.96 – 4.70 x 10^{-5} mol/m^2.s. This is possibly due to the greater role of surfactant solution concentration for SSOEP (DW) baths in comparison with the SSOEP (PW) baths. With respect to the SSOEP baths, it can be hypothesized that DW baths do not maintain the required concentration profile to improve adhesion strength of the as deposited film on the membrane surface. Therefore, it appears that further optimization of the process parameters is required.

Table 3.2 Time dependency of average plating rate for SIEP (DW) and SSOEP (DW) processes.

Rate enhancement technique	Average plating rate (mol/m^2.s)x10^5 for various total plating time(h))				
	2	**4**	**5**	**6**	**7**
SIEP (DW)	2.17	1.77	-	-	-
SSOEP (DW)	4.81	4.57	4.45	4.22	3.95

From a hypothesis perspective, the DW processes should have better depositional characteristics than PW processes, which is not the case.

3.4.3 Nitrogen flux profiles

Figure 3.10a and 3.10b depicts the nitrogen permeation flux trends for Pd-PSS membranes fabricated with SIEP (DW) and SSOEP (DW) plating baths. It can be observed that the SIEP process enabled the flux reduction from 0.252 - 10.11 mol/m^2.s (for an average pressure of 1.05 - 2.05 bar) to 0.237 - 9.66 mol/m^2.s (for an average pressure of 1.05 - 2.05 bar) after 4 h of sequential Pd ELP. For SSOEP, the nitrogen permeation flux reduced from 0.162 - 6.02 mol/m^2.s (for an average pressure of 1.06 - 2.05 bars) to 3.94 x10^{-5}- 1.24 x 10^{-3} mol/m^2.s for an average pressure of 1.17 - 2.05 bars) after 7 h sequential deposition. The maximum reduction of nitrogen flux was obtained after 6 h sequential deposition and is about 0 - 5.42 x 10^{-4} mol/m^2.s for an average pressure of 1.2 - 2.05 bars. The possible reason for the enhancement in the nitrogen permeation flux in the later stages of ELP is due to the higher concentration of surfactant which contributes to higher negative charge density on the substrate surface that enabled an uneven deposition of Pd metal. This is also confirmed by the continued enhancement in metal thickness on the membrane surface after 7 h of plating. Therefore, it is apparent that controlling

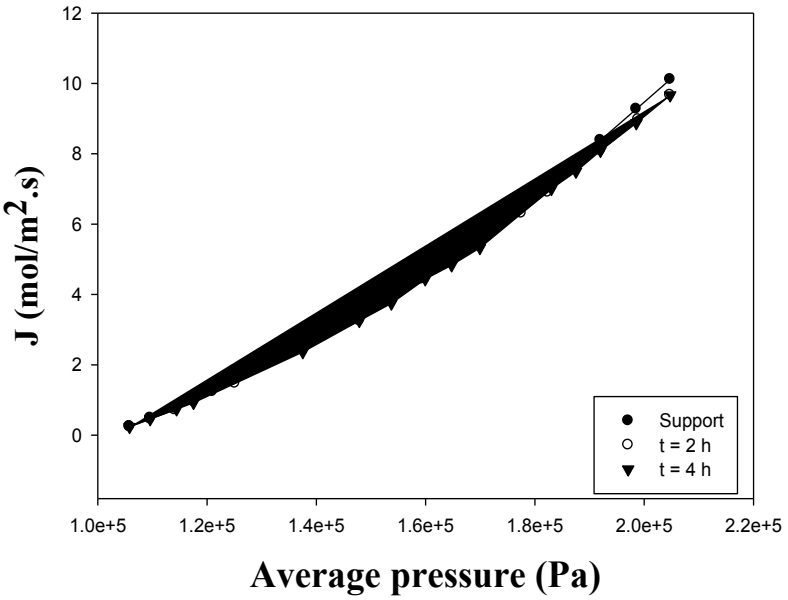

(a)

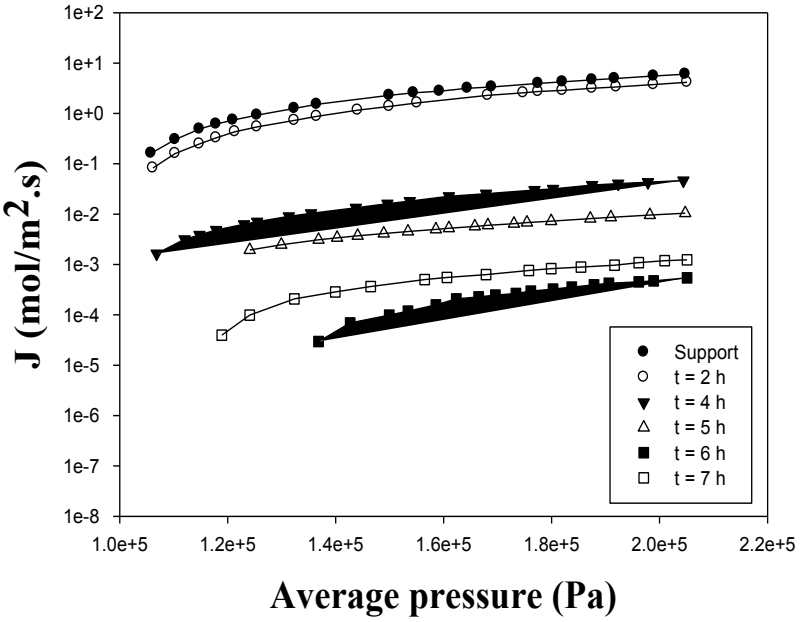

(b)

Figure 3.10: N_2 flux vs. average pressure plots for various membranes achieved with SIEP (DW) and SSOEP (DW) processes.

the film deposition characteristics during complete densification scenario appears to be the most challenging task using surfactant induced electroless plating baths and drop wise contacting pattern of the reducing agent is found to have insignificant affect towards minimization of such effects.

3.4.4 Percent pore densification

The dependency of percent pore densification on plating time for SIEP and SSOEP (DW) baths are shown in Figure 3.11a. For SIEP baths, it can be observed that after 4 h of sequential Pd deposition, the PPD is about 20.2% whereas for SSOEP (DW) baths, a PPD of 37.2% is achieved after 2 h of sequential Pd deposition. Also, for SSOEP process, a maximum PPD of 99.994% is obtained after 6 h of plating but in the 7^{th} h of plating, the PPD reduced to 99.98%. For comparison purposes, it can be observed that for the SSOEP (PW) processes, a maximum PPD of 99.82% is obtained after 6h of plating which is lower than that achieved in SSOEP (DW) bath. The probable reason for reduction of PPD after further plating is that once depositional saturation is achieved, higher concentration of surfactant would have enhanced the negative charge density on the substrate surface which enabled uneven metal deposition. This hypothesis has been reported in the literature [39]. The same is also confirmed with the enhancement in weight gain in the sequential plating steps but with a reduction in the PPD.

3.4.5 Thickness

Figure 3.11b shows the effect of plating time on deposited palladium film thickness for SIEP (DW) and SSOEP (DW) baths. For a total plating time variation from 2 – 4 h, it can be observed that for SIEP baths, the thickness of palladium film varied from 1.38 – 2.26 μm. However, for SSOEP plating baths, the time dependent enhancement in the Pd film thickness varied from

3.06-8.81 µm for a total plating time variation from 2 – 7 h, thus indicating that the SSOEP baths provided higher metal film thickness in comparison with the SIEP baths.

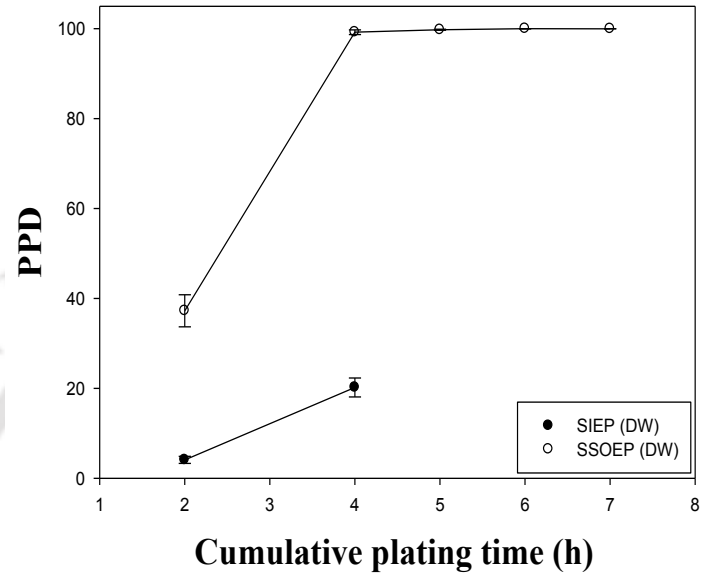

(a)

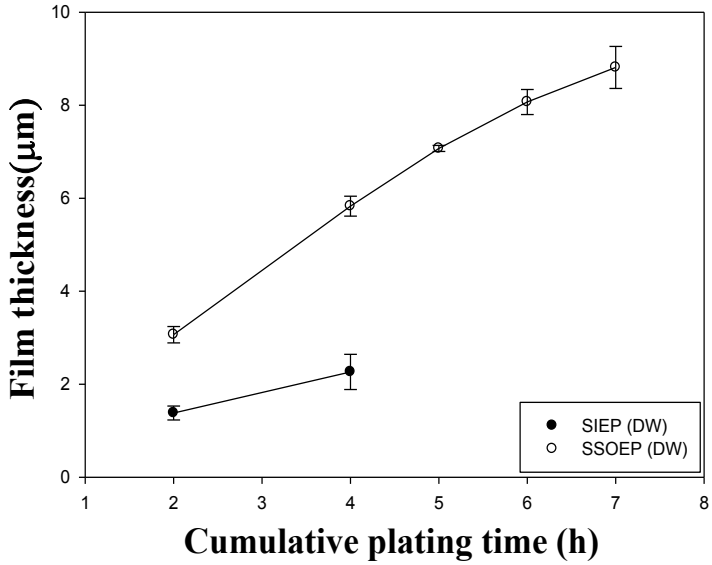

(b)

Figure 3.11: Variation of (a) PPD and (b) film thickness with plating time for SIEP (DW) and SSOEP (DW) processes.

(a) (b)

Figure 3.12: Photographs of (a) spent plating solution and (b) Pd/PSS membrane obtained for SSOEP (DW) process.

3.4.6 Physical Examination

The images of plating solution (obtained after Pd ELP) and the palladium membrane are shown in Figure 3.12 a and b respectively. In the novel SSOEP (DW) process, the formation of metal ions was not observed in plating solution during and after plating. After plating, it was also observed that palladium adhered properly onto the porous stainless steel substrate surface.

3.4.7 Advanced Characterization

3.4.7.1 Particle size distribution in solution after SSOEP (DW) process

The particle size distribution in the plating bath solution during drop wise addition of reducing agent was measured using Delsa Nano instrument. This Delsa nano can detect the particle size from the range of 0.1 - 6 nm. This instrument didn't detect the presence of particles in the plating solution after plating and hence the SSOEP (DW) can be regarded to be a very promising process for the ELP towards dense Pd membrane fabrication.

3.4.7.2 Morphological and surface characterization

Figure 3.13a shows the FESEM micrograph of Pd/PSS membranes fabricated with SSOEP (DW) bath at 4 CMC surfactant concentration. From the figure, it can be observed that finer Pd grains are distributed more uniformly on the substrate surface and do not exhibit small pin holes on the

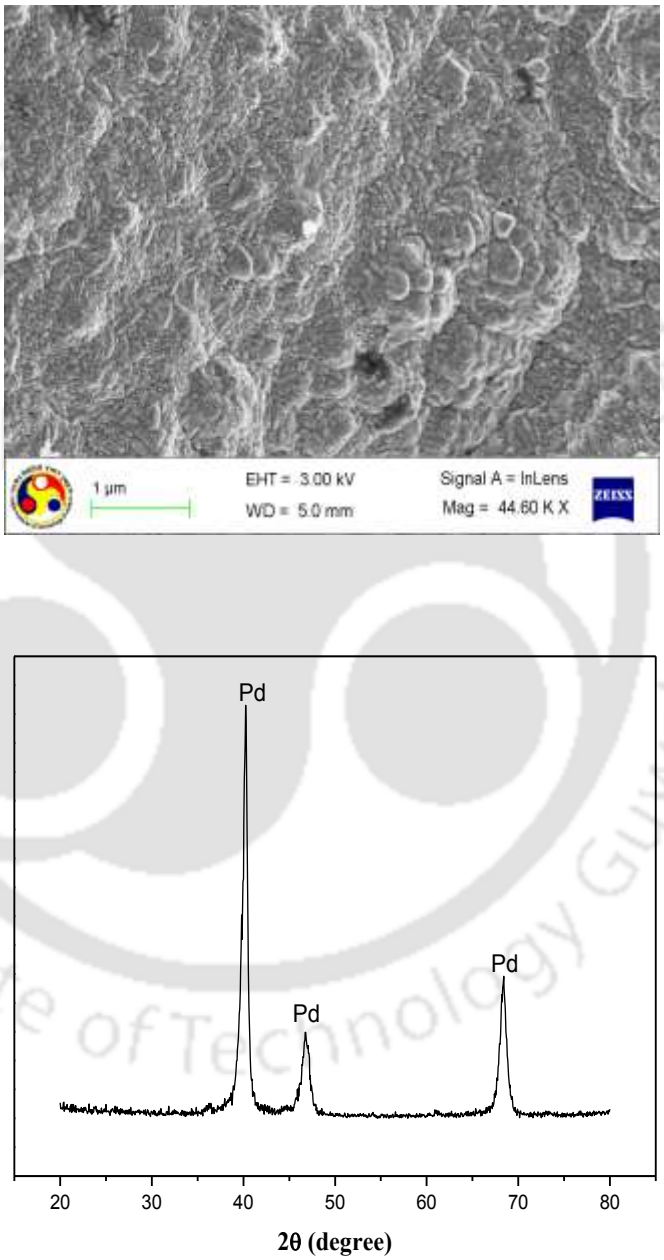

Figure 3.13: (a) FESEM micrograph and (b) XRD pattern of the Pd/PSS membrane fabricated with SSOEP (DW) bath at 0.005 M and 4 CMC CTAB initial concentration.

surface at the chosen magnification. However, room temperature nitrogen permeation experiments confirmed that the membrane had small pinholes by providing nitrogen permeance of 1.36×10^{-10} $m^3/m^2.s.Pa$.

Figure 3.13b shows the XRD pattern of Pd/PSS composite membrane fabricated with SSOEP (DW) bath at 4 CMC surfactant concentration. The XRD spectra indicate the existence of Pd reflection peaks at a diffraction angle (2θ) of 40.2°, 46.76° and 68.28° due to diffraction of (1 1 1), (2 0 0) and (2 0 2) plane and it confirmed the deposited Pd metal to be highly pure. No peaks associated to stainless steel composite membrane (that are not shown in a separate figure) have been observed and this indicates that the deposition has been dense from the perspective of the XRD analysis. However, in this case, fully dense membranes have not been obtained and this can be only confirmed with the gas permeation characteristics.

3.4.8 Tradeoffs

Figure 3.14a shows the dependence of $\frac{PPD}{\delta}$ on PPD for SIEP (DW) and SSOEP (DW) baths. For SIEP (DW) baths, after 4 h of Pd sequential plating, the $\frac{PPD}{\delta}$ values varied from 2.95 – 8.92 only. However, for SSOEP baths, the $\frac{PPD}{\delta}$ values varied from 12.14 – 11.34 for a variation in plating time from 2 to 7 h. For SIEP baths, the $\frac{PPD}{\delta}$ values are too low and this is due to poor pore densification using SIEP (DW) case. On the other hand, for SSOEP baths, $\frac{PPD}{\delta}$ profiles indicated reducing trend after 4 h of sequential plating, but played significant role towards the membrane pore densification. After 6 h of total plating time for these baths, the $\frac{PPD}{\delta}$ profile indicated saturation towards the membrane densification. Therefore, it is evident that SSOEP baths are beneficial towards the cost effective fabrication of dense Pd composite membranes.

Figure 3.14b illustrates (100-PPD) vs. selective conversion profiles for SIEP (DW) and SSOEP (DW) baths. For SIEP baths, the selective conversion and PPD varied from 14.5 – 13.75% and 4.1 – 20.2%, respectively, whereas for SSOEP baths, the selective conversion and PPD varied from 30.6 – 26.31% and 37.24 – 99.98%, respectively. For SIEP baths, the selective conversions and PPD values are much lower than the SSOEP baths, thus indicating that SSOEP (DW) provides the best conditions for Pd electroless plating to fabricate dense palladium membranes.

Figure 3.14c shows the profiles $\frac{PPD}{\delta}$ vs. α^{th} for SSOEP baths. It can be evaluated that the $\frac{PPD}{\delta}$ and α^{th} varied from 17.02 – 11.34 and 5.0 – 480.2, respectively. After 4 h of Pd sequential plating, the theoretical selectivities enhanced to values above Knudsen selectivity. The maximum selectivity of 480.2 is obtained after 6 h of Pd sequential deposition. After 7th h of plating, the selectivities further reduced to 114.3. This is due to the de-lamination of Pd film from the membrane surface due to inefficient deposition on the membrane surface, which is brought forward by uneven distribution of negative charge densities on the membrane surface at higher surfactant concentrations. Thus, surfactant concentrations need to be further optimized to achieve dense palladium membranes and this will be addressed in the next chapter.

A plot of average theoretical hydrogen flow rate (with in the pressure range of 0.01 – 5 bar) vs. α^{th} for various membranes fabricated using SSOEP (DW) baths are shown in Figure 3.14d. Ideally, the best process shall indicate maximum combinations of both these values and hence the profiles shall be located in the extreme right and top portion of the plot. The membranes fabricated using SSOEP (DW) baths have been evaluated to offer average theoretical hydrogen flow rates of 0.148 – 0.072 LPM and selectivities of 5 – 480. The maximum selectivity of 480 is obtained after 6 h of Pd plating which reduced to 114 after 7th h of plating. For comparison

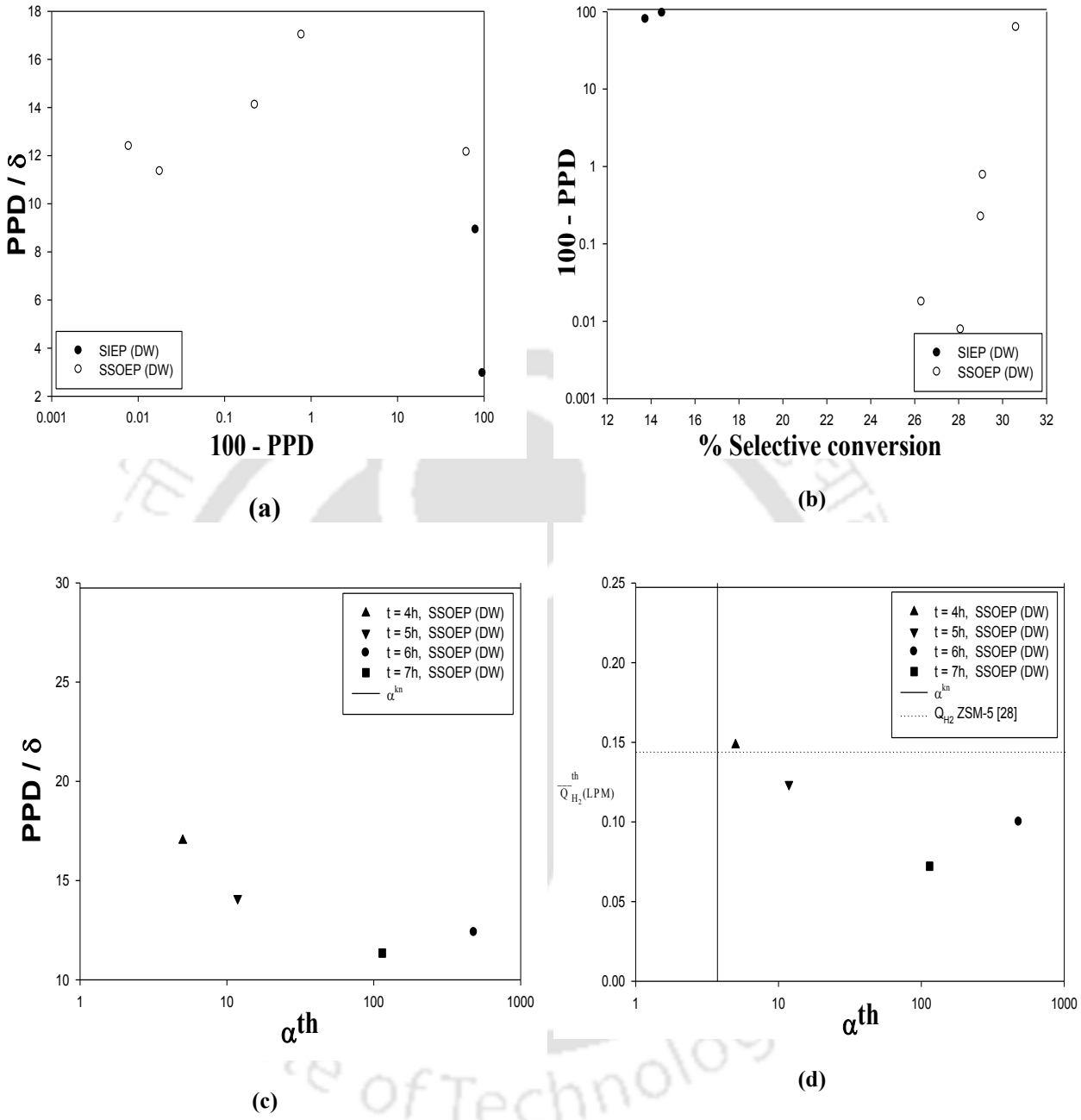

Figure 3.14: Tradeoffs of (a) PPD/ δ vs. (100 - PPD) (b) (100 - PPD) vs. Selective conversion (c) $\frac{\text{PPD}}{\delta}$ vs. α^{th} and (d) $\overline{Q}^{th}_{H_2}(\text{LPM})$ vs. α^{th} for SIEP (DW) and SSOEP (DW) processes.

purpose, the average hydrogen flow rate of ZSM-5 [63] is also presented in the figure and the obtained theoretical hydrogen flow rates of the prepared membranes are comparable with the

average hydrogen flow rate of the ZSM-5 [63] membrane. An important trade-off for the comparison of various rate enhanced Pd electroless plating processes is with respect to pore densification vs. average plating rate. While average plating rate may remain fairly constant for several rate enhanced electroless plating processes, the PPD profiles need not be. Such interesting tradeoffs for the investigated surfactant induced plating baths are summarized in Figure 3.15, which presents tradeoffs in terms of (100 – PPD), which is a convenient measure of the extent of non-densification. Ideally (100 – PPD) shall be zero for dense Pd composite membranes. As shown, for SOEP (PW) and SSOEP (PW) baths, for a total plating time of 6 h, the extent of non–densification and plating rates varied from 90.05 to 15.26%, 5.28×10^{-5} to 4.77×10^{-5} mol/m^2.s and 86.65 to 0.18%, 3.96×10^{-5} to 4.70×10^{-5} mol/m^2.s, respectively. For SSOEP (DW) baths, for a total plating time of 7 h, the extent of non-densification and plating

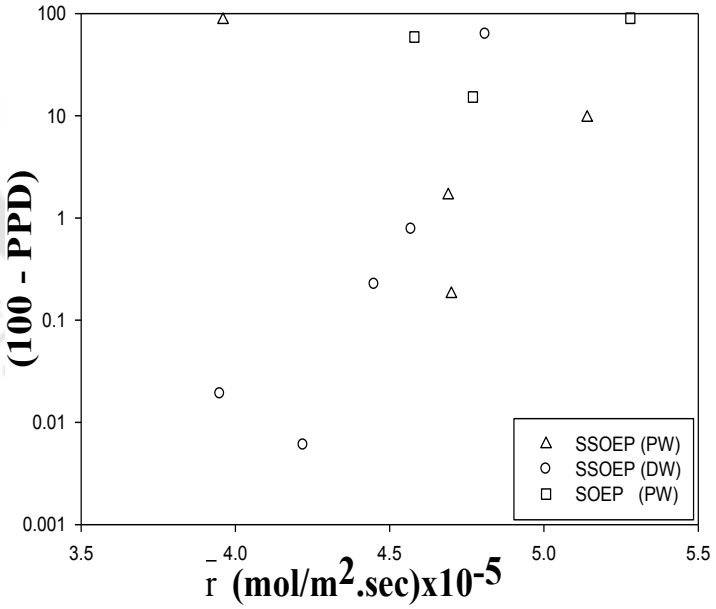

Figure 3.15: Tradeoffs of (100 - PPD) vs. $\bar{r}_{Pd}$ for SOEP (PW), SSOEP (PW) and SSOEP (DW) processes.

rates varied from 62.76 to 0.0178% and 4.81×10^{-5} to 3.95×10^{-5} mol/m^2.s, respectively. For SOEP baths, even though the plating rates are high, the extent of non-densification is much higher than that in SSOEP (PW) and SSOEP (DW) baths. The desired combination of minimal non-densification and maximum plating rate is obtained only for SSOEP (DW) baths, which also indicate a synchronized reduction in the profiles with increasing periods of total plating time.

3.4.9 Summary

This chapter identified an efficient Pd electroless plating process for the fabrication of dense Pd composite membranes. Three important inclusions namely reduction of Pd solution concentration, coupling of sonication and drop wise contacting pattern of the reducing agent are the principal features of the suggested novel plating process, which has not been reported till date in the literature for the fabrication of dense Pd membranes. The identified process refers to a combination of sonication under degas mode of operation, cationic surfactant CTAB and drop wise contacting pattern of the hydrazine reducing agent to achieve dense Pd composite membranes using highly improved rate enhanced Pd electroless plating process. The identified method i.e., SSOEP (DW) process provided higher combinations of plating efficiencies (80.69%), selective conversions (26.31%), pore densification (99.994%) and plating rates (3.95×10^{-5} mol/m^2.s) and minimal combinations of palladium solution concentration (0.005 mol/L), CTAB surfactant solution concentration (4 CMC) and total plating time (7 h).

The methodology indicated in the chapter addresses the combinatorial process - product perspective for the fabrication of dense palladium composite membranes and is generic in nature for extension towards materials engineering research. Also, this thesis highlighted upon significant number of tradeoffs that could serve as guidelines towards materials fabrication engineering research and development. Conceptually, the utilization of theoretical selectivity

concept to foster upon the efficacy of rate enhanced electroless plating processes is a significant development that is anticipated to receive fair contribution from other researchers across the world in the field of materials science and engineering associated to metal membrane fabrication research.

Chapter 4:

Optimality of Process Parameters for Optimal Rate Enhanced Pd ELP Process

Chapter 4

Optimality of Process Parameters for Optimal Rate Enhanced Pd ELP process

This chapter addresses parametric studies for SSOEP (DW) Pd ELP baths for dense Pd composite membrane fabrication. The results for various investigated cases are presented in three sections. Section 4.2 addresses the effect of Pd solution concentration on the combinatorial plating characteristics. Section 4.3 presents the results obtained for the variation in surfactant concentration at the optimal Pd solution concentration. Section 4.4 outlines upon the effect of loading ratio on the combinatorial plating characteristics. Section 4.5 summarizes results from surface characterization studies. Section 4.6 addresses the cost analysis of prepared membranes with best conditions in this work and those presented in the literature.

4.1 Introduction

In the previous chapter, a novel process has been identified to provide the best combinations of various process and membrane characteristics for dense Pd composite membrane fabrication. Precisely, refers to surfactant and sonication assisted Pd ELP baths supplemented with drop wise addition of the hydrazine reducing agent (SSOEP (DW)). In this chapter, the results obtained from the parametric studies conducted with the SSOEP (DW) plating baths are being presented. The parametric studies specifically refer to variations in Pd solution concentration (0.005 and 0.010 M), surfactant solution concentration (1 – 4 CMC) and loading ratio (203 and 407 cm^2/L). The next section addresses the effect of Pd solution concentration on the combinatorial Pd ELP characteristics.

4.2 Effect of Pd solution concentration on the combinatorial electroless plating characteristics

To evaluate upon the effect of Pd solution concentration on combinatorial plating characteristics, the Pd solution concentrations are taken as 0.005 M and 0.01 M and the surfactant solution concentration was taken as 4 CMC. All plating experiments were conducted using Pd ELP process setup shown in Figure 2.2b.

4.2.1 Selective conversion and plating efficiency

Figure 4.1a and 4.1b shows the variation of selective conversion and plating efficiencies with plating time for Pd ELP baths containing Pd solution concentration of 0.005 M and 0.01 M respectively. As shown, with an increase in Pd solution concentration from 0.005 M to 0.01 M, both selective conversion and plating efficiencies reduced from 30.61 – 26.31% to 25.56 – 26.54 and 72.53 – 80.69% to 59.77 – 69.99 %, respectively. Even though the concentrations of reactants are higher in 0.01 M plating baths, both selective conversions and plating efficiencies are much lower due to the presence of limited active sites on the membrane surface. In other words, excess Pd solution concentration did not enhance selective conversions and plating efficiencies. The Pd electroless plating process is an autocatalytic surface reaction and therefore, higher solution concentrations did not enhance the conversions and this indicates that the surface reaction is rate limiting but not solution concentration. However, this does not indicate that the plating rates could be lower for higher Pd solution concentration, as the conversion evaluation is a function of the Pd solution concentration. Therefore, even though lower selective conversions were obtained at higher solution concentration, the selective conversions were evaluated with respect to higher solution concentration and this indicates higher average plating rates.

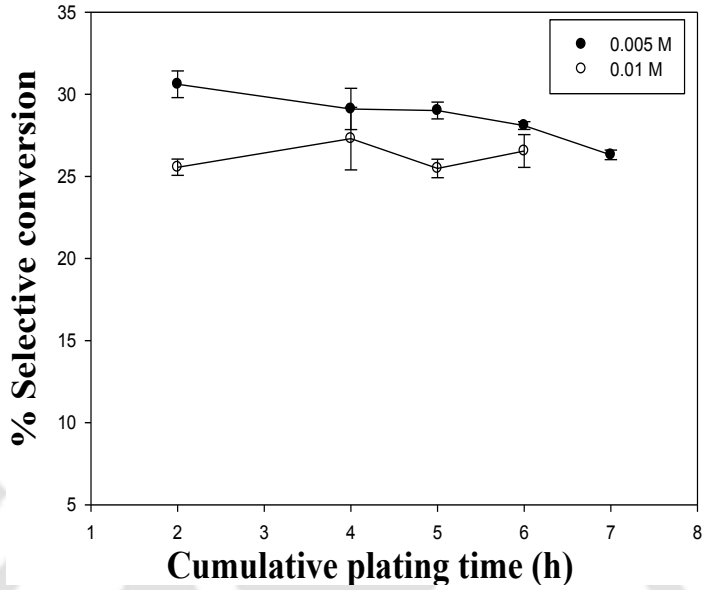

(a)

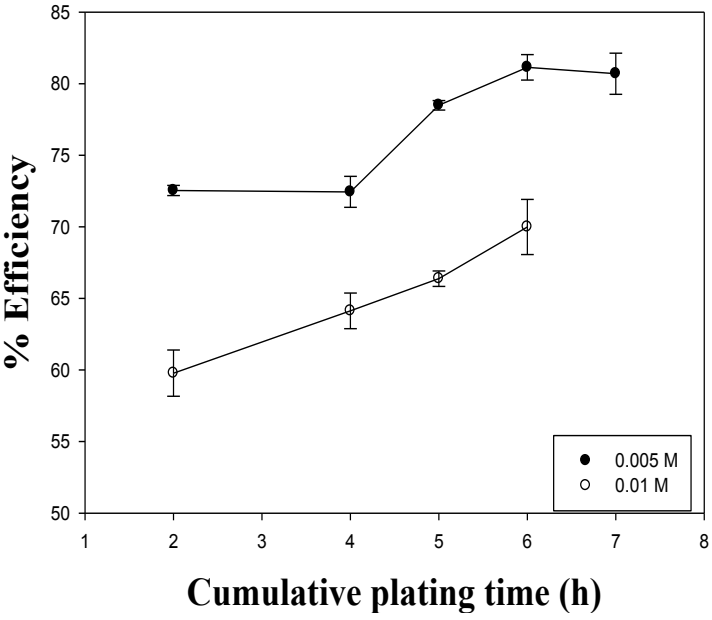

(b)

Figure 4.1: Effect of Pd solution concentration on the time dependent profiles of (a) Selective conversion and (b) Plating efficiency for SSOEP (DW) process.

Table 4.1: A summary of the variation in the time dependent average plating rate with Pd solution concentration for SSOEP (DW) process.

Pd solution concentration (M)	Average plating rate (mol/m^2.s)× 10^5 for various total plating time (h)				
	2	**4**	**5**	**6**	**7**
0.005	4.81	4.57	4.45	4.22	3.95
0.01	6.97	7.45	6.95	7.24	-

4.2.2 Plating rate

Table 4.1 presents the variation in average plating rates with respect to plating time for Pd solution concentrations of 0.005 M and 0.01 M plating baths. It can be observed that for 0.005 M plating baths, the average plating rates varied from 4.81 – 3.95 x 10^{-5} (mol/m^2.s), which is significantly lower than the corresponding values obtained at 0.01 M Pd ELP baths (6.97 – 7.24 x 10^{-5} mol/m^2.s). The increase in metal plating rates with increasing solution concentration is due to the presence of more availability of Pd metal in the plating bath.

4.2.3 Nitrogen permeation flux tradeoffs

Figure 4.2a and 4.2b shows the nitrogen permeation flux trends for Pd-PSS membranes fabricated using SSOEP baths containing palladium solution concentrations of 0.005M and 0.01M respectively. Using 0.005 M Pd solution concentration, the SSOEP (DW) baths enabled the flux reduction from 0.162 – 6.018 mol/m^2.s (for an average pressure of 1.06 – 2.05 bars) to 3.94 – 1.24 x 10^{-3} mol/m^2.s (for an average pressure of 1.19 – 2.05 bar) after 7 h of sequential Pd ELP. For a Pd solution concentraton of 0.01 M, the flux reduced from 0.204 – 8.48 mol/m^2.s (for an average pressure of 1.05 – 2.05 bar) to 5.33x10^{-4} – 6.11x10^{-3} mol/m^2.s (for an average pressure of 1.12 – 2.04 bar) after 6 h of sequential Pd ELP. Also, for both these cases, during the first 2 h of plating, the reduction in nitrogen permeation flux is low. This is possibly due to

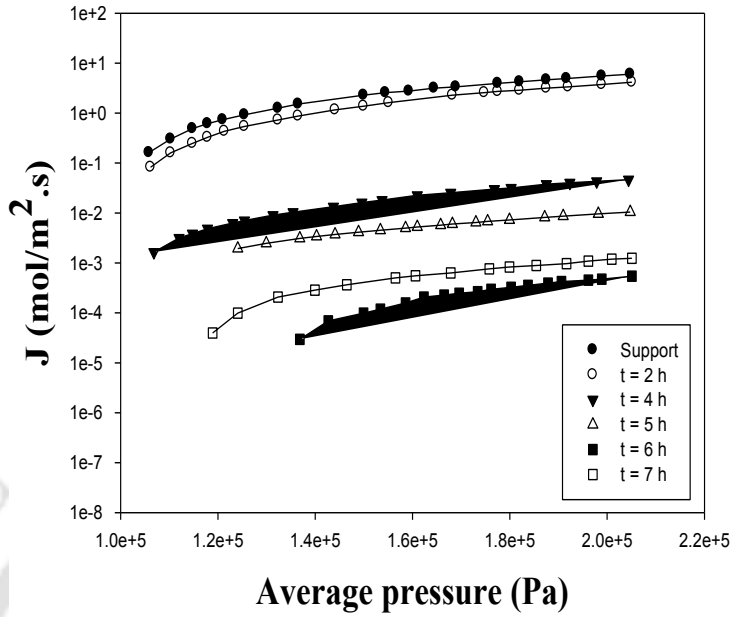

(a)

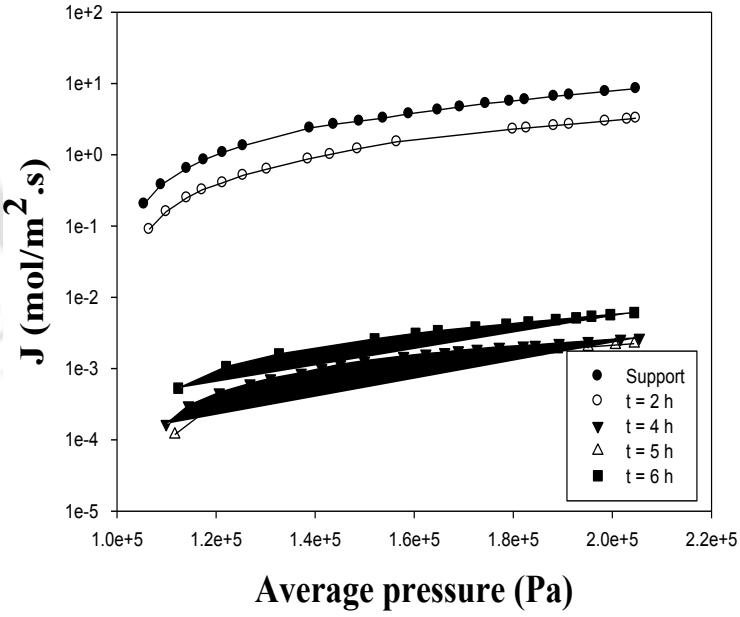

(b)

Figure 4.2: N_2 flux profiles for Pd/PSS membranes fabricated with (a) 0.005 M and (b) 0.01 M Pd solution concentration.

normalization of palladium deposited on the surface. For 0.005M Pd solution concentration, the maximum reduction of nitrogen permeation flux was obtained after 6 h plating and thereafter the flux increased to $3.94x10^{-5}$ – $1.24x10^{-3}$ mol/m^2.s (for an average pressure of 1.19 – 2.05 bar) for further 1h plating. Similarly, for 0.01M Pd solution concentration, the maximum reduction of nitrogen flux is obtained after 5 h of sequential plating and the permeate flux increased to $5.33x10^{-4}$ – $6.11x10^{-3}$ mol/m^2.s (for an average pressure of 1.12 – 2.04 bar) after 6 h of Pd sequential plating. In summary, it can be analyzed that higher Pd solution concentration using SSOEP (DW) ELP baths enhanced N_2 flux. This indicates that faster Pd deposition on the support surface did not enable better surface pore coverage. These aspects would be further elaborated in the next section. In summary, the chosen lower solution concentration is optimal to provide good Pd plating characteristics.

4.2.4 Percent pore densification

Figure 4.3a illustrates the time dependent PPD profiles for Pd ELP baths containing 0.005 M and 0.001 M Pd solution concentrations. It can be observed that for 0.005 M case, the PPD varied from 37.24 – 99.982% after 7 h of sequential ELP. However, for the 0.01 M case, the PPD varied from 66.76 – 99.94% after 6 h of sequential ELP. Further, it can be also observed that for 0.005 M bath, the maximum PPD of 99.992% was achieved after 6 h of Pd ELP which reduced to 99.982% after 1 h of additional ELP. For 0.01 M case, the maximum PPD of 99.97% was achieved after 5 h of plating time which reduced to 99.94% after 1 h of additional plating. For both cases, the plating bath could not provided fully dense membranes within the set maximum time of deposition. The reduction of PPD at higher plating times is due to higher negative charge density on the substrate surface at higher CMC values of the surfactant which contribute to

uneven deposition of palladium. Due to this reason, it is anticipated that metal delamination occurs selectivity from densified zones of the membrane surface.

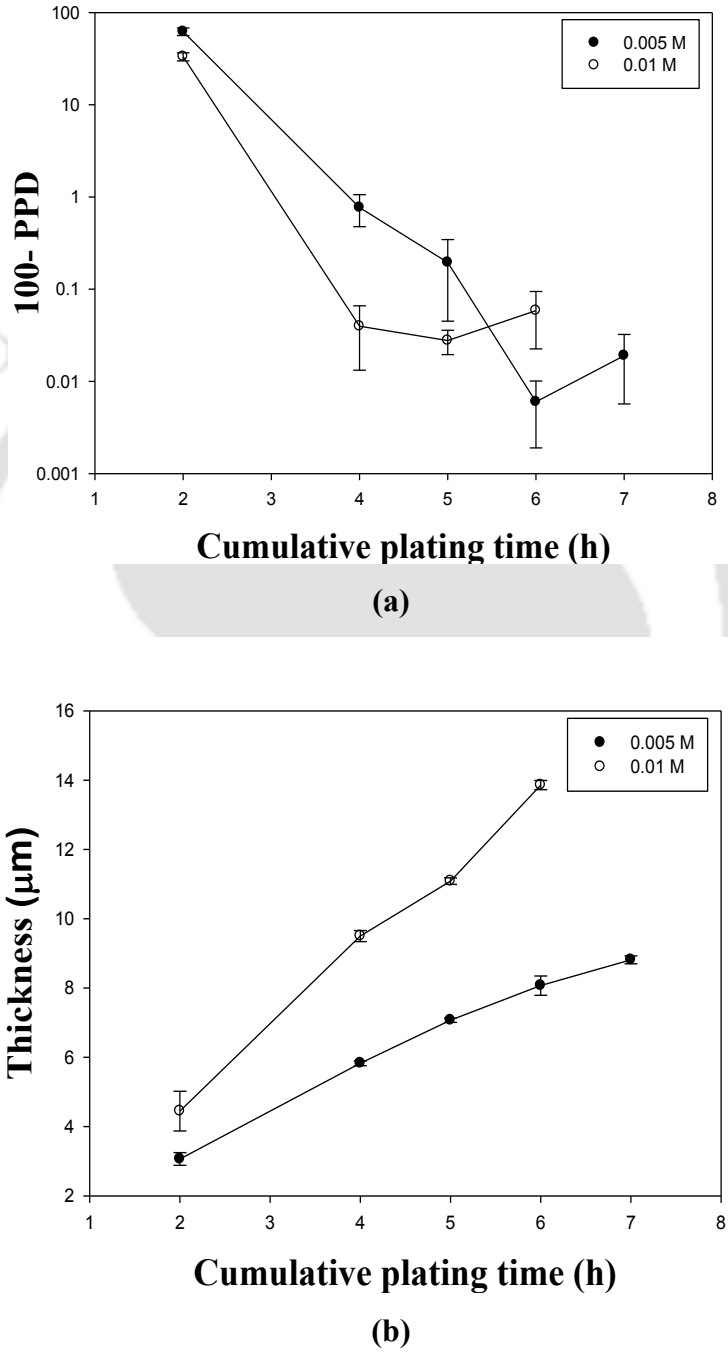

Figure 4.3: Variation of time dependent (a) (100 – PPD) and (b) Pd film thickness with Pd solution concentration (0.005 and 0.01 M).

4.2.5 Metal film Thickness

Figure 4.3b shows the variation of palladium film thickness with plating time for ELP baths containing 0.005 M and 0.01 M Pd solution concentration. It can be observed that the palladium film thickness varied from 3.06 – 8.81µm for 0.005 M case and 4.44 – 13.85 µm for 0.01 M case. Thus, higher Pd solution concentrations provided higher deposition rates of Pd, but could not enhance the PPD. This is due to faster deposition on the membrane surface which did not enable further surface mobility of the as deposited film to other sections of the membranes where porous structures are significantly prevalent. Therefore, from the perspective of achieving dense Pd composite membranes, lower Pd solution concentration of 0.005 M is only recommendable.

4.2.6 PPD tradeoffs

Figure 4.4a illustrates the tradeoffs associated with $\frac{PPD}{\delta}$ vs. PPD for SSOEP baths containing palladium solution concentrations of 0.005 and 0.01 M. For 0.005 and 0.01 M Pd solution concentrations, it can be observed that the $\frac{PPD}{\delta}$ varied from 12.15 – 12.39 and 15.01 – 7.21 respectively. Further, it can be observed that the lower Pd solution concentration case indicated a declining trend in $\frac{PPD}{\delta}$ without any lapse mode which was not the case for the higher Pd solution concentration case. For the case of 0.01M Pd solution concentration, the $\frac{PPD}{\delta}$ profile indicated reducing trend after first 2 h of Pd ELP which eventually reached saturation after 5 h of total plating time. Therefore, it is apparent that higher solution concentration is not favourable towards dense metal composite membrane fabrication using SSOEP (DW) process.

Figure 4.4b illustrates (100 – PPD) vs. selective conversion profiles for SSOEP baths with Pd solution concentration of 0.005 and 0.01 M. For the case of 0.005 M Pd solution concentration,

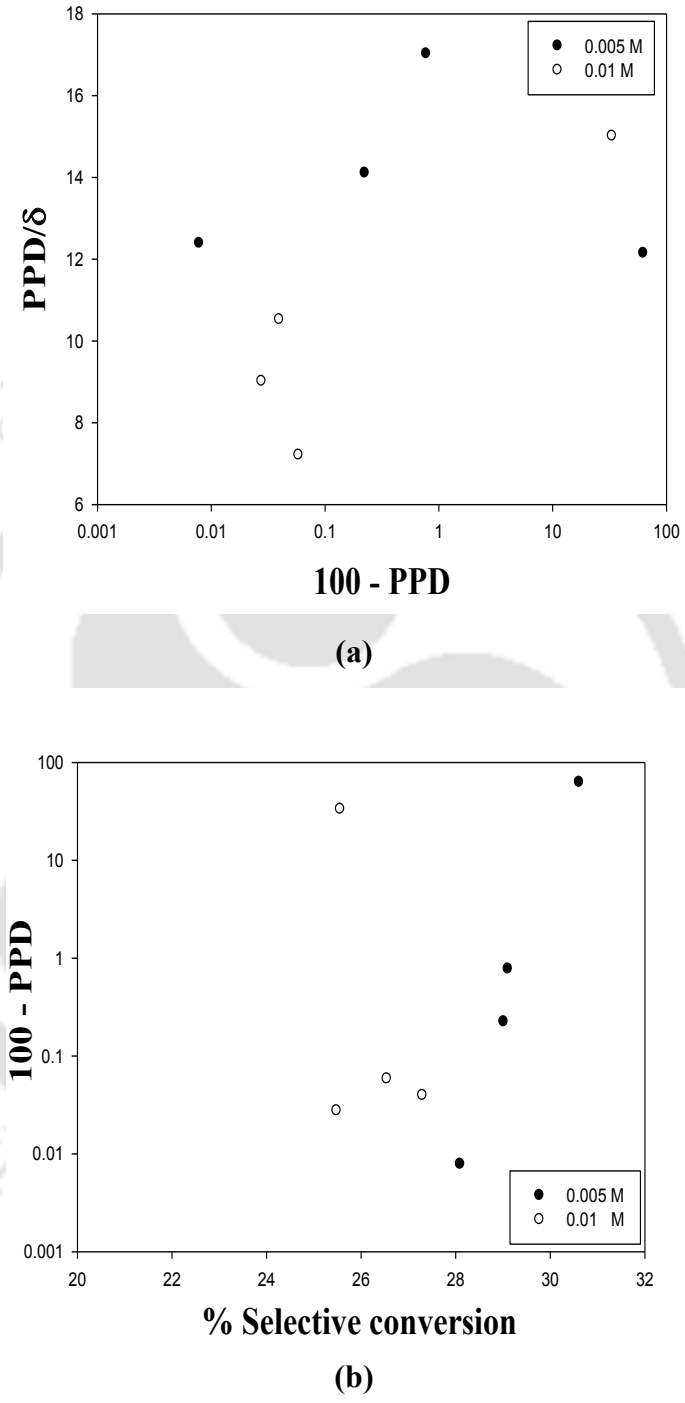

Figure 4.4: Tradeoffs for (a) PPD/δ vs (100 – PPD) and (b) Selective conversion vs (100 – PPD) for SSOEP (DW) processes at 0.005 and 0.01 M Pd solution concentrations.

the selective conversion and PPD varied from 30.61 – 28.09% and 37.24 – 99.992% respectively. However, for 0.01 M Pd solution concentration case, the selective conversion and PPD varied from 25.55 – 26.54% and 66.76 – 99.94 % respectively. Further, it can be also observed that there is a lapse mode in the profile corresponding to the 0.01 M case which is indicating its non-optimality. In other words, the best combination of selective conversion and PPD were identified for SSOEP (DW) baths with 0.005 M Pd solution concentration.

4.2.7 Summary

An enhancement in Pd solution concentration did not provide better pore densification and improve the pore densification of fabricated dense Pd composite membranes. Therefore, higher Pd solution concentration of 0.01 M with 4 CMC surfactant concentrations is not favourable for the fabrication of dense Pd membranes. Since surfactant concentration plays a crucial role in membrane densification, the next section addresses the results obtained with variation of surfactant solution concentration. Thereby, the objective of the next section is to identify optimal surfactant solution concentration.

4.3 Effect of surfactant concentration on the combinatorial electroless plating characteristics

The section addresses the effect of surfactant solution concentration (1, 2 and 4 CMC) on the combinatorial plating characteristics of Pd composite membranes. For these experiments, the initial Pd solution concentration was maintained at 0.005 M. Based on the obtained combinatorial plating characteristics, the optimal surfactant concentration would be identified for SSOEP (DW) process.

4.3.1 Selective conversion and Plating efficiency

Figure 4.5a and 4.5b illustrate the time dependent selective conversion and plating efficiency profiles for the surfactant solution concentration of 1 CMC, 2 CMC and 4 CMC. It can be

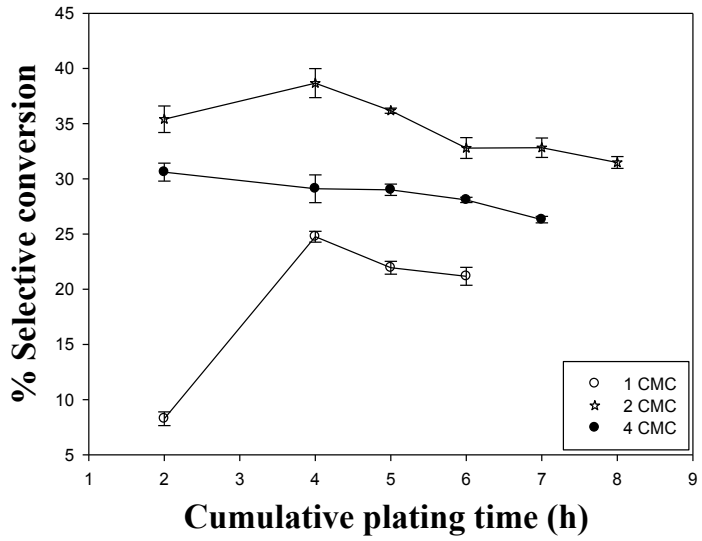

(a)

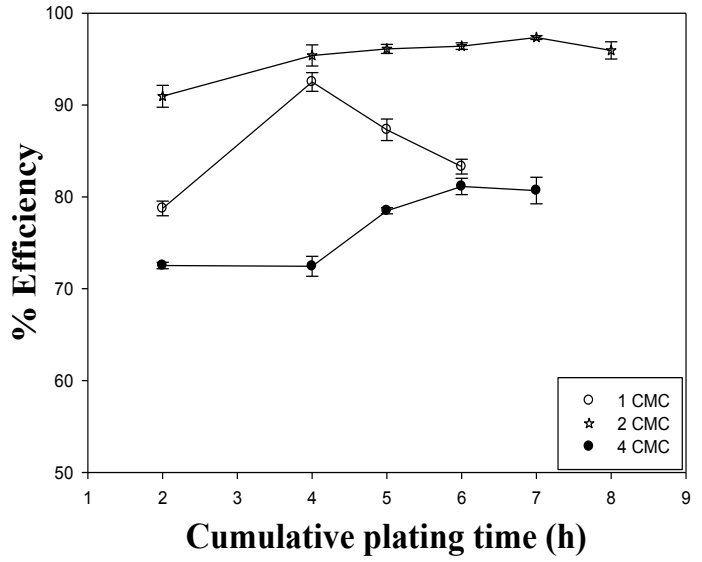

(b)

Figure 4.5: Effect of surfactant solution concentration on the time dependent profiles of SSOEP (DW) processes (a) selective conversion and (b) plating efficiency.

observed that, with an increase in surfactant concentration from 1 to 2 CMC, both selective conversion and plating efficiency values increased from 8.27 – 21.17% to 35.4 – 31.48% and 78.74 – 83.29% to 90.95 – 95.94%, respectively. A further enhancement in surfactant solution concentration from 2 to 4 CMC indicated a reduction in the trends for both selective conversion (30.61 – 26.31%) and plating efficiency (72.53 – 80.69 %) profiles. This is possibly due to the aggregation of surfactant molecules on the substrate surface at 4 CMC surfactant concentration. These observations are in agreement with Chen et al. [39] who reported that at high concentration, surfactant molecules forms cylindrical aggregates on substrate surface, which enable variations in the charge distributions on the surface. These variations promote plating in-efficiency due to the undesired metal delamination. Further, surfactant adsorption to the support surface could inhibit the metal plating on the surface and hence the conversions would decrease.

4.3.2 Plating rate

The variation of average Pd plating rate with total plating time for surfactant concentrations of 1, 2, and 4 CMC in the baths are presented in Table 4.2. It can be observed that the plating rates varied in the range of 1.13 – 2.89×10^{-5} mol/m^2.s for 1 CMC, 4.92 – 4.38×10^{-5} mol/m^2.s for 2 CMC, and 4.81 – 3.95×10^{-5} mol/m^2.s for 4 CMC cases. With an increase in surfactant concentration from 1 to 2 CMC, the nitrogen gas bubbles are removed more quickly from the substrate surface. Thereby, average plating rates are enhanced. However, a further increase in surfactant concentration (from 2 to 4 CMC) may have caused the surfactant molecules to form cylindrical aggregates on the substrate surface and inhibit the metal deposition rate. Similar hypothesis was presented by Chen et al. [39].

Table 4.2: Effect of surfactant solution concentration on the time dependence of average plating rate

Surfactant concentration	Average plating rate (mol/m^2.s)× 10^5 for various total plating time (h)					
	2	**4**	**5**	**6**	**7**	**8**
1 CMC	1.13	3.38	2.99	2.89	-	-
2 CMC	4.92	5.38	5.03	4.56	4.56	4.38
4 CMC	4.81	4.57	4.45	4.22	3.95	-

4.3.3 Nitrogen flux tradeoffs

Figure 4.6 (a-c) presents the nitrogen flux through palladium membrane fabricated with 1, 2 and 4 CMC CTAB solution concentrations. For 1 CMC case, the nitrogen flux reduced from 0.146 – 6.41 mol/m^2.s (for an average pressure of 1.05 – 2.05 bar) to 5.72x10^{-3} mol/m^2.s (for an average pressure of 1.09 – 2.05 bar). However, for the 2 CMC case, the nitrogen flux reduced from 0.211 – 8.77 mol/m^2.s (for an average pressure of 1.05 – 2.047 bar) to 0 – 0 mol/m^2.s (for an average pressure of 1.17 – 2.05 bar) after 8 hours of sequential plating. In other words, a dense Pd membrane has been successfully fabricated, which is the major objective of this work and has been fulfilled through a novel fabrication process involving surfactant, sonication under degas mode and drop wise addition of hydrazine to the plating solution. This is not the case in the literature where it was indicated that SIEP with 4 CMC DTAB surfactant solution concentration is optimal to obtain a dense Pd membrane using stainless steel support of average pore size of 200 nm, Pd solution concentration of 0.015 M and a total plating time of 10 h [38]. This work corresponds to the dense Pd membrane fabrication using SSOEP (DW) process using 2 CMC of CTAB surfactant, stainless steel support of 100 nm average pore size, Pd solution concentration of 0.005 M and a total plating time of 8 hours (16 plating steps of 30 minutes duration each).

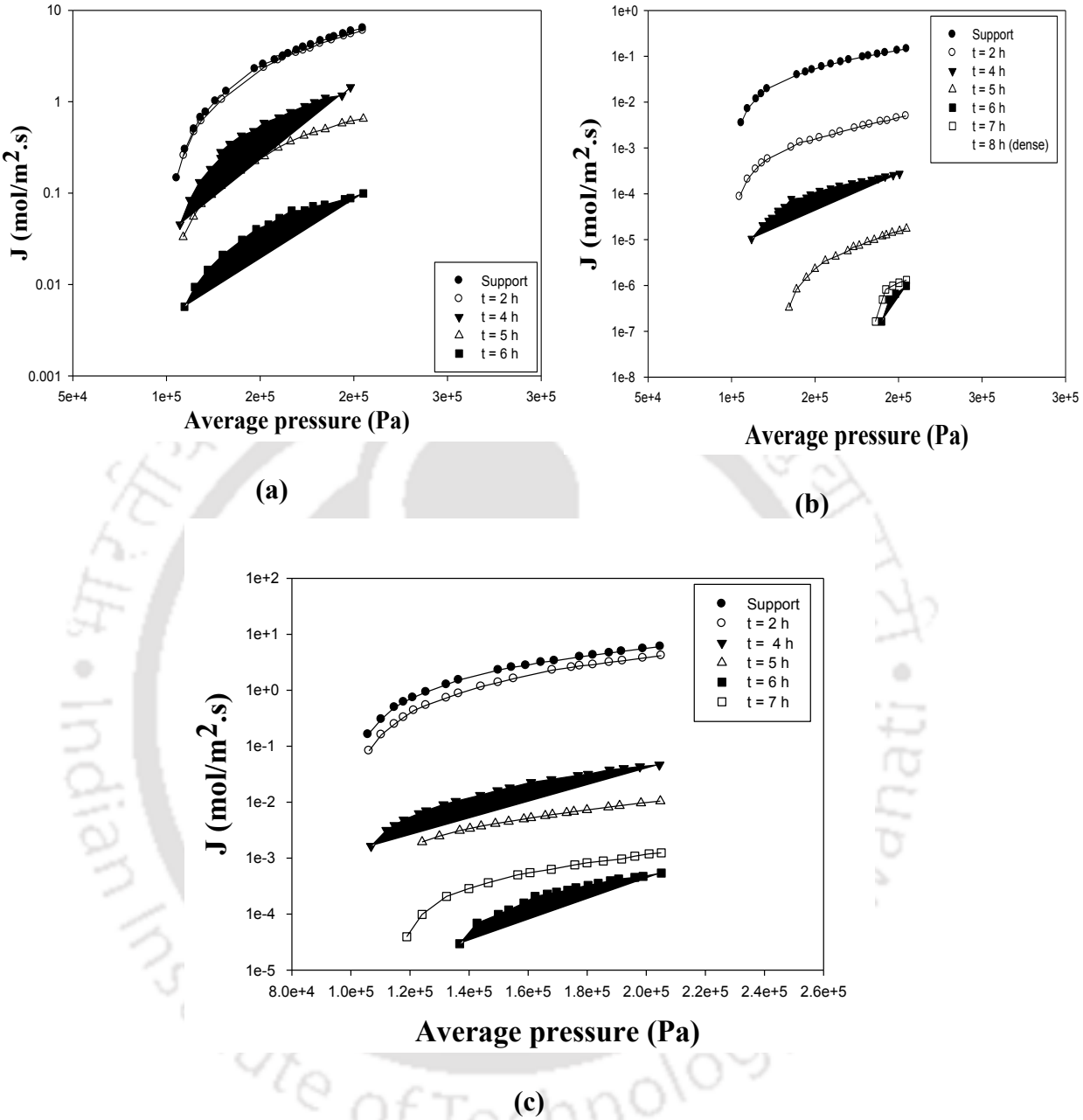

Figure 4.6: N_2 flux vs average pressure plots for Pd/PSS membranes fabricated with (a) 1 CMC (b) 2 CMC and (c) 4 CMC surfactant solution concentrations.

Comparatively, it can be observed in the figure that the nitrogen flux profiles of 2 CMC case are placed below the profiles obtained using 4 CMC case. Hence, 2 CMC concentration is the

recommended surfactant concentration for the electroless fabrication of dense Pd composite membranes using SSOEP (DW) process.

4.3.4 Percent pore densification

Figure 4.7a presents the time dependent PPD for plating baths with surfactant solution concentrations of 1, 2, and 4 CMC. It can be observed that after 6 h of Pd ELP, the PPD values are 98.29, 99.9999 and 99.994% for 1, 2 and 4 CMC Pd ELP baths respectively. For an additional 1 h Pd ELP, the PPD values reduced to 99.9998% and 99.981% for 2 and 4 CMC surfactant concentrations respectively. Also, it can be observed that the lapse mode of densification profile is also evident in the 2 and 4 CMC cases. However, the lapse mode of the PPD profile is not very significant for the 2 CMC case. In other words, the 2 CMC solution concentration of the surfactant has been able to negate the variations in charge densities on the membrane surface to foster towards 100% metal densification. This was not the case for the 4 CMC bath where the lapse at the later stage of the plating (from 6 to 7 h) is very significant. The minimization of the lapse in the profile of the PPD is a very important phenomenon that has not been reported so far in the literature. While generalized reasons for lapse have been presented in the literature in terms of the negative surface charge density distributions, their minimizations have not been reported and especially towards 100% Pd metal composite membrane fabrication. Therefore, the role of surfactant concentration to induce various desired and undesired surface affects is apparent with the observed trends. The desired effect of surfactant addition is minimization of pitting and wettability alteration and the undesired effect of surfactant addition is the strong variation in the surface charge density and inhibition of metal plating, which is apparent at higher surfactant concentrations (4 CMC).

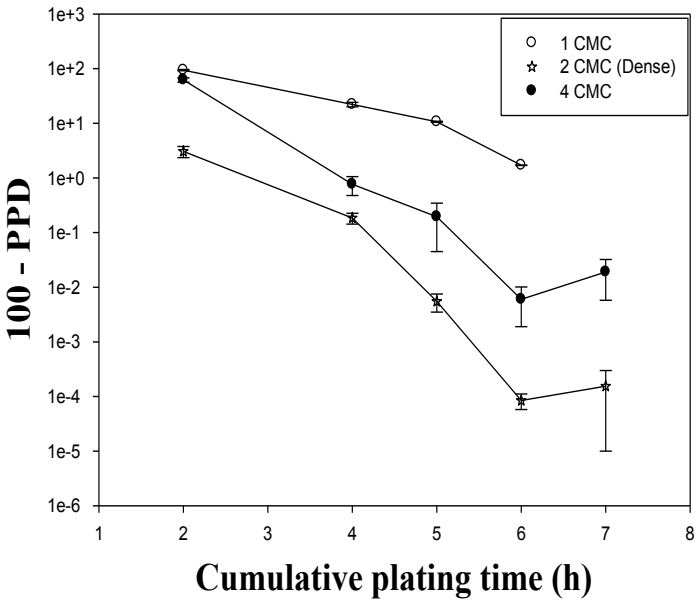

(a)

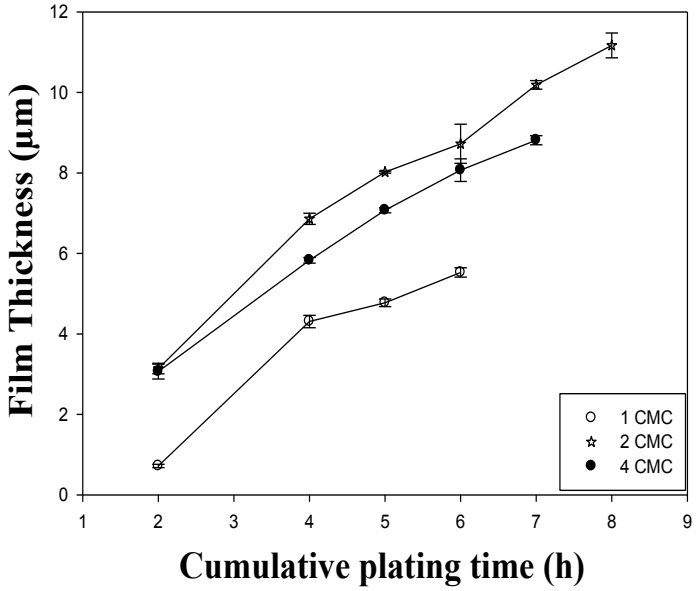

(b)

Figure 4.7: Time dependent (a) PPD and (b) metal film thickness profiles for Pd/PSS membranes fabricated at 1, 2 and 4 CMC surfactant solution concentrations.

4.3.5 Metal film Thickness

Figure 4.7b illustrates the variation in time dependent dense Pd film thickness for surfactant solution concentrations of 1, 2 and 4 CMC. It can be observed that the film thickness varied from 0.72 – 5.52 μm after 6 h for 1 CMC, 3.14 – 11.6 μm after 8 h for 2 CMC and 3.06 – 8.81 μm after 7 h for 4 CMC Pd ELP bath. With increasing surfactant concentration (1 – 2 CMC), the film thickness increased. However, a further enhancement in surfactant concentration (2 – 4 CMC) reduced the film thickness values due to uneven surface charge densities on substrate surface at 4 CMC surfactant concentration. Similar observations have been reported by Chen et al. [39] for the surfactant induced nickel - phosphorous electroless plating baths. The authors inferred that at moderately high concentrations, surfactant enhanced the metal deposition rates. However, at even higher solution concentration, the surfactant molecules form cylindrical aggregates on the substrate surface and inhibit the metal deposition rates.

4.3.6 Tradeoffs

a) $\frac{PPD}{\delta}$ vs. (100 – PPD)

Figure 4.8a shows the tradeoffs associated for $\frac{PPD}{\delta}$ vs. (100 – PPD) for 1, 2 and 4 CMC baths at a loading ratio of 203 cm^2/L. The $\frac{PPD}{\delta}$ varied from 8.17 – 17.78 for 1 CMC, 30.87 – 8.95 for 2 CMC and 12.34 – 11.34 for 4 CMC, respectively. Further, the 100 – PPD profile for the 2 CMC bath extended more towards the left side of the x-axis in comparison to the 4 CMC bath and 1 CMC baths. Even though the $\frac{PPD}{\delta}$ profile reduced significantly for the 2 CMC bath, a value of 8.95 at near densification is highly attractive, given the fact that the

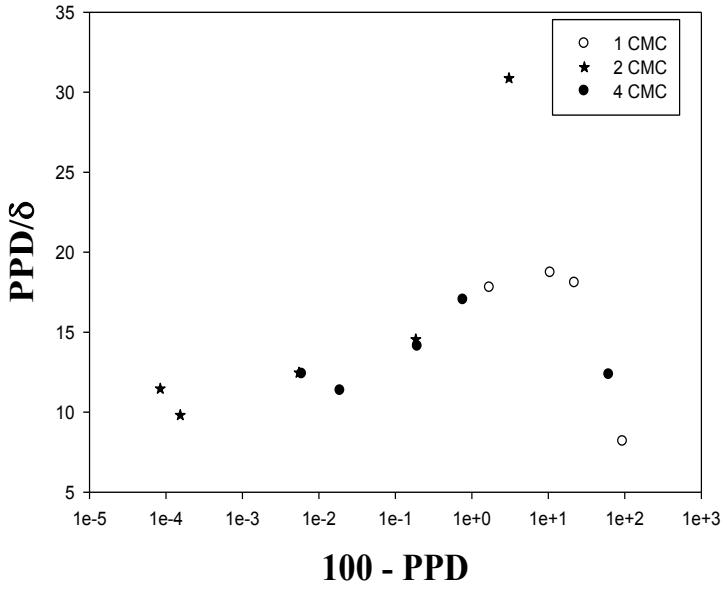

(a)

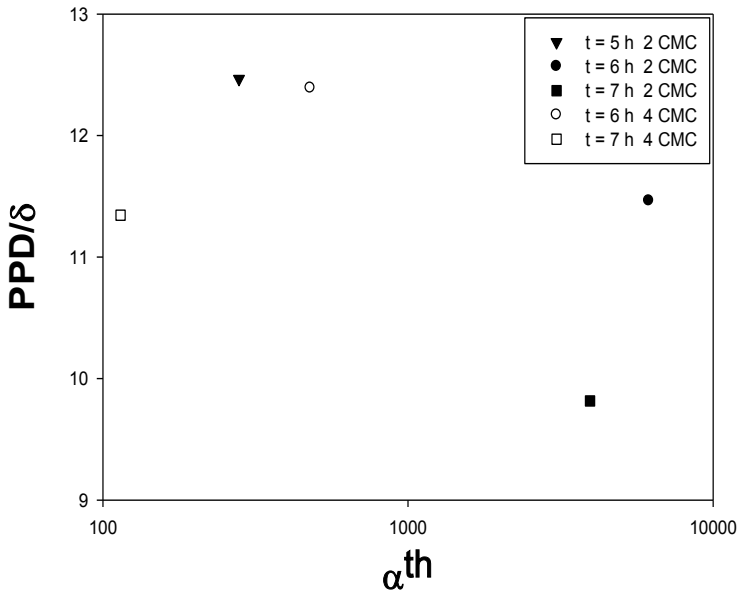

(b)

Figure 4.8: Tradeoffs for (a) $\frac{\text{PPD}}{\delta}$ vs. (100 – PPD) and (b) $\frac{\text{PPD}}{\delta}$ vs. α^{th} b) $\frac{\text{PPD}}{\delta}$ vs. α^{th} for various Pd/PSS membranes fabricated with 1, 2 and 4 CMC surfactant solution concentrations.

$\frac{PPD}{\delta}$ reduces significantly (to values lower than 1) for CEP baths. In the literature [37], the $\frac{PPD}{\delta}$ can be estimated to be 11.14, which is higher than the value obtained for the SSOEP baths. However, considering the 50% lower Pd solution concentrations in this work, the obtained $\frac{PPD}{\delta}$ for 2 CMC surfactant concentration is promising for further process engineering studies. In addition, the existence of lapse mode in the profiles for both 2 CMC and 4 CMC baths can be also observed in the figure. However, as explained earlier, the PPD profile lapse mode of 2 CMC case is not significant when compared to that for the 4 CMC bath. This is evident from the fact that the lapse has been in the order of 10^{-5} to 10^{-4} for the 2 CMC bath which is significantly lower than the lapse in the order of 10^{-3} to 10^{-2} for the 4 CMC bath.

Figure 4.8b shows the trend of $\frac{PPD}{\delta}$ vs. α^{th} with plating time for the plating baths containing surfactant concentrations of 2 CMC and 4 CMC. For the 2 CMC bath, the theoretical selectivities obtained after 5, 6 and 7 h of sequential plating are 279.23, 6154 and 3953. The maximum selectivity of infinity was obtained after completion of 8 h of Pd ELP. For 4 CMC Pd ELP bath, the selectivities obtained after 6 and 7 h sequential plating are 478.5 and 114.3 only. Thus it is apparent that the SSOEP (DW) with 2 CMC is promising to provide very high theoretical selectivities for the separation of H_2/N_2.

4.4 Effect of Loading Ratio on the combinatorial electroless plating characteristics

Based on the combinatorial plating characteristics presented in the previous two sections, it can be inferred that the optimal Pd and surfactant solutions correspond to 0.005M and 2 CMC respectively. In this section, the optimality of loading ratio is being addressed in the context of combinatorial plating characteristics for two different values of the loading ratio.

4.4.1 Selective conversion and Plating Efficiency

Figure 4.9a and 4.9b illustrates the time dependent profiles of selective conversion and plating efficiencies for loading ratio values of 407 and 203 cm^2/L. As shown, for an increase in loading ratio from 203 to 407 cm^2/L, the selective conversions enhanced from 35.4 – 31.48% to 46.04 – 41.34%. However, corresponding plating efficiencies reduced from 90.96 – 95.94 to 89.54 – 89.01%. The enhancement in selective conversions with increasing loading ratio is possibly due to the significant mass transfer limitations for Pd ions to reach the active membrane surface for lower loading ratio values. On the other hand, doubling the loading ratio marginally affected plating efficiencies, which might be due to insignificant metal nucleation in the solution. The reduction in plating efficiencies with increasing loading ratio is indicative towards greater metal nucleation in the solution which is possibly due to the greater attrition of the metal from the support surface during Pd ELP. Therefore, it is apparent that loading ratio affects metal adhesion strength to the porous metallic structure. These variations in metal adhesion are due to the variations in the average Pd plating rate with loading ratio. At higher loading ratio, the Pd ELP solution volume is low and the total metal available in the solution would be as well low. Thus, lower average plating rates exist and it is apparent that lower plating rates translate to lower

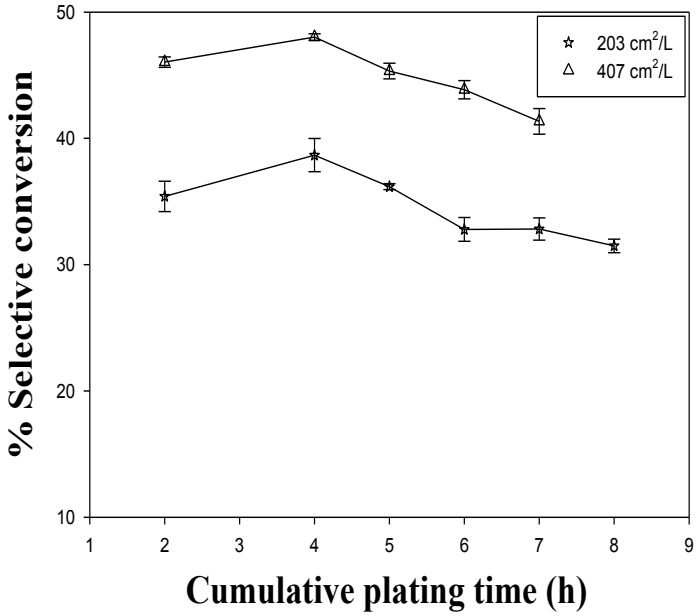

(a)

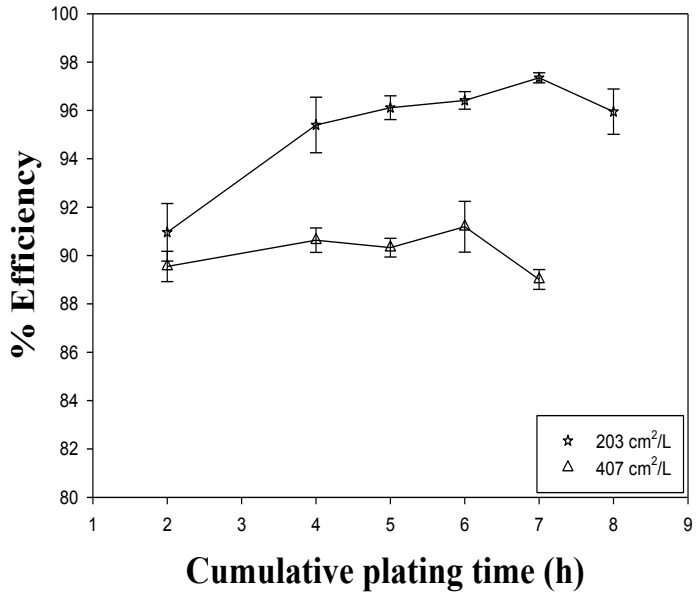

(b)

Figure 4.9: Effect of loading ratio on (a) selective conversion and (b) plating efficiency of SSOEP (DW) processes.

adhesion strength of the metallic film to the surface. In other words, higher solution concentrations coupled with higher loading ratios might provide better performance characteristics. However, a tradeoff exists for the enhancement in metal plating rate at higher Pd solution concentrations. At very high Pd solution concentrations, it has been observed during Pd ELP that metal nucleation is intense in the solution and this is due to very fast deposition of Pd on the support surface whose adhesion characteristics are very poor. Based on the experimental investigations carried out in this work, a loading ratio of 203 cm^2/L is the recommended choice for the electroless fabrication of dense Pd composite membranes.

4.4.2 Plating rate

The average Pd plating rate for the loading ratio of 203 cm^2/L and 407 cm^2/L at various sequential plating time durations are presented in Table 4.3. It can be observed that with increasing loading ratio, the metal deposition rates reduced from $4.92x10^{-5}$ – $4.38x10^{-5}$ $mol/m^2.s$ to $3.14x10^{-5}$ – $2.82x10^{-5}$ $mol/m^2.s$. Even though for both cases Pd solution concentration remained the same (0.005 M), the case corresponding to lower loading ratio provided greater quantity of Pd metal in the solution due to which higher Pd plating rates have been achieved. Based on the explanation presented in the previous section, the higher Pd plating rates are affordable to provide higher plating efficiencies. Based on membrane support morphology (pore size distributions, porosity and roughness), it is hypothesized that there exists an optimal range of the average plating rate that provides maximum adhesion strength of the as deposited Pd film. The maximum adhesion strength of the dense Pd film is a function of the plating process parameters and therefore the outlined approach of evaluating combinatorial plating characteristics in this work is anticipated to serve as a guideline to screen, scope and judiciously

select the optimal electroless process parameters for the cost effective fabrication of dense Pd composite membranes.

Table 4.3: Effect of loading ratio on average plating rates of SSOEP (DW) process.

Loading ratio (cm^2/L)	**Average plating rate $\bar{r}_{Pd}$ ($mol/m^2.s$) x 10^5 for various total plating time (h)**					
	2	**4**	**5**	**6**	**7**	**8**
203	4.92	5.38	5.03	4.562	4.57	4.38
407	3.14	3.28	3.09	2.99	2.82	-

4.4.3 Nitrogen flux tradeoffs

Figure 4.10a and 4.10b shows the nitrogen permeation flux trends for Pd-PSS membranes fabricated using ELP baths at a loading ratio's of 203 and 407 cm^2/L, respectively. It can be observed that, at a loading ratio of 407 cm^2/L, the room temperature nitrogen flux reduced significantly from 0.18 – 8.68 $mol/m^2.s$ (for an average pressure of 1.1 – 2.05 bar) to $5.79x10^{-3}$ – 0.08 $mol/m^2.s$ (for an average pressure of 1.09 – 2.05 bar) during the initial 2 h plating. An additional 5 h Pd ELP did not alter the nitrogen flux significantly ($3.41x10^{-3}$ – $6.35x10^{-3}$ $mol/m^2.s$ for an average pressure of 1.05 – 2.05 bar). However, for a loading ratio of 203 cm^2/L, the nitrogen flux reduced from 0.211 – 8.77 $mol/m^2.s$ (for an average pressure of 1.05 - 2.047 bar) to 0-0 $mol/m^2.s$ (for an average pressure of 1.17 – 2.05 bar) after 8 h of Pd ELP to enable the realization of a fully dense Pd/PSS composite membrane. Hence, from the nitrogen flux tradeoffs, a lower loading ratio is recommended for dense Pd composite membrane fabrication.

4.4.4. Percent pore densification

Figure 4.11a shows the comparison of time dependent PPD for 407 cm^2/L loading ratio case with that obtained for the 203 cm^2/L loading ratio case. For the 407 cm^2/L case, after 2 h sequential plating the membrane densified to 99.14%, which only enhanced to 99.9% after an additional Pd

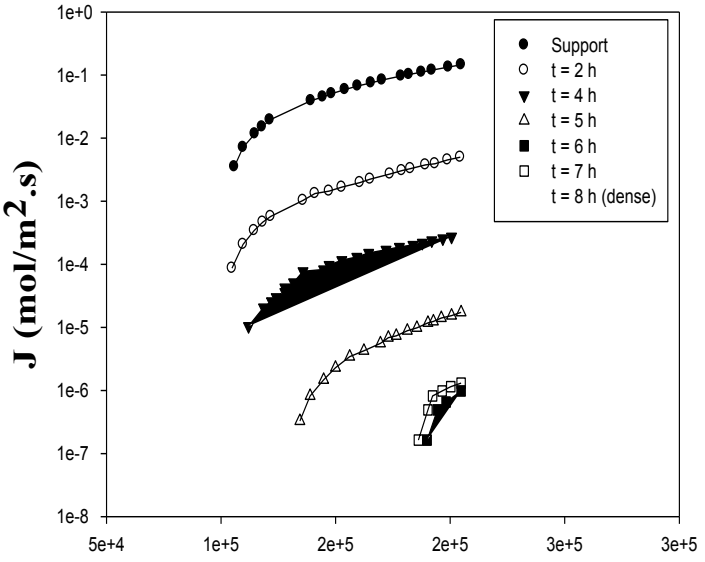

(a)

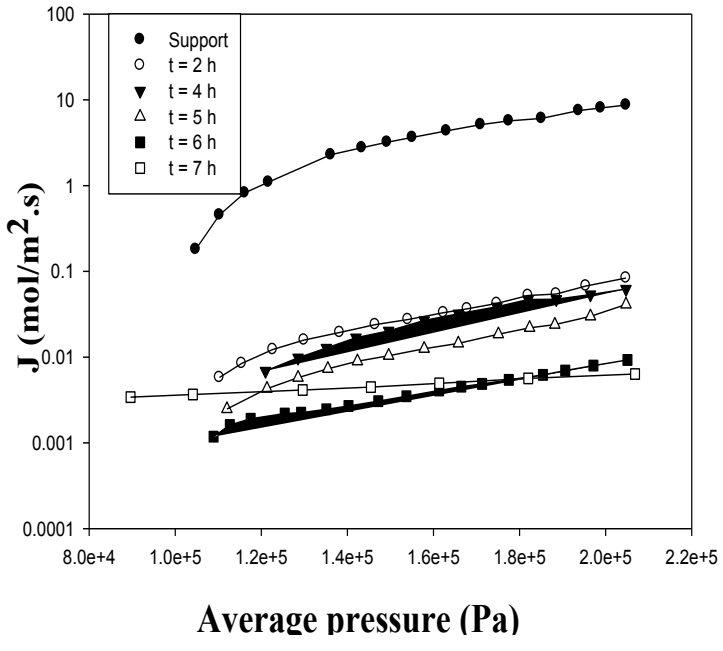

(b)

Figure 4.10: N_2 flux plots for Pd/PSS membranes fabricated at a loading ratio of (a) 203 cm^2/L and (b) 407 cm^2/L.

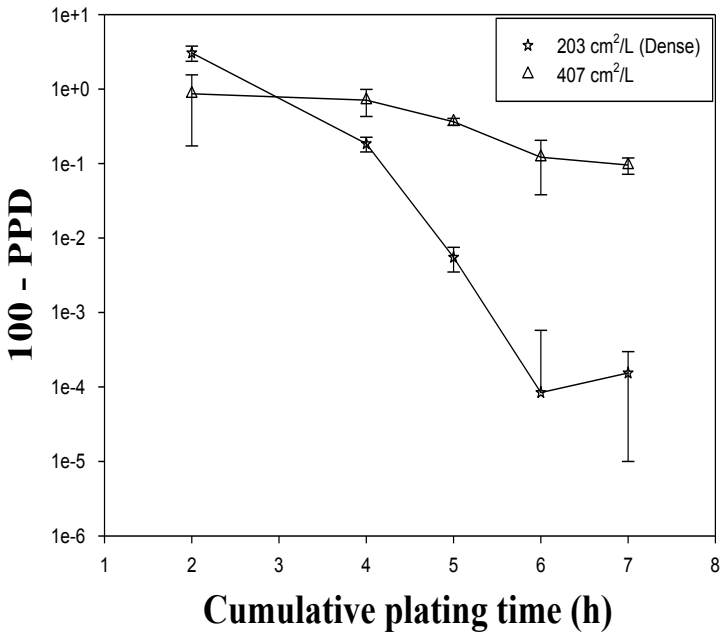

(a)

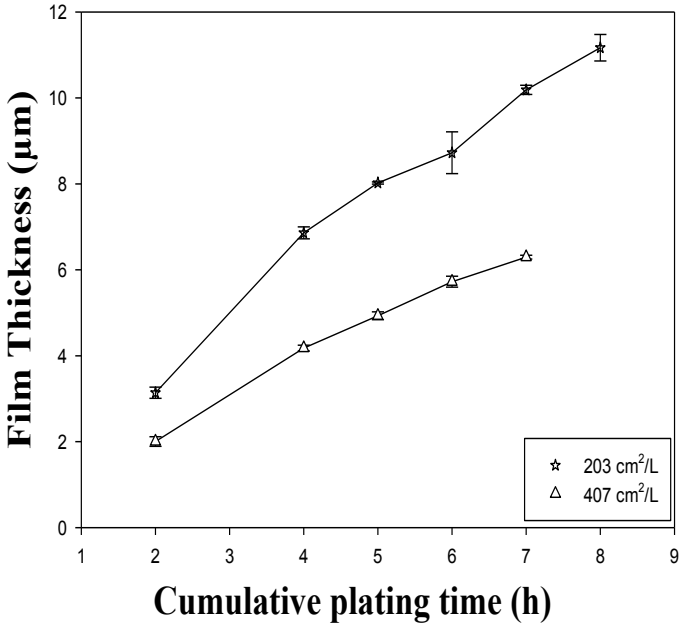

(b)

Figure 4.11: Variation of time dependent (a) (100 – PPD) and (b) metal film thickness profiles with loading ratio for SSOEP (DW) process.

ELP for 5 h. On the other hand, for the lower loading ratio case, the PPD values increased significantly upto 6 h of sequential plating and reached 100% densification after another 2 h sequential plating. For all the durations, maximum PPD values were achieved in 203 $cm^{2/}L$ case due to the presence of more quantity of Pd metal in the plating solution that effectively catered towards surface pore coverage and complete densification.

4.4.5. Metal film Thickness

Figure 4.11b shows the incremental metal film thickness variation with plating time for 203 and 407 cm^2/L loading ratio cases. It can be observed that for an increase in the loading ratio from 203 to 407 cm^2/L, the film thickness reduced from 3.13 – 11.17 μm to 2.0 – 6.29 μm. This is due to the reduction in the amount of Pd metal available in the ELP bath for a loading ratio of 407 cm^2/L. Despite achieving lower thickness at higher loading ratio, the PPD values are significantly lower for the case in comparison to the PPD values obtained for the lower loading ratio. Hence, the higher loading ratio is not recommended for dense Pd/PSS composite membrane fabrication with SSOEP (DW) Pd baths.

4.4.6 Tradeoffs

The tradeoffs associated to the higher loading ratio (407 cm^2/L) are not presented, considering the fact that better tradeoffs have been obtained for the lower loading ratio (203 cm^2/L).

4.5 Surface characterization

The surface morphology and cross section of the dense Pd/PSS membrane fabricated with SSOEP (DW) Pd ELP bath at optimal process parameters (0.005 M Pd solution concentration, 2 CMC surfactant solution concentration and loading ratio of 203 cm^2/L) was examined by Field Emission Scanning Electron Microscopy (FESEM). Figure 4.12a presents the dense Pd/PSS

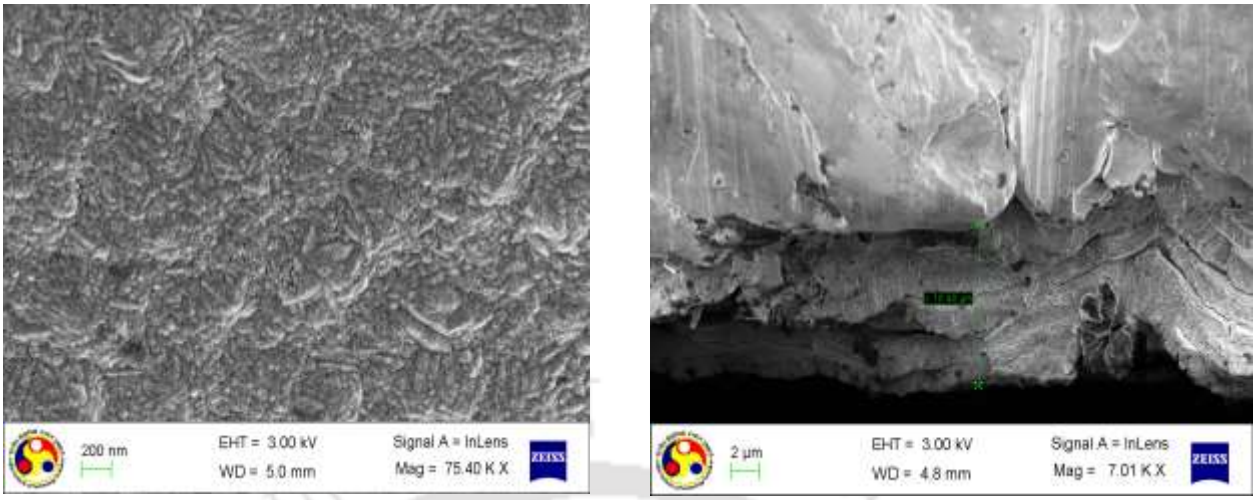

(a) **(b)**

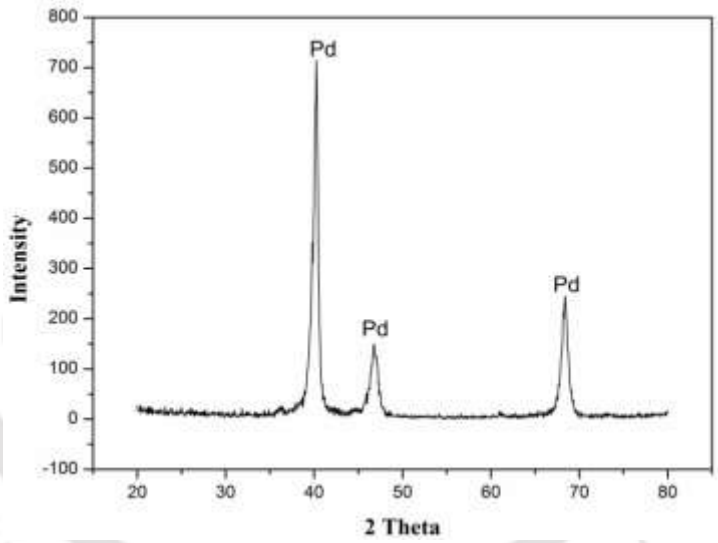

(c)

Figure 4.12: (a) Surface FESEM image (b) Cross-sectional FESEM image and (c) XRD pattern of 100% dense Pd/PSS composite membrane.

membrane surface morphology. In this figure, it can be observed that smooth and uniform grain agglomeration exists without any pores on the surface. Figure 4.12b presents the cross section of dense Pd/PSS membrane and it can be observed that the thickness of the deposited dense Pd film is about 10.48 µm which is in good agreement with that evaluated using weight gain method

(11.16 μm). Figure 4.12c illustrates the XRD pattern of dense Pd/PSS composite membrane fabricated with optimal process conditions summarized in the earlier paragraph. The XRD spectra indicate the existence of Pd reflection peaks in the face centred cubic (f.c.c.) phase at (1 1 1), (2 0 0) and (2 0 2) planes. Further, no other reflection peaks were detected for the dense Pd composite membrane. In this regard, it shall be noted that minor peaks of Fe, Cr, Ni and Mn/Mo were detected for the PSS support. Hence, observed XRD pattern also confirms towards the uniformity of the dense Pd metal on the support.

4.6 Cost Analysis

The invented SSOEP (DW) Pd ELP process needs to be analyzed with respect to its cost effectiveness to fabricate low cost dense Pd composite membranes. Therefore, a retail cost analysis has been carried out for the fabricated dense Pd composite membranes in conjunction with the literature available data. Further, it shall be noted that retail cost analysis has not been presented in the literature and this work addresses the retail cost analysis of the Pd composite membranes prepared with literature reported process parameters and conditions. Various parameters assumed and considered for the retail cost analysis of dense Pd composite membranes is presented in Table 4.4.

Various cases considered include dense Pd composite membrane fabrication with SSOEP (DW) on PSS (this work), SIEP (bulk addition of hydrazine) on PSS [37], CEP (bulk addition of hydrazine) on PSS [37], and SIEP (bulk addition of hydrazine) on alumina [36]. The overall retail cost comparability plot is presented in Figure 4.13. As shown, the cost of fabricated dense Pd membrane is 13.2 $/cm^2, which is significantly lower than the cost of the membrane fabricated with conditions mentioned by Islam et al. [37] (32.45 $/cm^2) and Zhang Ke et al. [36]

(35.69 $/cm^2). Therefore, it is apparent that the invented SSOEP process reduces the fabrication costs significantly by about 60%. Further, it is important to note that Islam et al. [37] did not mention total plating volume used for Pd membrane fabrication and therefore, the assumed value of 20 mL plating solution for a membrane area of 5.06 cm^2 in one plating step is to be noted. Also, for the CEP, it can be noted that, utilizing the process parameter data presented by Islam et al. [37], the cost of the membrane increased to 61.2 $/cm^2 which is atleast 4 times higher than the cost obtained using parameters reported in this work. Compared to all other processes, the retail fabrication cost of the invented SSOEP (DW) Pd ELP process is lowest. This is due to the following facts. Firstly, the utilized surfactant (CTAB) is highly inexpensive (retail cost of CTAB is 0.077 $/g, whereas the cost of DTAB (literature reported best cationic surfactant) is

Table 4.4: Cost parameters for the evaluation of retail fabrication cost of dense Pd composite membranes.

S.No	Name of composition		Quantity	Cost ($)
		PSS	3.6 cm dia	44
1	Support			
		α-Al_2O_3	100 (cm^2)	38.45
2	Palladium	($PdCl_2$)	1 (g)	67.62
		CTAB	100 (g)	7.763
3	Surfactant			
		DTAB	25 (g)	90.84
4	Na_2EDTA		100 (g)	3.49
5	Acetone		2.5 (L)	14.72
6	Hydrazine		0.5 (L)	21.49
7	Electrical		1 (kW)	0.16
8	Man Power		1 (h)	4.54

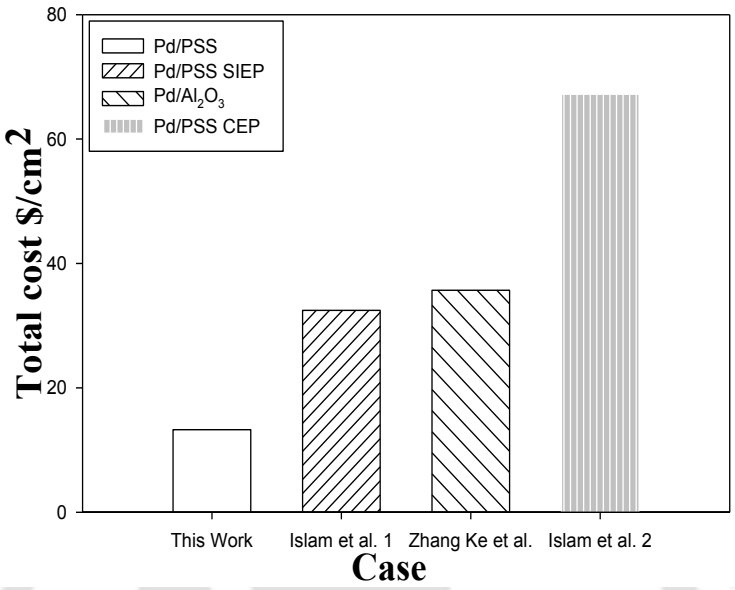

Figure 4.13: Comparative assessment of SSOEP (DW) process with most efficient ELP processes reported in the literature.

3.62 $/g in India). In addition, the CMC concentration of DTAB (4.93 g/L) is significantly higher than the CMC concentration of CTAB (0.335 g/L). Therefore, higher concentrations of DTAB need to be deployed for SIEP Pd ELP baths. In other words, the DTAB surfactant has a double impact on its cost contribution due to higher cost and higher CMC concentration. Secondly, SSOEP (DW) utilizes 0.005 mol/L of 50 mL plating solution for one 30 min depositional step, whereas patented SIEP process utilizes 0.015 mol/L for 1 h plating step. Thirdly, the total time of plating in this work is atleast 2 h lower than the time of plating reported by Islam et al. [37]. Fourthly, the membrane area considered in this work is significantly higher than the values reported in the literature.

A summary of various component contributions towards the membrane cost is summarized in Figure 4.14 for all membranes. It can be observed that for the present case, manpower, stainless steel support and palladium chemical cost contributed very uniformly towards the total cost of

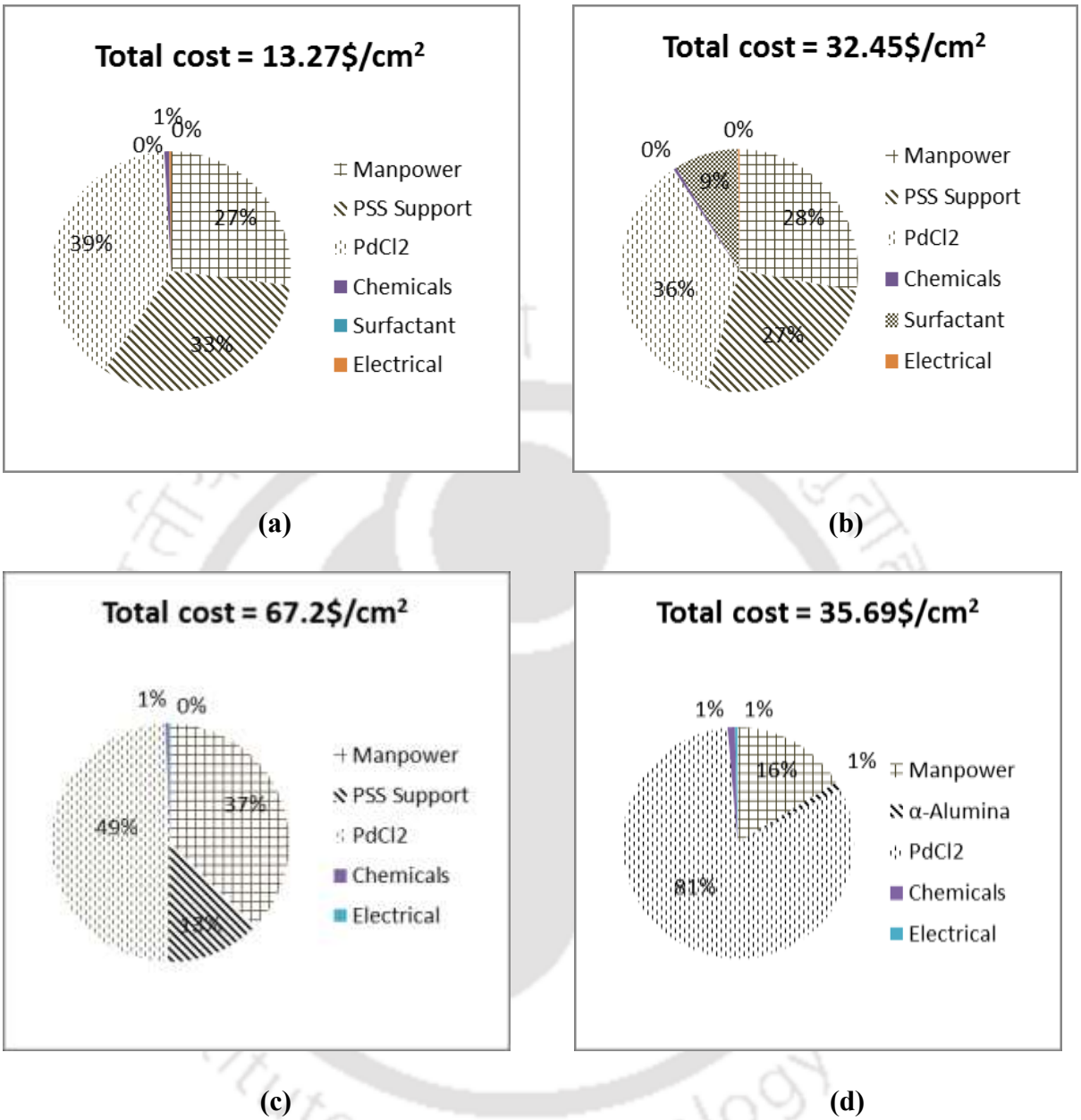

Figure 4.14: Pie-charts for the cost contribution of various sectors towards the overall cost of dense Pd/PSS membranes (a) SSOEP (DW) on PSS (this work) (b) SIEP process with 10 h plating time (literature, [37]) (c) CEP (bulk) with 28 h total plating time (literature, [37]) (d) SIEP process for α-Al_2O_3 (literature, [36]).

the membrane. The cost contribution of the surfactant is insignificant towards the retail cost of the membrane. However, for the membrane fabricated by Islam et al. [37], the cost of the

surfactant is significant and is upto 9% and Pd chemicals contributed about 36%. For the Pd dense membrane fabricated using alpha-alumina support, the support cost contribution is not more than 1% and Pd chemicals contributed towards 81% of the total cost. On the other hand, the dense Pd composite membrane prepared using CEP process indicated significant contributions from, both manpower and Pd chemicals to the total cost. Thus, based on the retail cost analysis, it can be inferred that the carried out research in this work has been able to successfully optimize the cost contributions of various important components and hence indicated towards the lowest retail cost of the dense Pd composite membranes.

4.7 Summary

Three important inclusions namely reduction of Pd solution concentration, coupling of sonication, surfactant and drop wise contacting pattern of the reducing agent are the principal features of the suggested novel plating process in this work which has been not reported so far. All other ELP processes reported in the literature have not been able to provide a dense Pd membrane using the said concentration of palladium (0.005 M). Thus, SSOEP needs further research emphasis by Pd membrane fabrication researchers to enhance its optimality for the successful fabrication of dense Pd membranes on low cost basis.

Based on the observed plating and depositional characteristics of SSOEP plating baths, the optimal combinations of plating and process parameters corresponds to palladium solution concentration of 0.005 M, loading ratio of 203 cm^2/L, CTAB surfactant solution concentration of 2 CMC, total plating time of 8 h (16 depositional steps of 30 min duration each). The process provided 11.16 μm thick dense palladium composite membrane with plating efficiencies greater than 90%, selective conversions of about 30 – 35 % and plating rate of 4.38 x 10^{-5} $mol/m^2.s$. The SSOEP with these combinations of plating and process parameters provided minimal lapse in the

PPD profiles and provided very high PPD values after 2 h of plating itself. The overall fabrication cost of identified dense Pd/PSS composite membrane is 13.24 \$/cm^2 which is 60% cost effective with respective to the best known SIEP process [37]. Further, it has been analyzed that enhancing the loading ratio from 203 to 407 cm^2/L enhanced selective conversion, reduced plating efficiency and provided lower PPD values, thus indicating that the non-optimality of the higher loading ratio.

Chapter 5:

Role of electroless Nickel diffusion barrier on the combinatorial plating characteristics of dense Pd composite membranes

Chapter 5

Role of electroless Nickel diffusion barrier on the combinatorial plating characteristics of dense Pd composite membranes

This chapter addresses the combinatorial plating characteristics of SSOEP-DW Pd ELP baths to fabricate Pd/Ni/PSS composite membranes. The membranes were fabricated using porous PSS supports with an average pore size of 0.1 and 0.5 μm. For comparative purposes, the combinatorial plating characteristics of dense Pd/PSS membranes were considered. The reported combinatorial plating characteristics refer to selective conversion, plating efficiency, plating rate, percent pore densification and thickness. Further, surface characterization results including XRD analysis and FESEM analysis have also been presented for the fabricated dense membranes.

5.1 Introduction

The primary objective of this chapter is to identify the various challenges associated to the fabrication of dense Pd/Ni/PSS composite membranes. The membranes were fabricated using SSOEP (DW) Pd ELP bath that was identified to provide the best performance in terms of combinatorial plating characteristics for Pd/PSS membranes. The role of support morphology (in terms of its pore size distributions) has been investigated for the said membranes. The next section briefly outlines the results obtained in terms of combinatorial plating characteristics. For all cases, dense Pd/PSS membrane plating characteristics have been considered as a reference.

5.2 Results and Discussion

5.2.1 Selective conversions and plating efficiency

Figure 5.1a and 5.1b respectively illustrate the effect of cumulative plating time on selective conversion and plating efficiencies of palladium electroless plating baths for the fabrication of Pd/Ni/PSS membranes (on 0.5 and 0.1 μm average pore size supports) and Pd/PSS membranes (on 0.1 μm average pore size supports). In comparison with the Pd/PSS membranes where moderate conversions were achieved (35.40 – 31.48%), it can be observed that the selective conversions were significantly low (20.38 – 17.98%) for 0.5 μm nominal pore size supports and comparable (33.73 – 30.92%) for 0.1 μm nominal pore size PSS supports. Thus, it is apparent that wider support morphology did not provide good selective Pd conversions during the fabrication of Pd/Ni/PSS membranes.

On the other hand, the plating efficiencies for Pd/Ni/PSS membrane fabrication varied from 30.50 – 48.77% and 76.54 – 87.01% for 0.5 and 0.1 μm average pore size supports respectively. For comparison purpose, it can be analyzed that the plating efficiencies for Pd/PSS membranes were significantly higher (90.95 – 95.94%). It can be also inferred that the plating efficiencies are in the order of Pd/PSS (0.1 μm) > Pd/Ni/PSS (0.1 μm) > Pd/Ni/PSS (0.5 μm). Thus, compared to the stainless steel substrate, nickel did not allow significant metal deposition to occur on the membrane surface and this could be due to the poor Pd surface activation on the Ni/PSS support in comparison with the PSS support. Further, lower plating efficiencies for the Ni/PSS supports are indicative towards greater metal nucleation in the solution, which is an undesired feature. Also, it can be observed from both Figure 5.1a and b that while selective conversions reduced with increasing total plating time, the plating efficiency values increased with total plating time. This indicates that for both cases of Pd/PSS and Pd/Ni/PSS membranes,

plating rates increased with increasing plating time due to the deposition of Pd on the membrane surface.

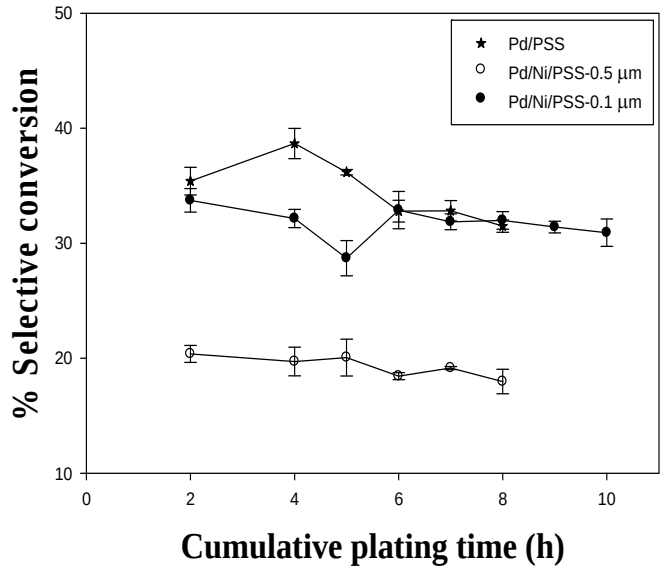

(a)

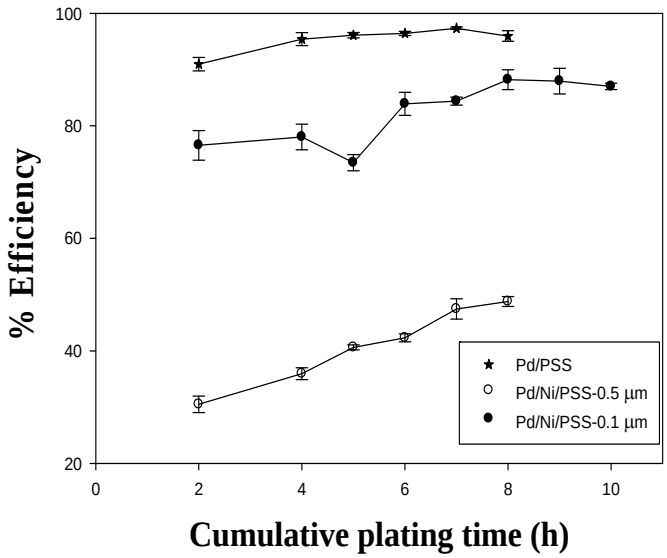

(b)

Figure 5.1: Time dependent profiles for Pd/Ni/PSS and Pd/PSS membranes: (a) selective conversion and (b) plating efficiency.

Table 5.1: Comparison of time dependent average plating rates for Pd/Ni/PSS and Pd/PSS membranes.

Type of Membrane	Average plating rate $\bar{r}_{Pd}$ (mol/m^2.s)x10^5 for various total plating time (h)								
	Ni	2	4	5	6	7	8	9	10
Pd/PSS	-	4.92	5.38	5.03	4.56	4.57	4.38	-	-
Pd/Ni/PSS-0.5 μm	6.74	3.95	3.82	3.89	3.57	3.71	3.45	-	-
Pd/Ni/PSS- 0.1 μm	3.58	3.35	3.19	2.85	3.27	3.17	3.18	3.12	3.07

5.2.2 Plating rates

The variation of Pd plating rates with plating time for Pd/Ni/PSS and Pd/PSS membranes has been summarized in Table 5.1. It can be observed that for Pd/PSS (on 0.1 μm PSS support) and Pd/Ni/PSS membranes (0.5 and 0.1 μm PSS supports), the plating rates varied from 4.92 – 4.38x10^{-5}, 3.95 – 3.45x10^{-5} and 3.35 – 3.07x10^{-5} mol/m^2.s, respectively. The plating rates on nickel modified stainless steel substrate are about 20 – 30% lower than those obtained for the PSS substrate. Thus, in comparison to the Pd/PSS membranes, lower average plating rates were obtained for Pd/Ni/PSS membranes. This is due to the poor surface activation of Pd for the Pd/Ni/PSS membranes.

5.2.3 Nitrogen flux profiles

Figure 5.2 (a-c) depicts the nitrogen permeation flux trends for Pd-PSS membranes on 0.1 μm PSS and Pd/Ni/PSS membranes on 0.1 and 0.5 μm PSS supports. For Pd/Ni/PSS membrane on 0.1 μm PSS supports, after depositing 1.7 μm thick Ni film, the N_2 flux reduced from 0.256 – 9.12 mol/m^2.s (for an average pressure of 1.06-2.05 bar) to 0.162 – 6.904 mol/m^2.s (for an average pressure of 1.06 – 2.05 bar) which further reduced to 0 – 9.07x10^{-4} mol/m^2.s (for an average pressure of 1.06 – 2.04 bar) after 10 h Pd sequential plating steps. On the other hand, for Pd/Ni/PSS membrane on 0.5 μm PSS supports, the 8 μm thick Ni film reduced the N_2 flux from

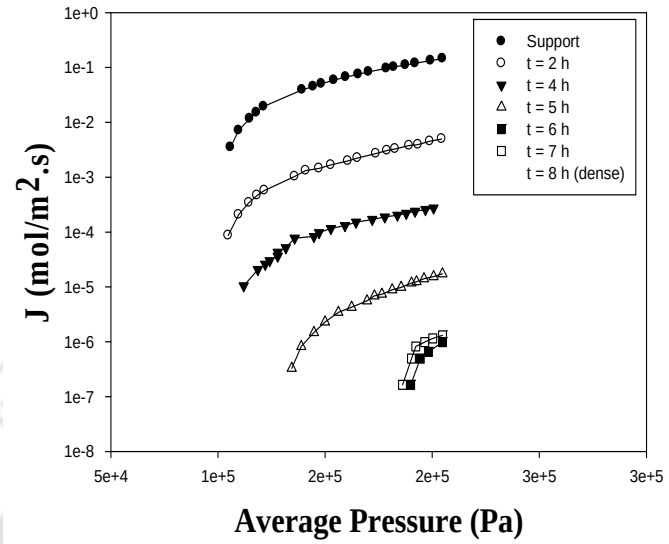

(a)

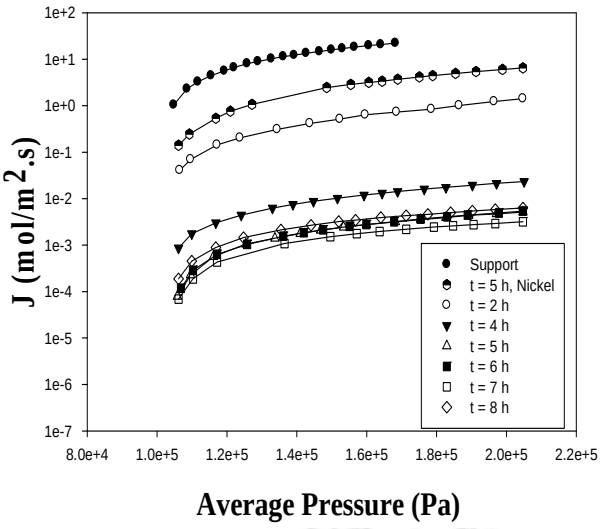

(b)

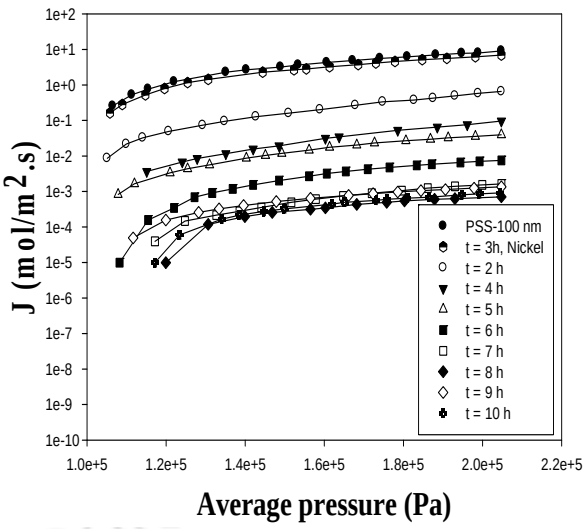

(c)

Figure 5.2: N_2 flux plots for various Pd composite membranes (a) Pd/PSS (b) Pd/Ni/PSS-0.5 µm and (c) Pd/Ni/PSS-0.1 µm.

1.03 – 22.19 mol/m^2.s (for an average pressure of 1.04 – 1.68 bars) to 0.139 – 6.51 mol/m^2.s (for an average pressure of 1.06 – 2.05 bar) which further reduced to $1.87x10^{-4}$ – $6.32x10^{-3}$ mol/m^2.s

(for an average pressure of 1.06 – 2.05 bar) after 8 h Pd sequential plating. It can be observed that after 8 h sequential plating the Pd/PSS membrane enabled the flux reduction from 0.211 – 8.77 mol/m^2.s (for an average pressure of 1.05 – 2.05 bar) to 0 – 0 mol/m^2.s (for an average pressure of 1.2 – 2.05 bars). For further 1 h plating the flux slightly enhanced to 0 – 1.31×10^{-6} mol/m^2.s (for an average pressure of 1.17 – 2.05 bar). Thus, it is apparent that the introduction of Ni interdiffusion barrier significantly altered and increased the room temperature N_2 flux profiles in comparison with those obtained for the Pd/PSS membranes.

5.2.4 Percent pore densification

Figure 5.3a shows the comparative performance of Pd/Ni/PSS and Pd/PSS membranes in terms of (100 - PPD) variation with total plating time. The PPD for Ni/PSS is about 84.5% and 25% after depositing 8 μm and 1.7 μm thick Ni films on 0.5 and 0.1 μm supports, respectively. Eventually for the Pd/Ni/PSS membrane cases, the PPD profiles have been considered for Ni/PSS membrane but not for the PSS support. After 2 h of Pd plating, the PPD for Ni/PSS membrane of 0.5 μm is only 79.01% which is significantly lower than that obtained for the Pd/PSS membrane (96.94%). Also, it can be observed that the PPD profiles varied from 79.01 – 99.9% for a variation in total plating from 2 – 8 h for the Pd/Ni/PSS membrane fabricated with 0.5 μm nominal pore size support. These PPD values were significantly lower than the corresponding PPD profiles (96.94 – 100%) obtained for Pd/PSS membrane. On the other hand, after 2 h sequential plating, the Pd/Ni/PSS membrane fabricated with 0.1 μm nominal pore size support provided 92.98 % PPD and it could not be subjected to 100% pore densification even after 10 h of sequential total plating time. Further, for all cases, it can be observed that for prolonged periods of total plating time, lapse mode of PPD was existent which indicates that uneven surface charge distributions contributed enormously towards poorer deposition. Also, in

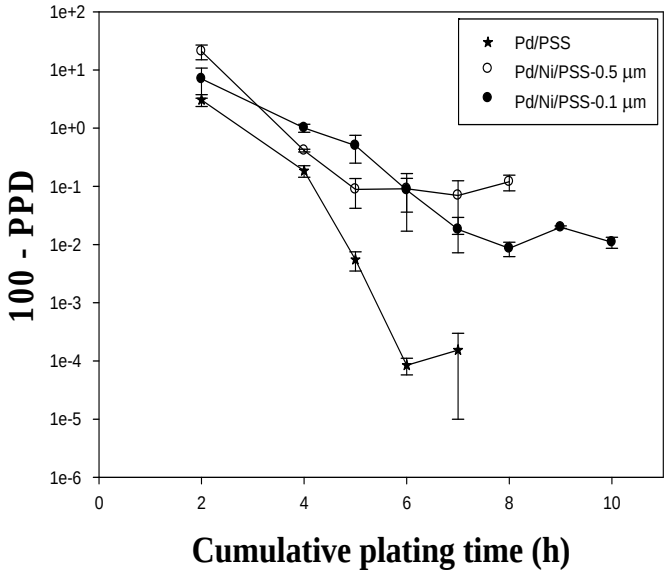

(a)

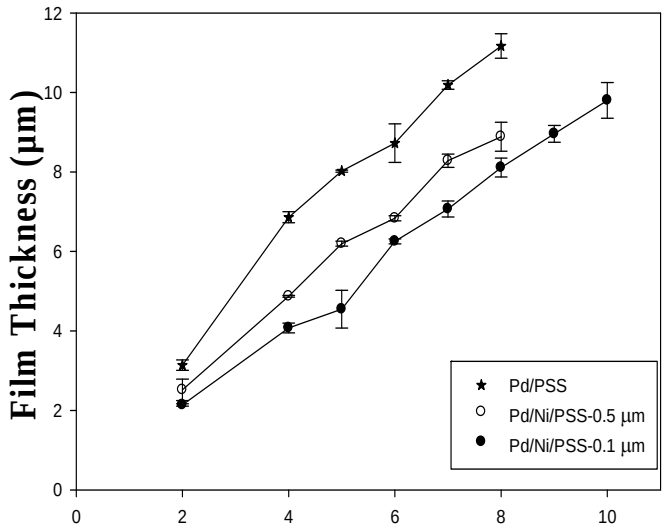

(b)

Figure 5.3: Variation of (a) (100 – PPD) and (b) metal film thickness with time for dense Pd/PSS, Pd/Ni/PSS-0.5 and Pd/Ni/PSS-0.1 membranes.

due course of prolonged plating, the metal delamination for the Pd/Ni/PSS membranes was significantly higher than that observed for the Pd/PSS membranes. In addition, the metal delamination during plating has been found to be significant for the nickel film deposited on 0.5 μm nominal pore size support. Thus, the metal delamination has been inferred to exist as per the following order: Ni/PSS (0.5 μm) > Ni/PSS (0.1 μm) > PSS (0.1 μm). Thus, it is apparent that the adhesion strength between Pd-Ni interface was not as strong as it exists for Pd/PSS interface. These important evaluations indicate and infer upon the poor depositional characteristics for Pd/Ni/PSS membranes in comparison with Pd/PSS membranes.

5.2.5 Metal film Thickness

The effect of plating time on the deposited Pd film thickness for Pd/Ni/PSS and Pd/PSS membranes are presented in Figure 5.3b. It can be observed that for Pd/Ni/PSS membranes, the Pd film thickness respectively varied from 2.52 – 8.88 μm and 2.14 – 9.80 μm for 0.5 and 0.1 μm nominal pore size supports, respectively. On the other hand, for Pd/PSS membranes, the time dependent Pd film thickness varied from 3.14 – 11.16 μm. Thus, it is apparent that, for the Pd/Ni/PSS membrane, lower Pd film thickness was obtained which refers to poor depositional characteristics in comparison with the Pd/PSS membrane. While lower Pd film thickness could ensure higher fluxes, the poor adhesion strength of the Pd to the Ni film is an important issue for future research investigations to address upon, as the ultimate target of the Pd composite membranes is to achieve Pd composite membranes with good combinations of mechanical strength, flux and separation factors.

5.2.6 Membrane characterization

Figure 5.4a and 5.4b respectively present the FESEM micrographs of Ni/PSS membranes on 0.1 and 0.5 μm PSS supports. From Figure 5.4a, it can be observed that the deposited 1.7 μm thick nickel film on 0.1 μm PSS support did not cover the surface pores completely. However, for Ni/PSS membranes fabricated with 0.5 μm PSS support, the 8 μm thick Ni film was thick enough to cover the maximum pores present on the surface. Figure 5.4c and 5.4d illustrate the FESEM micrographs of Pd/Ni/PSS and Pd/PSS membranes on 0.5 and 0.1 μm PSS supports after 8 h of sequential Pd ELP. It can be observed that for both cases, finer Pd grains exist on the membrane surface and no pinholes are visible for the chosen magnification which corresponds to the maximum magnification affordable with the instrument. Thus, the basic limitation of the FESEM imaging technique to elaborate upon the PPD characteristics of the membrane are evident and gas permeation experiments are very important for the analysis of the efficacy of Pd deposition in both cases.

Figure 5.5 presents the XRD (Make: Shimadzu Corporation, Model: D8 Advance) pattern of Ni/PSS and Pd/Ni/PSS composite membranes on 0.5 μm PSS supports. Bucker X-ray D8 advance diffractometer with a Cu-Kα radiation at 45 kV and 40 mA was used to record the XRD patterns within the range of 20 - 70^{o} at an increment of 0.05^{o}. The phase analysis of the diffraction profiles was carried out using ICDD-JCPDS database. It can be observed that the XRD spectra indicates upon the existence of Ni peaks at a diffraction angle (2θ) of 44.6^{o} and 52^{o} due to the diffraction of (1 1 1) and (2 0 0) planes [Pdf No 00-001-1260]. Further Pd peaks were observed at diffraction angles (2θ) of 40.2^{o}, 46.76^{o} and 68.28^{o} due to diffraction of (1 1 1), (2 0 0) and (2 0 2) planes respectively. The existence of Ni and Pd phases only for Ni/PSS and

Pd/Ni/PSS membranes confirms upon uniform deposition. This is also due to the fact that for the Pd/Ni/PSS membranes, neither Ni or stainless steel peaks were detected.

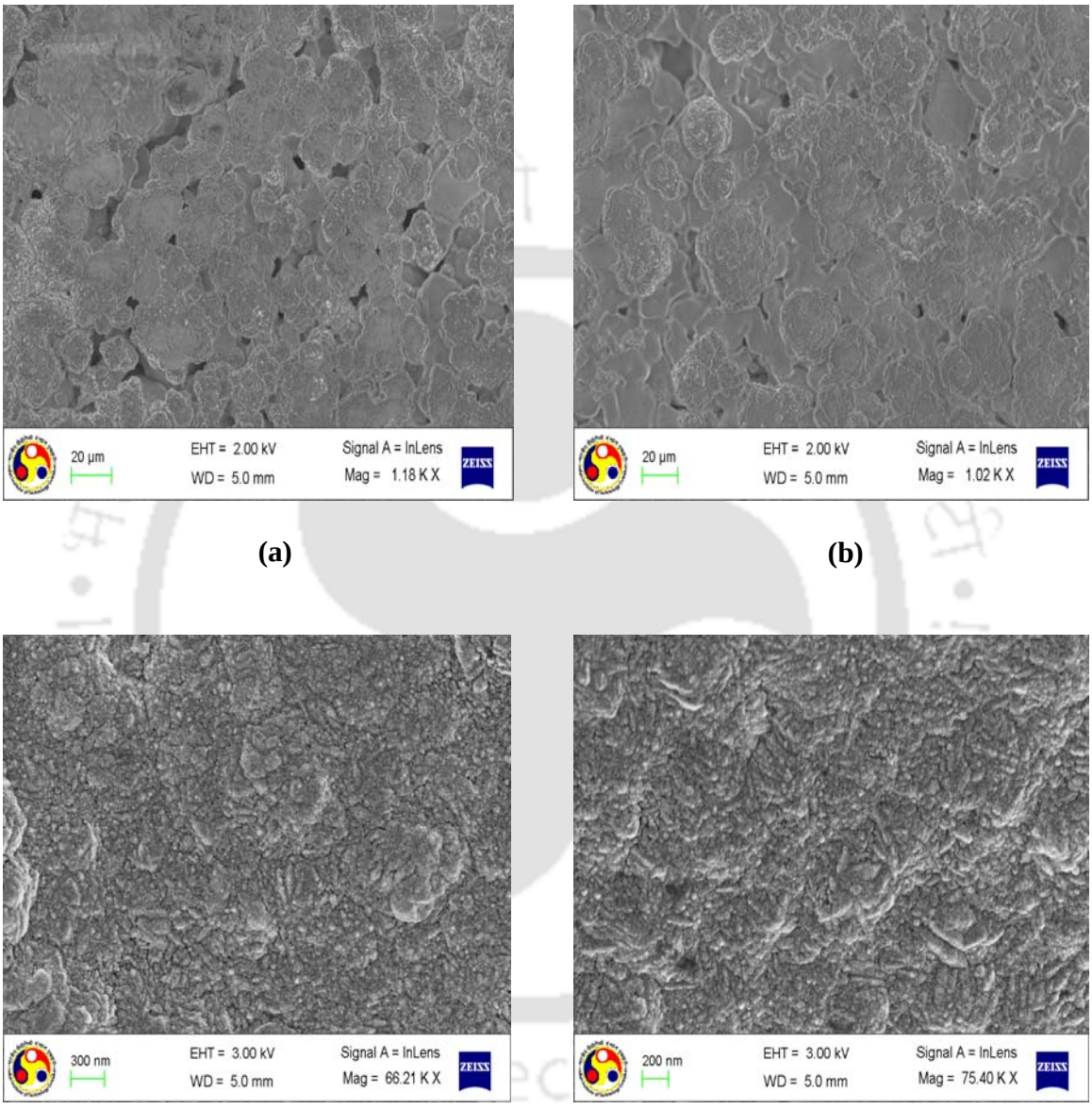

Figure 5.4: FESEM micrographs of (a) Ni/PSS membrane (0.1 µm PSS support) (b) Ni/PSS membrane (0.5 µm PSS support) (c) dense Pd/Ni/PSS membrane (0.5 µm PSS support) and (d) dense Pd/PSS membrane (0.1 µm PSS support).

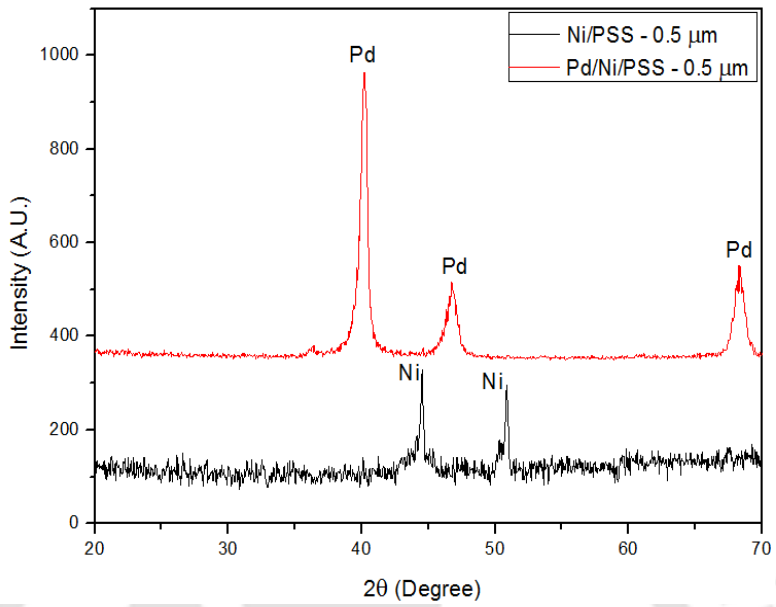

Figure 5.5: XRD pattern of the Pd/Ni/PSS membrane fabricated with 0.5 µm PSS support.

5.2.7 Tradeoffs

Figure 5.6 shows the $\frac{PPD}{\delta}$ vs. $\bar{\alpha}_{av}$ values for various Pd/Ni/PSS and Pd/PSS membranes. For Pd/Ni/PSS membrane fabricated with 0.5 µm nominal pore size support, the theoretical selectivities obtained after 6 and 7 h of sequential Pd ELP are 41.99 and 54.92 only. For the Pd/Ni/PSS membrane fabricated with 0.1 µm nominal pore size support, the theoretical selectivities are in the range of 140 – 170 after 7 – 9 h of total plating time. On the other hand, for Pd/PSS membrane, the theoretical selectivities obtained after 5, 6 and 7 h of sequential plating are 279.23, 6154 and 3953 respectively. For the same membrane, maximum selectivity of infinity was obtained after 8 h of Pd ELP. Thus it is apparent that lower theoretical selectivies exist for Pd/Ni/PSS membranes in comparison with the Pd/PSS membrane which is due to lower PPD profiles for the former cases. Also, it can be observed that $\frac{PPD}{\delta}$ is about 12 – 14 for

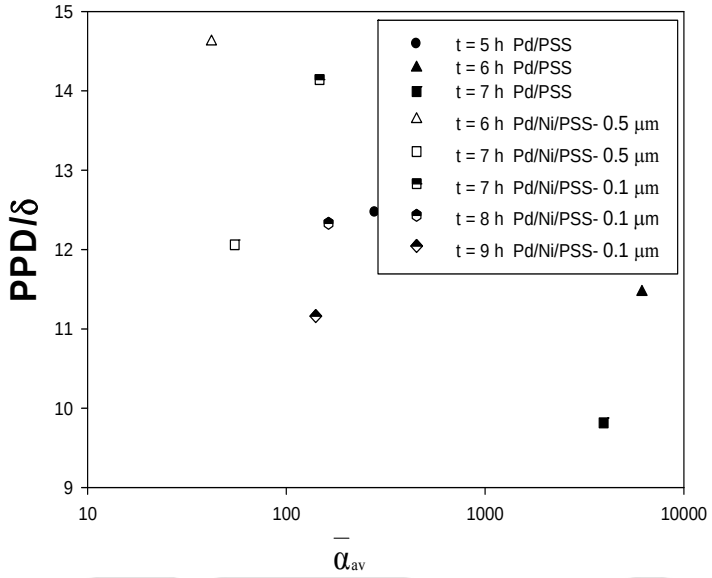

Figure 5.6: $\frac{PPD}{\delta}$ vs. $\bar{\alpha}_{av}$ tradeoffs for dense Pd/Ni/PSS and dense Pd/PSS membranes.

Pd/Ni/PSS but is only 10 - 12.5 for the Pd/PSS membrane. However, since higher PPDs were obtained for the Pd/PSS membranes, it is inferred that the nickel interdiffusion barrier deposited using electroless plating is not effective to simultaneously enhance PPD and reduce metal film thickness.

5.3 Summary

The experimental investigations confirmed that the fabrication of Pd/Ni/PSS membranes with 0.1 μm nominal pore size support have better combinatorial plating characteristics (selective conversion, plating efficiency, plating rate, PPD and theoretical selectivity) in comparison with the Pd/Ni/PSS membranes fabricated with 0.5 μm nominal pore size. For the Pd/Ni/PSS membrane fabricated with 0.1 μm PSS support, the combinatorial plating characteristics have been evaluated as 33.73 – 30.92% for selective conversion, 76.54 – 87.01% for plating efficiencies, 2.13 – 9.8 μm thick Pd films, average plating rates of 3.35 – 3.07 x 10^{-5} mol/m^2.s and PPDs of 92.98 – 99.989% for 2-10 h sequential Pd ELP. On the other hand, the Pd/PSS

membrane fabricated with 0.1 μm nominal pore size support, the best optimal combinatorial plating characteristics of 35.40 – 31.48% selective conversion, 90.95 – 95.94% plating efficiency, 4.92 – 4.38x10^{-5} mol/m^2.s average plating rate, 3.14 – 11.16 μm and 96.94 – 100% PPD were obtained for a total plating time of 2 – 8 h. This indicates that despite using the best Pd ELP deposition process, the nickel interdiffusion barrier was not effective to improve the plating characteristics. Thus, it is apparent that the combinatorial plating charecteristics of support surfaces is characterized with poor surface activation due to non-conducting surfaces. This is a major challenge for the cost effective fabrication of dense Pd composite membranes using electroless plating technique. In summary, while interdiffusion barriers such as Ni could be promising to enhance shelf life and hydrogen permeability of Pd composite membranes, they pose serious challenges during their fabrication and offer lower hydrogen selectivities. These complex tradeoffs are very important from the perspective of large scale fabrication and process scale up issues associated to Pd composite membranes.

Chapter 6:

Efficacy of novel electroless plating process or dense $Pd/Cr_2O_3/PSS$ membrane fabrication

Chapter 6

Efficacy of novel electroless plating process for dense $Pd/Cr_2O_3/PSS$ membrane fabrication

In this chapter, the combinatorial plating characteristics for the fabrication of dense Pd composite membranes were addressed for two cases namely (a) chromia interdiffusion barrier achieved with conventional electroplating method and (b) chromia interdiffusion barrier achieved with surfactant induced electroplating method. For both cases, the identified SSOEP (DW) Pd ELP process had been adopted to achieve dense Pd composite membranes. Thereby, the major objective of this chapter is to examine upon the role of surfactant engineered chromia interdiffusion barrier morphology on the combinatorial plating characteristics of Pd composite membranes. Among various intended features, the most essential feature of such investigations is to envisage whether surfactant induced chromia interdiffusion barrier has the potential to significantly reduce the critical thickness required to achieve dense Pd films with the identified SSOEP (DW) process which is the best among all processes investigated for Pd composite membrane.

6.1 Fabrication of $Pd/Cr_2O_3/PSS$ membranes

To study the role of chromia diffusion barrier on the combinatorial plating characteristics of Pd composite membranes, 7.8 and 20 μm thick chromia interdiffusion barrier films were deposited on 100 nm nominal pore size PSS supports using chromium electroplating process. The operating parameters of the process were chromium solution concentration of 250 g/L, current density of 133 mA/cm^2, plating temperature of 30 ^oC and a plating time of 10 – 30 min. Eventually, chromia interdiffusion barriers were achieved by oxidizing the chromium plated

membranes at 700 ^{o}C in a muffle furnace for 6 h. The investigated combinatorial plating characteristics were selective conversion, plating efficiency, plating rate, nitrogen flux profiles, percent pore densification and metal film thickness. Further, surface characterization was conducted using XRD and FESEM analyses. The obtained Pd-Cr_2O_3-PSS membrane characteristics were compared with those of Pd-PSS membranes to analyze upon the role of interdiffusion barrier.

The purpose of engineering chromia interdiffusion barriers with lower and higher chromia film thickness is to ensure whether uniformity of surface pore size distribution was achieved by enhancing the chromia interdiffusion barriers. In this regard two diverse cases can be presumed. In case the surface pore size distribution was not achieved with lower chromia film thickness, it should indicate that the dense Pd composite membranes should have lower saturated PPD values. For such a scenario, enhancing the chromia interdiffusion barrier would be relevant to enhance PPD values. On the other hand, enhancing chromia interdiffusion barrier thickness would reduce and the effective surface activation of the chromia/PSS membrane and therefore poses a further challenge towards the fabrication of dense Pd composite membranes. Thus, it will be interesting to evaluate upon the role of interdiffusion barrier thickness on the combinatorial plating characteristics of dense Pd/Cr_2O_3/PSS membranes.

In the following sections, the results obtained with respect to the combinatorial plating characteristics are presented.

6.1.1 Selective conversion and plating efficiency

Figure 6.1a and 6.1b presents the time dependent variation of selective conversion and plating efficiencies of Pd electroless plating baths for the fabrication of Pd/PSS and Pd/Cr_2O_3/PSS membranes. It can be observed that for Pd/PSS membranes, the selective

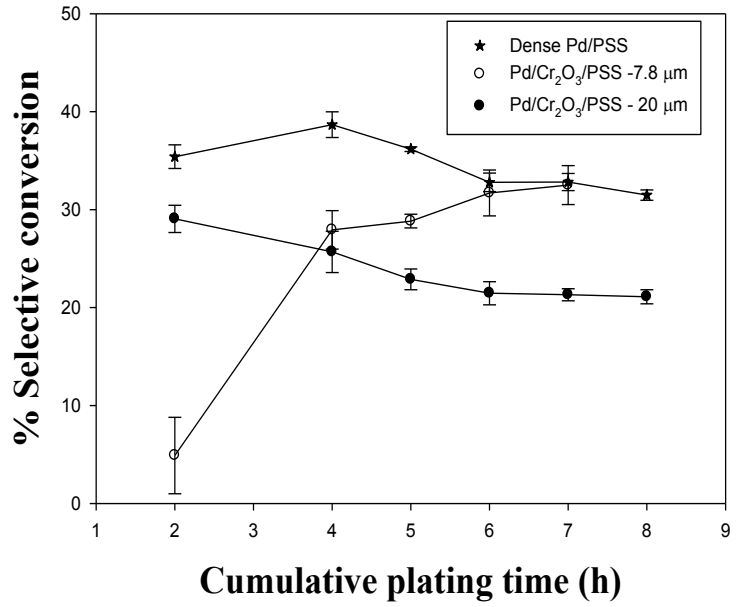

(a)

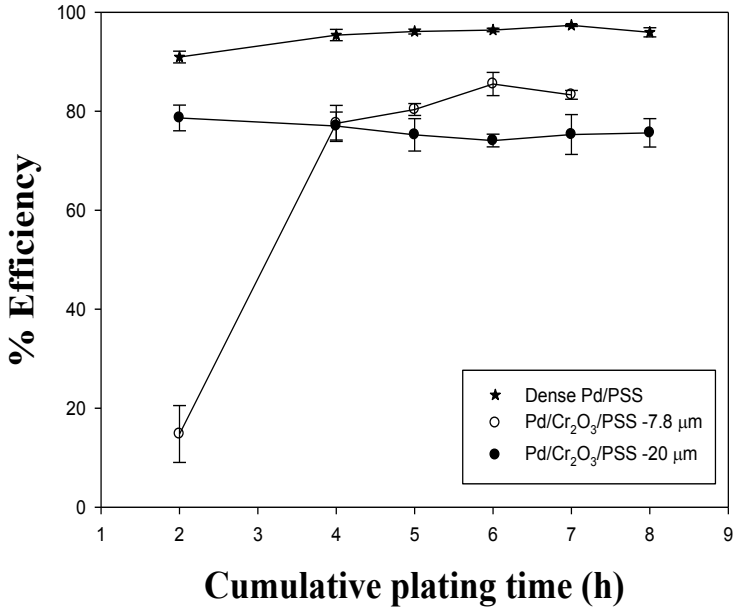

(b)

Figure 6.1: Effect of plating time on (a) selective conversion and (b) plating efficiency for Pd-Cr_2O_3-PSS membranes.

conversions and plating efficiencies varied from 35.4 – 31.48% and 90.95 – 95.94%. However, for Pd/Cr_2O_3/PSS membranes, for an increase in the thickness of Cr_2O_3 film from 7.8 to 20 µm, the selective conversions reduced from 4.90 – 32.51% to 29.06 – 21.11%. A similar reduction in plating efficiency has been evaluated from 14.78 – 83.31% to 78.65 – 75.64%. Thus, it is apparent that Pd/Cr_2O_3/PSS membranes exhibit lower selective conversions and plating efficiencies than Pd/PSS membranes due to the poor Pd surface activation on the chromia interdiffusion barrier.

6.1.2 Plating rate

The time dependent variation of Pd plating rates for Pd/PSS and Pd/Cr_2O_3/PSS membranes has been summarized in Table 6.1. For the Pd/Cr_2O_3/PSS membranes fabricated with 7.8 and 20 µm thick Cr_2O_3 films, the average plating rate values varied from 0.63 – 3.87 x 10^{-5} and 4.09 – 2.97 x 10^{-5} mol/m^2.s, respectively. It can be observed that the plating rates varied from 4.92 – 4.38 x 10^{-5} mol/m^2.s for Pd/PSS membranes. Thus, based on the obtained average plating rate trends, it can be inferred that an enhancement in chromia interdiffusion barrier thickness decreases the effective Pd activation of the membranes and hence lower plating rates.

Table 6.1: Comparison of time dependent average plating rates for Pd/PSS and Pd/Cr_2O_3/PSS membranes.

Type of Membrane	Average plating rate $\bar{r}_{Pd}$ (mol/m^2.s)x10^5 with time of plating (h)					
	2	4	5	6	7	8
Pd/Cr_2O_3/PSS -7.8 µm	0.63	3.13	3.33	3.73	3.87	-
Pd/Cr_2O_3/PSS-20 µm	4.09	3.61	3.22	3.02	3.0	2.97
Pd/PSS	4.92	5.38	5.03	4.56	4.57	4.38

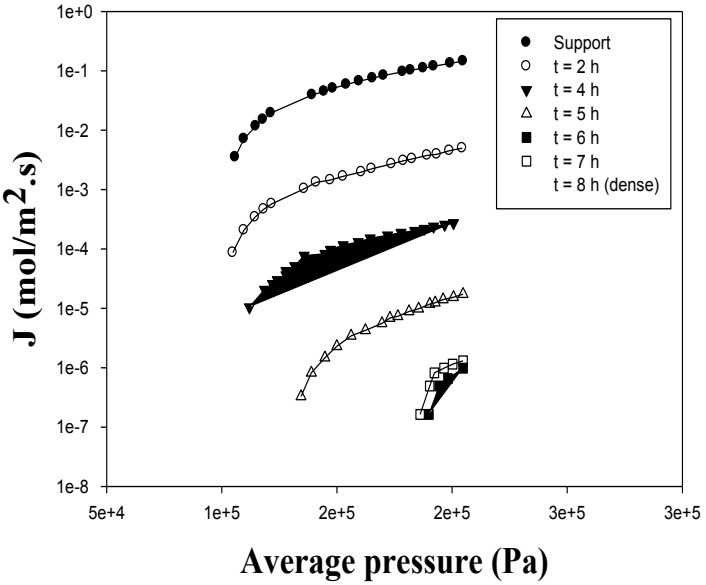

(a)

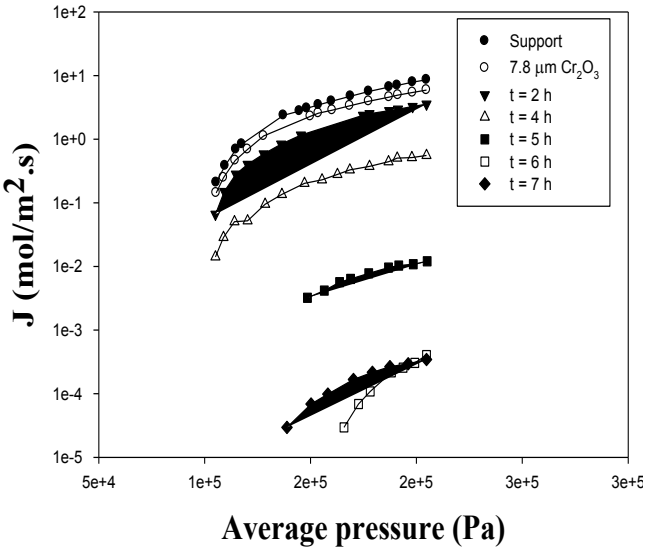

(b)

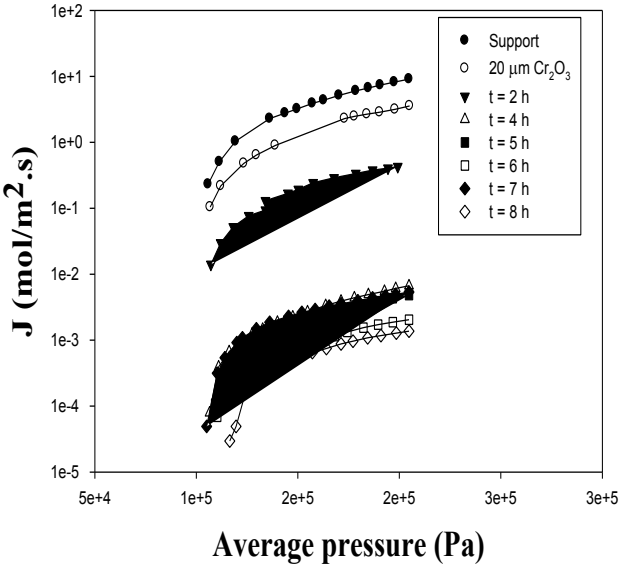

(c)

Figure 6.2: Nitrogen permeation flux Vs avg. Pressure profiles for (a) Pd/PSS and (b) Pd/Cr_2O_3/PSS membranes (7.8 and 20.0 µm thick Cr_2O_3 films).

6.1.3 Nitrogen flux tradeoffs

Figure 6.2 (a-c) depicts the nitrogen permeation flux trends for Pd/Cr_2O_3/PSS and dense Pd/PSS membranes on 0.1 µm PSS supports. For the case corresponding to 7.8 µm Cr_2O_3 on PSS supports, the Cr_2O_3-PSS membrane N_2 flux varied from 0.14 – 5.92 mol/m^2.s (for an average pressure of 1.05 – 2.05 bar) which further reduced to 0 – 3.45x10^{-4} mol/m^2.s (for an average pressure of 1.05 – 2.05 bar) after 7 h of sequential Pd ELP. Similarly, for the case corresponding to 20 µm Cr_2O_3 on PSS supports, the Cr_2O_3-PSS membrane N_2 flux varied from 0.10 – 3.55 mol/m^2.s (for an average pressure of 1.07 – 2.05 bar) which further reduced to 0 – 1.37x10^{-3} mol/m^2.s (for an average pressure of 1.05 – 2.05 bar) after 8 h of sequential Pd ELP. For comparative purposes, it can be observed that the Pd/PSS membrane enabled the flux reduction from 0.211 – 8.77 mol/m^2.s (for an average pressure of 1.05 – 2.05 bar) to 0 – 0 mol/m^2.s (for an average pressure of 1.17 – 2.05 bar) after 8 h of sequential Pd ELP. Thus, it can be inferred that for all cases (namely Pd/PSS and Pd/Cr_2O_3/PSS membranes), the metal delamination occurred after prolonged periods of total plating time. This is due to the uneven charge distributions on the membrane surface due to the CTAB surfactant present in the ELP solution for all cases [39].

6.1.4 Percent pore densification

Figure 6.3a shows the comparative performance of Pd/Cr_2O_3/PSS and Pd/PSS membranes in terms of time dependent variation of (100-PPD). For the Cr_2O_3/PSS membranes, it was evaluated that 7.8 and 20 µm thick chromia films densified the PSS support by 29.76% and 60% respectively. Further, based on the Cr_2O_3/PSS membrane N_2 flux data, it was evaluated that the time dependent PPD for Pd/ Cr_2O_3/PSS membranes varied from 29.8-99.994% (for a variation in time from 2 – 7 h) and 59.47 – 99.91% (for a variation in time from 2 – 8h) for 7.8 and 20 µm thick Cr_2O_3 interdiffusion barrier films respectively. Thus, it is apparent that, during the initial

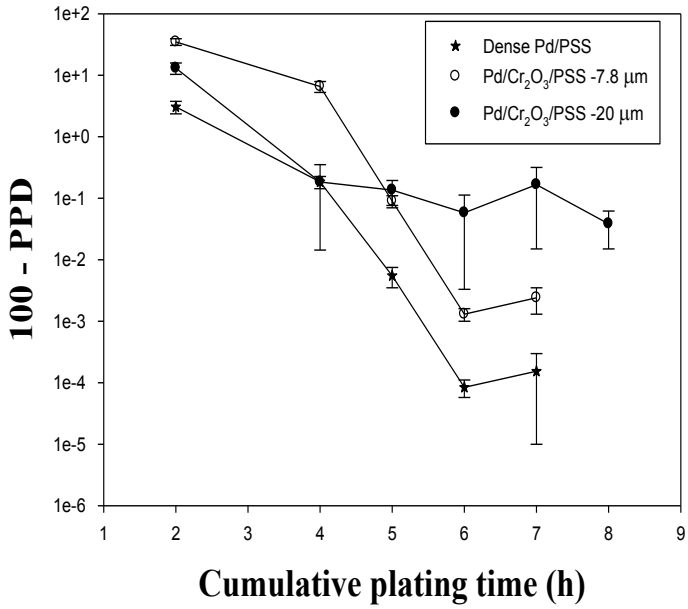

(a)

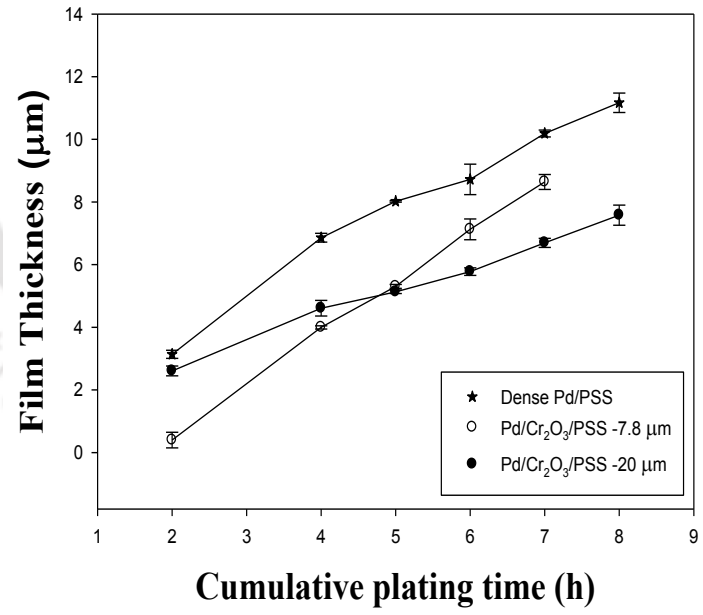

(b)

Figure 6.3: Time dependent variation of (a) PPD and (b) Pd film thickness for Pd/Cr_2O_3/PSS membranes.

4 h sequential plating, the Pd/Cr_2O_3/PSS membranes fabricated on 20 μm thick Cr_2O_3 films had higher PPD profiles than those fabricated with 7.8 μm thick Cr_2O_3 films. For prolonged time periods (5 – 8 h), the Pd/Cr_2O_3/PSS membranes fabricated on 20 μm thick Cr_2O_3 films had marginally lower PPDs (99.86 – 99.96%) in comparison with those obtained with 7.8 μm thick Cr_2O_3 films (99.91 – 99.998%). Also, for all cases, the PPD profiles indicated a lapse mode profile after 6h of sequential Pd ELP, where the PPD corresponds to 99.9%.

6.1.5 Metal film Thickness

Figure 6.3b presents the variation in time dependent metal film thickness with cumulative plating time for Pd/PSS and Pd/Cr_2O_3/PSS membranes. It can be observed that for Pd/Cr_2O_3/PSS membranes (on 7.8 and 20 μm thick Cr_2O_3 films) the time dependent Pd film thickness respectively varied from 0.4 – 8.64 μm and 2.6 – 7.58 μm for a variation in total plating time of 2 – 7 h and 2 – 8 h respectively. On the other hand, for Pd/PSS membranes the time dependent Pd film thickness varied from 3.14 – 11.16 μm. Thus, it is apparent that the Cr_2O_3 diffusion barrier reduced the critical thickness of dense Pd film by about 2 – 3 μm, but could not provide better pore densification than the Pd/PSS membranes. The reduction in the critical film thickness is possibly due to poor surface activation of the oxidized chromia interdiffusion barrier and it might be very unlikely that the chromia interdiffusion barrier normalized the pore size distributions of the support to such an extent that the critical Pd dense film thickness is significantly reduced. In other words, the introduction of chromia interdiffusion barrier is not promising from the perspective of fabrication engineering aspects of the Pd/PSS composite membranes.

6.1.6 Morphological and surface characterization

Figure 6.4a and 6.4b respectively illustrate the field emission scanning electron microscopy (FESEM) images of Cr_2O_3/PSS membrane (7.8 μm thick Cr_2O_3 film) and Pd/Cr_2O_3/PSS membrane (8.6 μm Pd film thickness) obtained after a total plating time of 7 h. From Figure 6.4a, it can be observed that after oxidation of deposited chromium metal, the surface morphology of chromium membrane is rough with homogeneous particle size distribution. Physically, the chromia membrane was observed to possess grey colour. From Figure 6.4b, it can be observed that the 8.6 μm thick Pd film on the surface is smooth with finer Pd grains and no pinholes/surface defects are visible for the composite membranes.

Figure 6.4c presents the X-ray diffraction (XRD) pattern of Cr_2O_3/PSS and Pd/Cr_2O_3/PSS composite membranes. The XRD profile of Pd/Cr_2O_3/PSS membrane is similar to that obtained for Pd/PSS membrane. For Cr_2O_3/PSS membrane, the reflection peaks appeared at a diffraction angle (2θ) of 33.7°, 41.6°, 46.7° and 65.2° which correspond to the peaks associated to chromium oxide. From Figure 6.4c, it was evaluated that the XRD spectra confirms the existence of Pd reflection peaks at diffraction angles (2θ) of 40.2°, 46.76° and 68.28° due to diffraction of (1 1 1), (2 0 0) and (2 0 2) plane, respectively. No other peaks were detected in the XRD pattern. The inability to detect Cr and stainless steel peaks in the XRD spectra for the Pd/Cr_2O_3/PSS membrane is indicative towards the achievement of a relatively dense Pd composite membrane.

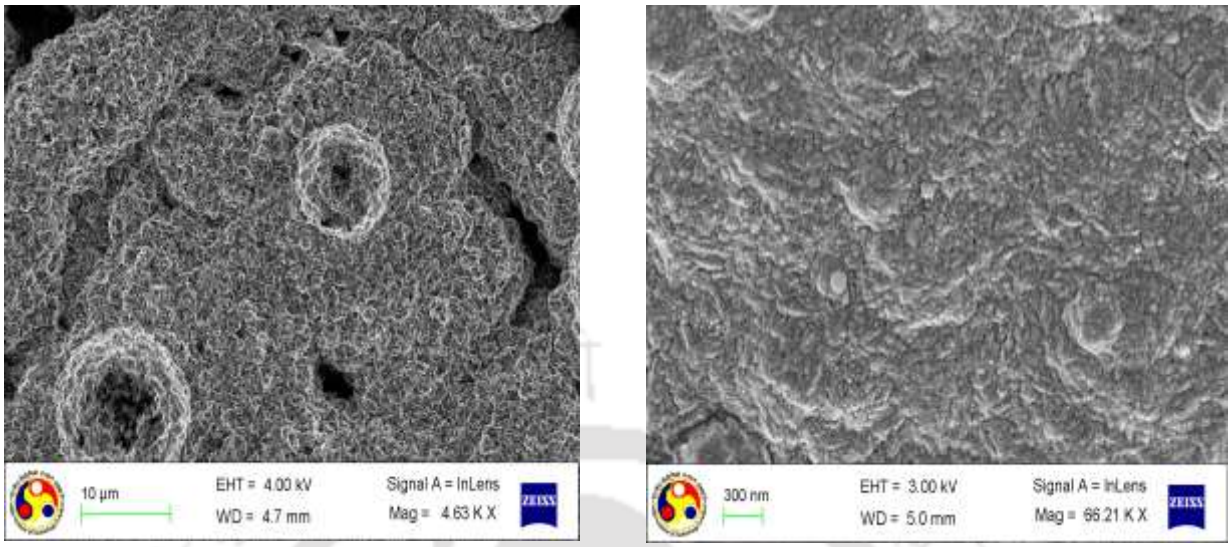

(a) **(b)**

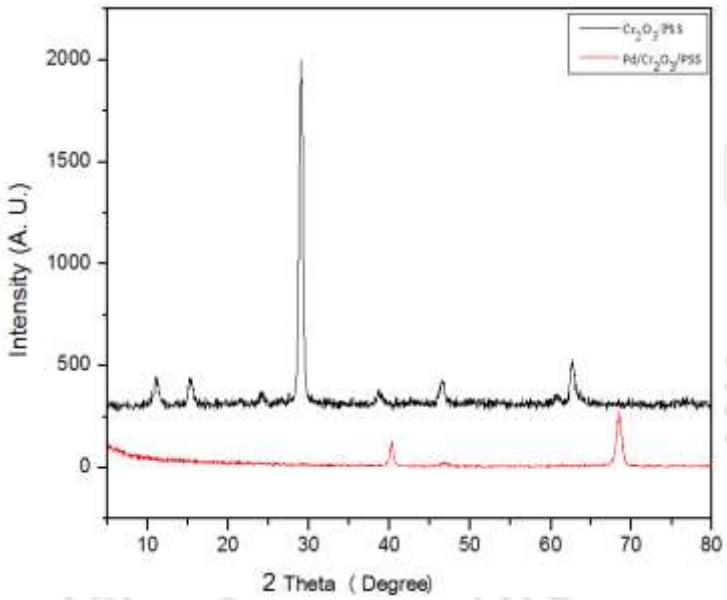

(c)

Figure 6.4: FESEM micrographs of (a) Cr_2O_3/PSS membrane (7.8 µm chromia film thickness) (b) dense Pd/Cr_2O_3/PSS membrane (7.8 µm chromia film thickness) and (c) XRD pattern of Pd/Cr_2O_3/PSS membrane (on 7.8 µm).

6.2 Fabrication of Pd/Cr_2O_3-surf/PSS membranes

To study the role of surfactant induced chromia diffusion barrier on combinatorial plating characteristics of Pd composite membranes, 7.1 and 12.5 μm thick Cr_2O_3 films were deposited by dispersing the CTAB cationic surfactant (2 CMC) in the chromium electroplating solution. Further, all the plating experiments were conducted as described earlier. Two cases with different chromia interdiffusion barrier thickness values were considered to evaluate upon the role of interdiffusion barrier uniformity on the combinatorial plating characteristics. In this regard two diverse hypothesis were presumed. Firstly, if it assumed that the chromia interdiffusion barrier enables uniformity of surface pore size distribution due to usage of surfactant during chromium electroplating, it should enable the achievement of dense Pd composite membranes. On the other hand, if surfactant induced chromia interdiffusion barrier fabrication does not promote significant variation in the uniformity of pore size distribution (which is eventually ensured by verifying whether dense Pd composite membranes can be achieved or not), it is indicative towards confirming that the surfactant utilization during chromium electroplating is not effective. Thus, it will be an interesting case study to consider the engineering aspects of chromium interdiffusion barrier using surfactant induced electroplating process.

6.2.1 Selective conversion and plating efficiency

Figure 6.5a and 6.5b illustrate the time dependent variation of selective conversion and plating efficiencies of Pd electroless plating baths during the fabrication of Pd/Cr_2O_3-surf/PSS membranes on 7.1, 12.5 μm thick Cr_2O_3 films and Pd/PSS membranes on 0.1 μm PSS supports. It can be observed that the selective conversions varied from 49.29 – 37.6, 41.84 – 28.65 and 35.4 – 31.48% for 7.1 μm thick surf-Cr_2O_3 films, 12.5 μm thick surf-Cr_2O_3 films and 0.1 μm

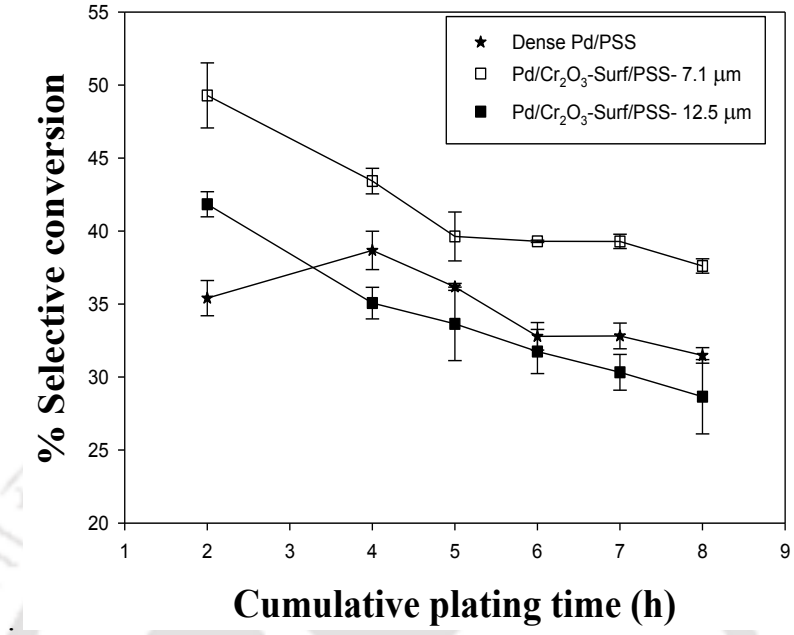

(a)

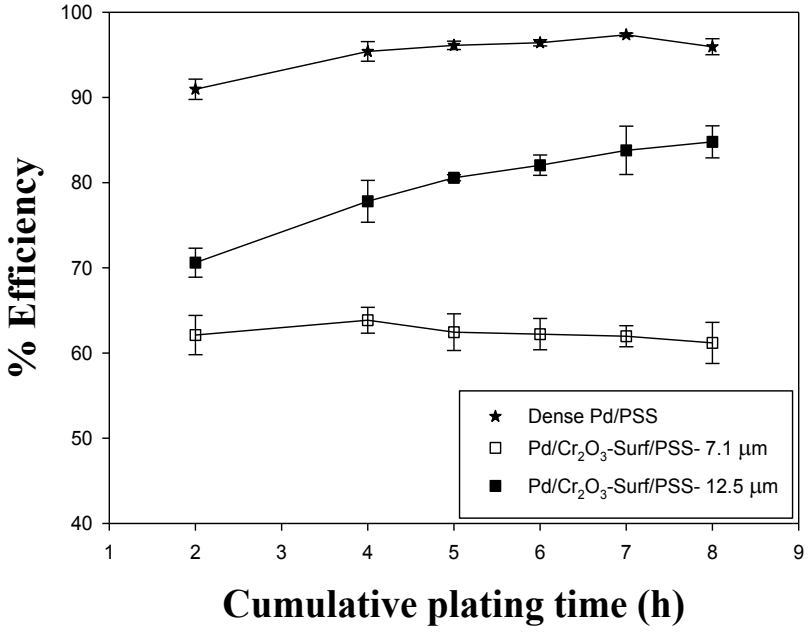

(b)

Figure 6.5: Variation of (a) selective conversion and (b) % efficiency with time for Pd/Cr_2O_3-surf/PSS membranes.

nominal pore size PSS membranes. Thus, it is apparent that lower surf-Cr_2O_3 film thickness provided higher selective conversions due to better engineering of the interdiffusion barrier in comparison to that of the support and 12.5 μm thick surf-Cr_2O_3 film. Compared to 12.5 μm thick surf-Cr_2O_3, higher conversions were obtained for the 7.1 μm thick surf-Cr_2O_3 film which is possibly due to poor surface activation for the former case.

On the other hand, the time dependent Pd plating efficiencies for 7.1 and 12.5 μm thick Cr_2O_3 films varied from 62.11 – 61.18 and 70.60 – 84.78% respectively, which were significantly lower than the corresponding values obtained for Pd-PSS membranes (90.96 – 95.94%). The reduction in plating efficiencies for the surf-chromia interdiffusion barrier cases is possibly due to greater metal nucleation in the solution due to the chromia interdiffusion barrier. This is also confirmed with the observed conversion profiles which indicated that conversions were very high for the chromia interdiffusion barrier cases in comparison with Pd/PSS membranes. Also, it is apparent that higher chromia film thickness enhanced plating efficiencies. This might be due to the fact that higher chromia film thickness ensures better surface uniformity in terms of pore size distributions which might reduce metal nucleation in the solution. Thus, the introduction of a non-conducting inter diffusion barrier with lower thickness is detrimental towards the plating efficiency profiles which are very important in the fabrication engineering aspects associated to Pd composite membrane fabrication. Further, it can be also observed for all cases that while selective conversions reduced, the plating efficiencies increased with increasing plating time. This is due to the lower metal nucleation in the solution at higher plating time, which might be due to the greater role of initially deposited Pd film in fostering adhesion strength of the later deposited Pd film to the chromia surface. Thus, it is apparent that the Pd adhesion with the chromia interdiffusion barrier was not significant in the initial stages of plating which improved

significantly with time. Also, among interdiffusion barriers, the best case of plating efficiencies was for 12.5 μm surf chromia-PSS case, which is possibly due to better surface pore size distribution uniformity for the case compared to the case of lower surf chromia interdiffusion barrier. All in all, the observed trends in selective conversion and plating efficiency are interesting features of the undertaken research, as they have clearly indicated that pertinent challenges associated to deposit Pd films on the surface of porous chromia.

6.2.2 Plating rate

The time dependent variation of Pd plating rates for Pd/Cr_2O_3-sur/PSS and Pd/PSS membranes has been summarized in Table 6.2. It can be observed that for Pd/Cr_2O_3-surf/PSS membranes fabricated with 7.1 and 12.5 μm thick surf-Cr_2O_3 films, the average plating rates were significantly higher and varied from 6.41 – 4.89 x 10^{-5} and 6.26 – 4.28 x 10^{-5} mol/m^2.s, respectively. Corresponding average plating rate values for the Pd/PSS membranes varied from 4.92 – 4.38 x 10^{-5} mol/m^2.s. Thus, it is apparent that higher plating rates were achieved for chromia interdiffusion barriers in comparison with the Pd/PSS membrane case. Also, in comparison with chromia interdiffusion barriers fabricated using chromium electroplating but

Table 6.2: A summary of time dependent average plating rates for Pd/PSS and Pd/Cr_2O_3-surf/PSS membranes.

Type of Membrane	Average plating rate $\bar{r}_{Pd}$ (mol/m^2.s)x10^5 for various total plating time (h)					
	2	4	5	6	7	8
Pd/Cr-surf/PSS- 7.1 μm	6.41	5.65	5.15	5.11	5.11	4.89
Pd/Cr-surf/PSS-12.5 μm	6.26	5.24	5.03	4.75	4.53	4.28
Pd/PSS	4.92	5.38	5.03	4.56	4.57	4.38

not surfactant, the trends were the opposite i.e., highest average plating rate was obtained for 12.5 μm thick surf-Cr_2O_3 film case. In other words, it is clearly evident that the utilization of surfactant during chromium electroplating favoured significant enhancement in the uniformity of the surface pore size distribution, for Cr_2O_3 films with higher thickness. This enabled efficient compatibility of chromia with as deposited Pd. Further, it is also hypothesized that the surfactant induced chromium electroplating might have significantly enhanced the surface area of the chromia films which thereby enabled significant enhancement in the average plating rate. Since higher average plating rates were obtained for the surf-chromia film cases, it is anticipated that higher thicknesses shall also exist for the same cases, as will be discussed in section 6.2.4. Also, the average plating rates were evaluated to reduce with increasing plating time. This is due to enhancement in surface Pd concentration which thereby reduces the potential of the electroless plating reaction with similar Pd solution concentrations.

Higher plating rates were obtained for lower Cr_2O_3-surf thickness values and this confirms that the films have better surface area for activation in comparison with those obtained for 12.5 μm Cr_2O_3-surf thickness. In other words, lower Cr_2O_3-surf thickness has better pore size distribution than higher Cr_2O_3-surf thickness.

6.2.3 Nitrogen flux tradeoffs

Figure 6.6 (a-c) depicts the nitrogen permeation flux trends for Pd-Cr_2O_3-surf/PSS and Pd/PSS membranes. It can be observed that for 7.1 μm thick surf-Cr_2O_3 film deposited on PSS support, the N_2 flux reduced from 0.173 – 8.58 mol/m^2.s (for an average pressure of 1.05 – 2.05 bars) to 0.178 – 6.21 mol/m^2.s (1.06 – 2.05 bar). Similarly, for the 12.5 μm thick surf-Cr_2O_3 film deposited on the PSS support, the N_2 flux reduced from 0.26 – 8.58 mol/m^2.s (for an average

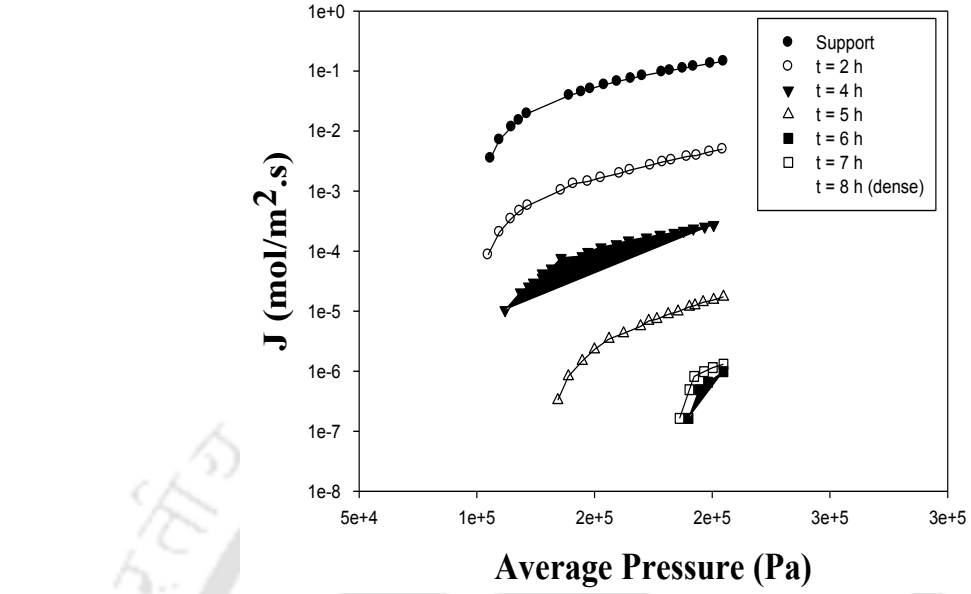

(a)

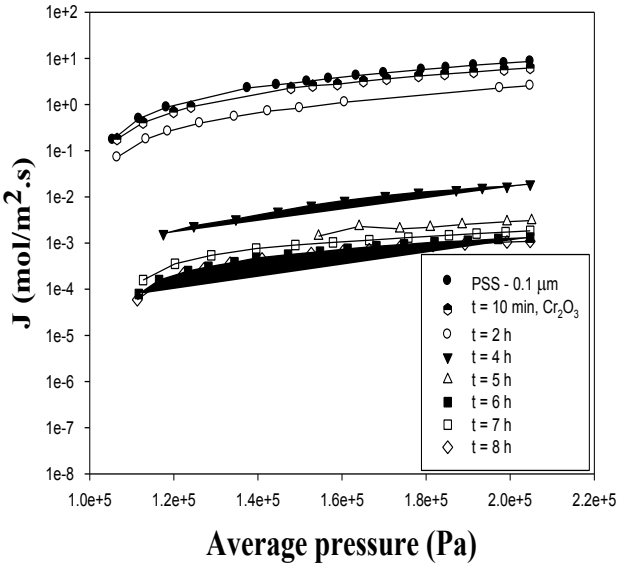

(b)

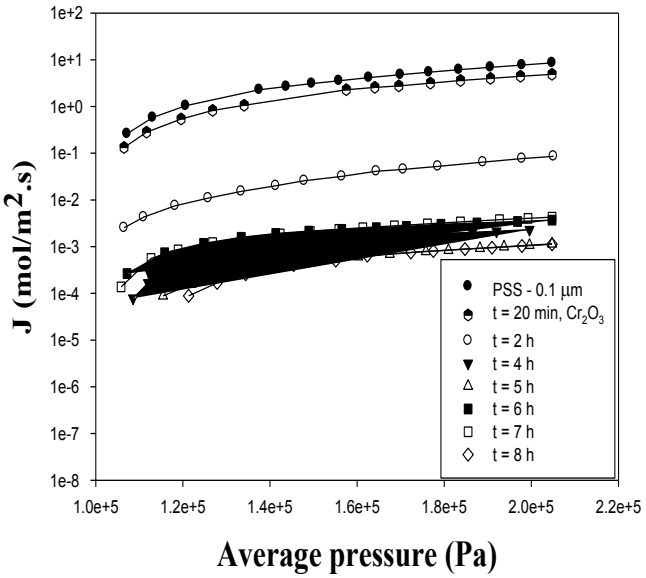

(c)

Figure 6.6: N_2 flux plots for various cases (a) Pd/PSS (b) Pd/Cr_2O_3-surf/PSS (7.1 µm chromia thickness) and (c) Pd/Cr_2O_3-surf/PSS (12.5 µm chromia thickness) membranes.

pressure of 1.07 – 2.05 bars) to 0.13 – 4.88 mol/m^2.s (for an average pressure of 1.06-2.05 bar). Thus, for the later case, significant reduction in flux was achieved during the deposition of the thicker chromia interdiffusion barrier. For Pd/surf-Cr_2O_3/PSS membranes fabricated with 7.1 μm thick surf-Cr_2O_3 film, the N_2 flux varied from 0 – $1.31x10^{-3}$ mol/m^2.s (for an average pressure of 1.05 – 2.05 bar) after 6 h of sequential Pd ELP. For the same case, with further 1 h plating, the flux enhanced to $1.58x10^{-4}$ – $1.84x10^{-3}$ mol/m^2.s (for an average pressure of 1.12 – 2.05 bar). After 8 h of sequential Pd ELP, for this case, the maximum reduction in nitrogen permeation flux was obtained in the range of $5.91x10^{-5}$ – $1.08x10^{-3}$ mol/m^2.s (1.13 – 2.05 bar).

On the other hand, for the 12.5 μm surf-chromia case, after 5 h of sequential Pd ELP, the N_2 flux reduced to 0.13 – 4.88 mol/m^2.s (for an average pressure of 1.06 – 2.05 bar) to 0 – $1.14x10^{-3}$ mol/m^2.s (for an average pressure of 1.09 – 2.05 bar). For the same case, an additional 2 h sequential plating enabled the flux reduction to $1.38x10^{-4}$– $4.29x10^{-3}$ mol/m^2.s (for an average pressure of 1.06 – 2.05 bar). For the same membrane, after 8 h of sequential Pd ELP, the maximum reduction in nitrogen permeation flux was obtained in the range of 0 – $1.12x10^{-3}$ mol/m^2.s (for an average pressure of 1.11 – 2.05 bar). Thus, it is apparent that for neither cases, a very significant reduction in N_2 flux was not prevalent and this confirmed not achieving very high values of pore densification. Further results with respect to the PPD are presented in the next section.

6.2.4 Percent pore densification

Figure 6.7a shows the comparative performance of Pd/Cr_2O_3-surf/PSS and Pd/PSS membranes in terms of (100 – PPD) variation with total plating time. It has been evaluated that after depositing 7.1 and 12.5 μm thick Cr_2O_3-surf films, the PSS membranes of 0.1 μm possessed PPD values of

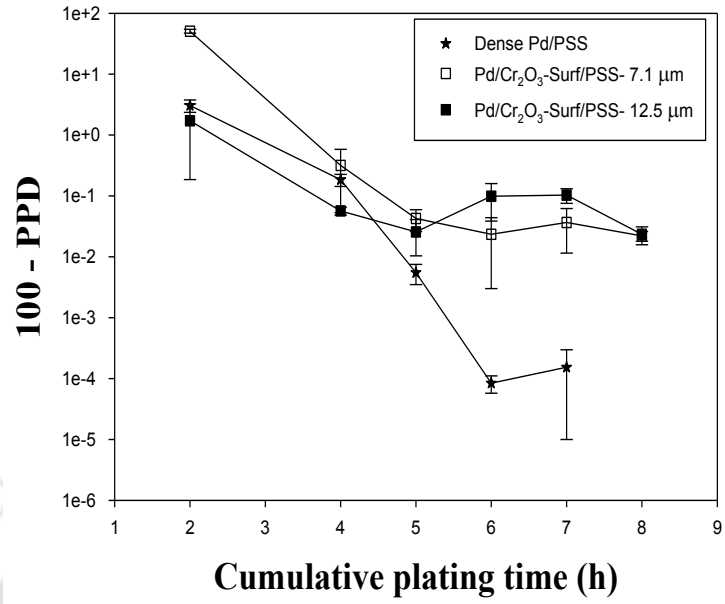

(a)

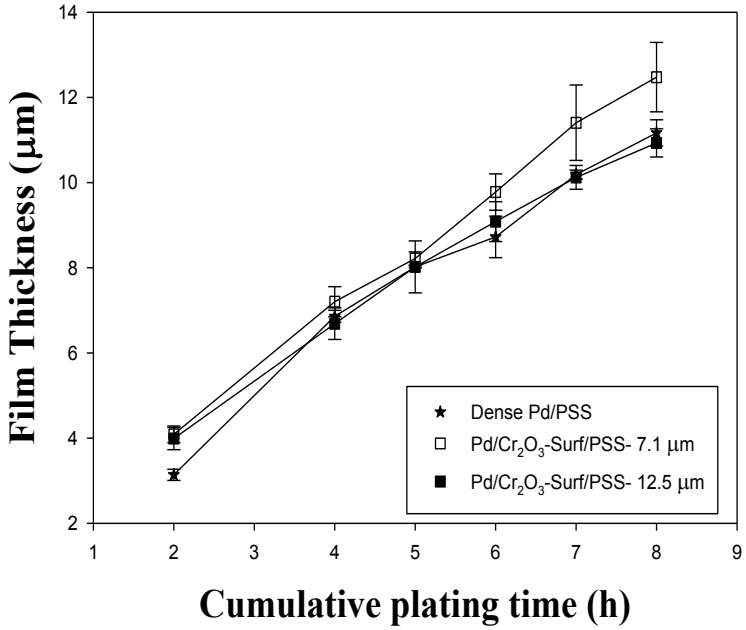

(b)

Figure 6.7: Time dependent profiles of (a) (100 – PPD) and (b) Metal film thickness for Pd/Cr_2O_3-surf/PSS membranes.

26.05 and 42.26% respectively. For 2 – 8 h Pd sequential plating on these Cr_2O_3-surf/PSS membranes, the PPD varied from 49.15 – 99.978% for 7.1 µm thick Cr_2O_3-surf interdiffusion barrier and 98.28 – 99.976% for the 12.5 µm thick Cr_2O_3-surf interdiffusion barrier. These are significantly lower than the PPD values obtained for the Pd/PSS membranes which were about 96.3 – 100%. Thus, it is apparent that the engineering of chromia interdiffusion barrier even with surfactant induced electroplating did not enable the achievement of very high PPD values in the longer periods of time. Instead, lower PPD values were obtained for both cases and among these two, lower PPD profile was obtained for the 12.5 µm thick Cr_2O_3-surf interdiffusion barrier case. Thus, it is apparent that despite using the best process (SSOEP (DW) for Pd ELP, the surfactant induced electroplating did not favor enhancement of the PPD. In other words, it appears that there exists a significant limitation of the ELP process in terms of engineering dense Pd films on chromia interdiffusion barrier. This important observation needs further insights from several research perspectives including variations in solution concentrations etc., Further, it is also interesting to note that the PPD was significantly higher during the early stage of plating for both cases corresponding to surfactant engineered chromia interdiffusion barriers. In comparison with the chromia interdiffusion barriers fabricated using conventional electroplating, the Pd composite membranes did not exhibit better PPD. Once again, this indicates that the surfactant induced electroplating is incompatible to further optimize the combinatorial plating characteristics associated to Pd/Cr_2O_3/PSS membranes.

6.2.5 Metal film Thickness

The variation in time dependent metal film thickness for Pd/Cr_2O_3-suf/PSS membranes is presented in Figure 6.7b. For a variation in total plating time from 2 to 8 h, the Pd/Cr_2O_3/PSS membrane Pd film thickness varied from 4.08-12.47 µm and 3.99 – 10.93 µm for 7.1 and 12.5

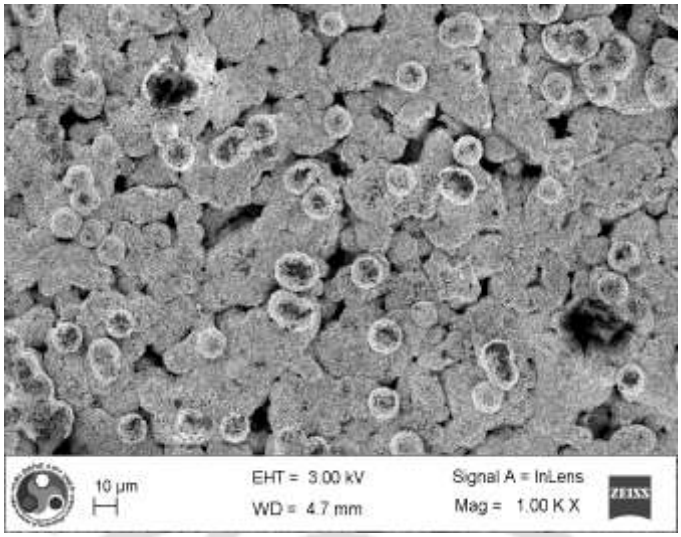

(a)

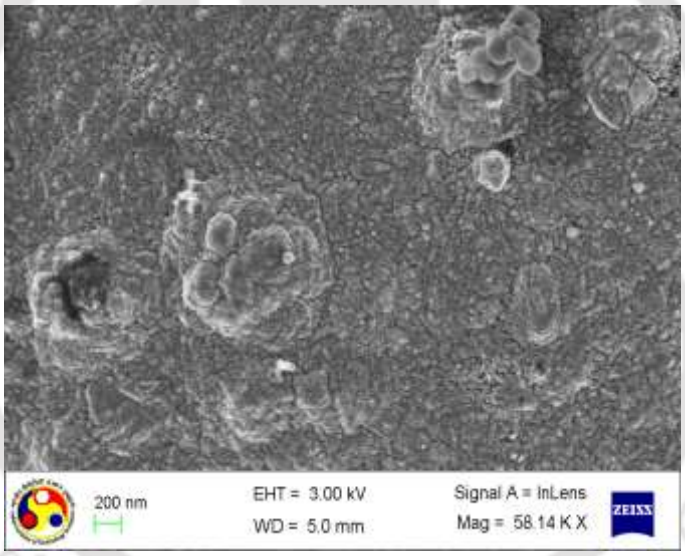

(b)

Figure 6.8: FESEM micrographs of Cr_2O_3-surf/PSS and Pd/ Cr_2O_3-surf/PSS membranes fabricated with 7.1 µm chromia interdiffusion barrier thickness.

µm thick Cr_2O_3-surf film cases respectively. Corresponding variation in Pd film thickness for Pd/PSS membranes is about 3.14 – 11.16 µm. Thus, it is apparent that the utilization of surfactant during chromia interdiffusion barrier engineering did not reduce the critical metal film thickness required to achieve dense Pd composite membranes. A significant increase in metal

film thickness is possibly due to higher average plating rates for the surfactant induced electroplating based fabrication of chromia interdiffusion barrier. Further details with respect to the same along with relevant reasons are presented in section 6.2.2 of the chapter.

6.2.6 Morphological and surface characterization

Figure 6.8a and 6.8b shows the FESEM micrographs of Cr_2O_3-surf/PSS membrane (7.1 μm thick Cr_2O_3-surf film) and Pd/ Cr_2O_3-surf/PSS membranes on porous stainless steel substrate of 0.1μm nominal pore size. From 6.8a, it can be observed that the resultant chromia grains (obtained with surfactant induced electroplating followed with oxidation) distributed more uniformly on the substrate surface. However, for Pd/ Cr_2O_3-surf/PSS membrane, the surface becomes even smoother with few grain agglomerations. Also, no pinholes are observed for the specified magnification of the FESEM instrument.

6.2.7 Tradeoffs

Figure 6.9 illustrates the $\frac{PPD}{\delta}$ vs. $\bar{\alpha}_{av}$ profiles for Pd/Cr_2O_3-surf/PSS membranes (on 7.1 and 12.5 μm thick Cr_2O_3-surf films), Pd/Cr_2O_3/PSS (on 20 μm thick Cr_2O_3 films) and Pd/PSS membranes. For Pd/Cr_2O_3-surf/PSS membrane fabricated with 7.1 μm thick Cr_2O_3 film, the selectivities obtained after 6, 7 and 8h of sequential Pd ELP are 90,109 and 222, respectively. Corresponding $\frac{PPD}{\delta}$ values are 11, 9.87 and 9.14 respectively. However, for Pd/Cr_2O_3-surf/PSS membrane fabricated with 12.5 μm thick Cr_2O_3 interdiffusion barrier, the selectivities obtained are 114 and 101 after 5 and 8 h sequential Pd ELP respectively. Corresponding $\frac{PPD}{\delta}$ values are 12.16 and 8.01 respectively. On the other hand, for Pd/PSS membrane, the theoretical

selectivities obtained after 5, 6 and 7 h of sequential Pd ELP are 279.23, 6154 and 3953 respectively. For this case, corresponding $\frac{PPD}{\delta}$ values are 12.46, 11.46 and 9.81. For the same membrane, maximum selectivity of infinity was obtained after completion of 8 h of Pd ELP. For Pd/Cr_2O_3/PSS membranes (on 20 μm thick Cr_2O_3 films) the selectivities are 150, 33 and 125 after 6, 7 and 8 h sequential plating steps, respectively for a corresponding $\frac{PPD}{\delta}$ values of 17.29, 14.91 and 13.19. Thus it is apparent that among all cases, lowest theoretical selectivities were evaluated for Pd/Cr_2O_3-surf/PSS membranes in comparison with the Pd/PSS membrane. The theoretical selectivities for Pd/Cr_2O_3/PSS membranes were located in between the values obtained for surfactant induced chromia interdiffusion barrier and conventional porous stainless steel supports. On the other hand, $\frac{PPD}{\delta}$ values obtained were highest for the chromia

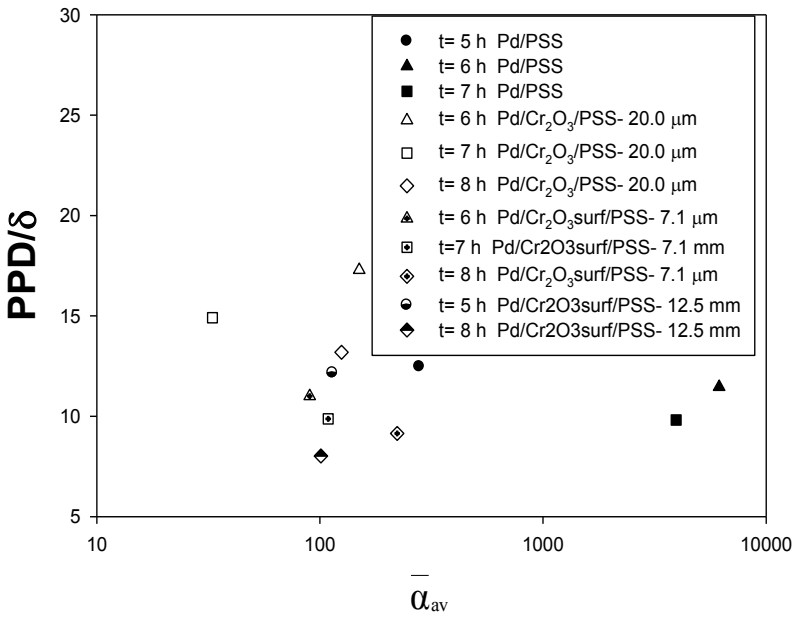

Figure 6.9: $\frac{PPD}{\delta}$ vs. $\bar{\alpha}_{av}$ tradeoffs for dense Pd/Cr_2O_3-surf/PSS, Pd/Cr_2O_3/PSS and Pd/PSS membranes.

interdiffusion barrier fabricated using conventional electroplating and lowest for conventional PSS supports. Nonetheless the variations in the $\frac{PPD}{\delta}$ for various cases is marginal and considering the highest values of selectivities for Pd/PSS membranes, it is apparent that an insignificant reduction in $\frac{PPD}{\delta}$ is justified.

6.3 Summary

From the experimental investigations, it has been evaluated that for a variation in total plating from 2 – 7 h, the Pd composite membranes fabricated with 7.8 μm thick Cr_2O_3 film (conventional electroplating case), the combinatorial plating characteristics such as selective conversion, plating efficiency, plating rate, thickness and PPD varied from 4.90 – 32.51%, 14.78 – 83.31%, 0.63 – 3.87x10^{-5} mol/m^2.s, 0.4 – 8.64 μm and 29.8 – 99.994%, respectively. In addition, these characteristics were marginally lower for the Pd/Cr_2O_3/PSS membranes fabricated with 20 μm thick Cr_2O_3 film (conventional electroplating case) and correspond to a variation in selective conversion from 29.06 – 21.11%, plating efficiency from 78.65 – 75.64%, plating rate from 4.09 – 2.97x10^{-5} mol/m^2.s, metal film thickness from 2.6 – 7.58 μm and PPD from 59.47 – 99.91%. While comparing these combinatorial plating characteristics with Pd/PSS membranes, the Pd/Cr_2O_3/PSS membranes fabricated with chromia interdiffusion barrier achieved with conventional electroplating possessed lower combinations of all combinatorial plating characteristics i.e., selective conversion, plating efficiency, plating rate, thickness and pore densifications.

For a variation in total plating time from 2 – 8h, the combinatorial plating characteristics of Pd/Cr_2O_3-surf/PSS membranes (for 7.1 μm thick Cr_2O_3 interdiffusion barrier) were evaluated to vary from 49.29 – 37.6%, for selective conversion, 62.11 – 61.18% for plating efficiency, 6.41

– 4.89×10^{-5} mol/m^2.s for average Pd plating rate, 4.08 – 12.47 μm for metal film thickness and 49.15 – 99.978% for PPD. On the other hand, for a variation in plating time from 2 – 8h, these characteristics were marginally better for the Pd/Cr_2O_3-surf/PSS membranes prepared with 12.5 μm thick Cr_2O_3 films for which case, the combinatorial plating characteristics were evaluated with selection conversion from 41.84 – 28.65%, plating efficiency from 70.60 – 84.78%, average plating rate from 6.26 – 4.28×10^{-5} mol/m^2.s, metal film thickness from 3.99 – 10.93 μm and PPD from 98.29 – 99.976%. In summary, the surfactant induced electroplating enabled the realization of higher Pd metal film thickness on the chromia interdiffusion barrier but did not enable the achievement of 100% pore densification. By using chromium interdiffusion barriers fabricated with conventional electroplating method, if it is assumed that the 100% Pd/PSS with higher Pd film thickness provides similar H_2 flux to that obtained for dense Pd/chromia/PSS membranes (with 99.99% PPD), a reduction in the critical dense Pd film thickness by 2 – 3 μm was feasible along with the relevant tradeoff associated to the PPD. Otherwise, the introduction of chromia interdiffusion barrier can be inferred to not enhance the hydrogen flux values, as similar dense Pd film thickness values were obtained for both Pd/PSS and Pd/chromia/PSS membranes for similar values of PPD (99.99%). All in all, the engineering of chromia interdiffusion barrier offers significant challenges to target in the near future using scalable rate enhancement techniques such as electroplating and electroless plating.

Chapter 7:

Conclusions and Future Work

CONCLUSIONS AND FUTURE WORK

In this chapter, Sections 7.1 and 7.2 address the conclusions and possible scope for future work respectively.

7.1 Conclusions

The thesis deals with the fabrication of dense Pd/PSS, Pd/Ni/PSS and Pd/Cr_2O_3/PSS composite membranes on porous stainless steel substrates of 0.1 and 0.5 μm nominal pore sizes using various rate enhancement Pd ELP processes such as sonication assisted electroless plating baths (SOEP), surfactant induced electroless plating baths (SIEP) and coupled surfactant and sonication assisted electroless plating baths (SSOEP). Emphasizing upon the combinatorial plating characteristics, the thesis addresses a comparative assessment of various Pd ELP processes supplemented with scalable rate enhancement techniques such as sonication and surfactant. The comparison study refers to combinatorial plating characteristics with time of plating for different rate enhancement techniques. The combinatorial plating characteristics refer to both process and membrane characteristics. While process characteristics were evaluated for selective conversion, plating efficiency, average plating rates, membrane characteristics refer to metal film thickness and percent pore densification.

It has been explicitly identified and inferred in this work that electroless plating technique cannot provide 100% dense Pd-PSS composite membranes despite utilizing rate enhanced ELP processes. Hence, high temperature experiments using H_2/N_2 and mixtures of H_2/N_2 were not conducted.

Various contacting patterns such as bulk, phasewise and continuous (drop wise) addition of the reducing agent have been targeted for the comparative assessment of Pd ELP baths and identification of optimal Pd ELP process for dense Pd composite membrane fabrication.

7.1.1 Thesis Novelty

- For the first time in the field of dense Pd composite membrane fabrication with Pd ELP, this thesis addressed the evaluation of time dependent combinatorial plating characteristics such as selective conversion, plating efficiency, average plating rate, metal film thickness and PPD.
- A framework has been presented to evaluate theoretical selectivity based on the room temperature nitrogen flux. Based on the said approach, high temperature experiments need not be conducted and the deviation of the fabricated membrane from 100% dense Pd composite membrane can be evaluated. These deviations are useful in the context of providing greater insight into the better fabrication aspects.
- The optimal process invented for Pd/PSS membrane fabrication refers to the sonication and surfactant coupled Pd ELP bath supplemented with dropwise addition of the reducing agent.
- Parametric optimality for dense Pd/PSS membranes have been identified for SSOEP (DW) Pd ELP baths. This refers to utilization of lower Pd solution concentrations.
- Combinatorial plating characteristics for dense Pd/Ni/PSS and Pd/ Cr_2O_3/PSS composite membranes have been evaluated.
- The role of chromia interdiffusion barrier morphology that was achieved using surfactant induced electroplating process to influence the combinatorial plating characteristics was

investigated. Using the obtained insights, further engineering aspects could be investigated.

- The optimality of SSOEP (DW) process for dense Pd/PSS membrane fabrication does not indicate upon its optimality for dense Pd/Ni/PSS and Pd/Cr_2O_3/PSS membrane fabrication.

For the fabrication of dense Pd/PSS, Pd/Ni/PSS and Pd/Cr_2O_3/PSS composite membranes using electroless plating technique, various important conclusions are summarized in the following sub-sections of this section.

7.1.2 Optimal process for dense Pd/PSS membrane fabrication

- For SOEP processes with 0.005 M Pd solution concentration and bulk addition of hydrazine reducing agent, metal nucleation was significant in the plating solution to eventually provide lower values of plating efficiency coupled with lower Pd film adhesion.
- Among CEP, SIEP, SOEP and SSOEP Pd ELP baths that were supplemented with phasewise (PW) addition of the reducing agent, SIEP and SSOEP provide better combinatorial plating characteristics for dense Pd/PSS composite membrane fabrication. The SIEP (PW) provided lower selective conversion (17.35%) but higher PPD values (98.46%) and did not provide dense Pd/PSS membrane. On the other hand, SOEP (PW) enabled high selective conversion (34.95%), with PPD reaching not more than 85%. On the other hand, CEP (PW) provided lower selective conversion (11.77%) and lower PPD (7.16%). Only SSOEP (PW) process provided higher combinations of selective conversion (34.45%) and PPD (99.82%). Henceforth, it can be inferred that only SSOEP process offers better opportunities to achieve 100% dense Pd composite membrane. A

summary of various optimal combinatorial plating characteristics of SIEP (PW) and SSOEP (PW) processes is presented in Table 7.1.

- Among SIEP (DW) and SSOEP (DW) Pd ELP baths, the SSOEP baths performed significantly better than SIEP baths in terms of combinatorial plating characteristics. The SSOEP Pd ELP bath indicated that the process provides better opportunities to achieve dense Pd/PSS composite membranes. Optimal combinatorial plating characteristics of SIEP (DW) and SSOEP (DW) processes are presented in Table 7.1.
- Among SSOEP (PW) and SSOEP (DW) Pd baths, except for PPD, PW provided better combinatorial plating characteristics than DW baths for the chosen parametric conditions (Table 7.1). However, a further improvement in the DW baths is inferred with process variations such as surfactant solution concentration.

Process	Optimal total plating time (h)	Selective conversion (%)	Plating efficiency (%)	Metal film thickness (µm)	Average plating rate (mol/m^2.s)	PPD (%)
SIEP (PW)	6	17.35	62.80	4.74	2.34x10^{-5}	98.46
SSOEP (PW)	6	34.95	95.18	8.99	4.70x10^{-5}	99.82
SIEP (DW)	4	13.75	45.23	2.26	1.77x10^{-5}	20.2
SSOEP (DW)	7	26.31	80.69	8.81	3.95x10^{-5}	99.98

Table 7.1: **A summary of optimal combinatorial plating characteristics for dense Pd/PSS composite membrane fabrication using SIEP and SSOEP Pd ELP baths (0.005 M Pd solution concentration, 4 CMC CTAB surfactant solution concentration and loading ratio of 203 cm^2/L).**

7.1.3 Parametric Optimality for SSOEP (DW) Pd ELP baths

- For SSOEP (DW) Pd ELP baths, for 4 CMC CTAB solution concentration and 203 cm^2/L loading ratio value, higher Pd solution concentration (0.01 M) did not enable the achievement of higher PPD values (Table 7.2). Hence, the optimal Pd solution concentration corresponds to 0.005 M at 4 CMC CTAB solution concentration and 203 cm^2/L respectively.
- The surfactant solution concentration has been evaluated to be a very sensitive parameter to influence the combinatorial plating characteristics. Lower surfactant solution concentration (1 CMC) provided lower PPD values and higher surfactant solution concentration (4 CMC) provided significant lapse mode in the time dependent PPD profiles. The 2 CMC CTAB solution concentration provided minimal lapse in the PPD profiles which was eventually overcome with additional plating. Hence, the surfactant solution concentration corresponds to 2 CMC CTAB solution concentration at 0.005 M Pd solution concentration and loading ratio of 203 cm^2/L respectively.
- For SSOEP (DW) Pd ELP baths, for 0.005 M Pd solution concentration and 2 CMC CTAB solution concentration, an enhancement in loading ratio did not increase PPD values (Table 7.2). Hence, the optimal loading ratio corresponds to 203 cm^2/L at 0.005 M Pd solution concentration and 2 CMC CTAB solution concentration.
- For SSOEP (DW) Pd ELP baths, the optimal combination of process parameters refers to 0.005M palladium solution concentration, 2 CMC surfactant solution concentration and a loading ratio of 203 cm^2/L, using which optimal combinatorial plating characteristics were achieved for the fabrication of 100% dense Pd/PSS composite membrane (Table 7.2). Apart from a PPD value of 100%, the optimal combinatorial plating characteristics refer to selective conversions of 30-35%, plating efficiency of 90-95%, average plating rate of

Parameters & Variables	**Case 1**	**Case 2**	**Case 3**	**Case 4**	**Case 5**	**Case 6**
Pd solution concentration (M)	0.005	0.010	0.005	0.005	0.005	0.005
CTAB concentration (CMC)	4	4	1	2	4	2
Loading ratio (cm^2/L)	203	203	203	203	203	407
Optimal plating time (h)	7	6	6	8	7	7
Selective Conversion (%)	26.31	26.54	21.17	31.48	26.31	41.34
Plating efficiency (%)	80.69	69.99	83.29	95.94	80.69	89.01
Average plating rate ($mol/m^2.s$)	$3.95x10^{-5}$	$7.24x10^{-5}$	$2.89x10^{-5}$	$4.38x10^{-5}$	$3.95x10^{-5}$	$2.82x10^{-5}$
Metal film thickness (μm)	8.81	13.85	5.52	11.16	8.81	6.29
PPD (%)	99.98	99.94	98.29	100	99.98	99.9

Table 7.2: A summary of results obtained during the parametric optimality studies conducted for SSOEP (DW) plating baths for dense Pd/PSS membrane fabrication.

Parameters & Variables	Case 1	Case 2	Case 3
Type of membrane	Pd/Ni/PSS (on 0.1 μm PSS)	Pd/Ni/PSS (on 0.5 μm PSS)	Pd/PSS (0.1 μm PSS)
Thickness of Nickel film	1.7	8	0
Optimal plating time (h)	10	8	8
Selective Conversion (%)	30.92	17.98	31.48
Plating efficiency (%)	87.01	48.77	95.94
Average plating rate ($mol/m^2.s$)	$3.07x10^{-5}$	$3.45x10^{-5}$	$4.38x10^{-5}$
Pd film thickness (μm)	9.80	8.88	11.16
PPD (%)	99.99	99.93	100

Table 7.3: Optimal combinatorial plating characteristics of dense Pd/Ni/PSS membranes fabricated with SSOEP (DW) plating baths.

$4.38x10^{-5}mol/m^2.s$.

- The overall fabrication cost of 100% dense Pd/PSS composite membrane is around 13.27 $\$/cm^2$. While comparing with best known SIEP process (Islam et al. [37]), which is 60% cost effective and noble Pd metal utilization is 40% only.

7.1.4 Fabrication of Pd/Ni/PSS composite membranes

- Among 0.1 and 0.5 μm nominal pore size PSS supports, highest PPD value (99.9%) was obtained for the PSS support with lower nominal pore size (0.1 μm).
- With an increase in Ni interdiffusion barrier from 1.7 to 8 μm, all combinatorial plating characteristics significantly reduced, thereby indicating poor surface activation of thicker nickel interdiffusion barriers (Table 7.3).

Parameters & Variables	Case 1	Case 2	Case 3	Case 4	Case 5
Type of membrane	Pd/Cr_2O_3/PSS		Pd/ Cr_2O_3-surf/PSS		Pd/PSS
Diffusion barrier thickness	7.8	20	7.1	12.5	0
Optimal plating time (h)	7	8	8	8	8
Selective Conversion (%)	32.51	21.11	37.6	31.48	31.48
Plating efficiency (%)	83.31	75.64	61.18	84.78	95.94
Average plating rate ($mol/m^2.s$)	$3.87x10^{-5}$	$2.97x10^{-5}$	$4.89x10^{-5}$	$4.28x10^{-5}$	$4.38x10^{-5}$
Pd film thickness (μm)	8.64	7.58	12.47	10.93	11.16
PPD (%)	99.99	99.91	99.98	99.97	100

Table 7.4: Optimal combinatorial plating characterstics of dense Pd/chromia/PSS membranes fabricated with SSOEP (DW) plating baths.

- Compared to Pd/PSS membranes, lower average plating rates were obtained for Pd/Ni/PSS membrane fabrication.
- Despite achieving normalization of support pore size distribution using SSOEP (DW) Ni plating baths, 100% PPD could not be obtained. This infers that the fabrication of dense Pd/Ni/PSS membranes is more challenging than Pd/PSS membranes.
- The Pd SSOEP (DW) plating baths provided higher PPD/δ values for dense Pd/Ni/PSS membranes in comparison with the Pd/PSS membranes. However, PPD values were comparatively lower for the Pd/Ni/PSS membranes. Thus, if it is assumed that the long term performance of 100% dense Pd/PSS membrane is similar to that of Pd/Ni/PSS membrane with optimal PPD (99.99%), it can be concluded that relatively higher hydrogen permeabilities could be obtained using dense Pd/Ni/PSS membranes in comparison with

those obtained from dense Pd/PSS membranes. If this is not the case, it can be inferred that the introduction of Nickel interdiffusion barrier is not at all effective to enhance hydrogen permeabilities.

7.1.5 Fabrication of Pd/Chromia/PSS composite membranes

- From the fabrication of Pd/Cr_2O_3/PSS and Pd/Cr_2O_3-surf/PSS composite membranes using SSOEP (DW) process, it can be inferred that, despite providing higher average Pd plating rates, the Pd/Cr_2O_3-surf/PSS composite membranes could not provide 100% pore densification (Table 7.4).
- Among all cases summarized in Table 7.4, the membranes with lower Cr_2O_3 interdiffusion barrier thickness (7.8 μm) provided optimal combinatorial plating characteristics along with higher PPD (Table 7.4).
- Compared to dense Pd/PSS membranes, the Pd/Cr_2O_3/PSS membrane fabricated with 7.1 μm of chromia interdiffusion barrier thickness provided similar PPD values (99.99% for Pd/chromia/PSS and 100% for Pd/PSS membranes) with lower Pd film thickness. Thereby, comparatively higher PPD/δ (from 8.96 for Pd/PSS and 11.57 for Pd/Cr_2O_3/PSS membranes) is obtained for the interdiffusion barrier case. Similar inferences provided for Pd/Ni/PSS membranes are applicable for the Pd/chromia/PSS membranes (first conclusion in page no. 181).
- Despite achieving chromia interdiffusion barrier with notable thickness using electroplating process, 100% dense Pd/chromia/PSS membranes could not be fabricated using SSOEP (DW). This indicates that further challenges exist for the fabrication of 100% dense Pd/chromia/PSS membranes. Also, the critical thickness required for dense Pd film thickness did not reduce significantly by introducing an interdiffusion barrier. This indicates that

further optimization of the interdiffusion barrier morphology and Pd SSOEP (DW) bath compositions needs to be targeted.

7.2 Recommendations for future work

Based on the research findings in this work, the following sub-sections elaborate upon the scope for further work in the field of dense Pd/PSS, Pd/Ni/PSS and Pd/Cr_2O_3/PSS composite membrane fabrication.

7.2.1 Minimization of total plating time for fabrication of dense Pd/PSS membranes using SSOEP (DW) Pd baths

In this work, a dense Pd/PSS membrane has been obtained after 8 h of total plating time. The evaluated selective conversions were about 30 – 35% for a corresponding plating efficiencies of 80 – 90%. Thus, significant amount of Pd metal in the solution has not undergone plating. Ideally, an industrial dense metal composite process shall have about 50 – 70% selective conversion and 75 – 90% plating efficiency. Such process characteristics could reduce the total plating time by 50 % (i.e., 4 h). To do so, the following areas of research can be targeted:

a) Enhancement of excess hydrazine reducing agent (100 – 300%) for 0.005 M plating baths. Since DW processes have better reducing agent concentrations in the baths, enhancement of hydrazine reducing agent concentration could be useful.

b) Shorter plating with lower Pd solution concentration (0.005 M) followed with ELP with higher solution concentration (0.010 M). Few preliminary experimental investigations indicated successful fabrication of 100% dense Pd composite membrane with such an approach. The most critical identification during the fabrication of dense Pd composite membranes is that once the PPD reached to 99.9%, saturation trend in PPD was observed

and therefore the lower Pd solution concentrations are unable to provide 100% pore densification in additional Pd ELP steps. The probable reason for the observed lapse in the PPD is the establishment of transport equilibrium between the metal concentration in the plating solution and on the membrane surface, which could not allow the metal to deposit on the membrane surface. The 100% dense Pd/PSS composite membranes can be fabricated by enhancing the metal solution concentration in the plating bath once the PPD reached to 99.9%.

c) It was observed that higher surfactant concentrations are detrimental to enhancement of the PPD and therefore, the reduction in surfactant solution concentration in the later stages of plating could also provide significant breakthrough in the dense membrane fabrication.

7.2.2 Minimization of total plating time for fabrication of dense Pd/PSS membranes using SSOEP (DW) with other fabrication techniques

The identified SSOEP (DW) process provided > 99% PPD after 4 h of total plating time and to achieve the remaining 1% PPD, the process took 4 h of additional PPD. This enhanced the membrane fabrication cost. Such high fabrication costs can be avoided by targeting coupling membrane repairing techniques such as ELP supplemented with osmosis, ELP supplemented with metal and reducing agent fed in opposite directions etc., could simultaneously reduce the fabrication cost and provide higher PPD/δ values. In this regard, studies with respect to the utilization of magnetron sputtering may not be advisable during later stages of Pd deposition, given the fact that sputtering technique is not a scalable technique for Pd deposition on porous substrates.

7.2.3 Further optimality of SSOEP (DW) processes for dense Pd/Ni/PSS and Pd/Chromia/PSS membrane fabrication

The dense Pd composite membranes fabricated in this work with Ni and chromia interdiffusion barriers are not 100% dense. Thus, it is apparent that the interdiffusion barrier provides more challenges to achieve 100% dense Pd composite membrane. The optimization of interdiffusion barrier morphology and SSOEP (DW) Pd ELP baths for the achievement of 100% dense Pd composite membranes with these interdiffusion barriers is required. Further concepts in this direction are not delineated due to intellectual property rights. The primary objective of such research investigations is to reduce the critical Pd film thickness using membrane supports with variant interdiffusion barrier thickness and morphologies.

7.2.4 Need for experimental research for the evaluation of membrane morphology without carrying out surface characterization techniques

One of the basic limitations of metal composite membrane fabrication research is the inability to deduce detailed morphological parameters such as pore size distributions from room temperature gas permeation experiments. Often researchers carry out surface characterization studies to justify the observed trends in plating and process characteristics. To carry out surface characterization studies, one needs to break the membrane and therefore, the membrane can no longer be used for the fabrication of metal composite membranes. Therefore, significant breakthrough in metal composite membrane fabrication can be obtained by developing experimental setup with which details with respect to pore size distribution on the membrane surface can be obtained at various sections of the membrane. Such experimental may involve significant number of pressure sensors located on either sides of the membrane to evaluate the

existing pressure drop profiles. A larger pore will have higher flux and variant pressure drop profile across the membrane in compared to the smaller pore. Therefore, such evaluations would be useful to further refine the existing knowledge in the field of Pd ELP using SSOEP (DW) Pd ELP baths.

7.2.5 Other areas of research

Few other areas of research have been outlined as follows for the SSOEP (DW) Pd baths:

Utilization of variable frequency sonicators and optimization of ultrasound schedule to achieve better parametric optimality of SSOEP (DW) Pd baths for 100% dense Pd composite membrane fabrication.

- Scalability of SSOEP (DW) Pd baths for the fabrication of dense Pd composite membranes in the context of mono-channel tubular and multichannel tubular stainless steel and ceramic porous supports.
- Further variations in the contacting pattern of the reducing agent by targeting a time dependent concentration profile in the Pd ELP bath.
- Targeting SSOEP (DW) Pd ELP baths for the development of noble metal supported catalysts.
- High temperature studies for the assessment of long term stability and intermetallic diffusion aspects of Pd composite membranes.

References

References

1. L. Sun, Y. Liu, W. Wang, R. Ran, Y. Huang, Z. Shao, "Methane catalytic decomposition integrated with on-line Pd membrane hydrogen separation for fuel cell application", International Journal of Hydrogen Energy 35 (2010) 2958 - 2963.
2. X. Li, Y. Fan, W. Jin, Y. Huang, N. Xu, "Improved photocatalytic deposition of palladium membranes", Journal of Membrane Science 282 (2006) 1 - 6.
3. J. Okazaki, T. Ikeda, D. A. P.Tanaka, K. Sato, T.M.Suzuki, F.Mizukami, "An investigation of thermal stability of thin palladium-silver alloy membranes for high temperature hydrogen separation", Journal of Membrane Science, 366 (2011) 212-219.
4. S.D. Sharma, "FUELS-HYDROGEN PRODUCTION/ Gas cleaning: Pressure Swing Adsorption", Encyclopedia of Electrochem. Power Sources 2009, 335-349.
5. D. Zhang, A. Kodama, M. Goto, T. Hirose, "Recovery of trace hydrogen by cryogenic adsorption", Separation and Purification Technology 35 (2004) 105-112.
6. K.D. Kreuer, "On the development of proton conducting polymer membranes for hydrogen and methanol fuel cells", Journal of Membrane Science 185 (2001) 29-39.
7. H.B. Zhao, K. Pflanz, J.H. Gu, A.W. Li, N. Stroh, H. Brunner, G.X. Xiong, "Preparation of palladium composite membranes by modified electroless plating procedure", Journal of Membrane Science 142 (1998) 147-157.
8. S.K. Ryi, N. Xu, A. Li, C.J. Lim, J.R. Grace, "Electroless Pd membrane deposition on alumina modified porous Hastelloy substrate with EDTA-free bath", International Journal of Hydrogen Energy 35 (2010) 2328-2335.

9. K.S Rothenberger, A.V. Cugini, B.H. Howard, R.P. Killmeyer, M.V. Ciocco, B.D. Morreale, R.M. Enick, F. Bustamante, I.P. Mardilovich, Y.H. Ma, "High pressure hydrogen permeance of porous stainless steel coated with a thin palladium film via electroless plating", Journal of Membrane Science 244 (2004) 55-68.
10. H. B. Zhao, G. X. Xiong, G. V. Baron, "Preparation and characterization of palladium-based composite membranes by electroless plating and magnetron sputtering", Catalysis Today 56 (2000) 89-96.
11. ECN, Netherlands, Energy efficient hydrogen separator, Available at:http://www.ecn.nl/newsletter-en/2010/September-2010/energy-efficient hydrogen separator/ (may2011).
12. Johnson Matthey Gas Purification Technology, USA, The Pure Guard Palladium Hydrogen Gas Purifiers, Available at: http://pureguard.net/cm/About_Us/About_JM_Gas Purification_Technology.html (May 2011).
13. K.J. Bryden, J.Y. Ying, "Nanostructured palladium membrane synthesis by magnetron sputtering", Material Science and Engineering: A 204 (1995) 140 - 145.
14. H.D. Tong, A.H.J. VandenBerg, J.G.E. Gardeniers, H.V. Jansen, F.C. Gielens, M.C.Elwenspoek, "Preparation of palladium-silver alloy films by a duel-sputtering technique and its application in hydrogen separation membrane", Thin Solid Films 479 (2005) 89 - 94.
15. G. Xomeritakis, Y.S. Lin, "Fabrication of a thin palladium membrane supported in a porous ceramic substrate by chemical vapour deposition", Journal of Membrane Science 120 (1996) 261-272.
16. S.Y. Lu, Y.Z. Lin, "Pd-Ag alloy films prepared by metallorganic chemical vapour deposition process", Thin Solid Films 376 (2000) 67-72.

17. L. Huang, C.S. Chen, Z.D. He, D.K. Peng, G.Y. Meng, "Palladium membranes supported on porous ceramics prepared by chemical vapor deposition", Thin Solid Films 302(1997) 98-101.
18. S.C. Chen, G.C. Tu, C.Y. Hung, C.A. Huang, M.H. Rei, "Preparation of palladium membrane by electroplating on AISI 316L porous stainless steel supports and its use for methanol steam reformer", Journal of Membrane Science 314 (2008) 5-14.
19. R. Bhandari, Y.H Ma, "Pd-Ag membrane synthesis: The electroless and electro-plating conditions and their effect on the deposits morphology", Journal of Membrane Science 334 (2009) 50- 63.
20. M. Kitiwan, D. Atong, "Effects of Porous Alumina Support and Plating Time on Electroless Plating of Palladium", Journal of Material Science & Technology 26 (2010) 1148 - 1152.
21. S.K Gade, P.M. Theon, J.D. Way, "Unsupported palladium alloy foil membranes fabricated by electroless plating", Journal of Membrane Science 316 (2008) 112-118.
22. D.A.P. Tanaka, M.A.L. Tanco, S.I. Niwa, Y. Wakui, F. Mizukami, T. Namba, T.M. Suzuki, "Preparation of palladium and silver alloy membrane on a porous α-alumina tube via simultaneous electroless plating", Journal of Membrane Science 247 (2005) 21 - 27.
23. Y.S. Cheng, K.L.Yeung, "Effects of electroless plating chemistry on the synthesis of palladium membranes", Journal of Membrane Science 182 (2001) 195-203.
24. K.L. Yeung, S.C. Christiansen, A.Verma, "Palladium composite membranes by electroless plating technique Relationships between plating kinetics, film microstructure and membrane performance", Journal of Membrane Science 159 (1999) 107-122.

25. Z. Shi, S. Wu, J. A Szpunar, M. Roshd, "An observation of Palladium membrane formation on a porous stainless steel substrate by electroless deposition", Journal of Membrane Science 280 (2006) 705-711.

26. S. Uemiya, T. Matsuda and E. Kikuchi, "Hydrogen permeable palladium-silver alloy membrane supported on porous ceramics", Journal of Membrane Science 56 (1991) 315-325.

27. J.N. Keuler, L. Lorenzen, R. D. Sanderson, V. Prozesky, W. J. Przybylowicz, "Characterization of electroless plated palladium-silver membranes", Thin Solid Films 347 (1999) 91-98.

28. S. Uemiya, N. Sato, H. Ando, Y. Kude, T. Matsuda and E. Kikuchi, "Separation of hydrogen through Palladium thin film supported on a porous glass tube", Journal of Membrane Science 56 (1991) 303-313.

29. F. Roa, J.D. Way, R.L. Mc Cormick, S.N. Paglieri, "Preparation and characterization of Pd-Cu composite membranes for hydrogen separation", Chemical engineering Journal 93 (2003) 11-22.

30. J.P. Collins and J.D. Way, "Preparation and characterization of a composite palladium-ceramic membrane", Industrial & Engineering Chemistry Research 1993, 32, 3006-3013.

31. A. Li, W. Liang, R. Hughes, "Fabrication of dense palladium composite membranes for hydrogen separation", Catalysis Today 56 (2000) 45-51.

32. R. Z. Souleimanova, A.S. Mukasyan, A.Verma, "Effect of osmosis on microstructure of Pd-composite membranes synthesized by electroless plating technique", Journal of Membrane Science 166 (2) 200 249-257.

33. A. Li, W. Liang, R. Hughes, "Characterisation and permeation of Palladium/stainless steel composite membranes", Journal of Membrane Science 149 (1998)259-268.

34. A. Li, W. Liang, R. Hughes, "Fabrication of defect-free Pd/α-Al_2O_3 composite membranes for hydrogen separation", Thin Solid Films 350 (1999) 106-112.
35. X. Zhang, G. Xiong, W. Yang, "A modified electroless plating technique for thin dense palladium composite membranes with enhanced stability", Journal of Membrane Science 314 (2008) 226-237.
36. Z. Ke, G. Huiyuan, R. Zebao, L. Yusheng and Li Yongdan, "Preparation of thin palladium composite membranes and application to Hydrogen/Nitrogen separation", Chinese Journal of chemical Engineering 15(5) (2007) 643-647.
37. M.S. Islam, M.M. Rahman, S. Ilias, "Characterization of Pd-Cu membranes fabricated by surfactant induced electroless plating (SIEP) for hydrogen separation", International Journal of Hydrogen Energy 37 (2012) 3477-3490.
38. S. Ilias and M.A. Islam, "Methods for preparing thin films by electroless plating", U. S. Patent Application #20100068391.
39. B.H. Chen, L. Hong, Y. Ma, T.M. Ko, "Effect of surfactants in an electroless nickel-plating bath on the properties of Ni-P alloy deposits". Industrial & Engineering Chemistry Research 41 (2002) 2668-78.
40. A.Chiba, H.Haijima, K.Kobayashi, "Effect of Sonication and vibration on the electroless Ni-B deposited film from acid bath", Surface and Coating Technology 169-170 (2003) 104-107.
41. M. Engin Ayturk, Yi Hua Ma, "Electroless Pd and Ag deposition kinetics of the composite Pd and Pd/Ag membranes synthesized from agitated plating baths", Journal of Membrane Science 330 (2009) 233-245.
42. G. Zeng, A. Goldbach, H. Xu, "Defect sealing in Pd membranes via point plating", Journal of Membrane Science 328 (2009) 6-10.

43. S. Samingprai, S. Tantayanon, Y. H. Ma, "Chromium oxide intermetallic diffusion barrier for palladium membrane supported on porous stainless steel", Journal of Membrane Science 347 (2010) 8-16.

44. J. Tong, C. Su, K. Kuraoka, H. Suda, Y. Matsumura, "Preparation of thin Pd membrane on CeO_2 modified porous metal by a combined method of electroless plating and chemical vapor deposition", Journal of Membrane Science 269 (2006) 101-108.

45. D. Zhang, S. Zhou, Y. Fan, N. Xu, Y. He, "Preparation of dense Pd Composite membranes on porous Ti-Al alloy supports by electroless plating", Journal of Membrane Science 387-388 (2012) 24-29.

46. A. Li, J. R. Grace, C. J. Lim, "Preparation of thin Pd-based composite membrane on planar metallic substrate Part 2 Preparation of membranes by electroless plating and characterization", Journal of Membrane Science 306 (2007) 159-165.

47. Y. Huang, R. Dittmeyer, "Preparation and characterization of composite palladium membranes on sinter-metal supports with a ceramic barrier against intermetallic diffusion", Journal of Membrane Science 282 (2006) 296-310.

48. V.M. Gryaznov, O.S. Serebryannikova, Y.M. Serov, M.M. Ermilova, A.N. Karavanov, A.P. Mischenko, N.V. Orekhova, "Preparation and catalysis over palladium composite membranes", Applied catalysis a-General 96 (1993) 15-23.

49. D. Yepes, L.M. Cornaglia, S. Irusta, E.A. Lombardo, "Different oxides used as diffusion barriers in composite hydrogen permeable membranes", Journal of membrane science 274 (2006) 92 - 101.

50. D. Wang, J. Tong, H. Xu, Y. Matsumura, "Preparation of palladium membrane over porous stainless steel tube modified with zirconium oxide", Catalysis Today, 93-95 (2004) 689-693.

51. X. Hu, W. Chen and Y. Huang, "Fabrication of Pd/ceramic membranes for hydrogen separation based on low-cost macro porous ceramics with pencil coating", International journal of hydrogen energy 35(2010) 7803-7808.
52. W.H. Lin, Y.C. Liu, H.F. Chang, "Autothermal reforming of ethanol in a Pd-Ag/Ni composite membrane reactor", International Journal of Hydrogen Energy 35 (2010) 12961-12969.
53. S. K. Ryi, J.S. Park, S.H. Choi, S.H. Cho, S.H. Kim, "Fabrication and characterization of metal porous membrane made of Ni powder for hydrogen separation", Separation and Purification Technology 47 (2006) 148-155.
54. D. Pizzi, R. Worth, M. Giachetti, G. C. Sarti, K. Noda, "Hydrogen permeability of 2.5 μm palladium-silver membranes deposited on ceramic supports", Journal of Membrane Science 325 (2008) 446-453.
55. X. Hu, Jian Yu, Jun song, X. Wang, Yan huang, "Toward low-cost Pd/Ceramic composite membranes for hydrogen separation: A case study of the recycled porous Al_2O_3 substrates in membrane fabrication", International journal of Hydrogen energy 36(2011) 15794-15802.
56. Z. Shi, S.Wu, J. A.Szpunar, "Microstructure transformation of Pd membrane deposited on a porous Inconel substrate in hydrogen permeation at elevated temperature", Journal of Membrane Science 284(2006) 424-430.
57. S.K. Ryi, J. Park, S.H. Kim, D.W. Kim, Kyu-II Cho, "Formation of a defect-free Pd-Cu-Ni ternary alloy membrane on a polished porous nickel support", Journal of Material Science 318 (2008) 346-354.

58. V.K.Bulasara, H.Thakuria, R.Uppaluri, M.K.Purkait, "Combinatorial performance Characteristics of agitated nickel hypophosphite electroless plating baths", Journal of Materials Processing Technology 211 (2011) 1488-1499.
59. V.K.Bulasara, H.Thakuria, R.Uppaluri, M.K.Purkait, "Combinatorial performance characteristics of agitated nickel hypophosphite electroless plating baths", Journal of Materials Processing Technology 211 (2011) 1488-1499.
60. N.Itoh, T. Akiha, T. Sato, "Preparation of thin palladium composite membrane tube by a CVD technique and its hydrogen permselectivity", Catalysis Today 104 (2005) 231-237.
61. V.K.Bulasara, R.Uppaluri, M.K.Purkait, "Effect of ultrasound on the performance of nickel hydrazine electroless plating baths", Materials and manufacturing processes 27 (2012) 201-206.
62. K. Karuppusamy, R. Anantharam, "Pit-Free Nickel Electroplating", Metal finish, 90 (5) (1992) 15-19.
63. H. Wang, Y.S. Lin, Synthesis and modification of ZSM-5/silicalite bi layer membrane with improved hydrogen separation performance, Journal of Membrane Science, 396 (2012) 128-137.

Appendix

Appendix A: Calibration Curves for the Estimation of Pd solution concentration using Atomic Absorption Spectroscopy

The calibration curves have been presented for the estimation of Pd solution concentration for two different cases namely (a) Pd solutions used for SIEP and SSOEP processes and (b) Pd solutions used for CEP and SSOEP processes. The following sections summarize the procedure adopted for the determination of the calibration curves for both cases.

Case A: SIEP and SSOEP Pd baths

The composition of standard solutions is similar to that presented for surfactant based baths in Chapter 2. Thus, the prepared standard solution consists of 18.7 mg of $PdCl_2$, 0.2979 g.Na_2EDTA, 2.1 mL NH_3 (25 %) and 27.8 mg CTAB surfactant in 100 mL solution. The solution has Pd solution concentration of 112.22 ppm. Using the standard solution, solutions with lower Pd solution concentrations (10, 20, 30, 40 and 50 ppm) have been

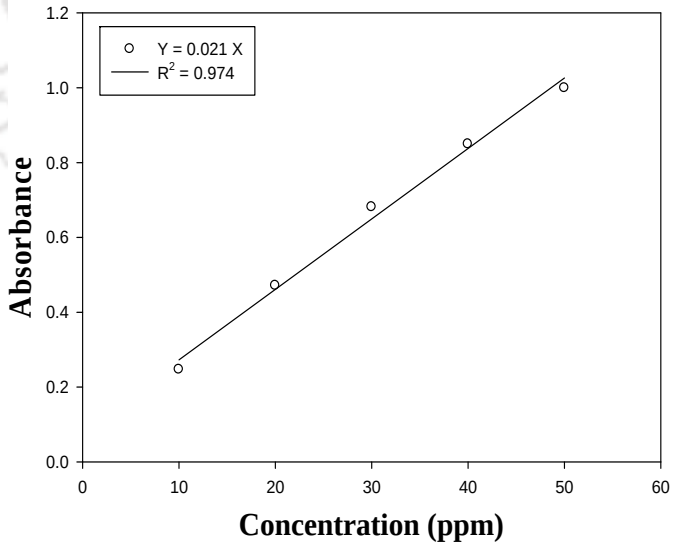

Figure A1: Standard curve for the evaluation of Pd solution concentration in SSOEP and SIEP baths

prepared using the molar mass balance expression for dilution systems:

$$C_0.V_0 = C_1V_1$$

where C_0, V_0 are the initial Pd solution concentration and Volume respectively and C_1, V_1 are the desired solution concentration and volume respectively. Subsequently, for the prepared solutions, the absorbance has been determined using Atomic Absorption Spectroscopy (AAS) instrument (Make: Varian AA240FS) at a wavelength of 247.6 nm using flame detection mode of operation. Fig. A1 presents the calibration curve thus obtained. For all spent electroless plating process solutions generated from SIEP and SSOEP processes, the calibration curve presented in Figure A1 has been used to determine the unknown concentration of these solutions by measuring the absorbance using AAS.

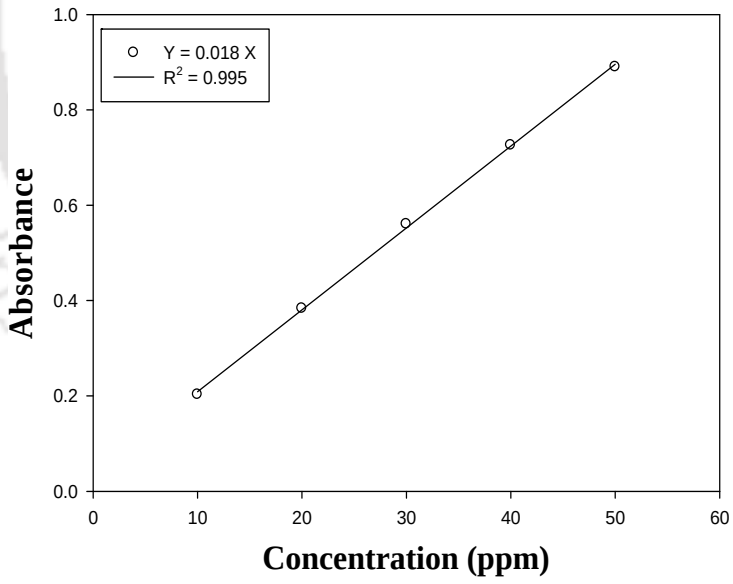

Figure A2: Standard curve for the evaluation of Pd solution concentration in SOEP and CEP baths.

Case B: Pd Electroless Plating Baths

The standard solution composition corresponds to that presented for CEP Pd baths in Chapter 2 of the thesis. Thus, the prepared standard solution consists of 18.7 mg $PdCl_2$, 0.2979 g Na_2EDTA and 2.1 mL NH_3 (25 %) in 100 mL solution. The solution consists of Pd solution concentration of 112.22 ppm. The standard solutions of desired Pd solution concentration (10, 20, 30, 40 and 50 ppm) were prepared using dilution expression presented for Case A in the Appendix A. Fig A2 presents the absorbance measured using flame mode equipped AAS instrument (Make: Varian AA240FS) at a wavelength of 247.6 nm. For all spent electroless plating process solutions obtained from CEP and SOEP processes, the calibration curve presented in Figure A2 had been used to determine the unknown concentration of spent ELP solutions by measuring their absorbance using AAS.

Appendix B: Sample Calculations for the Evaluation of Combinatorial Plating Characteristics

Below, the sample calculations for the evaluation of combinatorial plating characteristics are being presented.

The absorbance of feed (1ml diluted to 50 ml) is 0.2234 and the concentration of this solution is 10.64. Therefore, the concentration of feed is 532 ppm.

During 4 depositions of plating the amount of metal deposited is 0.0197 g.

After 4 depositions the volume of plating solution is 195.5 mL

Palladium metal concentration in 195.5 ml is 362.22 ppm

For 200 mL equivalent solution, the concentration is determined

$C_0.V_0 = C_1V_1$

$195.5 \times 362.22 = 200 \times C_1$

$C_1 = 354.07$ ppm

<u>After 4 depositions:</u>

Feed Concentration (C_i) 532 ppm

Final Concentration (C_f) 354.07 ppm

a) % Conversion (x) $= \dfrac{C_iV_i - C_fV_f}{C_iV_i} \times 100$

$$= \frac{(0.005 - 0.003327)}{(0.005)} \times 100$$

Conversion = 33.457

b) Plating efficiency (η) = $\frac{w}{(C_i - C_f) \times M.W_{Pd} \times V} \times 100$

$$\eta = \frac{0.0197}{(0.005 - 0.0033271) \times 106.421 \times 0.2} \times 100$$

= 55.32%

c) Selective conversion = Conversion × Plating Efficiency

= 33.44X 0.5532

= 18.5%

d) Film Thickness $\delta = \frac{w_2 - w_1}{\rho_{Pd} A_m}$

$$= \frac{(6.9287 - 6.909)}{(12.023 \times 0.00101736)} \times 10^{-6}$$

= 1.61066 μm

e) Average plating rate $\bar{r} = \frac{w_2 - w_1}{M.W_{Pd} \times A_m \times t}$

where M.W is molecular weight of Pd metal, t is plating time and A_m is area of the membrane

$$\bar{r} = \frac{6.9287 - 6.909}{106.421 \times 0.00101736 \times 2 \times 3600}$$

$= 2.52 \times 10^{-5}\ mol/m^2.s$

f) Percent Pore Densification $= \frac{\overline{J_0} - \overline{J_i}}{\overline{J_0}} \times 100$

$$= \frac{0.079 - 0.0341}{0.079} \times 100$$

= 56.835 %

Appendix C: Sample Calculation for the Estimation of Theoretical Selectivity

The following sample calculations are provided to estimate the theoretical selectivity using evaluated membrane and pore densification characteristics. Further details with respect to the termologies and methodologies can be obtained from section 2.5.

For surfactant induced sonication assisted electroless plating (DW) with 4 CMC surfactant concentration bath after 12 depositional steps, the membrane densification (PPD) was 99.992%. The nitrogen permeation experiments were conducted on this membrane at room temperature for the pressure range of 5.6-30.1 psi. Figure C1 presents the nitrogen permeability plot obtained for the membrane.

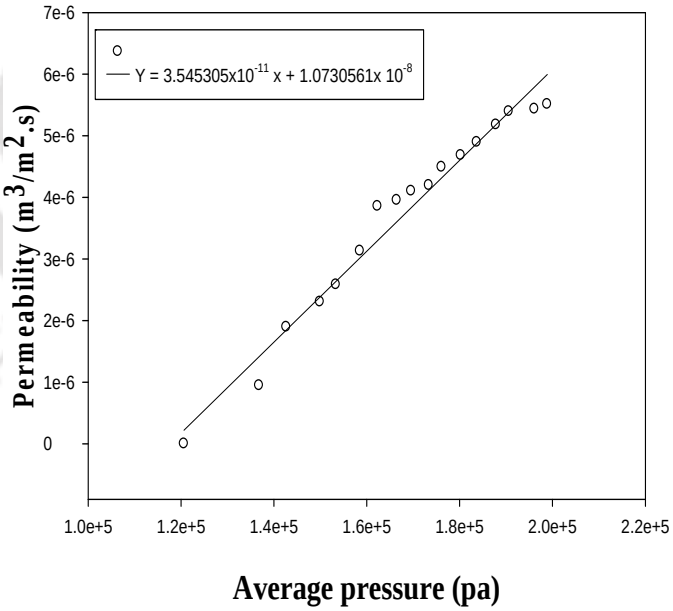

Figure C1: Nitrogen permeability plot for dense Pd/PSS membrane fabricated with SSOEP process.

The values of $KPern_{rt}^{pcm}$ and $ViPern_{rt}^{pcm}$ were evaluated by using equation (2.15). The obtained values of $KPern_{rt}^{pcm}$ and $ViPern_{rt}^{pcm}$ are $1.073x10^{-8}$ and $3.545x10^{-11}$. The values of $KPern_{ht}^{pcm}$ and $ViPern_{ht}^{pcm}$ at 550 ^{o}C are calculated by using eq. 2.16 and eq. 2.17.

$$KPern_{ht}^{pcm} = 1.073\times10^{-8}\times\frac{854.74}{510}$$

$$KPern_{ht}^{pcm} = 1.798\times10^{-8}\,mol.m/m^2.s.Pa$$

$$ViPern_{ht}^{pcm} = 3.545\times10^{-11}\times\frac{0.017}{0.0346}$$

$$ViPern_{ht}^{pcm} = 1.741\times10^{-11}\,mol.m/m^2.s.Pa$$

The permeability of nitrogen at 550 ^{o}C and pressure difference of 1.20 bar can be calculated by using Eq. (2.12): $Pern_{550^{o}C}^{pcm} = 1.798\times10^{-8} + 1.741\times10^{-11}\times(1{,}20{,}630.7)$

$=2.1183 \times 10^{-6}$ mol.m/m^2.s.Pa

The volumetric flow rate of nitrogen (LPM) at 550 ^{o}C and pressure difference of 1.20 bar is evaluated using Eq. (2.18)

$$Q_{550^{o}C}^{pcm} = \frac{120630.7}{101325}\times7.543\times10^{-4}\times2.1183\times10^{-6}\times60\times1000$$

$$Q_{550^{o}C}^{pcm} = 0.00011414\ LPM$$

Similarly the flow rates of nitrogen through Pd membrane at 550 ^{o}C, and PP = 1 bar was calculated for the average pressure range of 1.20 - 2.05 bars. The evaluated nitrogen flow rates variation with different pressure differentials at 550 ^{o}C are shown in Figure C2 (a).

Itoh et al. [60] fabricated dense Pd/PSS membrane with 2 µm thick palladium film. This membrane was subjected to hydrogen permeation experiments at 550^{o}C and the maximum permeance of hydrogen through this membrane was $3.34x10^{-6}$ mol/m^2.s.Pa. The permeance of

hydrogen is inversely proportional to thickness of Pd film. So, the hydrogen permeance through 8.07 μm thick Pd film is calculated as follows

$$P_2 = \frac{2}{8.07} \times (3.34 \times 10^{-6})$$

$$P_2 = 1.8319 \times 10^{-6}\, mol/m^2.s.Pa$$

The hydrogen flow rate is calculated by using eq. 2.20:

$$Q_{H_2}^{pcm} = \Delta P \times P_2 \times A_m \times 22.4 \times 60$$

$$Q_{H_2}^{pcm} = 4.04 \times 10^4 \times 7.543 \times 10^{-4} \times 1.8319 \times 10^{-6} \times 22.4 \times 60$$

$$Q_{550^oC}^{pcm} = 0.07506\, LPM$$

Similarly the flow rates of hydrogen through Pd membrane are calculated for the pressure range of 0.38-2.075 bars and at PP = 1 bar. The dependence of hydrogen flow rates on pressure differentials at 550 ^oC is shown in Figure C2.

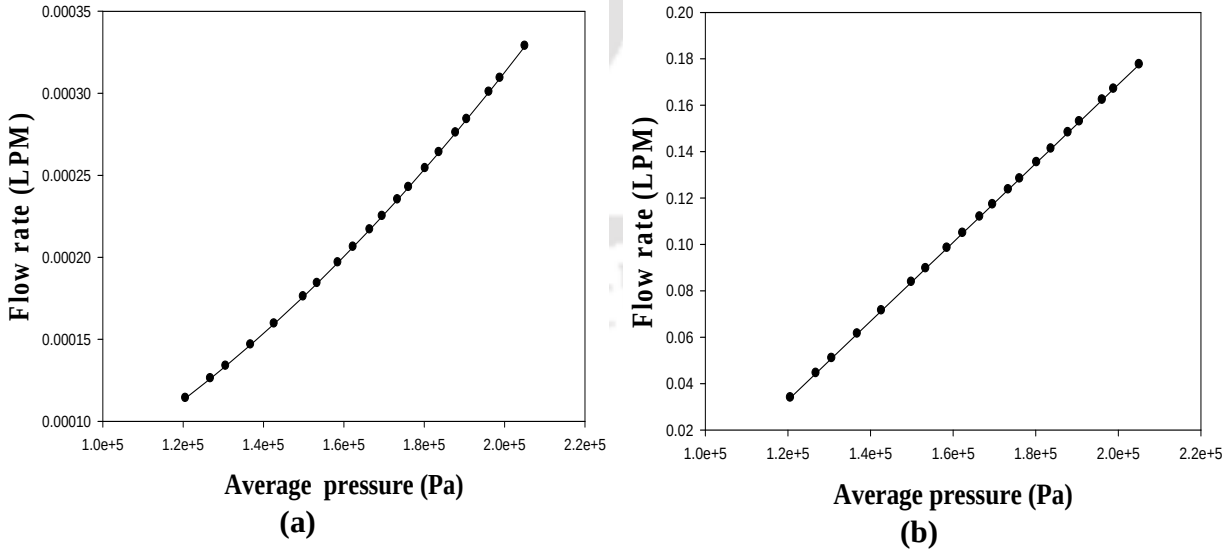

Figure C2: Simulated high temperature (a) N_2 and (b) H_2 flux vs. average pressure data.

For the pressure range of 0.38 – 2.075 bar, the flow rates of hydrogen at 550 ^{o}C varied in the range of 0.075 – 0.3929 LPM and the flow rates of nitrogen varied from 0.00011 – 0.000328 LPM. The H_2/N_2 theoretical selectivity at a particular value of pressure differential is evaluated using the expression:

$$\alpha = \frac{Q_{H_2}}{Q_{N_2}}$$

$$\alpha = \frac{0.033918}{0.000114149}$$

$$\alpha = 297.13$$

Similarly, the selectivities of hydrogen can be calculated at various other values of pressure differentials. The H_2/N_2 theoretical selectivities varied from 298.14 - 540.95 for the pressure range of 0.38 – 2.075 bar. From these selectivities, the average selectivity has been calculated using trapezoidal rule and was obtained as 481.

List of Publications

International Journals:

1. **Murali Pujari,** Amrita Agarwal, R.Uppaluri, A.Verma, "Effect of surfactant concentration and loading ratio on the electroless plating characteristics of dense Pd composite membranes", Industrial and Engineering Chemistry Research, 53(8) (2014) 3105-3115.

2. **Murali Pujari,** Amrita Agarwal, R.Uppaluri, A.Verma, "Role of electroless Nickel diffusion barrier on the combinatorial plating characteristics of dense Pd/Ni/PSS composite membranes", Applied Surface Science, 305 (2014) 658-664.

3. **Murali Pujari,** Amrita Agarwal, R.Uppaluri, A.Verma, "Efficacy of novel electroless plating process for dense Pd/Cr_2O_3/PSS membrane fabrication", Materials and Manufacturing Processes, In press, DOI: 10.1080/10426914.2014.880469 (2014).

4. **Murali Pujari,** Amrita Agarwal, R.Uppaluri, A.Verma, "Combinatorial electroless plating characteristic for dense Pd-PSS composite membrane fabrication", Materials and Manufacturing Processes (2014) (Accepted).

Patents:

1. **Murali Pujari,** Agarwal A., Uppaluri R. and Verma A. Composition and Method for Dense Palladium Composite Membrane Fabrication, Indian Patent filed (07-10-2013), Application No. 1150/KOL/2013.

Manuscripts Communicated:

1. **Murali Pujari,** Amrita Agarwal, R.Uppaluri, A.Verma, Effect of Pd concentration on electroless dense Pd-PSS membrane fabrication, Surface engineering (Under review).
2. **Murali Pujari,** Amrita Agarwal, R.Uppaluri, A.Verma, An investigation on critical thickness of diffusion barriers for fabrication of dense Pd/Cr_2O_3/PSS membranes, (Under preparation).

I&EC research
Industrial & Engineering Chemistry Research

Article

pubs.acs.org/IECR

Effect of Surfactant Concentration and Loading Ratio on the Electroless Plating Characteristics of Dense Pd Composite Membranes

Murali Pujari, Amrita Agarwal, Ramgopal Uppaluri,* and Anil Verma

Department of Chemical Engineering, Indian Institute of Technology Guwahati, Guwahati 781039, Assam, India

ABSTRACT: This article presents the effects of the concentration and loading ratios of a cationic surfactant (CTAB) on the performance characteristics of sonication-induced electroless plating baths for the fabrication of dense palladium composite membranes. The plating experiments were conducted with dropwise addition of reducing agent at loading ratios of 203 and 407 cm^2/L, a palladium solution concentration of 0.005 M, and surfactant solution concentrations of 1−4 CMC. A plating bath consisting of 0.005 M Pd with a surfactant concentration of 2 CMC at a loading ratio of 203 cm^2/L provided a 100% dense palladium composite membrane after 8 h of sequential plating with a Pd film thickness of 11.16 μm and a plating efficiency of 96%. The identified process can provide dense Pd/PSS composite membranes at a fabrication cost of 13.27 $/$cm^2$, which is 60% more cost-effective than the best-known SIEP process.

1. INTRODUCTION

Dense palladium composite membranes have been widely studied for hydrogen separation and purification because of their higher hydrogen permeabilities and selectivities.[1] Compared to thick palladium foils, these membranes provide higher hydrogen permeabilities and greater mechanical strength, and they are inexpensive. Typically, stainless steel supports are used to fabricate dense Pd composite membranes, because stainless steel supports have very high mechanical strengths, minimize temperature cycling effects, and enable efficient sealing through welding technologies. The fabrication of dense Pd composite membranes is achieved by one of the following fabrication methods: sputtering,[2,3] chemical vapor deposition (CVD),[4−6] electroplating,[7,8] and electroless plating (ELP).[9−11]

Among these fabrication methods, the electroless plating technique is promising because of its low cost, simple equipment, and ability to achieve uniform dense coatings on both conductive and nonconductive surfaces irrespective of their shapes and process scaleup.[12] Typically, in an electroless plating process, the redox reaction between a metal ion complex and a reducing agent produces gas bubbles that can adsorb on the substrate surface to prevent further deposition of metal on surface sites. This effect causes the formation of voids or pits on the substrate surface and lowers the metal plating efficiency. Therefore, to enhance the metal plating rates and reduce the time of plating for 100% pore densification, several researchers have coupled rate enhancement techniques such as stirring,[13] sonication,[13] agitation,[14] surfactant application,[15,16] and vacuum techniques[17] with conventional electroless plating baths. Among these approaches, sonication- and surfactant-based rate enhancement techniques are considered highly promising in terms of scalability, cost, and ease of operation.

Bulasara et al.[18] coupled sonication with conventional electroless plating baths during the fabrication of nickel composite membranes and evaluated parameters such as metal conversion, plating rate, and plating efficiency with rate enhancement. However, the authors failed to achieve pore densification to 100%.

To explore the role and optimality of a surfactant, Islam et al.[15] dispersed a cationic surfactant (dodecyltrimethylammonium bromide, DTAB) at a concentration of 4 times the critical micelle concentration (CMC) in conventional electroless plating baths containing 0.015 M Pd. They achieved a completely dense Pd composite membrane after 10 h of plating, which is significantly lower than the total plating time (28 h) required for conventional electroless plating baths. However, they used an expensive surfactant (DTAB, which costs 3.6 $/g) in the plating process.

On the other hand, high concentrations of reactants (Pd precursors and reducing agent) could provide higher plating rates but deteriorate the quality of the films deposited on the substrate surface in terms of adhesion strength. Variations in the concentration of reducing agent during ELP significantly influence the quality of plating and undesired metal nucleation in the solution.

In summary, available literature reports on combinatorial plating characteristics for the fabrication of dense palladium membranes have been sparse and do not necessarily present all of the parameters for evaluating the efficacy of the electroless plating process. Based on the state of the art, it is hypothesized that an optimal combination of surfactant, sonication, and dropwise (DW) contacting of the reducing agent could enable maximum transport of metal ions from solution to the metal surface. This promotes effective pore densification to achieve dense palladium membranes within shorter plating times. The major objective of this work was to optimize combinatorial plating characteristics by targeting various surfactant solution

Received: October 21, 2013
Revised: January 18, 2014
Accepted: January 22, 2014
Published: January 22, 2014

dx.doi.org/10.1021/ie4035412 | Ind. Eng. Chem. Res. 2014, 53, 3105−3115

concentrations and loading ratios along with lower Pd solution concentrations to achieve dense Pd composite membranes.

2. EXPERIMENTAL SECTION

2.1. Preparation of Pd Membranes on Porous Stainless Steel. Porous stainless steel circular disks (diameter of 36 mm and thickness of 1 mm) with a nominal pore size of 0.1 μm were purchased from Mott Corporation, Farmington, CT. Prior to Pd membrane fabrication, the stainless steel disks were sonicated (model S30H, Elma, Singen, Germany) with acetone to remove the grease, oil, dirt, corrosion products, and other contaminants present on the surface. The supports were subsequently dried at 393 K in an oven (model ROV/DG, REICO) for 2 h.

Electroless plating is an autocatalytic reaction, and to initiate the reaction, the supports were seeded by placing the stainless steel substrates in a sensitization bath ($SnCl_2$ solution) for 5 min and then rinsing with water. Subsequently, the disks were placed in an activation bath ($PdCl_2$ solution) for 5 min and rinsed in an acidic bath (0.1 N HCl) for 2 min. These steps were repeated 9 or 10 times to obtain a completely activated surface, as confirmed by the observation of a uniform dark-brown color on the membrane surface. After being seeded, the membrane was dried overnight in an oven at 393 K to measure its dry weight (w_1) before plating.

Table 1. Composition of Palladium Electroless Plating Baths[a]

no.	constituent	amount used in each bath
1	$PdCl_2$	0.8866 g/L
2	Na_2EDTA	14.89 g/L
3	$NH_3{\cdot}H_2O$ (25%)	110 mL/L
4	N_2H_4 (1.0 M)	1.81 mL/L
5	CTAB	1−4 CMC

[a]pH 11, temperature 60 °C.

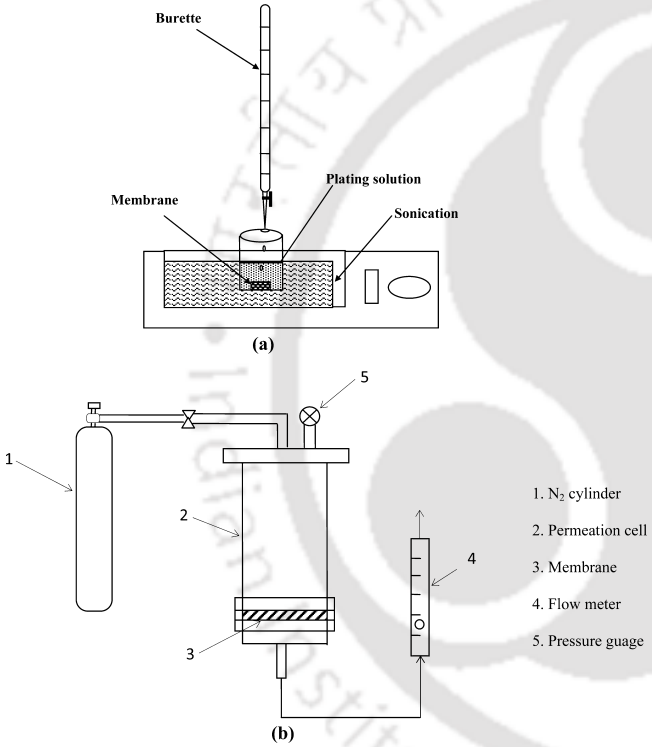

Figure 1. Experimental setups for (a) palladium electroless plating supplemented with controlled addition of reducing agent to SSOEP and (b) permeation tests.

Pd electroless plating experiments were conducted to evaluate time-dependent combinatorial Pd plating characteristics using a modified rate-enhanced ELP process. This term refers to surfactant- and sonication-assisted Pd electroless plating processes that are supplemented with dropwise addition of the reducing agent. For all experiments, a surfactant concentration of 1, 2, or 4 CMC along with a low palladium concentration of 0.005 M were used at a loading ratio of 203 cm^2/L. The time-dependent plating characteristics were evaluated initially after every four sequential plating steps whose duration was 30 min for each step. Later, after the percent pore densification (PPD) reached 90%, all relevant plating characteristics were evaluated after every two sequential plating steps of same duration for each plating step. The plating experiments were carried out using typical compositions listed in Table 1.

The experimental setup for the surfactant- and sonication-induced electroless plating (dropwise) [SSOEP (DW)] process is shown in Figure 1a. The experimental procedure for the plating process is presented as follows: The SSOEP (DW) process involves dispersing a cationic surfactant (cetyltrimethylammonium bromide, CTAB) into a plating solution containing palladium chloride, liquor ammonia, and the sodium salt of ethylenedinitrilo tetraacetic acid (Na_2EDTA). The plating solution was kept in an ultrasonic cleaning bath (Elmasonic, S30H) that also contained a heating element and the capacity for various modes of sonication operation (constant, degas, and sweep modes of sonication). During the SSOEP process, the Pd bath was maintained at a constant plating temperature of 333 K, a constant frequency of 50−60 Hz, and degas mode of sonication. Once the plating temperature was achieved, hydrazine was added to the plating solution continuously throughout the plating time using a burette.

For all membranes, 12−16 sequential plating steps were carried out with intermediate rinsing using hot deionized water to remove salts adsorbed in the pores of the porous support or entrapped in the Pd coating layer. Finally, the membrane was dried in an oven at 393 K for 6 h. The dry weight (w_2) of the membrane was measured to evaluate the amount of palladium deposited on the support surface during plating.

To evaluate the membrane performance and identify the presence of defects, nitrogen gas permeation experiments were conducted in the membrane module depicted in Figure 1b. The setup consisted of a stainless steel tubular cell with a flat circular steel base plate. The membrane was placed in the membrane housing provided on the base plate and sealed with rubber gaskets. The cell was pressurized with nitrogen gas, and the outlet was connected to a flow meter (rotameter/digital gas flow meter) for measuring gas flow rates at various transmembrane pressures. All permeation experiments were conducted at room temperature.

2.2. Evaluation of Plating Characteristics. The performance characteristics evaluated for the Pd electroless plating baths were plating bath conversion (χ), selective conversion, plating efficiency (η), palladium film thickness (δ), average plating rate ($\overline{r}_{Pd}$), average permeation flux ($\overline{J}$), and percent pore densification.

The plating bath conversion was evaluated as the ratio of the amount of Pd metal ion reacted to the amount of palladium present initially in the plating solution, expressed as

$$\chi\ (\%) = \frac{C_i - C_f}{C_i} \times 100 \quad (1)$$

where C_i and C_f are initial and final concentrations (mol/L), respectively, of Pd in the plating solution. These were determined using atomic absorption spectroscopy (AAS) (model FS 240, Varian, Palo Alto, CA) at a wavelength of 247.6 nm. Plating efficiency (η) was evaluated as the ratio of the amount of palladium deposited on the activated substrate surface to the amount of palladium converted during the plating step and is expressed as

$$\eta\ (\%) = \frac{w_2 - w_1}{w_o} \times 100 \quad (2)$$

where w_1 and w_2 are the dry weights (g) of the membrane before and after plating, respectively, and w_o is the amount of palladium metal converted during plating. w_o is calculated using the equation

$$w_o = (C_o - C_i) n V_o M_{Pd} \quad (3)$$

where n is the number of sequential plating steps, V_o is the volume of plating solution (L) in each plating step, and M_{Pd} is the molecular weight of palladium metal. The selective conversion is defined as the product of plating efficiency and conversion of the plating bath and is expressed as

$$\text{selective conversion}\ (\%) = \frac{\eta\chi}{100} \quad (4)$$

The thickness (δ) of deposited palladium film is evaluated by using weight gain method and is expressed as follows.

$$\delta = \frac{w_2 - w_1}{\rho_{Pd} A_m} \quad (5)$$

where ρ_{Pd} is the density of palladium metal (g/cm^3), A_m is the membrane surface area (cm^2). Because it was assumed that the palladium film was dense even for intermediate plating steps, the evaluated thickness corresponds to the theoretical value, and the actual value will be apparently higher than the evaluated value. This is also because porosity measurements could not be conducted because of the lack of availability of relevant experimental facilities (such as mercury porosimetry).The average plating rate $\bar{r}_{Pd}$ (mol/m^2·s) was evaluated using the expression

$$\bar{r}_{Pd} = \frac{w_2 - w_1}{M_{Pd} A_m t} \quad (6)$$

where t is the corresponding total plating time. Pore densification during the plating process is defined as the fractional volume of the pores covered by the deposited metal and is expressed as PPD, which is calculated using the expression

$$\text{PPD}\ (\%) = \frac{\bar{J}_o - \bar{J}_i}{\bar{J}_o} \times 100 \quad (7)$$

where $\bar{J}_o$ is the average room-temperature nitrogen permeation flux of the porous stainless steel substrate (mol/m^2·s) and $\bar{J}_i$ is the average room-temperature permeation flux of the palladium composite membrane fabricated after the ith depositional plating step. The average room-temperature nitrogen flux is calculated using the expression

$$\bar{J} = \frac{\int_{P_1}^{P_2} J\ dP}{P_2 - P_1} \quad (8)$$

where P_1 and P_2 correspond to the minimum and maximum retentate pressures during an experimental test to measure the nitrogen gas permeance at room temperature.

3. MODEL FOR THEORETICAL SELECTIVITY

Typically, for palladium composite membranes, high-temperature H_2/N_2 single and binary gas selectivities are determined after achieving a dense palladium membrane. However, depending on the PPD values of the palladium composite membranes, one can also estimate the theoretical selectivity. In this work, for the first time, we report a procedure for estimating the theoretical selectivity that will serve as an important guideline for the effectiveness of time-dependent pore densification of Pd composite membranes. Thus, using this procedure, one can avoid carrying out rigorous experimentation until one refines and obtains the best-quality palladium composite membranes. Thereby, one can also identify optimal combinations of plating process parameters with minimum experimentation. The procedure for evaluating the theoretical selectivity of palladium composite membranes is as follows:

(1) For a porous palladium composite membrane, conduct room-temperature permeation experiments with nitrogen gas.

(2) From room-temperature N_2 flow rate versus pressure differential data, calculate the average volumetric nitrogen permeance of the porous palladium composite membrane (pcm) using the expression

$$\text{Pern}_{rt}^{pcm} = \frac{Q_{rt}^{pcm}}{A_m} \frac{1}{(PR - PP)} \quad (9)$$

(3) Plot a graph between Pern_{rt}^{pcm} and (PR + PP)/2 to obtain the slope and intercept, which correspond to the room-temperature viscous and Knudsen nitrogen permeance values, respectively. Thus

$$\text{Pern}_{rt}^{pcm} = \text{KPern}_{rt}^{pcm} + \text{ViPern}_{rt}^{pcm} \frac{(PR + PP)}{2} \quad (10)$$

where KPern_{rt}^{pcm} and ViPern_{rt}^{pcm} correspond to the graphically determined Knudsen and viscous nitrogen permeance values at room temperature. Because the volumetric Knudsen permeance is proportional to the average velocity, corresponding the N_2 Knudsen permeance for the metal composite membrane at higher temperature (573K) can be estimated using the expression

$$\text{KPern}_{ht}^{pcm} = \text{KPern}_{rt}^{pcm} \frac{vn_{ht}}{vn_{rt}} \quad (11)$$

On the other hand, viscous permeance is inversely proportional to viscosity, and the high-temperature (573 K) N_2 gas viscous permeance for the metal composite membrane is determined using the expression

$$\text{ViPern}_{ht}^{pcm} = \text{ViPern}_{rt}^{pcm} \frac{\mu n_{rt}}{\mu n_{ht}} \quad (12)$$

Using the computed values of $KPern_{rt}^{pcm}$ and $ViPern_{rt}^{pcm}$, the high-temperature nitrogen flux is determined using the expression

$$JN_{ht}^{pcm} = \left[KPern_{ht}^{pcm} + ViPern_{ht}^{pcm}\frac{(PR + PP)}{2}\right]\frac{(PR - PP)}{PP} \times \frac{1000}{22.4} \quad (13)$$

The corresponding hydrogen flux through the porous palladium membrane is computed by assuming that the film is highly dense and consists of pinholes through which nitrogen and hydrogen gases pass through the dense palladium film. Thereby, the theoretical hydrogen flux of the palladium composite membrane at higher temperature is estimated using the expression

$$JH_{ht}^{pcm} = \frac{Perh^{dm}}{\delta^{pcm}}(PR^n - PP^n) = Pernh^{pcm}(PR^n - PP^n) \quad (14)$$

where $Perh^{dm}$ is assumed to be the dense palladium membrane permeability from literature data[19] (66.8×10^{-13} mol·m/m^2·s·Pa at 573 K) and δ^{pcm} corresponds to the thickness of the palladium film determined by the weight gain method. The theoretical hydrogen flow rate is evaluated as a function of membrane area and is expressed as

$$Q_{H_2}^{th} = JH_{ht}^{pcm}A^{pcm} \quad (15)$$

With the values of JH_{ht}^{pcm} and JN_{ht}^{pcm} at higher temperatures, the average hydrogen and nitrogen flux values can be determined using trapezoidal rule applied for the flux versus pressure differential data. The average hydrogen and nitrogen flux values are evaluated using the expressions

$$AJH_{ht}^{pcm} = \frac{\int_{PR_{min}}^{PR_{max}} JH_{ht}^{pcm}\, dP}{(PR_{max} - PR_{min})} \quad (16)$$

$$AJN_{ht}^{pcm} = \frac{\int_{PR_{min}}^{PR_{max}} JN_{ht}^{pcm}\, dP}{(PR_{max} - PR_{min})} \quad (17)$$

With the average flux values of the palladium composite membrane at higher temperature, the theoretical selectivity ($\bar{\alpha}_{av}$) for an equimolar feed mixture of H_2/N_2 is estimated using the expression

$$\bar{\alpha}_{av} = \frac{\frac{y_{H_2}}{y_{N_2}}}{\frac{0.5}{0.5}} = \frac{AJH_{ht}^{pcm}}{AJN_{ht}^{pcm}} \quad (18)$$

For tradeoff-related studies, the average theoretical hydrogen flow rate is estimated using expressions similar to eqs 16 and 17 and is presented as

$$\bar{Q}_{H_2}^{th} = \frac{\int_{PR_{min}}^{PR_{max}} Q_{H_2}^{th}\, dP}{(PR_{max} - PR_{min})} \quad (19)$$

The theoretical membrane selectivity has been evaluated using the literature hydrogen permeance value (33.4×10^{-7} mol/m^2·s·Pa for a 2-μm dense Pd film thickness) at 573 K.[19] However, in due course of sequential electroless deposition involving several plating steps, dense palladium films are obtained only in the last step, and all other intermediate palladium composite membranes are porous membranes. The contribution of hydrogen flux through the pinholes is ignored in the evaluation of the theoretical membrane selectivity, and therefore, the predicted theoretical selectivity values refer to slightly lower values. In due course of sequential plating, the palladium composite membrane theoretical selectivity values need to increase to about infinity, and identification of conditions that provide high selectivity values is an interesting issue during the fabrication of palladium composite membranes.

4. RESULTS AND DISCUSSION

In this section the performance characteristics of rate-enhanced electroless plating baths are reported in terms of plating bath characteristics and Pd/porous stainless steel (PSS) composite membrane characteristics at different loading ratios. The first subsection corresponds to a loading ratio of 203 cm^2/L for the identification of the optimal surfactant concentration, and the second subsection corresponds to the results obtained at a loading ratio of 407 cm^2/L with the identified optimum concentration of surfactant.

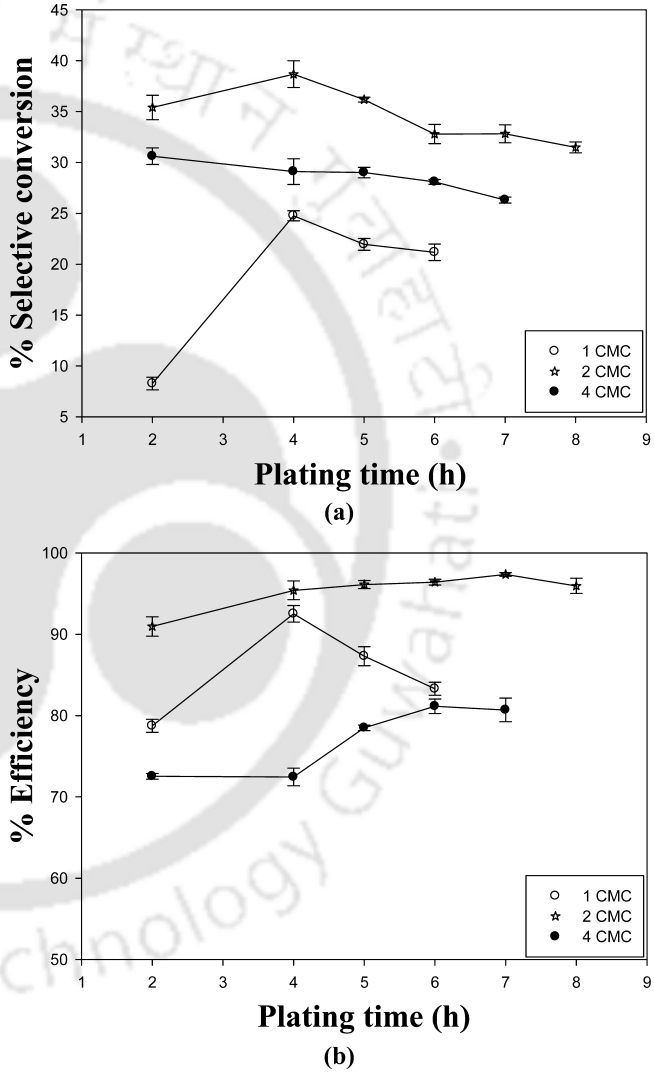

Figure 2. Effects of plating time on (a) selective conversion and (b) plating efficiency.

4.1. Effect of Surfactant Concentration on the Combinatorial Electroless Plating Characteristics.

Table 2. Effect of Surfactant Concentration on the Average Plating Rate ($\times 10^5$ mol/m^2·s) with Cumulative Plating Time

	surfactant concentration		
total plating time (h)	1 CMC	2 CMC	3 CMC
2	1.13	4.92	4.81
4	3.38	5.38	4.57
5	2.99	5.03	4.45
6	2.89	4.56	4.22
7	–	4.57	3.95
8	–	4.38	–

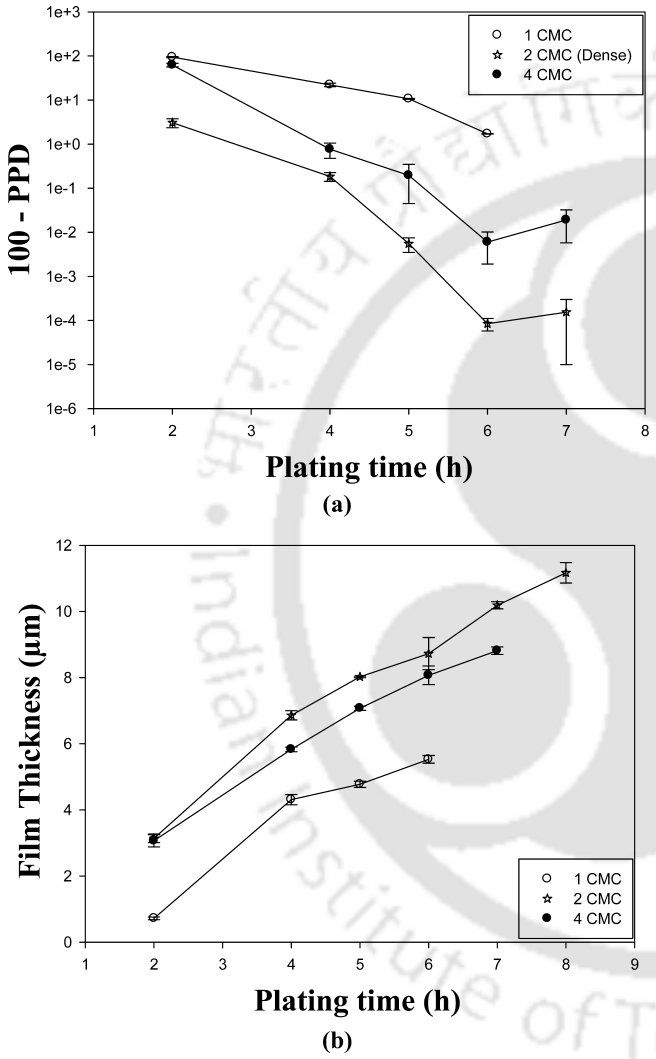

Figure 3. Dependencies of (a) PPD and (b) Pd film thickness on plating time.

4.1.1. Process Characteristics. Figure 2 shows the trends of the time-dependent selective conversion and plating efficiency for the surfactant solution concentration of 1, 2, and 4 CMC. It can be observed that, with an increase in surfactant concentration from 1 to 2 CMC, both the selective conversion and plating efficiency increased; for example, the selective conversion after 2 h increased from 8.27% to 35.4%, and the plating efficiency after 2 h increased from 78.74% to 90.95%. This might be due to a further reduction in the interfacial tension between the substrate surface and the solution, which, in turn, enabled faster removal of gas bubbles from the membrane surface without causing metal delamination. A further enhancement in surfactant solution concentration from 2 to 4 CMC did not improve the selective conversion or plating efficiency. This is probably due to the aggregation of surfactant molecules on the substrate surface at high surfactant concentration (4 CMC), which could hinder metal deposition. This observation is in agreement with the work of Chen et al.,[16] who reported that, at higher surfactant solution concentrations, the surfactant molecules form cylindrical aggregates on the substrate surface and promote plating inefficiency.

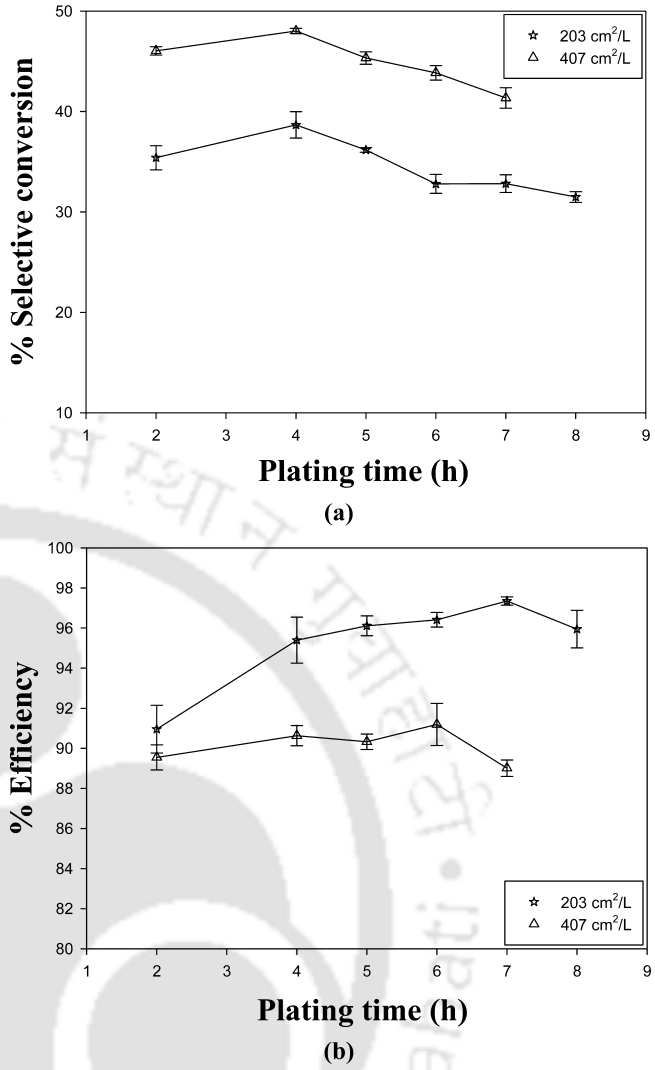

Figure 4. Effects of loading ratio on (a) selective conversion and (b) plating efficiency.

Table 3. Effect of Loading Ratio on the Average Plating Rate $\bar{r}_{Pd}$ ($\times 10^5$ mol/m^2·s) with Cumulative Time for Pd Electroless Plating Baths

	loading ratio (cm^2/L)	
total plating time (h)	203	407
2	4.92	3.14
4	5.38	3.28
5	5.03	3.09
6	4.56	2.99
7	4.57	2.82
8	4.38	–

dx.doi.org/10.1021/ie4035412 | Ind. Eng. Chem. Res. 2014, 53, 3105−3115

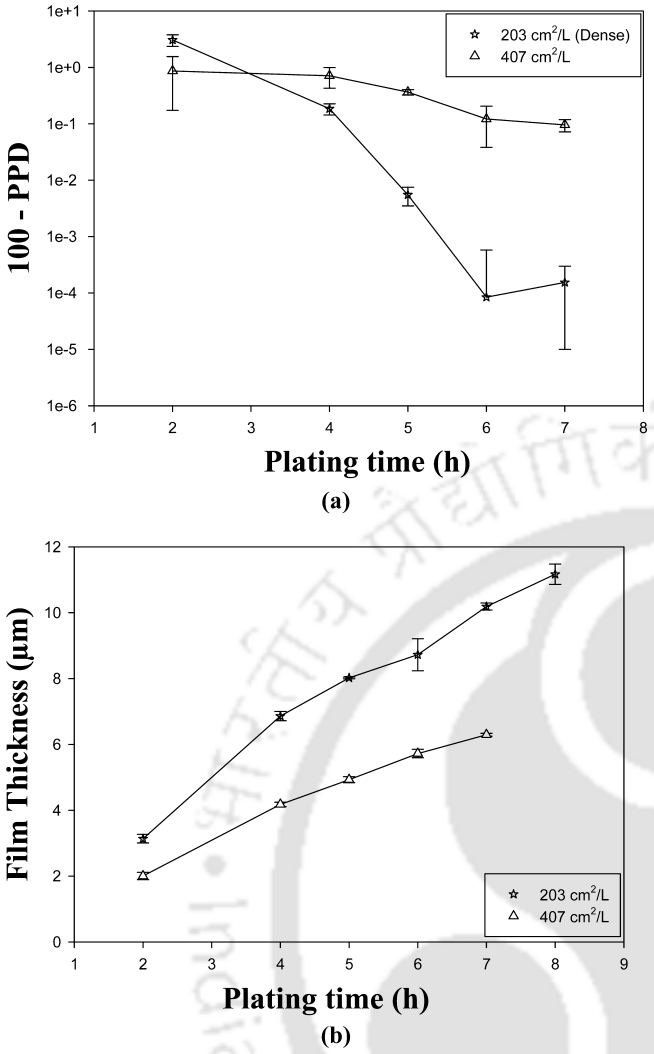

Figure 5. Dependencies of (a) PPD and (b) Pd film thickness on plating time for various loading ratios.

The variation of the Pd plating rate with the total plating time for surfactant concentrations of 1, 2, and 4 CMC in the baths are presented in Table 2. It can be observed that the plating rates varied in the ranges $(1.13-2.89) \times 10^{-5}$ mol/m^2·s for 1 CMC, $(4.92-4.38) \times 10^{-5}$ mol/m^2·s for 2 CMC, and $(4.81-3.95) \times 10^{-5}$ mol/m^2·s for 4 CMC. The variation in average metal plating rate with varying surfactant concentration is in accordance with the evaluated conversion and plating efficiency trends.

4.1.2. Membrane Characteristics. Figure 3a shows the time-dependent PPD for plating baths with surfactant concentrations of 1, 2, and 4 CMC. It can be observed that, after 2 h, significant differences existed in the (100 − PPD) values for various cases. This confirms that the surfactant solution concentration has a significant role in influencing the PPD. Lower (1 CMC) and higher (4 CMC) concentrations are not favorable for very good PPD achievement after 2 h of sequential Pd plating, indicating that complex tradeoffs exist with respect to the reduction of interfacial tension and surfactant adsorption on the surface. After 6 h of Pd ELP, the PPDs obtained were 98.29%, 99.9999%, and 99.994% for 1, 2, and 4 CMC baths, respectively. For further 1-h deposition, the PPDs decreased to 99.9998% and 99.981% for 2 and 4 CMC surfactant concentrations, respectively. The uncertainty in estimating PPDs ranges from about ±0.0092 for a PPD of 98.76% to $\pm 1.94 \times 10^{-7}$ for a PPD of 99.99997%. Thus, near dense Pd composite membranes, the PPD estimate has a lower uncertainty, and this is promising with progressive membrane densification in sequential electroless plating steps. It can be observed that the lapse mode of the densification profile is also evident in the 2 and 4 CMC cases but is not very significant for the 2 CMC case. In other words, the 2 CMC concentration of the surfactant is able to negate the surface density affects to foster toward 100% metal densification. This was not the case for the 4 CMC bath, where the lapse at the later stage of the plating (from 6 to 7 h) is very significant. The minimization of the lapse in the profile of the PPD is a very important phenomenon that has not been reported so far in the literature. Although generalized reasons for lapse have been presented in the literature in terms of negative surface charge density distributions, their minimizations have not been reported, especially toward 100% Pd metal composite membrane fabrication. Therefore, the role of surfactant concentration to induce various desired and undesired surface affects is apparent with the observed trends. The desired effect of surfactant addition is minimization of pitting and wettability alteration, and the undesired effect of surfactant addition is the strong variation in the surface charge density and inhibition of metal plating, which is apparent at higher surfactant concentrations.

Figure 3b shows the incremental variation in palladium film thickness with plating time for surfactant solution concentration of 1, 2, and 4 CMC baths. It can be observed that the film thickness varied in the ranges 0.72−5.52 μm after 6 h for 1 CMC, 3.14−11.6 μm after 8 h for 2 CMC, and 3.06−8.81 μm after 7 h for 4 CMC baths. With increasing surfactant concentration (from 1 to 2 CMC), the film thickness increased, but a further enhancement in surfactant concentration (from 2 to 4 CMC) reduced the film thicknesses as a result of uneven surface charge densities on the substrate surface at the 4 CMC surfactant concentration. Similar observations have been reported by Chen et al.[16] for surfactant-induced nickel−phosphorus electroless plating baths. They also inferred that, at moderately high concentrations, surfactant enhanced the metal deposition rates but, at higher concentration, the surfactant molecules form cylindrical aggregates on the substrate surface and inhibit the metal deposition rates.

To reduce the consumption of noble palladium metal, further plating experiments were conducted at a loading ratio of 407 cm^2/L with similar conditions maintained for the SSOEP baths at an optimal surfactant concentration of 2 CMC. This was identified at a loading ratio of θ = 203 cm^2/L. The performance characteristics are reported in terms of plating bath characteristics such as selective conversion, plating efficiency, plating rate, and Pd/PSS composite membrane characteristics such as thickness and percent pore densification and are compared with plating characteristics of 203 cm^2/L bath in the following section.

4.2. Effect of Loading Ratio on the Combinatorial Electroless Plating Characteristics. *4.2.1. Process Characteristics.* Figure 4 compares the selective conversion and plating efficiency with plating time for θ = 203 and 407 cm^2/L. As shown in the figure, an increase in the loading ratio from 203 to 407 cm^2/L enhanced the selective conversion (e.g., from 35.4% to 46.04% after 2 h) and reduced the plating efficiency (e.g., from 90.96% to 89.54% after 2 h). The enhancement in selective conversions with increasing loading ratio is possibly due to the significant mass-transfer limitations for Pd ions to

dx.doi.org/10.1021/ie4035412 | Ind. Eng. Chem. Res. 2014, 53, 3105−3115

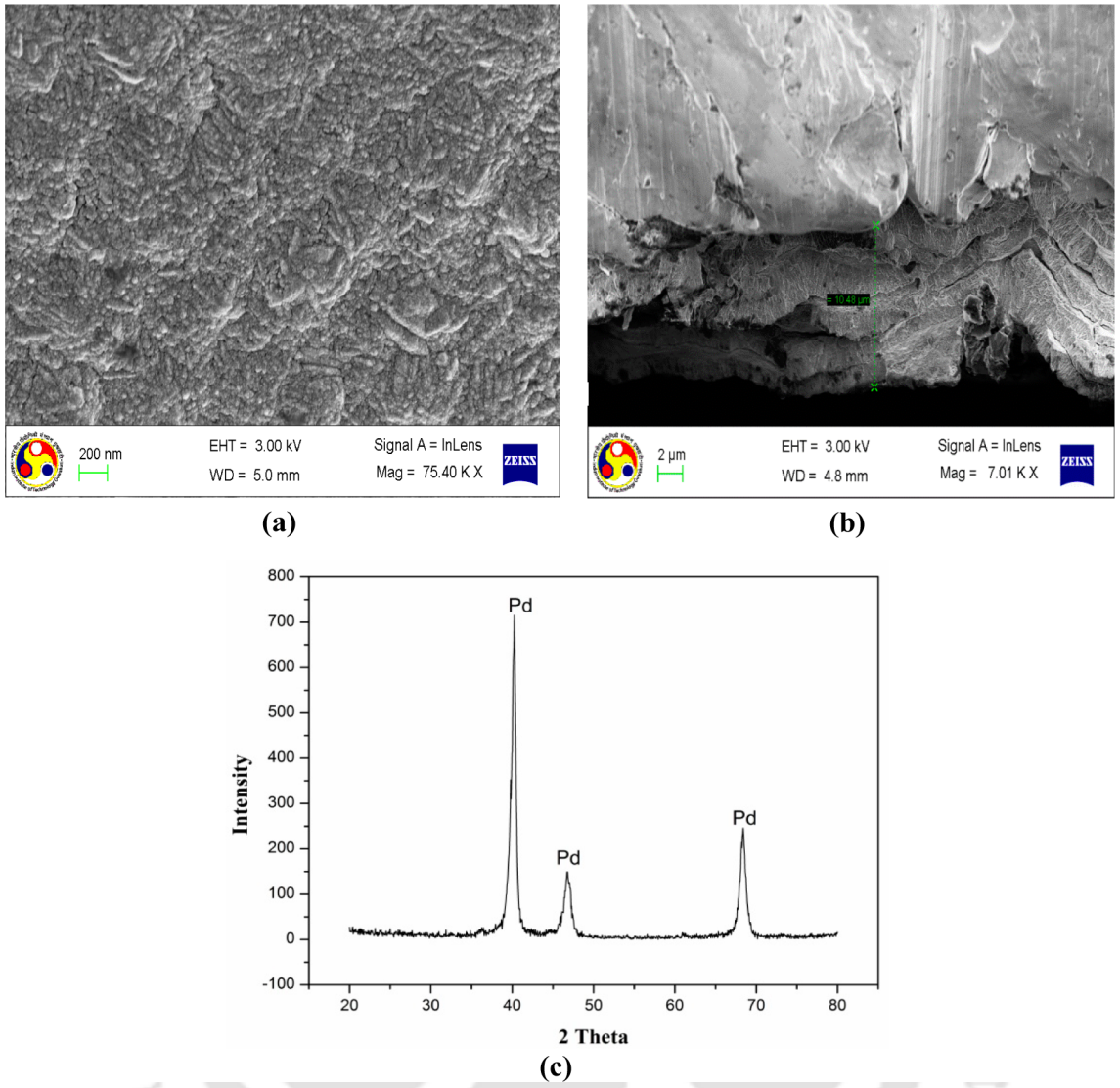

Figure 6. (a) Surface morphology, (b) cross section, and (c) XRD pattern of dense Pd/PSS composite membrane.

reach the active membrane surface for a lower loading ratio. On the other hand, doubling the loading ratio marginally affected the plating efficiency, which might be due to insignificant metal nucleation in the solution.

The average Pd plating rates for loading ratios of 203 and 407 cm^2/L at various sequential plating time steps are presented in Table 3. It can be observed that, with increasing loading ratio, the metal deposition rates decreased, for example, from 4.92×10^{-5} to 3.14×10^{-5} $mol/m^2 \cdot s$ after a total plating time of 2 h and from 4.57×10^{-5} to 2.82×10^{-5} $mol/m^2 \cdot s$ after a total plating time of 7 h. Even though the Pd solution concentration remained the same in the two cases, the case corresponding to the lower loading ratio provided a greater quantity of Pd metal in the solution, so that higher Pd plating rates were achieved in this case.

4.2.2. Membrane Characteristics. Figure 5a shows a comparison of the time-dependent PPD values obtained for loading ratios of 203 and 407 cm^2/L. For the 407 cm^2/L case, after 2 h of sequential plating, the membrane densified to 99.14%, which enhanced to 99.9% after another 5 h of sequential plating. On the other hand, for the lower loading ratio, the PPD values increased significantly up to 6 h of sequential plating and provided 100% densification after another 2 h of sequential plating. For all time durations, maximum PPD values were achieved in the 203 cm^2/L case because of the presence of a higher quantity of Pd metal in the plating solution that effectively carried out surface pore coverage and densification.

Figure 5b shows the variation of the incremental metal film thickness with time of plating for loading ratios of 203 and 407 cm^2/L. It can be observed that, for an increase in the loading ratio from 203 to 407 cm^2/L, the film thickness decreased, for example, from 3.13 to 2.0 μm at a plating time of 2 h. This is due to the reduction in the amount of Pd metal available in the ELP bath for the loading ratio of 407 cm^2/L.

4.3. Surface Characterization. The surface morphology and cross section of the dense Pd/PSS membrane fabricated in an SSOEP bath with a surfactant concentration of 2 CMC at a loading ratio of 203 cm^2/L was examined by field-emission scanning electron microscopy (FESEM; Zeiss model SIGMA). Figure 6a presents the surface morphology of a dense Pd/PSS membrane, and it can be observed that smooth and uniform grain agglomeration exists without any pores on the surface. Figure 6b presents the cross section of a dense Pd/PSS

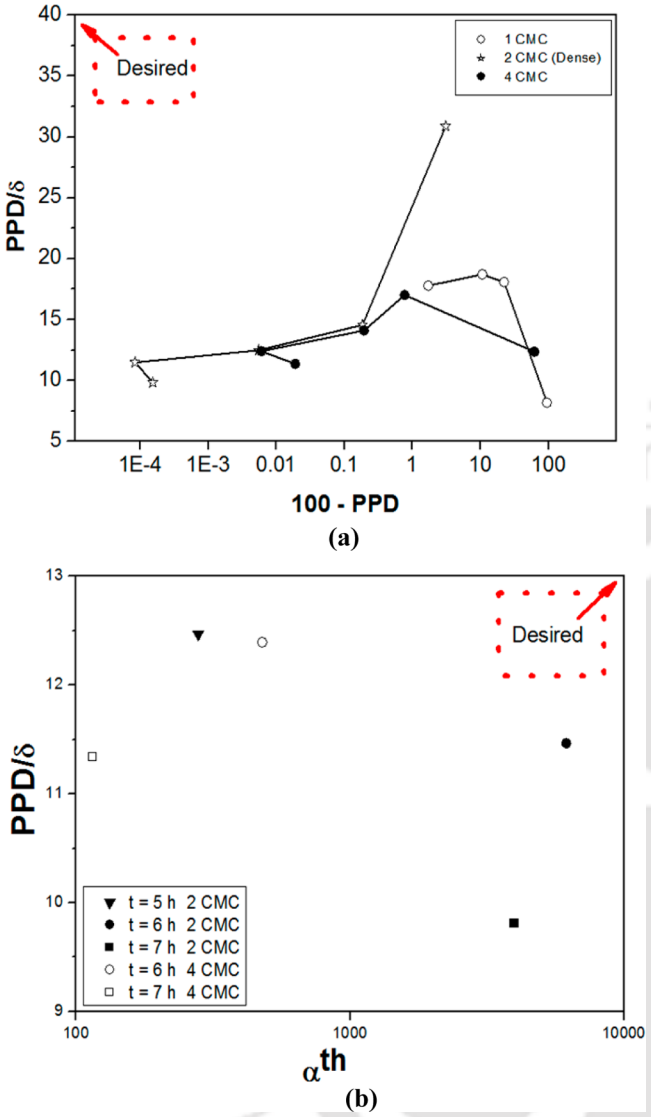

Figure 7. Tradeoffs associated with (a) PPD/δ vs (100 − PPD) and (b) PPD/δ vs α^{th}.

membrane, and it can be observed that the thickness of the palladium film was 10.48 μm, which is close to the thickness (11.16 μm) evaluated by the gravimetric method (eq 5).

Figure 6c shows the XRD spectrum of a dense Pd/PSS composite membrane fabricated with an SSOEP bath at a surfactant concentration of 2 CMC and a loading ratio of 203 cm^2/L. The XRD spectrum contains Pd reflection peaks in the face-centered-cubic (fcc) phase at the (111), (200), and (202) planes but no other reflection peaks for Fe, Cr, Ni, or Mn/Mo metals. These elements could exist at the PSS substrate, and hence, the XRD spectrum confirms the achievement of dense Pd membranes.

4.4. Tradeoffs. In this section, tradeoffs are presented for the loading ratio of 203 cm^2/L but not 407 cm^2/L. This is because a PPD of 100% was achieved for the loading ratio of 203 cm^2/L, whereas the PPD did not increase above 99.9% after 7 h of sequential deposition for the higher loading ratio.

4.4.1. PPD/δ versus (100 − PPD). Figure 7a shows the tradeoffs associated with PPD/δ versus (100 − PPD) for 1, 2, and 4 CMC baths at a loading ratio of 203 cm^2/L. The PPD/δ value varied in the ranges of 8.17−17.78 for 1 CMC, 8.95−30.87 for 2 CMC, and 11.34−12.34 for 4 CMC. Further, the 100 − PPD profile for the 2 CMC bath extended more toward the left side of the x axis in comparison to those for the 4 and 1 CMC baths. Even though the PPD/δ profile decreased significantly for the 2 CMC bath, a value of 8.95 at near-densification is highly attractive, given the fact that PPD/δ decreases significantly (to values less than 1) for conventional electroless plating (CEP) baths. In the literature,[15] the PPD/δ can be estimated to be 11.14, which is higher than the value obtained in this work for SSOEP baths. However, given the 50% lower Pd solution concentrations in this work, the obtained PPD/δ value for a 2 CMC surfactant concentration is promising for further process engineering studies. In addition, the existence of a lapse mode in the profiles for both 2 and 4 CMC baths can also be observed in Figure 7a. However, as explained earlier, the PPD profile lapse mode of the 2 CMC bath is not significant when compared to the PPD profile of the 4 CMC bath. The PPD profile lapse was on the order of 10^{-5}−10^{-4} for the 2 CMC bath, which is significantly lower than the lapse on the order of 10^{-3}−10^{-2} for the 4 CMC bath.

4.4.2. PPD/δ versus α^{th}. Figure 7b shows the trend with plating time of PPD/δ versus α^{th} for plating baths containing surfactant concentrations of 2 and 4 CMC. For the 2 CMC bath, the theoretical selectivities obtained after 5, 6, and 7 h of sequential plating were 279.23, 6154, and 3953, respectively. The maximum selectivity of infinity was obtained after completion of 8 h of Pd ELP. For the 4 CMC bath, the selectivities obtained after 6 and 7 h sequential plating were only 478.5 and 114.3. Thus it is apparent that SSOEP (DW) with a surfactant concentration of 2 CMC is promising to provide very high theoretical selectivities for the separation of H_2 and N_2.

5. COST ANALYSIS

Parameters assumed and considered for the retail cost analysis of various dense membranes are presented in Table 4. The retail costs of fabricating dense palladium membranes using various approaches, namely, SSOEP (DW) on PSS, surfactant-induced electroless plating (SIEP) (bulk) on PSS,[15] CEP (bulk) on PSS,[15] and SIEP (bulk) on alumina[20] are presented in Figure 8. As shown, the cost of the dense Pd membrane fabricated in this work is 13.2 \$/cm^2, which is significantly lower than the costs of the membranes fabricated under the conditions reported by Islam et al.[15] (32.45 \$/cm^2) and Ke et al.[20] (35.69 \$/cm^2). Therefore, it is apparent that the SSOEP

Table 4. Cost Parameters for the Evaluation of Retail Fabrication Costs of Dense Pd Composite Membranes

no.	name of composition	quantity	cost (\$)
1	support		
	PSS	3.6-cm diameter	44
	α-Al_2O_3	100 cm^2	38.45
2	palladium ($PdCl_2$)	1 g	67.62
3	surfactant		
	CTAB	100 g	7.763
	DTAB	25 g	90.84
4	Na_2EDTA	100 g	3.49
5	acetone	2.5 L	14.72
6	hydrazine	0.5 L	21.49
7	electrical	1 kW	0.16
8	manpower	1 h	4.54

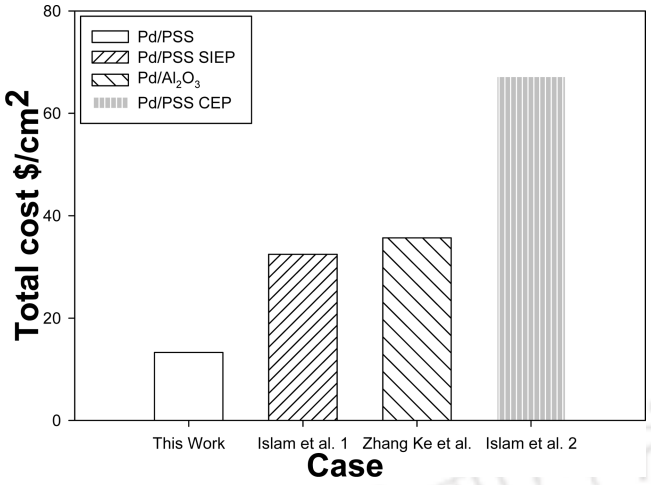

Figure 8. Cost comparison of existing SSOEP (DW) with literature data.

process developed herein reduces the costs significantly by about 60%. Further, it is important to note that Islam et al.[15] did not mention the total plating volume used for Pd membrane fabrication and, therefore, an assumed value of 20 mL of plating solution for a membrane area of 5.06 cm^2 in one plating step was used in the comparative assessment. Also, for CEP using the conditions reported by Islam et al.,[15] the cost of the membrane increased to 61.2 $/$cm^2$, which is atleast 4 times higher than the cost obtained using the parameters reported in this work. The cost of the SSOEP process was lower for the following reasons: First, the surfactant used (CTAB) is very inexpensive (retail cost of CTAB is 0.077 $/g, whereas the cost of DTAB is 3.62 $/g in India). In addition, the CMC concentration of DTAB (4.93 g/L) is significantly higher than that of CTAB (0.335 g/L). Second, SSOEP (DW) utilizes 50 mL of a 0.005 mol/L plating solution for one 30-min depositional step, whereas the patented SIEP process utilizes 0.015 mol/L for a 1-h plating step. Third, the total time of plating in this work was at least 2 h less than the time of plating reported by Islam et al.[15] Finally, the membrane area considered in this work was significantly higher than the values reported in the literature.

A summary of various component contributions to membrane costs is provided in Figure 9 for several membranes. It can be observed that, for the present case, the manpower, stainless steel support, and palladium chemical costs contributed very uniformly to the total cost of the membrane. The cost of the surfactant was an insignificant fraction of the retail cost of the membrane. However, for the membrane fabricated by Islam et al.,[15] the cost of the surfactant was significant at up to 9%, and the Pd chemicals contributed about 36%. For the Pd dense membrane fabricated using an α-alumina support, the cost contribution of the support was not more than 1%, but the Pd chemicals contributed 81% of the total cost. For membrane fabrication using CEP, both manpower and Pd chemicals contributed significantly to the total cost. Thus, the research in this work has been able to optimize the cost contributions of various important components and, hence, to minimize the overall cost of the Pd composite dense membrane.

6. CONCLUSIONS

Based on the observed plating and deposition characteristics of SSOEP plating baths, the optimal combination of plating and process parameters was found to be a palladium solution

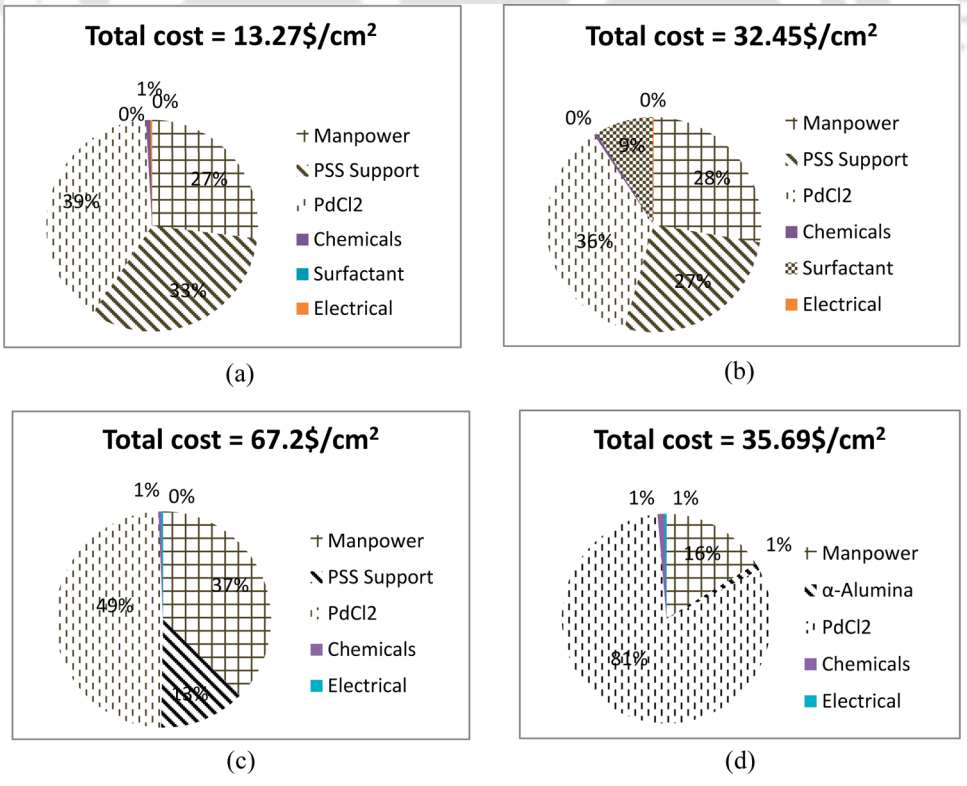

Figure 9. Cost analysis of (a) existing SSOEP (DW) on PSS (this work), (b) Pd/PSS SIEP (bulk, 10 h),[15] (c) Pd/PSS CEP (bulk, 28 h),[15] and (d) Pd/α-Al_2O_3 SIEP (bulk).[20]

concentration of 0.005 M, a loading ratio of 203 cm^2/L, a CTAB surfactant solution concentration of 2 CMC, and a total plating time of 8 h (16 depositional steps of 30-min duration each). The process provided 11.16-μm-thick dense palladium composite membranes with plating efficiencies greater than 90%, selective conversions of about 30−35%, and a plating rate of 4.38×10^{-5} $mol/m^2 \cdot s$. SSOEP with this combination of plating and process parameters provided minimal lapse in the PPD profiles and provided very high PPD values after 2 h of plating. The overall fabrication cost of the identified dense Pd/PSS composite membrane was estimated to be 13.24 $\$/cm^2$, which is 60% more cost-effective than the best-known SIEP process.[15] Further, it was observed that enhancing the loading ratio from 203 to 407 cm^2/L enhanced the selective conversion, reduced the plating efficiency, and provided lower PPD values, thus indicating the nonoptimality of the higher loading ratio.

Three important features, namely, reduction of the Pd solution concentration, coupling of sonication and a surfactant, and dropwise contacting of the reducing agent, are the principal characteristics of the plating process proposed in this work that have not previously been reported. All other processes that have been investigated have not been able to provide a dense Pd membrane using the specified concentration of palladium (0.005 M). Thus, SSOEP warrants further research emphasis by Pd membrane material scientists to enhance its optimality for the successful fabrication of dense Pd membranes at low cost.

AUTHOR INFORMATION

Corresponding Author

*E-mail: ramgopalu@iitg.ernet.in. Tel.: +91 361 2582260. Fax: +91 361 2582291.

Notes

The authors declare no competing financial interest.

ACKNOWLEDGMENTS

This work was partially supported by a grant from the DST (Department of Science and Technology), New Delhi, India. Any opinions, finding, and conclusions expressed in this paper are those of the authors and do not necessarily reflect the views of DST.

NOMENCLATURE

AAS = atomic absorption spectroscopy
CEP = conventional electroless plating
DW = dropwise
PPD = percent pore densification (%)
SIEP = surfactant-induced electroless plating
SSOEP = surfactant- and sonication-induced electroless plating
A_m = area of the membrane (cm^2)
AJH_{ht}^{pcm} = average H_2 flux of porous composite membrane at high temperature ($mol/m^2 \cdot s$)
AJN_{ht}^{pcm} = average N_2 flux of porous composite membrane at high temperature ($mol/m^2 \cdot s$)
C_f = final concentration of Pd^{2+} in the plating solution (mol/L)
C_i = initial concentration of Pd^{2+} in the plating solution (mol/L)
$\overline{J}_i$ = average permeation flux through the membrane ($mol/m^2 \cdot s$)
$\overline{J}_o$ = average permeation flux through the support ($mol/m^2 \cdot s$)
JH_{ht}^{pcm} = hydrogen flux of porous composite membrane at high temperature ($mol/m^2 \cdot s$)
JN_{ht}^{pcm} = nitrogen flux of porous composite membrane at high temperature ($mol/m^2 \cdot s$)
$KPern_{ht}^{pcm}$ = Knudsen nitrogen permeance at high temperature ($mol/m^2 \cdot s \cdot Pa$)
$KPern_{rt}^{pcm}$ = Knudsen nitrogen permeance at room temperature ($mol/m^2 \cdot s \cdot Pa$)
M_{Pd} = molecular weight of palladium metal (g/cm^3)
N = number of plating steps
$Perh^{dm}$ = hydrogen permeability of dense palladium membrane ($mol \cdot m/m^2 \cdot s \cdot Pa$)
$Pernh^{pcm}$ = hydrogen permeance through porous composite membrane ($mol/m^2 \cdot s \cdot Pa$)
$Pern_{rt}^{pcm}$ = nitrogen permeance of the porous composite membrane at room temperature ($mol/m^2 \cdot s \cdot Pa$)
PP = partial pressure on the permeate side (Pa)
PR = partial pressure on the retentate side (Pa)
PR_{max} = maximum allowed upstream pressure (5 bar)
PR_{min} = minimum upstream pressure (0.01 bar)
$\overline{Q}_{H_2}^{th}$ = Average theoretical hydrogen flow rate (mol/s)
Q_{rt}^{pcm} = volumetric flow rate of nitrogen at room temperature for the porous composite membrane (mol/s)
$\overline{r}_{Pd}$ = average plating rate of palladium metal ($mol/m^2 \cdot s$)
t = plating time (h)
V_o = volume of plating solution in each plating step (L)
$ViPern_{ht}^{pcm}$ = viscous nitrogen permeance at high temperature ($mol/m^2 \cdot s \cdot Pa$)
$ViPern_{rt}^{pcm}$ = viscous nitrogen permeance at room temperature ($mol/m^2 \cdot s \cdot Pa$)
vn_{ht} = velocity of nitrogen at high temperature (m/s)
vn_{rt} = velocity of nitrogen at room temperature (m/s)
w_1 = dry weight of membrane before plating (g)
w_2 = dry weight of membrane after plating (g)
w_o = amount of metal converted during plating (g)
x_{H_2} = Mole fraction of hydrogen in the feed stream
x_{N_2} = Mole fraction of nitrogen in the feed stream
y_{H_2} = Mole fraction of hydrogen in the permeate stream
y_{N_2} = Mole fraction of nitrogen in the permeate stream

Greek Letters

α_{av}^{pcm} = average selectivity of porous composite membrane
δ = palladium film thickness
δ^{pcm} = thickness of porous composite membrane (m)
η = plating efficiency
μn_{rt} = viscosity of nitrogen at room temperature (kg/m·s)
μn_{ht} = viscosity of nitrogen at high temperature (kg/m·s)
ρ_{Pd} = density of palladium metal (kg/m^3)
χ = conversion of Pd^{2+} to Pd in the plating

Subscripts and Superscripts

rt = room temperature
ht = high temperature
max = maximum
min = minimum
Pd = palladium
m = membrane
N_2 = nitrogen
H_2 = hydrogen
pcm = porous composite membrane
dm = dense membrane
th = theoretical

REFERENCES

(1) Shi, Z.; Wu, S.; Szpunar, J. A.; Roshd, M. An observation of palladium membrane formation on porous stainless steel substrate by electroless deposition. *J. Membr. Sci.* **2008**, *280*, 705−711.

(2) Bryden, K. J.; Ying, J. Y. Nanostructured palladium membrane synthesis by magnetron sputtering. *Mater. Sci. Eng. A* **1995**, *204*, 140−145.

(3) Tong, H. D.; VandenBerg, A. H. J.; Gardeniers, J. G. E.; Jansen, H. V.; Gielens, F. C.; Elwenspoek, M. C. Preparation of palladium−silver alloy films by a dual-sputtering technique and its application in hydrogen separation membrane. *Thin Solid Films* **2005**, *479*, 89−94.

(4) Xomeritakis, G.; Lin, Y. S. Fabrication of a thin palladium membrane supported in a porous ceramic substrate by chemical vapour deposition. *J. Membr. Sci.* **1996**, *120*, 261−272.

(5) Huang, L.; Chen, C. S.; He, Z. D.; Peng, D. K.; Meng, G. Y. Palladium membranes supported on porous ceramics prepared by chemical vapor deposition. *Thin Solid Films* **1997**, *302*, 98−101.

(6) Lu, S. Y.; Lin, Y. Z. Pd−Ag alloy films prepared by metallorganic chemical vapour deposition process. *Thin Solid Films* **2000**, *376*, 67−72.

(7) Chen, S. C.; Tu, G. C.; Hung, C. C. Y.; Huang, C. A.; Rei, M. H. Preparation of palladium membrane by electroplating on AISI 316L porous stainless steel supports and its use for methanol steam reformer. *J. Membr. Sci.* **2008**, *314*, 5−14.

(8) Bhandari, R.; Ma, Y. H. Pd−Ag membrane synthesis: The electroless and electro-plating conditions and their effect on the deposits morphology. *J. Membr. Sci.* **2009**, *334*, 50−53.

(9) Kitiwan, M.; Atong, D. Effects of Porous Alumina Support and Plating Time on Electroless Plating of Palladium. *J. Mater. Sci. Technol.* **2010**, *26*, 1148−1152.

(10) Gade, S. K.; Theon, P. M.; Way, J. D. Unsupported palladium alloy foil membranes fabricated by electroless plating. *J. Membr. Sci.* **2008**, *316*, 112−118.

(11) Tanaka, D. A. P.; Tanco, M. A. L.; Niwa, S. I.; Wakui, Y.; Mizukami, F.; Namba, T.; Suzuki, T. M. Preparation of palladium and silver alloy membrane on α-alumina tube via simultaneous electroless plating. *J. Membr. Sci.* **2005**, *247*, 21−27.

(12) Cheng, Y. S.; Yeung, K. L. Effects of electroless plating chemistry on the synthesis of palladium membrane. *J. Membr. Sci.* **2001**, *182*, 195−203.

(13) Bulasara, V. K.; Chandrasekhar, O.; Uppaluri, R. Effect of surface roughness and mass transfer enhancement on the performance characteristics of nickel-hypophosphite electroless plating baths for metal−ceramic composite membrane fabrication. *Chem. Eng. Res. Des.* **2011**, *89*, 2485−2494.

(14) Ayturk, M. E.; Ma, Y. H. Electroless Pd and Ag deposition kinetics of the composite Pd and Pd/Ag membranes synthesized from agitated plating baths. *J. Membr. Sci.* **2009**, *330*, 233−245.

(15) Islam, M. S.; Rahman, M. M.; Ilias, S. Characterization of Pd−Cu membranes fabricated by surfactant induced electroless plating (SIEP) for hydrogen separation. *Int. J. Hydrogen Energy* **2012**, *37*, 3477−3490.

(16) Chen, B. H.; Hong, L.; Ma, Y.; Ko, T. M. Effect of surfactants in an electroless nickel-plating bath on the properties of Ni−P alloy deposits. *Ind. Eng. Chem. Res.* **2002**, *41*, 2668−78.

(17) Nam, S. E.; Lee, S. H.; Lee, K. H. Preparation of a palladium alloy composite membrane supported in a porous stainless steel by vacuum electrodeposition. *J. Membr. Sci.* **1999**, *153*, 163−173.

(18) Bulasara, V. K.; Abhimanyu, M. S.; Pranav, T.; Uppaluri, R.; Purkait, M. K. Performance characteristics of hydrothermal and sonication assisted electroless plating baths for nickel−ceramic composite membrane fabrication. *Desalination* **2012**, *284*, 77−85.

(19) Itoh, N.; Akiha, T.; Sato, T. Preparation of thin palladium composite membrane tube by a CVD technique and its hydrogen permselectivity. *Catal. Today* **2005**, *104*, 231−237.

(20) Ke, Z.; Huiyuan, G.; Zebao, R.; Yuesheng, L.; Yongdan, L. Preparation of Thin Palladium Composite Membranes and Application to Hydrogen/Nitrogen Separation. *Chin. J. Chem. Eng.* **2007**, *15*, 643−647.

dx.doi.org/10.1021/ie4035412 | *Ind. Eng. Chem. Res.* 2014, 53, 3105−3115

Applied Surface Science 305 (2014) 658–664

Contents lists available at ScienceDirect

Applied Surface Science

journal homepage: www.elsevier.com/locate/apsusc

Role of electroless nickel diffusion barrier on the combinatorial plating characteristics of dense Pd/Ni/PSS composite membranes

Murali Pujari, Amrita Agarwal, Ramgopal Uppaluri*, Anil Verma

Department of Chemical Engineering Indian Institute of Technology Guwahati Guwahati 781039, Assam, India

ARTICLE INFO

Article history:
Received 28 October 2013
Received in revised form 17 March 2014
Accepted 23 March 2014
Available online 31 March 2014

Keywords:
Electroless plating
Sonication
Surfactant
Pd composite membrane
Interdiffusion

ABSTRACT

This work addresses the combinatorial plating characteristics of dense Pd/Ni/porous stainless steel (PSS) composite membranes in comparison with Pd/PSS membranes. While Pd/PSS membranes were fabricated using 0.1 μm nominal pore size PSS supports, Pd/Ni/PSS membranes were fabricated using 0.5 and 0.1 μm nominal pore size PSS supports. Both Ni and Pd films were deposited using an identified novel electroless plating process that characterizes the optimal utilization of surfactant, sonication and reducing agent contacting pattern in Pd electroless plating baths. It was observed that the combinatorial plating characteristics for Pd/Ni/PSS membranes were significantly different and poorer in comparison with those obtained for the Pd/PSS membranes. In summary, it has been inferred that the introduction of nickel interdiffusion barrier was not fruitful to reduce the critical thickness of dense Pd film without jeopardizing upon the pore densification.

Introduction

In comparison with pure palladium foils, palladium composite membranes possess superior combinations of hydrogen permeability, separation factor, mechanical strength and cost [1,2]. Typically, palladium composite membranes refer to a thin dense Pd film deposited on a macro porous support such as alumina or sintered stainless steel or inconel [3,4]. Amongst various types of macroporous supports, porous stainless steel (PSS) is promising. This is due to its several advantages such as better mechanical stability and ease to seal through welding technologies in experimental infrastructure [5–7]. The life cycle of palladium composite membranes is invariably affected by the temperature cycling effect due to which variations in the thermal expansion of Pd film and the support contribute towards intermetallic diffusion and thereby reduce hydrogen permeability and their shelf life. Therefore, interdiffusion barriers have been suggested by several authors to restrict the degradation of membrane performance due to repetitive temperature cycling effect [7,8]. Another advantage of the interdiffusion barrier is that they reduce the wider pore size distributions on the macro porous support and thereby reduce the critical thickness required to achieve dense Pd composite membranes. Till date, for the fabrication of Pd composite membranes various types of interdiffusion barriers investigated are yttria stabilized zirconia [2], TiO_2 [2], CeO_2 [7], α-Fe_2O_3 [8], γ-Al_2O_3 [8], W [9], ZrO_2 [10], Cr_2O_3 [11] and Ni [12].

Huang et al. [2] introduced ~10–70 μm thick yttria stabilized zirconia (YSZ) and ~40–60 μm thick TiO_2 diffusion barriers between palladium film and porous stainless steel substrate by using atmospheric plasma spraying and wet spraying techniques, respectively. The YSZ and TiO_2 modified substrates were densified after depositing ~15–20 μm and ~8–10 μm thick Pd films, respectively. Thus their work indicated that despite using larger thickness of the interdiffusion barriers, the dense Pd film thickness did not reduce substantially.

Tong et al. [7] introduced cerium hydroxide particles (1–4 nm) in the pores of porous stainless steel support (average pore size 200 nm) using ultrasonic bath and vacuum suction followed by electroless palladium deposition. The membrane was densified after depositing 13 μm thick Pd film and the composite membrane has not improved the hydrogen permeability in comparison with the palladium membranes fabricated on PSS supports.

Yepes et al. [8] introduced α-Fe_2O_3 and γ-Al_2O_3 as diffusion barriers between Pd–Ag alloy films and porous stainless steel substrate (200 nm average pore size). The γ-Al_2O_3 and α-Fe_2O_3 was deposited by wash coating of the support with γ-Al_2O_3 suspension and oxidation of PSS support, respectively, followed with the sequential electroless deposition of palladium and silver. The

* Corresponding author. Tel.: +91 361 2582260; fax: +91 361 2582291.
E-mail address: ramgopalu@iitg.ernet.in (R. Uppaluri).

http://dx.doi.org/10.1016/j.apsusc.2014.03.156
0169-4332/

membrane with α-Fe_2O_3 barrier exhibited higher selectivities than γ-Al_2O_3 barrier but the H_2 permeability was 2 times lower than those obtained with γ-Al_2O_3 interdiffusion barrier.

Gryaznov et al. [9] introduced thin Tungsten (W) film using magnetron sputtering technique on porous stainless steel membranes (average pore size of 200 nm) and achieved a dense Pd composite membrane using magnetron sputtering technique. The authors indicated that the introduced W interdiffusion barrier did not reduce the support pore size and a critical Pd film thickness of 10 μm was required to obtain a dense composite membrane. On the other hand, enhancing the W film thickness reduced the Pd film thickness but as well reduced hydrogen permeability. In other words, further engineering of the macro porous support has been suggested by the authors as an important future research issue.

Wang et al. [10] introduced zirconia oxide particles on the surface of a tubular porous stainless steel substrate (average pore size of 200 nm) using coupled sonication and vacuum application and eventually deposited 10 μm thick Pd dense film using electroless plating. The authors observed that the introduced zirconia oxide particles offered additional permeation resistance to reduce hydrogen flux in comparison with the Pd/PSS membranes.

Samingprai et al. [11] fabricated dense palladium membrane using electroless plating to achieve a Pd film thickness of 32 μm on a 2 μm thick Cr_2O_3 layer deposited on a porous stainless steel substrate (average pore size 100 nm) using electroplating and subsequent oxidation of the chromium film. It was analyzed by the authors that the chromia diffusion barrier did not reduce the minimal thickness required for the Pd film to achieve dense Pd composite membrane.

Researching upon nickel as interdiffusion barrier Lin et al. [12] addressed nickel electroplating on porous stainless steel substrate (4 μm average pore size) followed with sequential electroless deposition of palladium and silver. On 16.9 and 27.2 μm thick nickel films, 18.4 and 17.8 μm Pd thick films were deposited which were then subjected to hydrogen permeance studies. The authors observed that the enhancement of hydrogen flux was more critically dependent on the Pd film thickness but not nickel film thickness. This indicates that the interdiffusion barrier did not influence upon the minimum Pd film thickness required to achieve dense Pd composite membranes.

A critical analysis of the above literatures provides the following insights. First, magnetron sputtering had been utilized in several cases to introduce the interdiffusion barrier which is not a scalable fabrication technique. Second, amongst various techniques deployed to fabricate the interdiffusion barrier and Pd films, electroless and electroplating are highly promising due to their simplicity, susceptibility to process scale up and cost. Third, literatures addressing the role of interdiffusion barriers do not present a systematic investigation that highlights the interdependency of interdiffusion barrier permeation properties on the considered fabrication methods. For instance, literatures do not elaborate upon the metal transport efficiency when interdiffusion barriers have been introduced, which is a very important issue from the perspective of process efficacy. Fourth, amongst various interdiffusion barriers, Ni, Al_2O_3, Fe_2O_3 and Cr_2O_3 appear to be the most competent in terms of the cost of the interdiffusion barriers given the fact that ceria, zirconia and tungsten are expensive materials and cannot reduce the cost of the palladium composite membrane which has already been regarded to be expensive due to the utilization of Pd noble metal. Thus, research emphasis for the large scale fabrication of Pd composite membranes with interdiffusion barriers shall address the engineering aspects associated to the efficient fabrication of these interdiffusion barrier films.

On the other hand, the selection of an optimal fabrication technique to engineer the interdiffusion barriers on porous ceramic/stainless steel substrates is very important. Based on the existing literatures as well as scale up possibilities for various fabrication perspectives, electroless plating remains the most promising technique for the fabrication of inexpensive Pd composite membranes. Compared to electroless plating, electroplating is not comparatively promising given the fact that electroplating requires conducting surfaces and the utilization of non-conducting ceramic supports renders the process to be extremely cumbersome.

While electroless plating is advantageous from the perspective of scale up, it suffers from the basic limitation of lower plating rates and hence rate enhancement techniques need to be supplemented to enhance plating rates without affecting the quality of deposition and pore densification. Till date, several researchers addressed rate enhancement techniques such as stirring [13], sonication [13], agitation [14], surfactant [15] and vacuum [16] to enhance the plating rate and reduce total plating time. Even amongst these techniques, sonication and surfactant appear to be promising from the perspective of combinatorial plating characteristics and scale up. In our recent work, we have identified an optimal combination of surfactant, sonication and contacting pattern of the reducing agent (SSOEP-DW ELP process) to achieve maximum combinations of metal electroless plating combinatorial plating characteristics [17]. This work is a natural extension of these concepts for the evaluation of combinatorial plating characteristics of electroless plating baths in those circumstances, where nickel interdiffusion barrier is engineered to target the minimization of Pd film thickness desired for dense metal composite membranes.

This work addresses the combinatorial plating characteristics for the fabrication of dense Pd/Ni/PSS composite membranes in comparison with dense Pd/PSS membranes. The combinatorial plating characteristics include the estimation of time dependent variation of conversion, plating efficiency, plating rate, thickness and percent pore densification (PPD). Thereby, utilizing this data, significant insights are anticipated to foster upon improving the efficacy of electroless plating processes and their associated degrees of freedom for the smart fabrication of multi-metal membranes.

Experimental

Preparation of Pd membrane on porous stainless steel

Porous stainless steel circular discs (dia of 36 mm and thickness of 1 mm) with a nominal particle retention size of 0.1 μm and 0.5 μm were purchased from Mott Corporation, USA. Prior to the Pd membrane synthesis, the stainless steel discs were subjected to sonication in acetone for 30 min in an ultrasonic cleaning bath (Model: S30H, Make: ELMA) to remove the grease, oil, dirt, corrosion products and other contaminants present on the surface. The power consumption capacity of the ultrasonic cleaning bath is 280 W. The discs were subsequently dried at 393 K in an oven (Model: ROV/DG, REICO) for 2 h.

Eventually, these discs were seeded with Pd particles to initiate an autocatalytic electroless Pd plating process that involves the reduction of Pd metal complex ions on the substrate surface. The seeding process refers to placing the stainless steel substrates in the sensitization bath ($SnCl_2$ solution) to bond Sn^{2+} ions on to the substrate surface which are eventually displaced with metal Pd particles in the sequential activation step. About 8–10 times the sequence of sensitization and activation were repeated to achieve a completely activated Pd membrane surface which is confirmed by observing uniform dark-brown color on the membrane surface. After seeding, the membranes were dried overnight in an oven (Model: ROV/DG, REICO) at 393 K to measure its dry weight (w_1) before plating.

Table 1
Composition for nickel electroless plating bath.

S. no.	Constituent	Amount used in each bath
1	Nickel sulfate ($NiSO_4 \cdot 7H_2O$)	0.08 mol/L
2	Hydrazine hydrate (20%) ($N_2H_4 \cdot H_2O$)	40 ml/L
3	Trisodium citrate ($Na_3C_6H_5O_7 \cdot 2H_2O$)	0.16 mol/L
4	Sodium hydroxide (NaOH)	pH: 10–11
5	CTAB	4 CMC
6	Temperature	80 °C

To deliberate upon the role of diffusion barrier in influencing combinatorial plating characteristics, prior to palladium plating the seeded PSS supports (nominal pore size of 0.5 μm and 0.1 μm) were electroless plated with nickel to obtain Ni/PSS composite membranes. To achieve the desired average pore size of the Ni/PSS membranes, sequential electroless Ni plating was carried out for 5 and 2 h for 0.5 and 0.1 μm PSS supports, respectively. Corresponding nickel electroless plating bath compositions are summarized in Table 1. For the 0.5 μm PSS support, the higher total plating time (5 h) was considered due to the fact that the PSS support possessed wider pore size distributions and wider average pore size in comparison with the 0.1 μm PSS support. Thereby, the Ni–PSS support prepared with 0.5 μm PSS supports is anticipated to possess similar pore size distributions and average pore size to that of the 0.1 μm PSS supports. Also, a total plating time of 2 h was deployed for the 0.1 μm PSS support to ensure whether critical Pd film thickness can be reduced by introducing the Ni inter-diffusion barrier. On the other hand, the Pd/PSS composite membrane was fabricated with 0.1 μm PSS support. For both Ni/PSS and PSS membrane supports, seeding and activation steps were conducted to ensure upon the activation of the support surface with Pd particles.

All Pd electroless plating experiments were conducted with novel identified surfactant and sonication induced electroless plating baths supplemented with drop wise addition of reducing agent (SSOEP-DW) at a loading ratio of 203 cm^2/L. Further details of the process have been presented elsewhere [17]. Table 2 summarizes the composition of Pd electroless plating baths. Each Pd plating step duration is about 30 min. The performance characteristics of Pd electroless plating baths were determined initially after every four sequential plating steps (2 h of plating time). Later, after PPD reached 90%, all relevant plating characteristics were determined after every two sequential plating steps.

For all membranes, 12 to 16 sequential plating steps were carried out with intermediate rinsing using de-ionized water to remove salts adsorbed in pores of the porous support or entrapped in the Pd coating layer. Finally the membrane was dried in an oven at 393 K for 6 h. The dry weight (w_2) of the membrane was measured to evaluate the amount of palladium deposited on the support surface during plating.

Evaluation of plating characteristics

The performance characteristics evaluated for the electroless plating baths are namely plating bath conversion (χ), selective conversion, plating efficiency (η), Palladium film thickness (δ), average plating rate ($\bar{r}_{Pd}$), average permeation flux ($\bar{J}$), percent pore densification (PPD) and theoretical selectivity ($\bar{\alpha}_{av}$).

Table 2
Composition for palladium electroless plating bath.

S. no.	Constituent	Amount used in each bath
1	$PdCl_2$	0.886 g/L
2	Na_2EDTA	14.89 g/L
3	$NH_3 \cdot H_2O$ (25%)	110 ml/L
4	N_2H_4 (1.0 M)	1.81 ml/L
5	CTAB	2 CMC
6	pH	11
7	Temperature	60 °C

The plating bath conversion is evaluated as the ratio of the amount of Pd metal ion reacted to the amount of palladium present initially in the plating solution, and is expressed as:

$$\chi(\%) = \frac{C_i - C_f}{C_i} \times 100 \quad (1)$$

where C_i and C_f are initial and final concentration (mol/L) of Pd in the plating solution. These were determined using atomic absorption spectrophotometer (AAS) (Model: FS 240, Make: Varian Spectra) at a wavelength of 247.6 nm.

Plating efficiency (η) is evaluated as the ratio of amount of palladium deposited on active substrate surface to the amount of palladium converted during the plating step and is expressed as follows:

$$\eta(\%) = \frac{w_2 - w_1}{w_o} \times 100 \quad (2)$$

where w_1 is the dry weight of membrane before plating (g), w_2 is the dry weight of membrane after plating and w_o is the amount of palladium metal converted during plating. In the above expression, w_o is calculated using the equation:

$$w_o = \left(C_i - C_f\right)\, nV_oM_{Pd} \quad (3)$$

where n is the number of sequential plating steps, V_o is the volume of plating solution (L) in each plating step and M_{Pd} is the molecular weight of palladium metal (g/mol).

The selective conversion is defined as the product of plating efficiency and conversion of plating bath:

$$\text{Selective conversion}(\%) = \frac{\eta \times \chi}{100} \quad (4)$$

The thickness of deposited palladium film has been evaluated using weight gain method and is calculated using the expression:

$$\delta = \frac{w_2 - w_1}{\rho_{Pd} A_m} \quad (5)$$

where ρ_{pd} is the density of palladium metal (g/cm^3), A_m is the membrane surface area (cm^2). Since it was assumed that the palladium film is dense even in intermediate steps, the evaluated thickness corresponds to the theoretical value and the actual value will be apparently higher.

The average plating rate $\bar{r}_{Pd}$ (mole/m^2 s) is evaluated by using the expression:

$$\bar{r}_{Pd} = \frac{w_2 - w_1}{M_{Pd} \times A_m \times t} \quad (6)$$

where t is the corresponding total plating time.

Pore densification during the plating process is defined as the fractional volume of the pores covered by the deposited metal and is expressed as PPD. It is calculated by using the following expression.

$$\text{PPD}(\%) = \frac{\bar{J}_o - \bar{J}_i}{\bar{J}_o} \times 100 \quad (7)$$

where $\bar{J}_o$ is the average room temperature nitrogen permeation flux of the porous stainless steel substrate (mol/m^2 s) and $\bar{J}_i$ is the average room temperature permeation flux of the palladium composite membrane fabricated after ith plating step. The average room temperature nitrogen permeation flux has been calculated using the expression:

$$\bar{J} = \frac{\int_{P_1}^{P_2} J\, dP}{P_2 - P_1} \quad (8)$$

where P_1 and P_2 corresponds to the minimal and maximum retentate pressures during an experimental test to measure the nitrogen gas permeance.

The theoretical selectivity ($\bar{\alpha}_{av}$) of the membrane at higher temperature (573 K) has been estimated using the following procedure, which has been elaborated in our earlier work [18]. Firstly, using the room temperature nitrogen flux vs. average pressure data, a graph has been plotted for these parameters whose slope and intercept, respectively, correspond to the Knudsen ($KPern_{rt}^{pcm}$) and viscous ($ViPern_{rt}^{pcm}$) room temperature permeance of the palladium composite membrane. Using these values, the high temperature Knudsen ($KPern_{ht}^{pcm}$) and viscous ($ViPern_{ht}^{pcm}$) permeances were evaluated as ratio and inverse ratios of gas RMS velocities and viscosities at high and low temperatures, respectively. Eventually, the high temperature nitrogen flux was determined as a function of retentate (PR) and permeates pressure (PP) using the expression:

$$JN_{ht}^{pcm} = \left[KPern_{ht}^{pcm} + ViPern_{ht}^{pcm}\frac{(PR+PP)}{2}\right] \times \frac{[PR-PP]}{PP} \times \frac{1000}{22.4} \quad (9)$$

Assuming literature data for hydrogen permeability through dense Pd films, the theoretical hydrogen flux was estimated using the expression:

$$JH_{ht}^{pcm} = \frac{Permh^{dm}}{\delta^{pcm}} \times \left(PR^n - PP^n\right) = Perh^{pcm} \times \left(PR^n - PP^n\right) \quad (10)$$

where $Permh^{dm}$ is assumed to be the dense palladium membrane permeability from literature data and δ^{pcm} corresponds to the thickness of the palladium film determined with the weight gain method (Eq. (5)). Finally, the theoretical average selectivity of the palladium composite membrane was estimated using the expression:

$$\bar{\alpha}_{av} = \frac{AJH_{ht}{}^{pcm}}{AJN_{ht}^{pcm}} \quad (11)$$

where $AJH_{ht}{}^{pcm}$ and $AJN_{ht}{}^{pcm}$ corresponds to the average hydrogen and nitrogen fluxes of porous composite membrane at high temperature, which was estimated using the expressions:

$$AJH_{ht}^{pcm} = \frac{\int_{PR_{min}}^{PR_{max}} JH_{ht}^{pcm}\,dP}{(PR_{max}-PR_{min})} \quad (12)$$

$$AJN_{ht}^{pcm} = \frac{\int_{PR_{min}}^{PR_{max}} JN_{ht}^{pcm}\,dP}{(PR_{max}-PR_{min})} \quad (13)$$

Results and discussion

In this section, we present the comparative assessment of the combinatorial plating characteristics of SSOEP-DW Pd ELP baths for the fabrication of Pd/Ni/PSS composite membranes on 0.5 and 0.1 μm supports and Pd/PSS membranes on 0.1 μm supports. The reported combinatorial plating characteristics refer to selective conversion, plating efficiency, plating rate, percent pore densification and thickness. Further, surface characterization results including XRD analysis and FESEM analysis have also been presented for both Pd/Ni/PSS and Pd/PSS membranes.

Selective conversions and plating efficiency

Figs. 1 and 2, respectively, illustrate the effect of cumulative plating time on selective conversion and plating efficiencies of palladium electroless plating baths for the fabrication of Pd/PSS membranes (on 0.1 μm average pore size supports) and Pd/Ni/PSS membranes (on 0.5 and 0.1 μm average pore size supports). It can be observed that the selective conversion and plating efficiencies varied from 35.40 to 31.48% and 90.95 to 95.94% for Pd/PSS membranes. However, for Pd/Ni/PSS membranes, the selective conversions significantly reduced to 20.38–17.98% and 33.73–30.92%

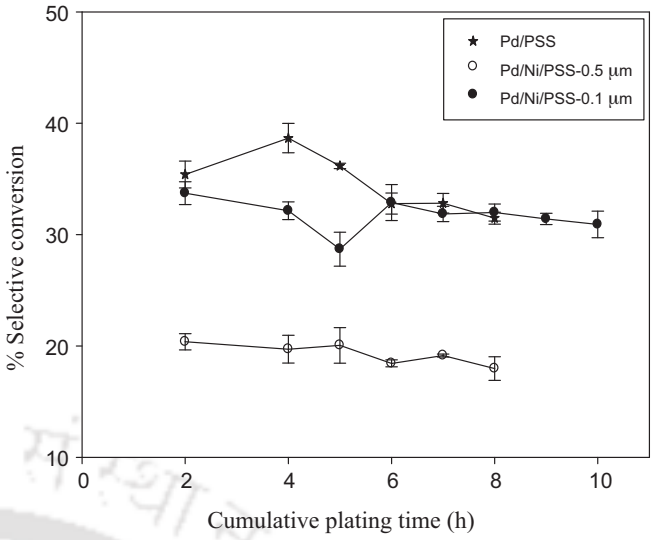

Fig. 1. Effect of plating time on selective conversion.

for 0.5 and 0.1 μm nominal pore size PSS supports, respectively. For these cases, corresponding plating efficiencies varied from 30.50–48.77% and 76.54–87.01%, respectively. Thus, it is apparent that higher nickel loading is not promising to enable good plating characteristics. Thus, compared to the stainless steel substrate, nickel did not allow significant metal deposition to occur on the membrane surface and this could be due to the poor conductivity and Pd surface activation. Further, lower plating efficiencies for the Ni/PSS supports are indicative towards greater metal nucleation in the solution, which is an undesired feature. Also, it can be observed from both Figs. 1 and 2 that while selective conversions reduced with increasing total plating time, the plating efficiency values increased with total plating time. This indicates that for both cases of Pd/PSS and Pd/Ni/PSS membranes, surface conductivities increased with increasing plating time due to the deposition of Pd on the membrane surface. It can be also inferred that the plating efficiencies are in the order of Pd/PSS (0.1 μm) > Pd/Ni/PSS (0.1 μm) > Pd/Ni/PSS (0.5 μm).

Plating rates

The variation of Pd plating rates with plating time for Pd/PSS and Pd/Ni/PSS membranes has been summarized in Table 3.

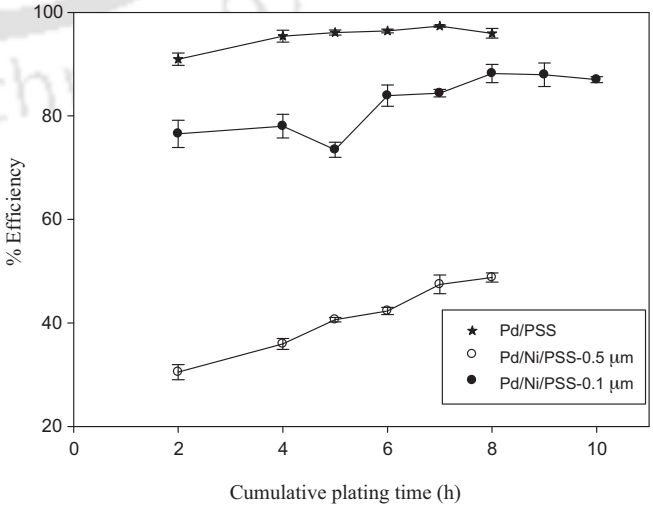

Fig. 2. Effect of plating time on plating efficiency.

Table 3
Comparison of time dependent average plating rates for Pd/Ni/PSS and Pd/PSS membranes.

Type of membrane	Average plating rate $\bar{r}_{Pd}$ (mol/m^2 s) $\times 10^5$ for various total plating time (h)								
	Ni	2	4	5	6	7	8	9	10
Pd/PSS	–	4.92	5.38	5.03	4.56	4.57	4.38	–	–
Pd/Ni/PSS-0.5 μm	6.74	3.95	3.82	3.89	3.57	3.71	3.45	–	–
Pd/Ni/PSS-0.1 μm	3.58	3.35	3.19	2.85	3.27	3.17	3.18	3.12	3.07

It can be observed that the plating rates varied from 4.92 to 4.38×10^{-5} mol/m^2 s for Pd/PSS membrane, 3.95–3.45 $\times 10^{-5}$ and 3.35–3.07 $\times 10^{-5}$mol/m^2 s for Pd/Ni/PSS membranes on 0.5 and 0.1 μm pore sizes, respectively. The plating rates on nickel modified stainless steel substrate are about 20–30% lower than those obtained for the PSS substrate. This is due to the poor conductivity and surface activation of Pd for the Pd/Ni/PSS membranes.

Percent pore densification

Percent pore densification is by far the most important parameter for the fabrication of dense Pd composite membranes. Fig. 3 shows the comparative performance of Pd/Ni/PSS and Pd/PSS membranes in terms of (100-PPD) variation with total plating time. The PPD for Ni/PSS is about 84.5% and 25% after depositing 8 μm and 1.7 μm thick Ni films on 0.5, 0.1 μm supports, respectively. Eventually for the Pd/Ni/PSS membrane cases, the PPD profiles have been considered for Ni/PSS membrane but not PSS membrane. After 2 h of Pd plating, the PPD for Ni/PSS membrane of 0.5 μm is only 79.01% which is significantly lower than that obtained for the Pd/PSS membrane (96.94%). Also, it can be observed that the PPD profiles varied from 79.01 to 99.9% for variation in total plating from 2 to 8 h for Pd/Ni/PSS (0.5 μm nominal pore size support) membrane case which was significantly lower than the corresponding PPD profiles (96.94–100%) obtained for Pd/PSS membrane. On the other hand, after 2 h sequential plating, the Pd/Ni/PSS membrane (0.1 μm nominal pore size support) provided 92.98% PPD and it could not be subjected to 100% pore densification even after 10 h of sequential total plating time. Further, for all cases, it can be observed that for prolonged periods of total plating time, lapse mode of PPD was existent which indicates that uneven surface charge distributions contributed enormously towards poorer deposition. Also, the metal delamination for the Pd/Ni/PSS membranes was significantly higher than that observed for the Pd/PSS membranes. In addition, the metal delamination during plating has been found to be significant for the nickel film deposited on 0.5 μm nominal pore size support. Thus, the metal delamination has been inferred to exist as per the following order: Ni/PSS (0.5 μm) > Ni/PSS (0.1 μm) > PSS (0.1 μm). Thus, it is apparent that the adhesion strength between Pd and Ni interface was not as strong as it exists for Pd/PSS interface. These important evaluations signify upon the poor depositional characteristics for Pd/Ni/PSS membranes in comparison with Pd/PSS membranes.

Thickness

The effect of variation in plating time on the deposited Pd film thickness for Pd/Ni/PSS and Pd/PSS membranes are presented in Fig. 4. It can be observed that for Pd/Ni/PSS membranes, the Pd film thickness, respectively, varied from 2.52 to 8.88 μm and 2.14 to 9.80 μm for 0.5 and 0.1 μm nominal pore size supports, respectively. On the other hand, for Pd/PSS membranes, the time dependent Pd film thickness varied from 3.14 to 11.16 μm. Thus, it is apparent that for the Pd/Ni/PSS membrane, lower Pd film thickness was obtained which refers to poor depositional characteristics in comparison with the Pd/PSS membrane. While lower Pd film thickness could ensure higher fluxes, the poor adhesion strength of the Pd to the Ni film is an important issue for future research investigations to deliver upon, as the ultimate target of the Pd composite membranes is to achieve Pd composite membranes with good combinations of mechanical strength, flux and separation factors.

Membrane characterization

Fig. 5a and b, respectively, presents the FESEM micrographs of Pd/Ni/PSS and Pd/PSS membranes on 0.5 and 0.1 μm PSS supports after 8 h sequential plating. It can be observed that for both cases finer Pd grains exist on the membrane surface and no pinholes are visible for the chosen magnification which corresponds to the maximum magnification affordable with the instrument. Thus, the basic limitation of the FESEM imaging technique to elaborate upon the PPD characteristics of the membrane are evident and gas permeation experiments are very important for the analysis of the efficacy of Pd deposition in both cases.

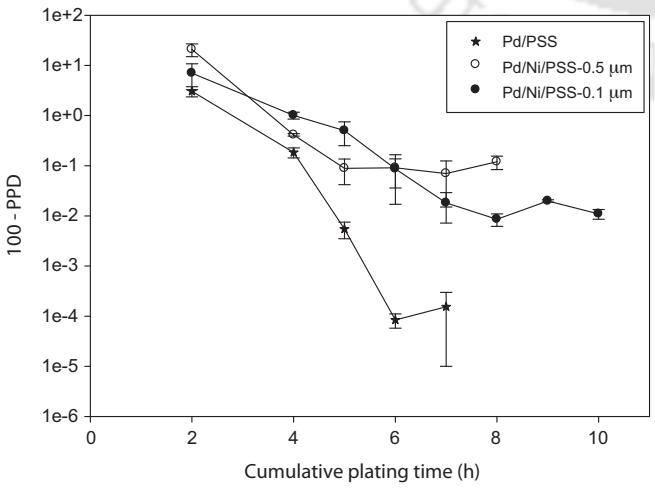

Fig. 3. Variation of PPD with plating time for all cases.

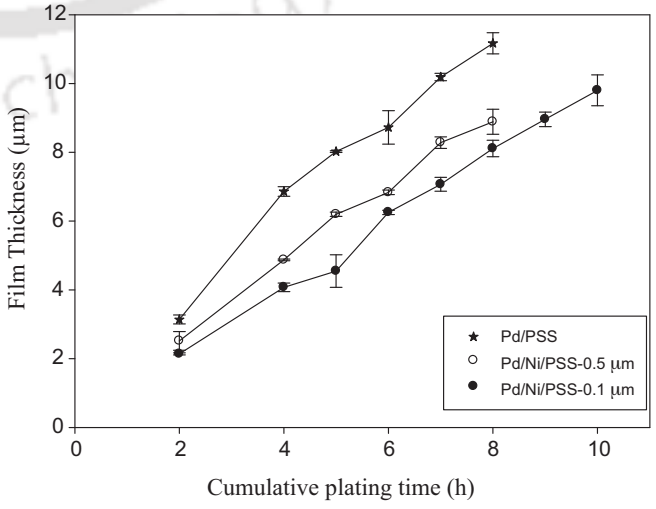

Fig. 4. Dependency of Pd film thickness on plating time.

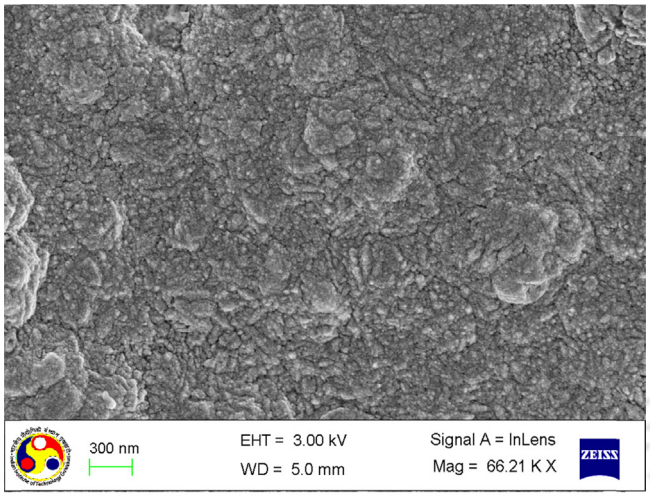

Fig. 5. (a) FESEM micrograph of Pd/Ni/PSS membrane. (b) FESEM micrograph of the Pd/PSS membrane.

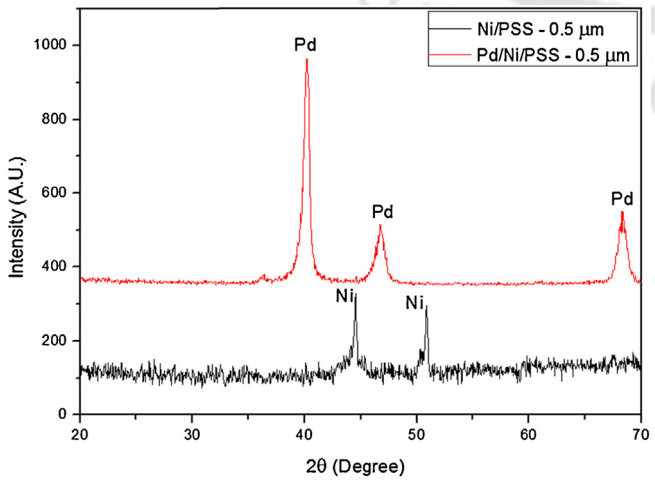

Fig. 6. XRD patterns of Ni/PSS and Pd/Ni/PSS membranes fabricated with 0.5 μm PSS supports.

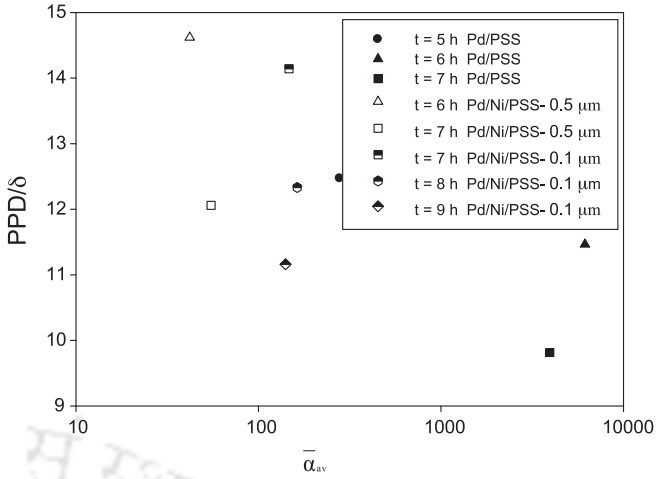

Fig. 7. Tradeoffs of PPD/δ vs. $\bar{\alpha}_{av}$.

Fig. 6 presents the XRD (Make: Shimadzu Corporation, Model: D8 Advance) pattern of Ni/PSS and Pd/Ni/PSS composite membranes on 0.5 μm PSS supports. Bucker X-ray D8 advance diffractometer with a Cu-$K\alpha$ radiation at 45 kV and 40 mA was used to record the XRD patterns within the range of 20–70° at an increment of 0.05°. The phase analysis of the diffraction profiles was carried out using ICDD-JCPDS database. It can be observed that the XRD spectra indicates upon the existence of Ni peaks at a diffraction angle (2θ) of 44.6° and 52° due to the diffraction of (1 1 1) and (2 0 0) planes [Pdf No 00-001-1260]. Further Pd peaks were observed at diffraction angles (2θ) of 40.2°, 46.76° and 68.28° due to diffraction of (1 1 1), (2 0 0) and (2 0 2) planes, respectively. Clear existence of nickel and Pd phases for Ni/PSS and Pd/Ni/PSS membranes confirms uniform depositions. Absence of Ni and stainless steel peaks in the XRD spectra for the Pd/Ni/PSS membrane confirms the achievement of purely dense Pd composite membranes.

Tradeoffs

Fig. 7 shows the trend of PPD/δ vs. $\bar{\alpha}_{av}$ for Pd/Ni/PSS and Pd/PSS membranes. For Pd/Ni/PSS membrane (0.5 μm nominal pore size support), the selectivities obtained after 6 and 7 h sequential plating have been 41.99 and 54.92 only. For the Pd/Ni/PSS membrane (0.1 μm nominal pore size support), the theoretical selectivities in the range of 140–170 after 7–9 h of total plating time. On the other hand, for Pd/PSS membrane, the theoretical selectivities obtained after 5, 6 and 7 h of sequential plating are 279.23, 6154 and 3953, respectively. For the same membrane, maximum selectivity of infinity was obtained after completion of 8 h of Pd ELP. Thus it is apparent that lower theoretical selectivities existed for Pd/Ni/PSS membranes in comparison with the Pd/PSS membrane which is due to lower PPD profiles for the former cases. Also, it can be observed that PPD/δ is about 12–14 for Pd/Ni/PSS but is only 10–12.5 for the Pd/PSS membrane. However, since higher PPDs were obtained for the Pd/PSS membranes, it is inferred that the nickel interdiffusion barrier deposited using electroless plating is not effective to simultaneously enhance PPD and reduce metal film thickness.

Conclusions

The experimental investigations confirmed that the fabrication of Pd/Ni/PSS membranes with 0.1 μm nominal pore size support have better combinatorial plating characteristics (selective conversion, plating efficiency, plating rate, PPD and theoretical selectivity) in comparison with the Pd/Ni/PSS membranes

fabricated with 0.5 μm nominal pore size. For the Pd/Ni/PSS membrane (0.1 μm), the combinatorial plating characteristics have been evaluated as 33.73–30.92% selective conversions, 76.54–87.01% plating efficiencies, 2.13–9.8 μm thick Pd films, plating rates of $3.35–3.07 \times 10^{-5}$ mol/m^2 s and PPD's of 92.98–99.989% for 2–10 h sequential plating steps. On the other hand, the Pd/PSS membrane (0.1 mm) fabrication possessed the best combinatorial plating characteristics of 35.40–31.48% selective conversion, 90.95–95.94% plating efficiency, $4.92–4.38 \times 10^{-5}$ mol/m^2 s average plating rate, 3.14–11.16 μm and 96.94–100% PPD for a total plating time of 2–8 h. This indicates that despite using the best Pd ELP deposition process, the nickel interdiffusion barrier was not effective to improve the plating characteristics. Thus, it is apparent that the combinatorial plating characteristics of support surfaces characterized with poor conductivities and non-conducting surfaces is a major challenge for the cost effective fabrication of dense Pd composite membranes using electroless plating technique. In summary, while interdiffusion barriers such as Ni could be promising to enhance shelf life and hydrogen permeability of Pd composite membranes, they pose serious challenges during their fabrication and offer lower hydrogen selectivities. These complex tradeoffs are very important from the perspective of large scale fabrication and process scale up issues associated to Pd composite membranes.

Acknowledgments

This work is partially supported by a grant from the DST (Department of Science and Technology) (grant no. SR/S3/CE/070/2010) New Delhi. Any opinions, finding and conclusions expressed in this paper are those of the authors and do not necessarily reflect the views of DST, New Delhi.

References

[1] K.S. Rothenberger, A.V. Cugini, B.H. Howard, R.P. Killmeyer, M.V. Ciocco, B.D. Morreale, R.M. Enick, F. Bustamante, I.P. Mardilovich, Y. Ma, High pressure hydrogen permeance of porous stainless steel coated with a thin palladium film via electroless plating, J. Membr. Sci. 244 (2004) 55–68.
[2] Y. Huang, R. Dittmeyer, Preparation and characterization of composite palladium membranes on sinter-metal supports with a ceramic barrier against intermetallic diffusion, J. Membr. Sci. 282 (2006) 296–310.
[3] X. Zhang, G. Xiong, W. Yang, A modified electroless plating technique for thin dense palladium composite membranes with enhanced stability, J. Membr. Sci. 314 (2008) 226–237.
[4] S.C. Chen, G.C. Tu, C.C.Y. Hung, C.A. Huang, M.H. Rei, Preparation of palladium membranes by electroless plating on AISI 316L porous stainless steel supports and its use for methanol steam reformer, J. Membr. Sci. 314 (2008) 5–14.
[5] S.K. Ryi, J.S. Park, S.H. Choi, S.H. Cho, S.H. Kim, Fabrication and characterization of metal porous membrane made of Ni powder for hydrogen separation, Sep. Purif. Technol. 47 (2006) 148–155.
[6] I.P. Mardilovich, E. Engwall, Y.H. Ma, Dependence of hydrogen flux on the pore size and plating surface topology of asymmetric Pd-porous stainless steel membranes, Desalination 144 (2002) 85–89.
[7] J. Tong, Y. Matsumura, H. Suda, K. Haraya, Thin and dense Pd/CeO_2/MPSS composite membrane for hydrogen separation and steam reforming of methane, Sep. Purif. Technol. 46 (2005) 1–10.
[8] D. Yepes, L.M. Cornaglia, S. Irusta, E.A. Lombardo, Different oxides used as diffusion barriers in composite hydrogen permeable membranes, J. Membr. Sci. 274 (2006) 92–101.
[9] V.M. Gryaznov, O.S. Serebryannikova, Y.M. Serov, M.M. Ermilova, A.N. Karavanov, A.P. Mischenko, N.V. Orekhova, Preparation and catalysis over palladium composite membranes, Appl. Catal., A: Gen. 96 (1993) 15–23.
[10] D. Wang, J. Tong, H. Xu, Y. Matsumura, Preparation of palladium membrane over porous stainless steel tube modified with zirconium oxide, Catal. Today 93–95 (2004) 689–693.
[11] S. Samingprai, S. Tantayanon, Y.H. Ma, Chromium oxide intermetallic diffusion barrier for palladium membrane supported on porous stainless steel, J. Membr. Sci. 347 (2010) 8–16.
[12] W.H. Lin, Y.C. Liu, H.F. Chang, Autothermal reforming of ethanol in a Pd–Ag/Ni composite membrane reactor, Int. J. Hydrogen Energy 35 (2010) 12961–12969.
[13] V.K. Bulasara, O. Chandrasekhar, R. Uppaluri, Effect of surface roughness and mass transfer enhancement on the performance characteristics of nickel-hypophosphite electroless plating baths for metal-ceramic composite membrane fabrication, Chem. Eng. Res. Des. 89 (2011) 2485–2494.
[14] M.E. Ayturk, Y.H. Ma, Electroless Pd and Ag deposition kinetics of the composite Pd and Pd/Ag membranes synthesized from agitated plating baths, J. Membr. Sci. 330 (2009) 233–245.
[15] M.S. Islam, M.M. Rahman, S. Ilias, Characterization of Pd–Cu membranes fabricated by surfactant induced electroless plating (SIEP) for hydrogen separation, Int. J. Hydrogen Energy 37 (2012) 3477–3490.
[16] S.E. Nam, S.H. Lee, K.H. Lee, Preparation of a palladium alloy composite membrane supported in a porous stainless steel by vacuum electrodeposition, J. Membr. Sci. 153 (1999) 163–173.
[17] M. Pujari, A. Agarwal, R. Uppaluri, A. Verma, Composition and method for dense palladium composite membrane fabrication, in: Indian Patent (filed), 2013, Application No. 1150/KOL/2013.
[18] M. Pujari, A. Agarwal, R. Uppaluri, A. Verma, Effect of surfactant concentration and loading ratio on the electroless plating characteristics of dense Pd composite membranes, Ind. Eng. Chem. Res. (2014), http://dx.doi.org/10.1021/ie4035412.

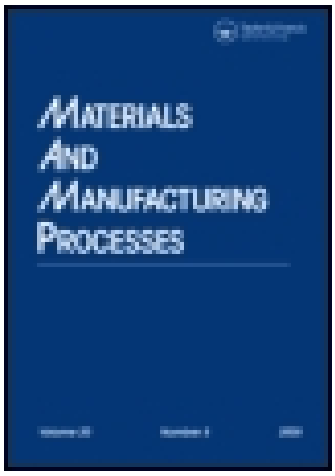

Materials and Manufacturing Processes
Publication details, including instructions for authors and subscription information:
http://www.tandfonline.com/loi/lmmp20

Efficacy of Novel Electroless Plating Process for Dense Pd/Cr_2O_3/PSS Membrane Fabrication

Murali Pujari [a], Amrita Agarwal [a], Ramgopal Uppaluri [a] & Anil Verma [a]
[a] Department of Chemical Engineering, Indian Institute of Technology Guwahati, Guwahati, Assam, 781039, India
Accepted author version posted online: 10 Feb 2014.

To cite this article: Murali Pujari, Amrita Agarwal, Ramgopal Uppaluri & Anil Verma (2014): Efficacy of Novel Electroless Plating Process for Dense Pd/Cr_2O_3/PSS Membrane Fabrication, Materials and Manufacturing Processes, DOI: 10.1080/10426914.2014.880469

To link to this article: http://dx.doi.org/10.1080/10426914.2014.880469

Efficacy of novel electroless plating process for dense Pd/Cr_2O_3/PSS membrane fabrication

Murali Pujari[1], Amrita Agarwal[1], Ramgopal Uppaluri[1,], Anil Verma[1]

[1]Department of Chemical Engineering, Indian Institute of Technology Guwahati, Guwahati, Assam 781039, India

Corresponding author: , Tel: +91 361 2582260, Fax: +91 361 2582291, Email: ramgopalu@iitg.ernet.in, ru.aissq@gmail.com

Received November 1, 2013; Accepted December 28, 2013

Abstract

This work addresses the role of chromia diffusion barrier on the combinatorial plating characteristics of Pd plating baths during fabrication of dense Pd/Cr_2O_3/porous stainless steel (PSS) composite membranes and is compared with those obtained during fabrication of Pd/PSS membranes. Cr_2O_3 was deposited by electroplating technique followed with oxidation at 700 ^oC and Pd films were deposited using a novel Pd electroless plating process that provides optimal performance. Apart from providing similar process characteristics, the Pd/Cr_2O_3/PSS membrane provided 15.2% lower Pd film thickness in comparison with Pd/PSS membrane for similar pore densification values.

KEYWORDS: ultrasonic,deposition, oxidation, stainless, characterization, membrane, pores, plating

1. INTRODUCTION

In addition to be being cost effective, palladium composite membranes offer higher combinations of hydrogen permeability, selectivity [1].However, frequent temperature cycling causes intermetallic diffusion between the Pd film and the support and thereby reduces the shelf life of the membrane [2]. To circumvent this problem, various types of interdiffusion barriers were investigated. Further, interdiffusion barriers enhance narrow pore size distributions of the macroporous support and thereby reduce the critical Pd film thickness required to achieve a dense composite membrane.

Till date, various interdiffusion barriers investigatedinclude yttria stabilized zirconia (YSZ) [3], TiO_2 [3], CrO_2 [4], CeO_2 [5], α-Fe_2O_3 [6], □-Al_2O_3 [6], Tungsten [7] and ZrO_2 [8]. Few of these investigations indicated that despite achieving 100% dense Pd composite membranes, the interdiffusion barrier could not reduce the achieved critical dense Pd film thickness [3,4]. On the other hand, while interdiffusion barriers reduced the critical dense Pd film thickness, they did not enhance hydrogen flux due to additional transport resistance contributed by the barrier itself [5-8]. Amongst several diffusion barriers, Cr_2O_3 can be regarded as the most competent due to higher chemical stability under high pressure hydrogen environment. Also, Cr_2O_3 offer lower additional cost of fabrication, which is not the case for other interdiffusion barriers such as ZrO_2, CeO_2 and YSZ.

Till date, only Samingprai et al. [4] reported the membrane charecteristics of dense Pd (32 μm) composite membranes using an interdiffusion barrier of Cr_2O_3 (2 μm) that was prepared using electroplating and subsequent oxidation of chromium film deposited on a

porous stainless steel (PSS) substrate. The authors inferred that the chromia diffusion barrier did not reduce the critical (minimal) thickness of Pd film to achieve a dense Pd composite membrane.

All investigations reported till date with respect to interdiffusion barriers [3-8] ignored the combinatorial plating characteristics for dense Pd composite membranes. Also, while only one literature is available with respect to dense Pd-Cr_2O_3-PSS membranes, a comparative assessment of Pd-Cr_2O_3-PSS membranes with Pd-PSS membranes had not been carried out. Such studies could provide significant insights with respect to the quality of deposition and the associated challenges in fabrication engineering of dense Pd composite membranes.

The objective of this work is to examine the combinatorial plating characteristics of Pd electroless plating baths for the fabrication of dense Pd-Cr_2O_3-PSS composite membranes in comparison with dense Pd-PSS membranes. Thecombinatorial performance characteristics evaluated for the electroless plating baths are namely plating bath conversion (χ), selective conversion, plating efficiency (η), Pd film thickness (δ), average plating rate $\left(\bar{r}_{Pd}\right)$, average permeation flux $\left(\bar{J}\right)$, percent pore densification (PPD). The process conditions refer to the identified novel Pd electroless plating process that provided maximum combinations of desired plating characteristics [9]. The novelty in the plating process especially refers to the optimal combination of surfactant, sonication, Pd solution and reducing agent concentrations and their contacting patterns. The process has been identified after enormous research was conducted on the combinatorial plating

characteristics of metal electroless plating baths on metal composite membrane fabrication [10].

The identified process-product combination is promising for the manufacture of highly efficient Pd-Cr_2O_3-PSS membranes. The identified optimal process parameters and process variants for Pd electroless plating have been proven to be highly relevant for the deposition of noble metals on non-conducting surfaces such as oxides. The outlined combinatorial plating characteristics are relevant from the context of process design, scale up and research commercialization. The carried out research is totally new in the context of process development and optimization in the context of large scale fabrication of dense Pd membranes.

2. EXPERIMENTAL

Prior to Pd ELP, porous stainless steel circular discs (dia of 36 mm, thickness of 1 mm, nominal pore size of 100 nm purchased from Mott Corporation, USA) were sonicated (Model: S30H, ELMA) with acetone to remove the contaminants present on the surface. Subsequently, the discs were dried at 393 K in oven (Model: ROV/DG, REICO) for 2 h.

Eventually, seeding and activation steps have been followed to achieve an activated PSS support [4]. Two different types of membranes were fabricated, one corresponding to Pd-PSS membrane and other referring to Pd-Cr_2O_3-PSS membranes. The chromia interdiffusion barrier was fabricated using electroplating of H_2CrO_4 solution (250 g/L) at a current density of 133 mA/cm^2 for 5 min, followed with oxidation at 700 ^oC. The average plating rate (expressed in terms of Cr_2O_3) and thickness (Cr_2O_3layer) have been evaluated as 8.9×10^{-4} mol/m^2.s and 7.8 µm, respectively. For both Pd

composite membranes, the novel Pd ELP process had been followed. This refers to the surfactant and sonication induced Pd electroless plating baths supplemented with drop wise addition of reducing agent (SSOEP-DW) at a loading ratio of 203 cm^2/L [9]. Table 1 summarizes the composition of Pd electroless plating baths. The evaluation of combinatorial plating parameters was carried out using the expressions presented for these parameters in our earlier work [11,12].

3. RESULTS AND DISCUSSION

In this section, we present the time dependent combinatorial plating characteristics of SSOEP-DW Pd ELP baths during the fabrication of Pd/Cr_2O_3/PSS and Pd/PSS composite membranes. Further, surface characterization results including XRD analysis and FESEM analysis have also been presented for both Pd-Cr_2O_3-PSS and Pd-PSS membranes.

3.1 Process Characteristics

Fig. 1a and 1b illustrate the time dependent variation of selective conversion and plating efficiencies for Pd electroless plating baths during the fabrication of Pd/Cr_2O_3/PSS and Pd/PSS membranes. While the selective conversion varied from 35.40-32.82% and 4.90-32.51% for Pd/PSS and Pd/Cr_2O_3/PSS membranes respectively, corresponding plating efficiencies varied from 90.95-97.35% and 14.78-83.31%, respectively. Thus two important inferences can be drawn. Firstly, during the early stages of Pd ELP, the introduction of Cr_2O_3 provided lower initial conversions and plating efficiencies due to poor Pd surface activation and greater metal nucleation in the solution. Secondly, prolonged plating enabled achieving similar selective conversions and plating efficiencies for theCr_2O_3 case in comparison with the PSS case.

The time dependent variation of Pd plating rates for Pd/PSS and Pd/Cr_2O_3/PSS membranes has been summarized in Table 2. It can be observed that the plating rates varied from $4.92-4.57\times10^{-5}$ mol/m^2.s and $0.63-3.87\times10^{-5}$ mol/m^2.s for Pd/PSS and Pd/Cr_2O_3/PSS membranes, respectively. Thus, the introduction of Cr_2O_3 interdiffusion barrier reduced the average plating rates to 12.8% in the early stages and 85% in the final stages of Pd ELP in comparison with that of the PSS support. Once again, the significant role of poor Pd activation in the early stages of Pd plating has been evident.

3.2Membrane Characteristics

Percent pore densification is by far the most important parameter for the fabrication of dense Pd composite membranes. For the Cr_2O_3/PSS case, it can be evaluated that 7.8 □m thick chromia film densified the PSS support by 29.76%. Fig.2a shows the comparative performance of Pd/Cr_2O_3/PSS and Pd/PSS membranes in terms of (100-PPD) variation with total plating time. It has been evaluated that the time dependent PPD varied from 65.08-99.998% and 96.94-99.9998% for Pd/Cr_2O_3/PSS and Pd/PSS membranes respectively for a variation in total plating time from 2-7 h. Thus, it is apparent that the PPD profiles at prolonged time periods were insignificantly better for the Pd/PSS case in comparison with the Pd/Cr_2O_3/PSS case. This is an important observation to infer that similar PPD profiles were achieved for Pd/Cr_2O_3/PSS with lower Pd film thickness. Also, for both cases, lapse mode of PPD existed for prolonged periods of total plating time, which is due to the uneven surface charge distributions contributed by the surfactant [13].

The mechanism associated to the optimal plating process involves the optimal utilization and contacting of Pd ionic species, reducing agent distributions in the plating solution and on the surface, metal nucleation in the solution as well as on the surface. While sonication assisted electroless plating has been not able to enhance pore densification, the combination of surfactant, sonication and reducing agent contacting pattern has been able to provide necessary conditions on the plated surface to simultaneously maximize metal transport to the surface and minimize metal nucleation in the solution.

The variation in time dependent metal film thickness with cumulative plating time is presented in Fig. 2b for both Pd/Cr_2O_3/PSS and Pd/PSS membranes. It can be observed that for Pd/Cr_2O_3/PSS and Pd/PSS membranes, the time dependent Pd film thickness respectively varied from 0.4-8.64 μm and 3.14-10.18 μm for a variation in total plating time from 2 to 7 h. Thus, it is apparent that for the Pd/Cr_2O_3/PSS membrane, lower Pd film thickness was obtained which indicates better performance in terms of hydrogen flux.

The introduction of chromia interdiffusion barrier normalizes the wider pore size distributions and favours towards the reduction in the critical thickness required to achieve a dense Pd composite membrane. This is also in agreement with Mardilovich et al. [14] who suggested that the maximum pore size of the membrane support strongly influences the critical dense Pd film thickness required to achieve very high pore densification conditions.

3.3Morphological And Surface Characterization

Fig. 3a and 3b shows the FESEM micrographs of Pd/Cr_2O_3/PSS and Pd/PSS membranes obtained after a total plating time of 7 h. It can be observed that for both cases finer Pd grains exist on the membrane surface and no pinholes/surface defects are visible for the composite membranes.

Fig. 3c presents the XRD pattern of Pd/Cr_2O_3/PSS composite membrane. Similar XRD profile was obtained for the Pd/PSS membrane. It can be observed that the XRD spectra indicates upon the existence of Pd reflection peaks at diffraction angles (2θ) of 40.2°, 46.76° and 68.28° due to diffraction of (1 1 1), (2 0 0) and (2 0 2) plane respectively and confirms that the membrane surface consists of Pd metal only. The inability to detect Ni, Cr and stainless steel peaks in the XRD spectra for the Pd/Cr_2O_3/PSS and stainless steel peaks for the Pd-PSS membrane is indicative towards the achievement of dense Pd composite membranes for both cases.

4. CONCLUSIONS

Thecombinatorial plating characteristics of Pd/Cr_2O_3/PSS membranes for selective conversion, plating efficiency, plating rate, thickness and PPD varied from 4.90-32.51%, 14.78-83.31%, $0.63-3.87\times10^{-5}$ mol/m^2.s, 0.4-8.64 μm and 65.08-99.998%, respectively for a variation of total plating time of 2-7 h. On the other hand, these characteristics were slightly better for the Pd/PSS membranes (selective conversion of 35.40-32.82%, plating efficiency of 90.95-97.35%, plating rate of $4.92-4.57\times10^{-5}$ mol/m^2.s, thickness of 3.14-10.18μm and PPD of 96.94-99.9998%).The evaluated parameters indicate that the high temperature hydrogen flux can be enhanced by 17.8% with minimal variation in the

separation characteristics, thus indicating the relevance of novel identified Pd ELP process for the large scale fabrication of Pd composite membranes.

In the context of materials and manufacturing process, the suggested methodology of process-product optimality is highly relevant in the context of developing cost effective manufacturing processes for depositing noble metals such as palladium on porous non-conducting substrates. The demonstrated results are anticipated to be of paramount relevance for research commercialization of said optimal combinations of support morphology, support modification, Pd, hydrazine and surfactant solution concentrations.

ACKNOWLEDGEMENTS

This work is partially supported by a grant from the DST (Department of Science and Technology) New Delhi. Any opinions, finding and conclusions expressed in this paper are those of the authors and do not necessarily reflect the views of DST, New Delhi.

REFERENCES

[1] Zhang, X.; Xiong, G.; Yang, W. A modified electroless plating technique for thin dense palladium composite membranes with enhanced stability. J*ournal of Membrane Science***2008**, 314 (1-2), 226-237.

[2] Chotirach, M.; Tantayanon, S.; Tungasmita, S.; Kriausakul, K. Zr-based intermetallic diffusion barriers for stainless steel supported palladium membranes. *Journal of Membrane Science*. **2012**, 405-406, 92-103.

[3] Huang, Y.; Dittmeyer, R. Preparation and characterization of composite palladium membranes on sinter-metal supports with a ceramic barrier against intermetallic diffusion. J*ournal of Membrane Science***2006**,282 (1-2), 296-310.

[4] Samingprai, S.; Tantayanon, S.; Ma, Y.H. Chromium oxide intermetallic diffusion barrier for palladium membrane supported on porous stainless steel. J*ournal of Membrane Science***2010**,347 (1-2), 8-16.

[5] Tong, J.; Matsumura, Y.; Suda, H.; Haraya, K. Thin and dense Pd/CeO_2/MPSS composite membrane for hydrogen separation and steam reforming of methane. S*eparation and Purification Technology* **2005**,46 (1-2), 1-10.

[6] Yepes, D.; Cornaglia, L.M.; Irusta, S.; Lombardo, E.A. Different oxides used as diffusion barriers in composite hydrogen permeable membranes. J*ournal of Membrane Science***2006**, 274(1-2), 92-101.

[7] Gryaznov, V.M.; Serebryannikova, O.S.; Serov, Y.M.; Ermilova, M.M.; Karavanov, A.N.; Mischenko, A.P.; Orekhova, N.V. Preparation and catalysis over palladium composite membranes. A*pplied catalysis a: General***1993**, 96 (1), 15-23.

[8] Wang, D.; Tong, J.; Xu, H.; Matsumura, Y. Preparation of palladium membrane over porous stainless steel tube modified with zirconium oxide. C*atalysis Today***2004**, 93-95, 689-693.

[9] M. Pujari, A. Agarwal, R. Uppaluri, A. Verma. Composition and method for dense palladium composite membrane fabrication. I*ndian patent filed* (07-10-2013) Application No. 1150/KOL/**2013**.

[10] Bulasara, V.K.; Babu, Ch. S.N.M, Uppaluri, R. Effect of surfactants on performance of electroless plating baths for nickel-ceramic composite membrane fabrication, *Surface engineering***2012**, 28 (1), 44-48.

[11] Bulasara, V.K.; Uppaluri, R.; Purkait, M.K,Manufacture of nickel-ceramic composite membranes in agitated electroless plating baths. *Materials and Manufacturing Process***2011** 26 (6)862-867.

[12] Agarwal, A.; Pujari, M.; Uppaluri, R.; Verma, A. Preparation, optimization and characterization of low cost ceramics for the fabrication of dense nickel composite membranes. C*eramics International***2013**, 39 (7), 7709-7716.

[13] Chen, B. H.; Hong, L.; Ma, Y.; Ko, T. M. Effect of surfactants in an electroless nickel-plating bath on the properties of Ni-P alloy deposits. *Industrial & Engineering Chemistry Research***2002**, 41 (11), 2668-2678.

[14] Mardilovich, I.P.; Engwall, E.; Ma, Y.H. Dependence of hydrogen flux on the pore size and plating surface topology of asymmetric Pd-porous stainless steel membranes. *Desalination***2002,** 144 (1-3), 85-89.

Table 1. Composition for palladium electroless plating bath

S.No	Constituent	Amount used in each bath
1	$PdCl_2$	0.886 g/L
2	Na_2EDTA	14.89 g/L
3	$NH_{3.\ H2}O$ (25%)	110 ml/L
4	N_2H_4 (1.0 M)	1.81ml/L
5	CTAB	2 CMC
6	pH	11
7	Temperature	60 ^oC

Table 2. Comparison of time dependent averageplating rates for $Pd/Cr_2O_3/PSS$ and Pd/PSS membranes.

Type of Membrane	Average plating rate $\bar{r}_{Pd}$ (mol/m^2.s)x10^5 for various total plating time (h)				
	2	4	5	6	7
$Pd/Cr_2O_3/PSS$	0.63	3.13	3.33	3.73	3.87
Pd/PSS	4.92	5.38	5.03	4.56	4.57

Figure 1. Effect of plating time on (a) selective conversion and (b) plating efficiency.

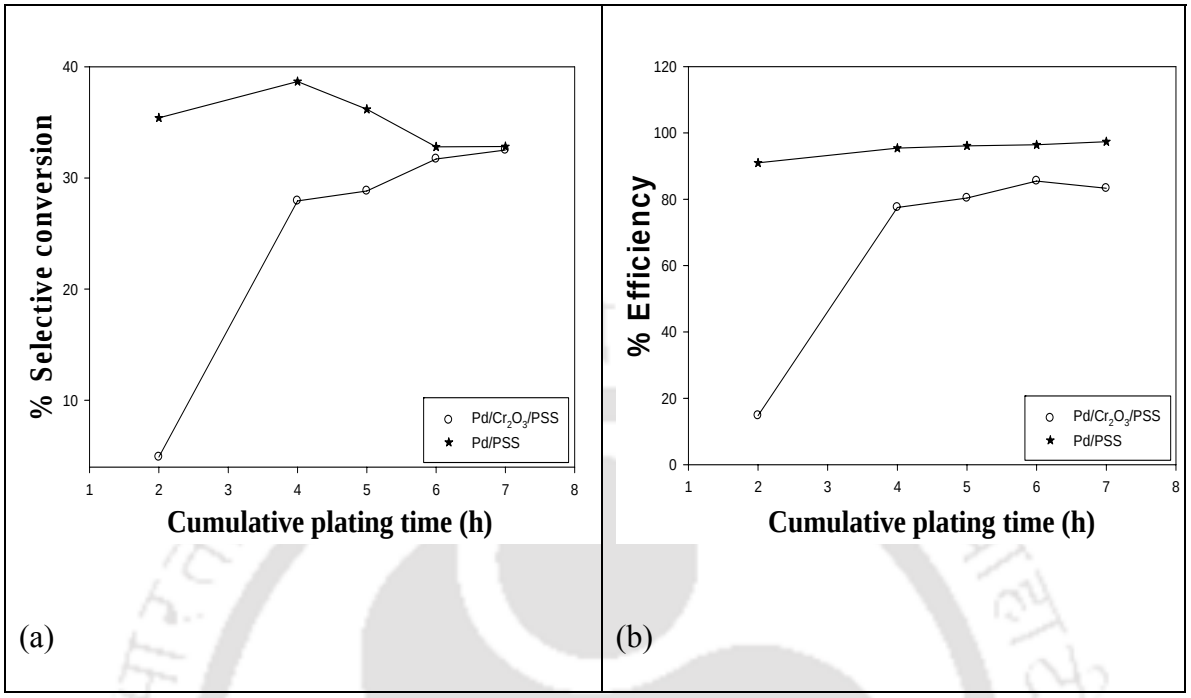

Figure 2. (a)Dependency of PPD and (b) Pd film thickness on plating time.

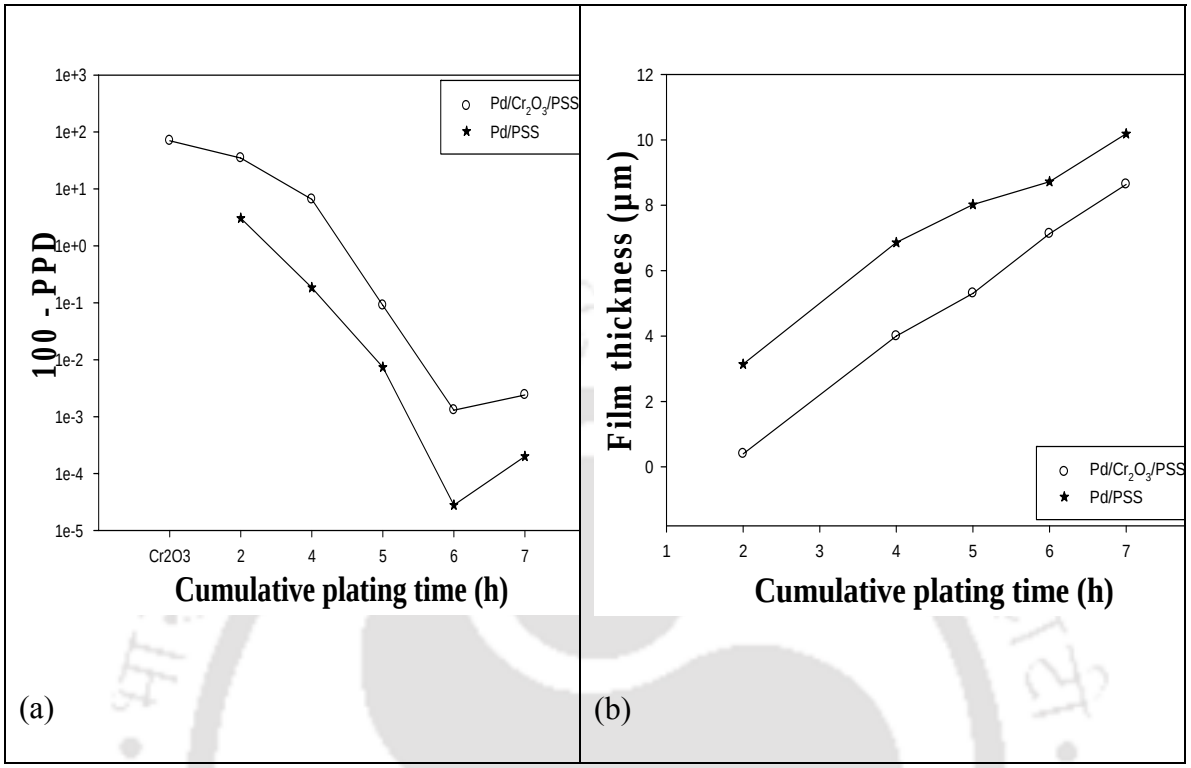

Figure 3. FESEM micrograph of (a) Pd/Cr_2O_3/PSS membrane and (b) Pd/PSS membrane

(c) XRD pattern of Pd/Cr_2O_3/PSS membrane.

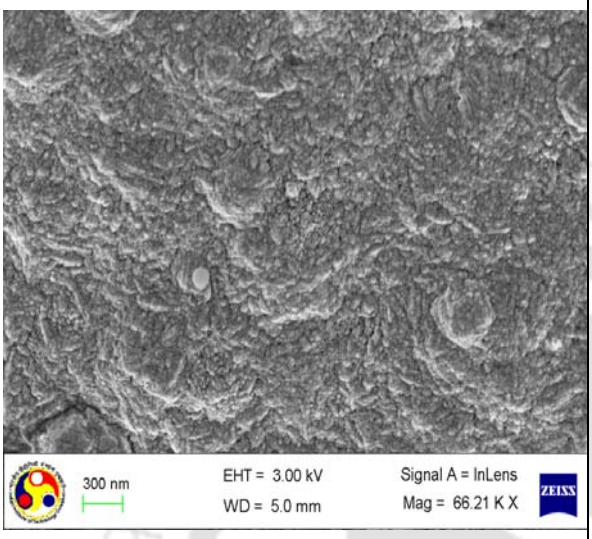

(a)

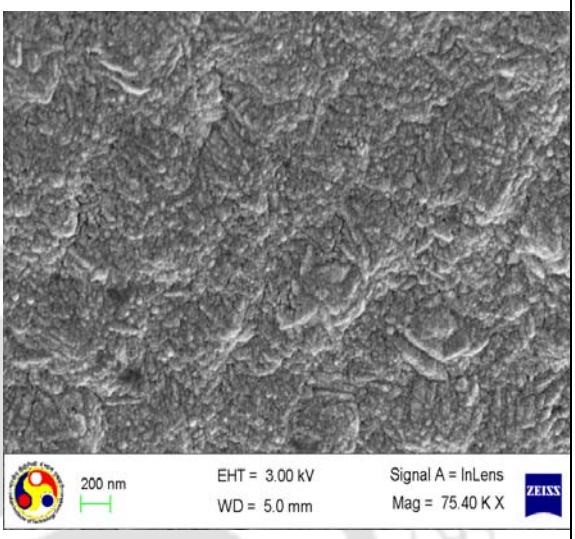

(b)

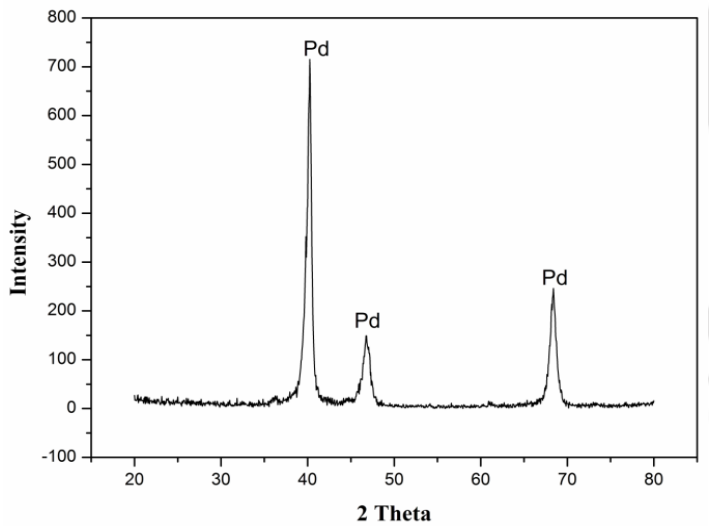

(C)